Dynamic loading of existing quay structures by induced earthquakes

F.S. (Frans) de Haan

Technical University Delft

TU Delft Delft University of Technology

Challenge the future

Dynamic loading of existing quay structures by induced earthquakes

A case-study regarding the quay structures of Groningen Seaports

by

F.S. (Frans) de Haan

in partial fulfillment of the requirements for the degree of

Master of Science

in Hydraulic Engineering

at the Delft University of Technology.

Chairman:	Prof. dr. ir. S.N. Jonkman	TU Delft; Hydraulic Engineering
Thesis committee:	Ir. A. van der Toorn	TU Delft; Hydraulic Engineering
	Ing. H.J. Everts	TU Delft; Geotechnical Engineering
	Ir. R.A.J van de Kamp	Arcadis - Rijkswaterstaat
	Dr. Ir. P. Meijers	Deltares

Status: Final Report

TU Delft

ARCADIS Design & Consultancy for natural and built assets

Abstract

As a consequence of extracting gas from gas fields in the subsoil of the Groningen province during the last decades, seismic activity is increasingly encountered. As The Netherlands is not located in a seismic active area, dynamic loads due to earthquakes historically are not taken into account in structural design. The dynamic loads from induced earthquakes in Groningen were therefore not included in the design conditions for the existing quay structures in the port of Groningen. The occurrence of seismic loads on existing structures is likely to be more common and the phenomenon of seismic activity might now be an important consideration for future design loading of these marine structures. For Groningen Seaports, the port authority, it is of importance to know the consequences of the (predicted) seismic activity on their quay infrastructure and to determine whether safety and functionality are at stake. This thesis research investigates if modifications are required and possible for an existing quay structure in the Eemshaven of Groningen Seaports.

In the analysis, an assessment to indicate the effect of an induced earthquake on an existing quay structure in Groningen is performed. As a case for the assessment, a quay structure consisting of a combined wall with grout anchors positioned at the northern side of the Juliana basin is used as reference structure, visualised in Figure 1. In order to determine if modifications of this existing combined walls are required, an assessment on the current state of the quay structure including dynamic loads from induced earthquakes is performed.

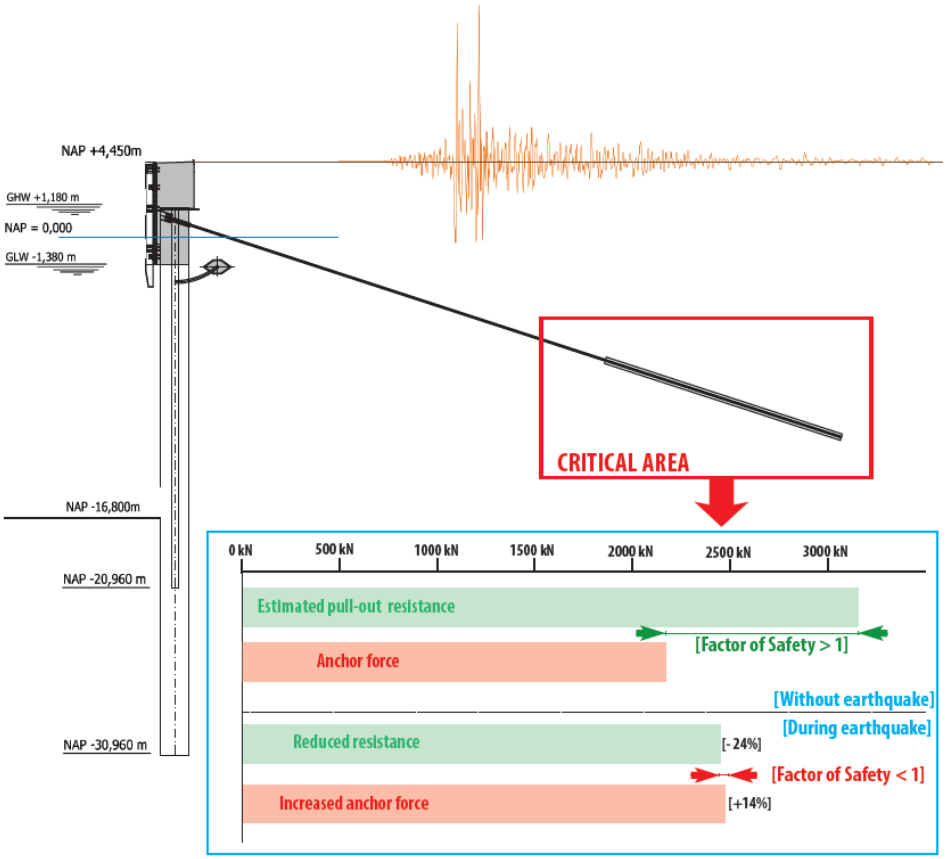

Figure 1: Impact from earthquake with respect to existing anchors of the reference structure

The assessment on the current quay structure state is subdivided into a static and dynamic approach. The static state refers to the state without an earthquake, for which the existing design report of the quay structure is applied as a baseline reference. The dynamic state includes the influence of an earthquake and is approached in a pseudo static and dynamic approach. The pseudo static and dynamic approaches both indicate that the increased anchor force is in all likelihood the most critical mechanism. The expected failure mechanism is therefore likely to occur with respect to the existing anchors. A significant difference of about 55% in output magnitudes for the increased anchor forces between the pseudo static and dynamic approaches is observed. This relatively large deviation is in line with the expectations from earlier research. The pseudo static approach includes many simplifications and assumptions which result in a conservative method to determine the influence of an earthquake. The results from the dynamic approach are therefore assumed to be governing for further research.

In addition to the results of increased anchor forces, the resistance of a grout anchor during an earthquake was investigated. From the obtained qualitative resistance development of the anchor during an earthquake, an initial quantitative estimation of the resistance development is also made. No detailed information regarding the behaviour of grout anchors under dynamic loading was available which required the introduction of a new approach. Existing literature from reference subjects was compared with the results from a modelled grout anchor in a finite element model. During an earthquake, excess pore pressures develop close to the grout body which cause decreased shear stresses between soil and grout body, which was observed from the model. A reduced anchor resistance of about 25% was initially estimated to appear during an earthquake in this research.

It is to be concluded that an induced earthquake will affect the existing quay structure. The determined factor of safety of the structure, defined as the ratio between dynamic anchor resistance and force, might be 0.98 during an earthquake, which refers to the possibility of failure of the quay structure. This factor of safety is however determined for design conditions which include a combination of several load components. The applied combination of loads, i.e. loads from soil and water, a design surface load and loads from a moored vessel might not occur often in practice, which results in a higher factor of safety during an earthquake. Therefore, further (probabilistic) studies are required for a risk-based decision on the implementation of reinforced measures. The assumed earthquake represents the Near Collapse State with a repetition of 800 years. Under the assumption that the existing structure is operational for another 40 years, an occurrence probability of about 5% for the observed design earthquake is assumed.

Due to the uncertainty regarding the influence of an earthquake, two improvement measures have been elaborated with respect to their effectiveness on reducing the acting anchor force. Both improvements, i.e. applying lightweight material (at the left of Figure 2) or a relieving structure behind the quay (at the right of Figure 2), result in an increased factor of safety during an earthquake. The decision whether to apply such an improvement measure should be based on the probability of the load component combination for a given quay and the corresponding investment costs, which are determined for both measures.

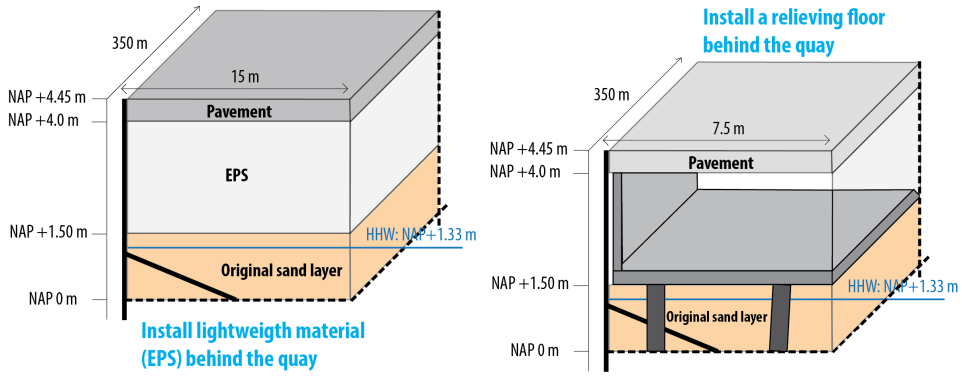

Figure 2: Proposed improvement measures to increase the factor of safety with respect to the anchors

Samenvatting

Vanwege het boren naar gas in de grond van de provincië Groningen, is daar de afgelopen jaren een sterke toename van seismische activiteit waargenomen. Normaliter wordt in Nederland weinig tot geen seismische activiteit gemeten, waardoor dynamische belastingen als gevolg van aardbevingen doorgaans niet worden meegenomen als randvoorwaarde voor het ontwerp van gebouwen en constructies. Zo is ook bij de bestaande kade constructies in Groningen Seaport geen rekening gehouden met de optredende dynamische belastingen door het winnen van gas uit de grond. Het is voor de havenautoriteit van Groning Seaport belangrijk om te weten wat de voorspelde aarbevingskrachten voor gevolgen hebben op de bestaande infrastructuur in de haven. Op deze manier kan worden beoordeeld of de functionaliteit en veiligheid van de bestaande infrastructuur in het geding komt. Dit afstudeeronderzoek richt zich daarom op de vraag of aanpassingen nodig en mogelijk zijn met betrekking tot een bestaande kademuur in de Eemshaven van Groningen Seaports.

Tijdens de analyse wordt beoordeeld wat het effect is van een geinduceerde aardbeving op een bestaande kademuur in de haven van Groningen. Een kademuur opgebouwd uit een combiwand met groutankers die gepositioneerd is aan de noordzijde van het Juliana haven basin, zoals weergeven in Figuur 3, wordt gebruikt als referentie constructie in dit onderzoek. Om het effect van een aardbeving inzichtelijk te maken en te bepalen of aanpassingen aan de bestaande kade nodig zijn, wordt een assessment uitgevoerd waarbij de huidige kade wordt onderworpen aan de dynamische belastingen van een geïnduceerde aardbeving.

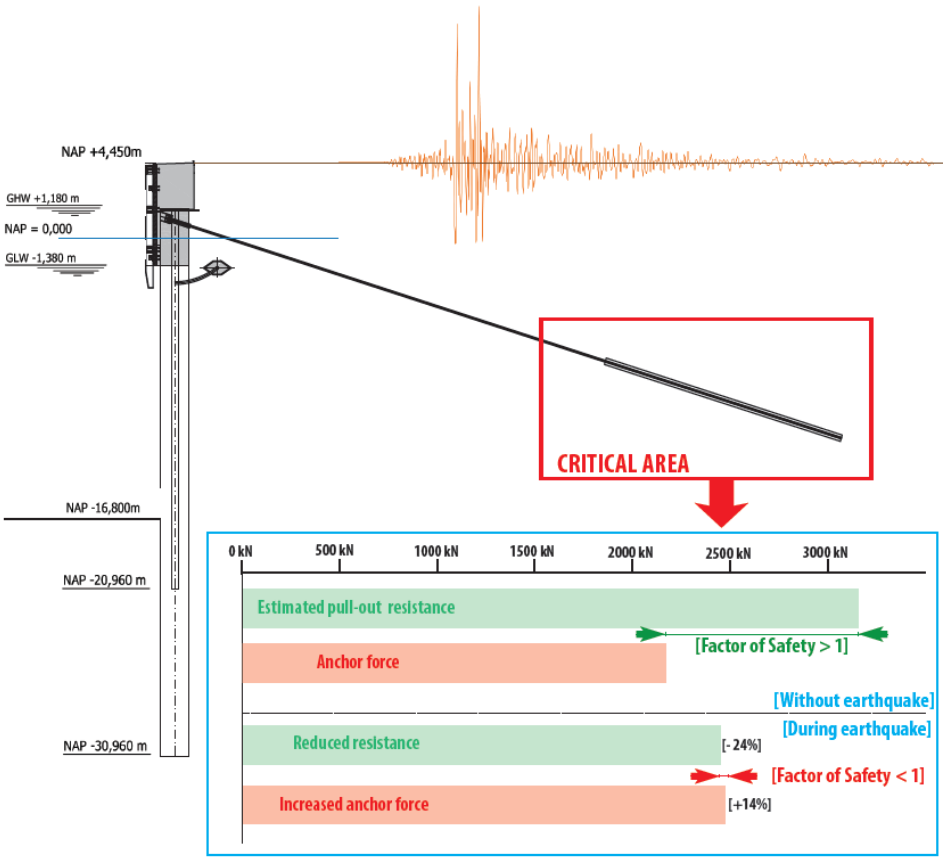

Figure 3: Overzicht van het effect van ontwerp aardbeving met betrekking tot bestaande ankers

De uitgevoerde assessment met betrekking tot dynamische belastingen op de huidige kadeconstructie is opgesplits in een statische en dynamische benadering. De statische benadering neemt geen aardbevingskrachten mee en daarin staat het huidige ontwerprapport van de bestaande kade dan ook centraal. De dynamische benadering neemt wel het effect van aardbevingen mee en is opgedeeld in een pseudo statische en dynamische methode. Een indicatie dat de bestaande anchors het meest kritieke punt vormen en dat daar in alle waarschijnlijkheid het eerste faalmechanisme optreedt, komt uniform naar voren als resultaat uit beide methodes. De pseudo statische en dynamische methode voorspellen een verschil in toename van ankerkracht van bijna 55 % als gevolg van een aardbeving. Dit relatief grote verschil in krachtstoename ligt in de lijn der verwachting vanuit eerder uitgevoerd onderzoek. De pseudo statische methode neemt veel aannames en grote versimpelingen aan wat tot concervatieve resultaten leidt. De resultaten van de dynamische methode worden daarom als leidend gezien tijdens verder onderzoek.

Vanuit de observatie dat het effect van een aardbeving zich uit in een toename van ankerkrachten, is onderzoek naar de invloed van een aardbeving met betrekking tot de weerstand van het anker ook van toegevoegde waarde. Het doel van dit onderzoek is om uit te drukken hoe de weerstand van de groutankers zich ontwikkelt tijdens een aardbeving. Nadat de verandering van weerstand kwalitatief is onderzocht, is ook een eerste kwantitatieve uitspraak gedaan over de verwachte weerstand van een groutanker tijdens een aardbeving. Hiervoor is een nieuwe relatie geïntroduceerd die de houdkracht van een groutlichaam benadert, omdat er nog geen bestaande informatie over dit aspect gevonden is. Bestaande literatuur van referentieonderwerpen is vergeleken met de resultaten van een eindig elementenmodel. Een afname van schuifspanningen tussen grond en groutlichaam treedt op vanwege de ontwikkelde wateroverspanningen dichtbij het groutlichaam tijdens een aardbeving. Een afname van de weerstand van het groutanker tijdens een aardbeving van 25 % wordt geschat op basis van dit initiële onderzoek.

Er kan worden geconcludeerd dat een geïnduceerde aarbeving invloed heeft op de bestaande constructies. De veiligheidsfactor, bepaald als de ratio tussen ankerweerstand en kracht, kan een waarde van 0.98 bereiken tijdens een aardbeving. Deze waarde zou mogelijk falen van de ankers en constructie kunnen betekenen. Er moet echter opgemerkt worden dat voor deze waarde een aantal krachtcombinaties bij elkaar opgeteld zijn. De aangenomen combinatie van krachten, voortkomend uit de aanwezige grond- en waterdrukken achter de kade, de aangenomen bovenbelasting en de troskrachten, zal in werkelijk wellicht niet optreden, wat de veiligheidsfactor aanzienlijk omhoog doet gaan. Er is daarom nader (probabilistisch) onderzoek nodig voor de beslissing met betrekking tot het toepassen van verbetermaatregelen. De aangenomen aardbevingsintensiteit vertegenwoordigt de 'Near Collapse State' met een herhalingstijd van 800 jaar. Onder de aanname dat de kade nog 40 jaar in operationeel gebruik is, ontstaat er kans van ongeveer 5 % dat de aangenomen aardbeving voor zal komen tijdens de levensduur van de kade.

Door het ontbreken van inzicht in de exacte invloed van een mogelijke aardbeving zijn twee kadeaanpassigen voorgesteld. De nadruk ligt hierbij vooral op het aantonen van de effectiviteit voor een verhoogde veiligheid van de bestaande ankers. Beide aanpassingen, het toepassen van lichtgewicht materiaal (zie linker optie van Figuur 4) of een ontlastvloer (zie rechter optie van Figuur 4) resulteren in een verhoogde veiligheid met betrekking tot de bestaande ankers. De beslissing voor het toepassen van een dergelijke aanpassing hangt af van een aanname van de aanwezige combinatie van krachten tijdens een aardbeving en de bijbehorende kosten van een dergelijke aanpassing.

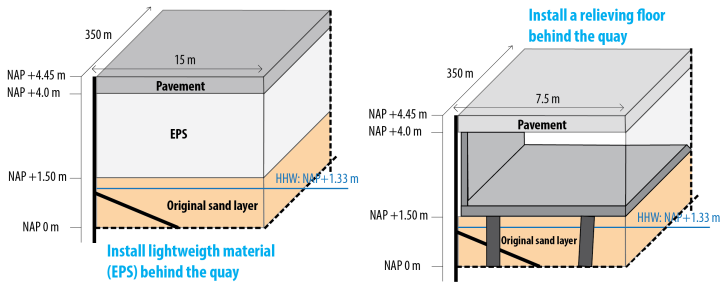

Figure 4: Voorgestelde verbetermaatregelen voor bestaande kade

Preface and Acknowledgments

This report describes my thesis research I have conducted as part of my thesis to obtain the Master of Science degree Hydraulic Engineering. For a long period of time I have been interested into structures which are related to water. They fulfil the function of protection against environmental influences and contribute to infrastructure which is important for the people nowadays in the Netherlands and in other countries all over the world. I experienced this research as a challenge and I enjoyed working at it very much. This project would, however, not be possible without the help and guidance of some people. Arcadis offered me the opportunity to work on this research for the last seven months. Many colleagues from different offices supported me if necessary, for which I am very grateful. Three colleagues from Arcadis I want to thank in particular are Ad Verweij, Rick Pijpers and Gavin Lloyd for their support during and outside office hours and their valuable feedback regarding the contents and report. Many thanks to Renger van de Kamp for his daily guidance and to be a member of my committee on behalf of Arcadis. I learned a lot from our discussions and the feedback I received during the research period.

This research would not have been able to succeed without the guidance and feedback from my committee members. In addition to Renger van de Kamp, I would like to thank Bas Jonkman for being the chairman of my graduation committee and also many thanks to Ad van der Toorn, Piet Meijers and Bert Everts for the support and feedback during and outside the meetings. I would also like to thank Hans Tanis for the discussion meetings we had during the research period from which I learned a lot.

Last but not least a special thanks towards my family and friends is reserved. They supported me in multiple ways during my whole study period at the Delft University of Technology for which I would like to thank them a lot.

Delft, May 2016
Frans

Contents

List of Figures

List of Tables

1

Introduction

1.1. Background information

Recently in the North of the Netherlands, specifically in the Groningen area, the residents and existing infrastructure are confronted with seismic events. These events are the consequence of gas extraction from gas fields, located at relatively shallow depths in the subsoil. These so called 'induced earthquakes' have a different cause and appearance compared to the well known tectonic earthquakes, which have their source at relatively great depths (Ontw.NPR9998, 2015). The knowledge about induced earthquakes and its consequences for the Groningen area are still limited because of their recent occurrence. Different institutions, like KNMI, Deltares and TNO, were therefore asked, commissioned by the NAM, to predict the likelihood of future induced earthquakes and to analyse the causes and effects for the areas surrounding the drilling fields.

Gas extraction in Groningen is nowadays a hot topic and subject to political debates. On the one hand it provides energy sources and a national income for the government, while on the other hand, it creates damage to buildings and infrastructure. As the seismic events only occurred recently, earthquakes were not taken into account during design which makes the existing buildings and infrastructure susceptible to damage. The possible damage to the houses and infrastructure is of great concern to the inhabitants. Predictions of the scale and seismic risk hazard for the future are done by the NPR9998-commission. The commissions task is to gain a better understanding of the exact and future effects which are still not known. Based on the available information, this research aims to contribute in the understanding regarding the effects of induced earthquakes for the port of Groningen.

1.2. Problem description

For a long period of time the phenomenon of seismic activity was not uppermost in the minds of the Dutch citizens in the Netherlands and it was not a common design issue taken into account. Dynamic loads from earthquakes did not play a major part in design calculations of structures. Due to the extraction of gas from the subsoil, the actuality of this topic has changed and seismic activity has become an issue to be considered.

For structures designed before the occurrence of seismic activity in the Groningen area, the dynamic loads from induced earthquakes were not included in the design conditions. Therefore the problem of unexpected seismic forces on existing structures is now appearing. For quay structures in the port of Delfzijl and the Eemshaven, also titled as Groningen Seaport (GSP), these unexpected forces from the soil may have a huge influence on the stability and structural integrity of the quay structure. Due to the large interaction between structure and soil, the phenomenon of seismic activity is expected to play an important role in loading these marine structures. For the Groningen Seaport authority it is of importance to know the consequences of the predicted seismic activity on their quay infrastructure to ensure safety. The port is not safe or operational if the structures are out of their allowable vertical and horizontal tolerances or if their structural capacity is exceeded.

1.3. Research question

To clarify the consequences of these unexpected additional dynamic loads from induced earthquakes on the quay structures, research on the effect on strength and stability is required. In case the results indicate that the allowable movement and strength or instability of the existing structure during an induced earthquake is reached, modifications of the existing quay structures may be required. The result of additional improvement measures to the existing structure may improve the strength or decrease the load. An improvement measure is assumed applicable if it results in a proper improvement regarding the earthquake resistance and is accepted by Groningen Seaport. Complete or partial failure of the structure may be the result if no measures are applied. The following research question is therefore defined:

"*Are modifications to the existing combined walls in the Groningen Seaport required and applicable to resist seismic loading from induced earthquakes?*"

From the general research question a number of sub-questions are derived:

- What is the effect of an induced earthquake on a combined wall located in the GSP with respect to the allowable deformations and strength of the structure?
- What are the expected failure mechanisms of the combined wall?
- Which measures are applicable against the possible failure mechanisms?
- Which modification to the existing structure provides the most optimal solution for improvement against induced earthquakes?

1.4. Methodology

The approach for this research is presented in a flow chart below. A brief description of each step in the flow chart is given.

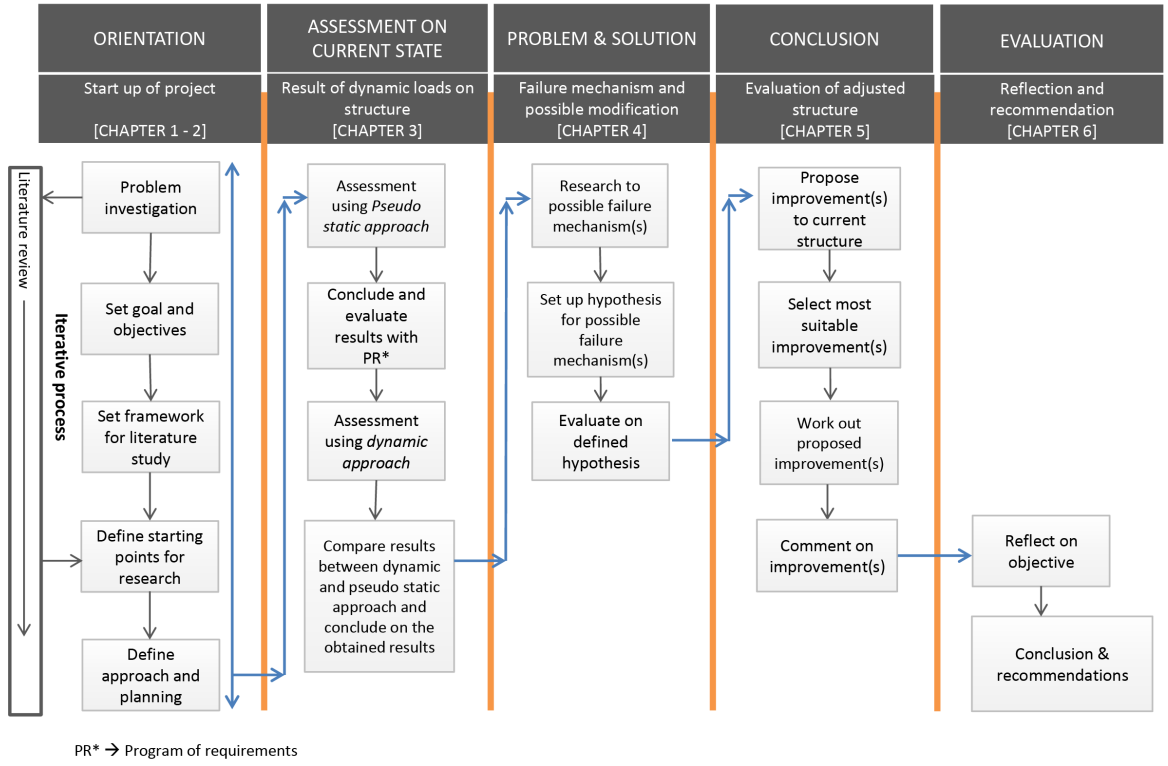

Chapter 1-2

Orientation and literature, which will provide information and starting points for the defined research question

Chapter 3

- *Assessment using Pseudo static approach*
By checking the new load conditions, a first estimation of the result of an added earthquake force on the structure is performed. The advantage of this method is the relatively fast and simple outcome to gather first insights in the influence of an earthquake to the structure.

- *Conclude and evaluate results with PR*
Evaluating the results of the Pseudo static approach with the program of requirements (PR*) of the structure can provide up a first approximation of exceeding strengths.

- *Assessment using dynamic approach*
To include the soil behaviour for a more reliable insight regarding the influence of an earthquake, an advanced model is required. During the dynamic approach, the reaction of the specific soil structure in the port to dynamic loading is obtained using a finite element method.

- *Compare results between dynamic and pseudo static approach and conclude on the obtained results*
Differences between both approaches should be evaluated to conclude on the assessment of the current quay structure state.

Chapter 4

- Research to possible failure mechanism(s)
Indicate the most critical part based on the assessment results for the reference quay structure.

- Set up hypothesis for possible failure mechanism(s)
The hypothesis for the expected failure mechanism forms the basis for further research to the failure of the structure. The hypothesis should be drafted from literature study, results from the assessment and engineering insights.

- Evaluate on defined hypothesis
From a trail to initially validate the proposed hypothesis, more detailed investigation to the expected failure mechanism is required. The result of this evaluation provides additional insight in the possible failure mechanism.

- Propose improvement(s) to current structure
Propose several improvement measures after defining the expected failure mechanism.

- Select most suitable improvement(s)
By using a trade off matrix, a quick selection regarding the most suitable improvement measures can be made.

Chapter 5

- Work out proposed improvement(s)
Implementing the selected improvement in the normative assessment from part 1 provides information regarding the effectiveness of the improvement. Results between part 1 and 3 should be compared to evaluate the improvement including additional assessment criteria from the trade off matrix.

- Comment on improvement(s)
Comment on obtained results from the improvement(s).

Chapter 6

- Reflect on objective
Elaborate on the goals and research questions which have been set at the start of the project to reflect on the objective and the extend to which this objective is pursued.

- Conclusion and recommendations
From the gathered results and pursued goals and objectives a conclusion to the research question and sub-questions can be given. From this conclusion further recommendations are advised.

1.5. Framework for research

Starting points

To create a clear view on the scope for this project, an overview of starting points and input is required. Without the use of starting points, the risk for an overload of research subjects is possible for the relatively new phenomenon of induced earthquakes. As a result, several assumptions might be made. These assumption should be kept in mind during the research. For some of the assumptions sensitivity analysis have been performed. For now, the following aspects are included as starting points and will be applied without intensive research:

- Apply the design Peak Ground Acceleration (PGA) value for the expected earthquake magnitude for an induced earthquake in Groningen Seaport. This design value will be gathered from the published NPR document in Section 2.2.
- The specific location of the quay structure including the related soil conditions will be determined at the start of the research, elaborated in Section 2.3. The research question will be worked out for a single quay structure. Findings and conclusions from this type of structure can be used to assess the influence from an earthquake for other existing structure types in Groningen Seaport.

- The program of requirements and operational requirements from the corresponding design report of the combined quay wall is used as input, which is elaborated in Section 2.4.
- Operational requirements during daily use from Groningen Seaport with respect to the existing quay structures will be gathered during literature.

Focus

The main focus of this research is to assess the influence of an induced earthquake regarding an existing quay structure in addition to the normal static loads. Subsequently, this research aims to recommend a structural improvement regarding the existing structure. This improvement should increase the obtained safety in case this is observed to become critical during or after the earthquake. To perform this research, knowledge from three main disciplines should be combined, visualised in Figure **??**.

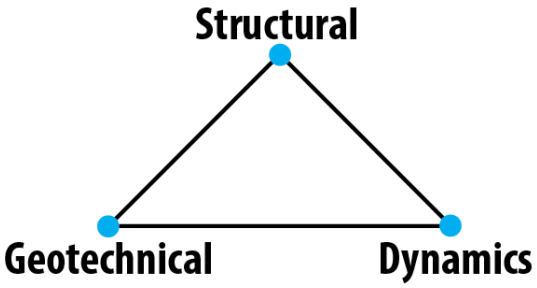

Figure 1.1: Involved disciplines from research topic

The interaction of disciplines is required to assess the behaviour from soil and structure as a result of dynamic loading from an earthquake. To prevent the research to become focussed on only one discipline, assumptions might be done for a specific complex aspect involved for that specific discipline.

1.6. Thesis outline

The outline of this thesis is schematically visualised in the flowchart of Section 1.4. Chapter 1 serves as an introduction to the project in which the context, methodology and objectives are discussed. Chapter 2 presents the general findings from literature with respect to the proposed topic. In Chapter 3 the assessment on current quay structure state is described. The effect of an earthquake regarding the existing structure is obtained using a pseudo static and dynamic approach. Chapter 4 contains the resistance investigation of grout anchors under dynamic loading to gather more insight regarding the possible failure mechanism. Chapter 5 reflects on the results as described in Chapter 3 and 4, in order to provide insight in the reduced safety of the existing structure. In addition to the indicated safety, several improvement measures are proposed. Finally, Chapter 6 describes the conclusions following from this research and recommendations for future research are presented.

2

Literature

In order to bring focus in the literature study, the following key points have been used as framework for the available information.

Earthquakes in general, Induced earthquakes Groningen, Groningen seaport area (including the specific quay and soil structure), Failure mechanisms, Loads from earthquakes and Liquefaction

It is tried to compare conclusions and statements from different sources to create a better view on the subject. Most important findings from the literature study are summarised in Table 2.4 and are applied in the assessment of the next chapter.

2.1. Earthquakes in general

To get an understanding of the influence of earthquakes on a structure, the source and characteristics of seismic events should be known. The ground motion plays a huge role between the interaction of structure and soil at different depths.

2.1.1. Source

There are different causes for seismic activity and resulting in different types of earthquakes. The type of earthquake depends mainly on the geology of the soil and the location of the source. The primary cause for earthquakes worldwide is the movement of tectonic plates. Due to the relative movement of plates to each other, sudden release of strain energy between the rocks at plate boundaries can suddenly appear which may result in seismic activity. The amount of released energy determines the magnitude of the earthquake. In addition to tectonic plate movement other possible reasons for seismic activity are (Kramer, 1996):

Volcanic activity, sudden movement of magma within a volcano can cause or trigger an earthquake.

Underground detonation, in case chemical explosives or nuclear devices create seismic activity.

Reservoir-induced earthquakes (man made), due to the extraction of gas or other natural materials from the ground.

In this research the focus is on the reservoir-induced earthquakes due to gas extraction from the Groningen gas field.

2.1.2. Energy transport by seismic waves

The energy release of an earthquake will develop and travel by waves. Two different types of seismic waves are body waves and surface waves. First the body waves will be briefly introduced and after

that the surface waves will be described. Information from (Kramer, 1996) is applied to introduce the different types of seismic waves.

Body waves

There are two types of body waves, p-waves (also called primary or longitudinal waves) and s-waves (also called secondary or transverse waves). The direction of the particles that travel in p-waves is parallel to the direction of the waves itself. The waves travel through the soil due to compression and rarefaction, see Figure 2.1a. The direction of the particles that travel in s-waves are perpendicular to the direction of the s-wave. During travelling through the soil, these waves cause shearing deformation, see Figure 2.1b. S-waves can be subdivided into two components, vertical plane movement (SV) and horizontal plane movement (HV), caused by the different directions of the particle movement.

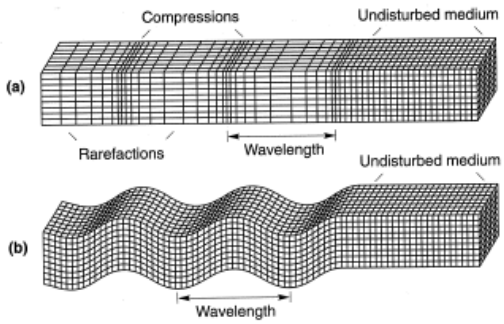

Figure 2.1: Body waves (Kramer, 1996)

The stiffness of the soil influences the travelling speed of a body wave through soil. The stiffer the soil, the higher the speed. The highest stiffness will be reached by compression of the soil with p-waves. Therefore this type of seismic wave will travel faster through the soil than s-waves.

Surface waves

This type of seismic wave travels along the surface with decreasing amplitudes in depth. A surface wave is the result of interaction between a body wave and a soil layer. Therefore this type of wave becomes more important further from the source. Two important surface waves are Rayleigh waves and Love waves, both presented in Figure 2.2a&b

In Rayleigh waves horizontal and vertical particle motion is involved. This type of wave is the result of interaction between the soil, p-waves and SV-waves. Love waves on the contrary have only horizontal particle motion and are the result of interaction between soft surficial layers and SH-waves.

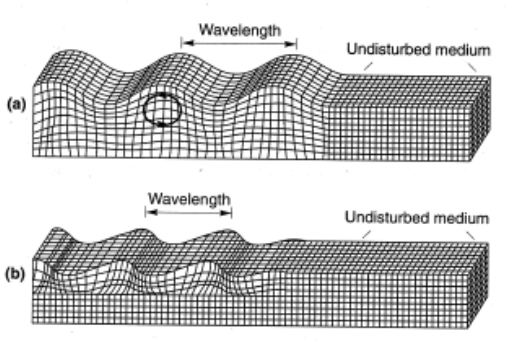

Figure 2.2: Surface waves (Kramer, 1996)

2.1.3. Parameters

During seismic activity instruments recording the ground motion can be set up which obtain valuable information about the characteristics of that earthquake. In Figure 2.3 an example of a time history is presented. Different parameters are optional to describe a seismic ground motion. The most used parameters are acceleration, velocity and displacement. By determining one of those parameters from a earthquake motion, the other two can be approached in a mathematical way. Due to the integral functions between the parameters a smoothening in the frequency domain occurs, which is visible in Figure 2.3 (Kramer, 1996). The motions from this figure are measured at Gilroy for rock at the left and soil at the right.

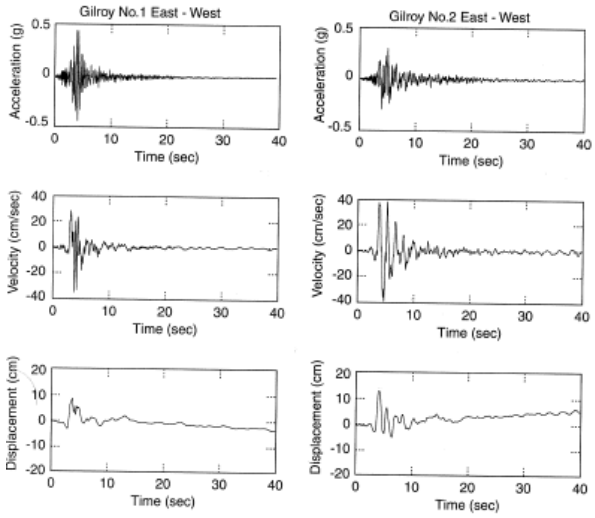

Figure 2.3: Time history of rock (left) and soil (right) from motion record at Gilroy (Kramer, 1996)

Peak acceleration

The peak acceleration can be subdivided in horizontal and vertical peak accelerations. The peak horizontal acceleration (PHA) represents the largest horizontal acceleration value in a motion from an accelerogram. This value is widely used to describe a ground motion because of the close relation with dynamic forces. The peak vertical acceleration (PVA) is less used because of the in general higher resistance of structures against vertical dynamic forces. The ratio between the horizontal and vertical acceleration is depending on the distances of the source of the earthquake. The peak acceleration provides no information on the duration or frequency of the ground motion. To determine the earthquakes level of destruction, the frequency and duration should be also taken into account (Kramer, 1996). For engineering purposes the scale of the peak ground motion is defined in most cases in the peak ground acceleration (PGA), which refers to the horizontal ground motion (PIANC, 2001). In this research the highest peak acceleration in horizontal direction will be therefore described as the PGA value.

Peak velocity and peak displacement

The advantage of the peak horizontal velocity PHV in comparison with the PHA is the sensibility to higher frequency components. The PHV is less sensible and presents therefore the amplitude of the ground motion more accurate at intermediate frequencies. The peak displacement is not commonly used as a measure of the ground motion, because it is for a different reason hard to determine this value accurately.

2.1.4. Local site effects

Due to dynamic response characteristics of the soil, the ground motion signal may significantly change during traveling through the soil. The frequency, amplitude and duration of the travelling motion can be changed between the source of the earthquake, named the hypocentre, and the location of measure at surface level, named the epicentre, due to local site effects. Damping of the amplitudes signal from the hypocentre is caused by material damping and geometric damping. The geometric damping is decisive in the area near the hypocentre, whereas the material damping becomes normative further away from the source.

A reduction in strength and stiffness of the soil layers can amplify the motion and the frequency (PIANC, 2001). On the other hand soft soil layers can also create a dampening system for the seismic waves (Visschendijk et al., 2014b). Smoothening of the signals amplitude and frequency is also a possibility with weak soil layers. The exact behaviour and influence on a signal should be determined for each specific location and soil structure itself.

2.1.5. Magnitude - intensity

A common way to express the size of an earthquake is by using the intensity and or magnitude. Both terms will be clarified briefly below.

Intensity

Using (Kramer, 1996) the intensity of an earthquake can be described indirectly as follows: "The intensity is a qualitative description of the effects of the earthquake at a particular location, as evidenced by observed damage and human reactions at that location". In other words, it describes what someone feels/observes during an earthquake. One earthquake can therefore produce different intensities at different locations. The most widely used scale for intensity is the Modified Mercalli Scale.

Magnitude

After the invention of instrumentation to measure the ground motion during an earthquake, a more objective manner of determining the size of an earthquake became possible. The measurements of ground shaking were related to a certain earthquake magnitude. The amount of energy release influences the size and amount of seismic waves and therefore the amount of shaking at surface level. No value from the observed damage is included in the magnitude, as is used for the intensity, but the ground motion and released energy determine the values of magnitude.

For this research, the size of induced earthquakes will be expressed using their magnitude. Based on measurements instead of personal observations, the size is then defined. This includes a more objective manner of earthquake scale expression.

2.2. Induced earthquakes Groningen

Important differences between induced earthquakes compared to tectonic earthquakes are the depth of the hypocentre and the time duration of the signal. The shallow depth of the hypocentre can create large effects at surface level in relation to the given magnitude of the earthquake. Also the time duration of the signal is of great influence on the damage to structures. For the induced earthquakes in the Groningen area, relatively short time duration is measured.

2.2.1. Magnitudes

Till now, the largest induced earthquake magnitude measured in the Groningen area is 3.6 which took place in 2012 at a depth of about 3 kilometres. The current expectation for the future magnitude of an earthquake in the Groningen area has been set on a magnitude of 5 (Dost et al., 2013). This value is however still a point of discussion and might change in the future.

To investigate the consequence of an earthquake with a certain magnitude at surface level, the magnitude value can be translated to the Peak Ground Acceleration (PGA) [g or m/s^2]. The KNMI has done this translation by using a Probabilistic Seismic Hazard Analysis. Soil conditions and certain characteristics of the earthquake are required to determine the PGA value for a specific location. The result of this analysis, see Figure 2.4, are the expected PGA in the Groningen area. The PGA values have a repetition time of 475 years, which corresponds to an exceedance probability of 10% in 50 years.

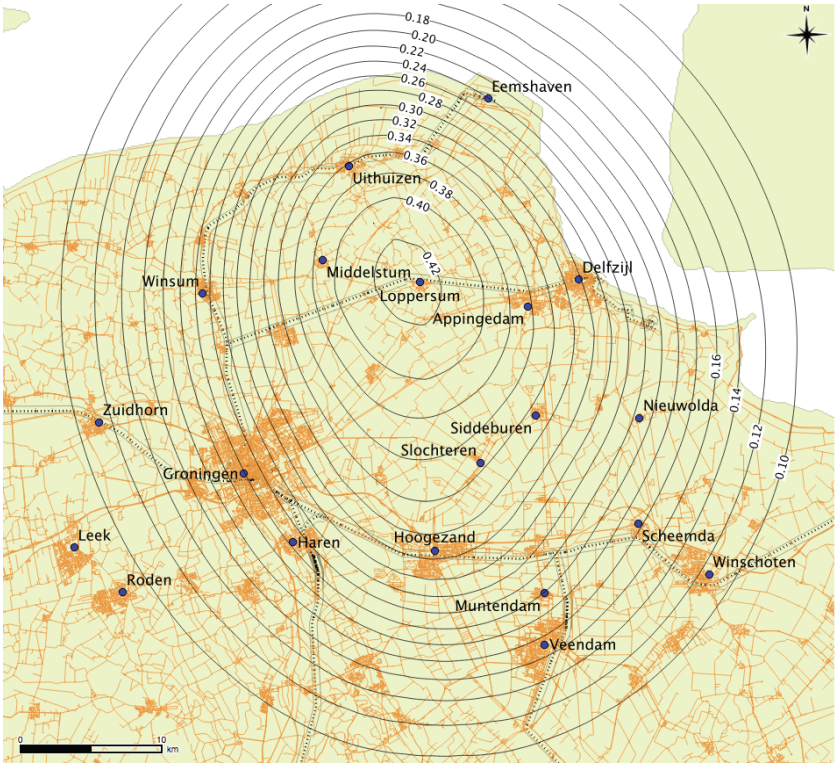

Figure 2.4: Expected of PGA values [in g] (Ontw.NPR9998, 2015)

Translation to structural loading condition

The design values for the PGA can be found by multiplying the values from 2.4 with the importance factors γ, using Fig 2.5 (in Dutch). Multiplying the PGA value with the γ factor represents the 'Near Collapse State'. This is the state in which the structure is heavily damaged. Large deformations have appeared and in case of reloading, failure of the complete structure is expected (Ontw.NPR9998, 2015).

The class CC1B is applied for quay wall structures in the GSP. This class refers to a non-public location which is comparable to quay areas in a port with low danger to lost of human life. This class is applied in agreement with GSP.

Gevolgklasse	Belangrijkheidsfactor γ_I	
	Nieuwbouw	Verbouw en afkeuren
CC1A	[a]	[b]
CC1B	1,3	1,2
CC2	1,5	1,4
CC3	1,7	1,6

Figure 2.5: Importance factors (Ontw.NPR9998, 2015)

From the data given above the design values for the Eemshaven in Groningen can be estimated. This results in a desing PGA of $0.24 * 1.2 =$ **0.29g** (equal to 2.84 m/s^2). From the included importance factor, the design PGA value corresponds to a repetition time of 800 years (Ontw.NPR9998, 2015).

The design PGA values are presented in the NPR9998. The 'green' version of this report was available during the start of this research. This document was till December 2015 the most recent version of a design guideline which includes induced earthquakes for the Netherlands. Therefore, reference is made to this document in this research. The 'white' version, which is more definitive, has been published quite recently. It can be stated that the 'green' version of the NPR9998 is more conservative than the recently published 'white' version. **All calculations made in this research before December 2015 are based on the 'green' version of the NPR9998. The committee approves to continue the research based on the earlier made calculations.**

It should be noted that the NPR9998 is made as a guideline for buildings at surface level, like houses, in the Groningen area. Therefore it does not include quay structure. A publication to indicate the initial effect from the induced earthquakes for the structures in the Eemshaven and Delfzijl has been presented by Deltares (Meijers and Steenbergen, 2015). From this report, which is also partly based on the information from the 'green' version of the NPR9998, a design PGA value for the Eemshaven of 2.6 m/s^2 is advised, which is equivalent to **0.27g** and corresponds to a repetition time of 800 years.

The advised value of 0.27g will be applied in the analysis in Chapter 3, because this value is especially determined for the Eemshaven. As mentioned before this acceleration value represents the 'Near Collapse State'. A second manner is not to apply the 'Near Collapse State' value, but a lower value with a shorter return period to determine the risk on the possible continuity of daily work during seismic events, also referred as the Operation Basis Earthquake (Meijers and Steenbergen, 2015) in a 'Serious Damage State'. The partial load and strength factors will be taken into account in this situation. This second option will not be applied in the analysis, because it is of interest to determine first the extreme effects from the appearing earthquake.

For some type of structures a reduction in PGA value is applicable (NEN-EN:1998-5, 2005), section 7.3.3.2. for the pseudo static approach. Sheet pile walls with a height over 10 meters may be reduced with a certain factor. From estimations this factor is assumed at 0.8 (Visschendijk et al., 2014b). The reduction is based on the fact that a constant acceleration in space and time is assumed in the pseudo static approach. Therefore, an average acceleration instead of an peak acceleration may be applied over the depth of the wall.

From Visschendijk et al. (2014b) it becomes clear that for the Groningen area in most cases the horizontal peak acceleration is governing and the vertical peak acceleration may be neglected. This statement is confirmed by NEN-EN:1998-5 (2005) article 7.3.2.2 section 7. Still, it should be kept in mind that there are examples of situations where the vertical peak acceleration was governing instead of the horizontal acceleration (de Gijt and Broeken, 2014). In Meijers and Steenbergen (2015) the advise is given to include the vertical PGA as 1.0 times the horizontal PGA for the Eemshaven. The decision whether to include the vertical acceleration should be made on engineering judgement and available reference cases during the assessment.

2.2.2. Source of induced earthquakes

To predict the future seismic events in the Groningen area it is important to get insight in the cause and occurrence of those earthquakes. Different relationships have been found between the current seismic activities and the locations of the drilling pits by the research work of TNO (TNO, 2009). It is hard to find the exact cause for the relationship between the seismic activity and the drilling in the Groningen area due to limited data of the soil conditions.

two optional sources for the earthquakes are discussed below. (TNO, 2009). The first optional source relates the seismic activity to tensions due to compaction of the reservoir. A reservoir filled with gas has a certain stable pressure level. Lowering of this level due to the drilling and extraction of the gas can create unequal compaction of surrounding ground. Unequal sudden compaction of soil along a fault creates vibration in the soil. The second optional cause relates differential pressure differences between different compartments to vibrations of the soil. Contiguous compartments can be separated with a fracture. If one of the two compartments has a reduction in pressure due to gas extraction, compaction differences over the fracture may arise.

Even though the exact cause between the seismic activity and the extraction of gas from the reservoirs is not yet know, the similarity between both approaches seems to be related to compaction Therefore it is assumed that induced earthquakes are a result of compaction of the soil along present fault (Ontw.NPR9998, 2015).

For this research it is important the understand the corresponding soil response from the source of the occurring induced earthquakes. The seismic activity recorded at surface level is therefore important to observe. These observations are used in the assessment in the next chapter.

Seismic wave development

The development of seismic waves in the soil of Groningen is relatively unknown due to the deviating source and soil layers compared to normal tectonic earthquakes. The compaction of soil appears at a depth of about 3 kilometres in the sand stone layer due to extraction of gas from this layer (Scientias, 2013). The Eemshaven of Groningen Seaport, which will be introduced in the next section, is positioned about 14 kilometres from the epicentre of the highest measured earthquake in Huizinge. The introduced body and surface waves are schematically visualid in Figure 2.6. The exact development of the seismic waves which will reach the port is not known. This development is depending on the soil characteristics, for example the stiffness of the soil layers. The goal of Figure 2.6 is to visualise the ratio between the source depth and distance from the port regarding the applied design earthquake. The amount and types of waves reaching the port should be investigated further before a specific forecast can be done. It is important to keep in mind that soil shaking due to an earthquake is not a 2-dimensional problem as indicated from Figure 2.4 and 2.6. The introduced waves develop in all directions which causes a 3-dimensional load effect on the existing structures.

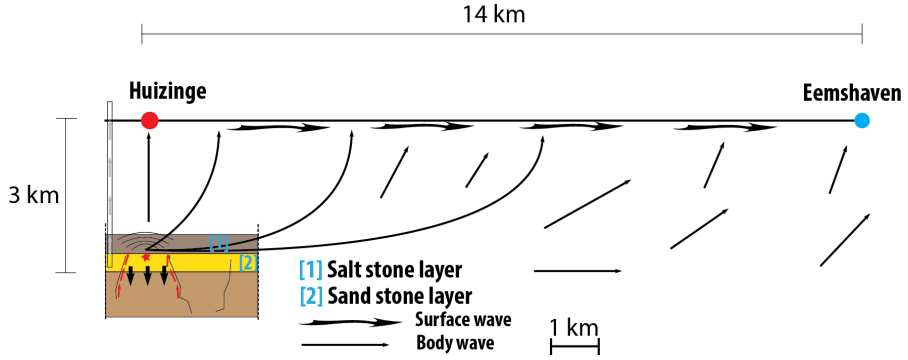

Figure 2.6: Schematic overview Groningen situation

2.3. Groningen Seaport

Groningen Seaport is the port authority of the two ports located in Groningen. The port of Delfzijl and Eemshaven play an important role for industry of energy and chemicals. In this research the focus will be on the Eemshaven.

The industry in the Eemshaven is mainly focused on energy. Due to the increasing demand of the energy market, gas heated power stations, a coal power station and almost 90 wind turbines are positioned in the Eemshaven. Besides that, space is available for the facilities needed for the transshipment and storage of dry and wet bulk goods. Facilitating the wind offshore industry is one of the newer functions of the Eemshaven (GSP).

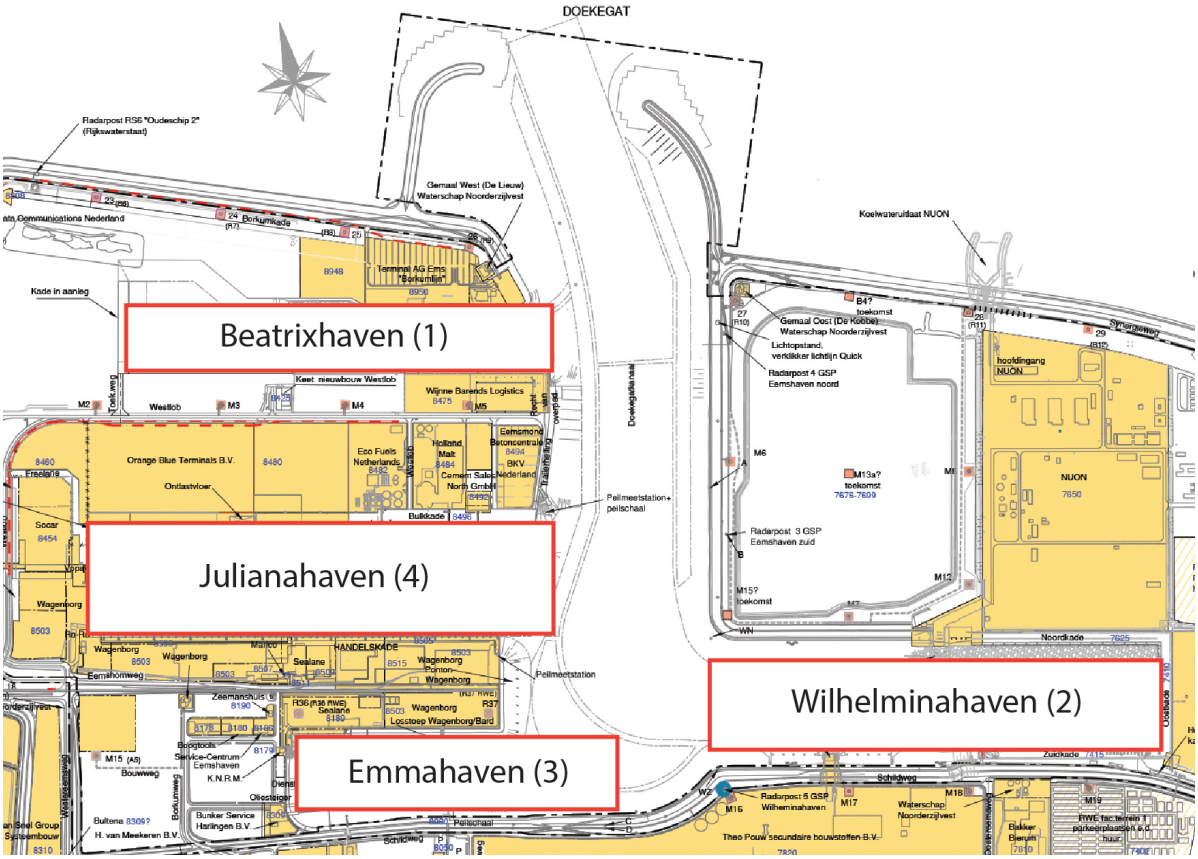

Figure 2.7: Overview map of Eemshaven in GSP

The Eemshaven is subdivided in four basins, which are be briefly elaborated in Appendix **A.2**. The corresponding quay structures are also presented in the appendix. The focus of this research regarding a specific quay structure is explained in the next section.

2.3.1. Focus of research

As a starting point for the analysis of this research the scope will be restricted to a specific quay structure. The decision scheme on which quay location to investigate is illustrated with the help of Figure 2.8.

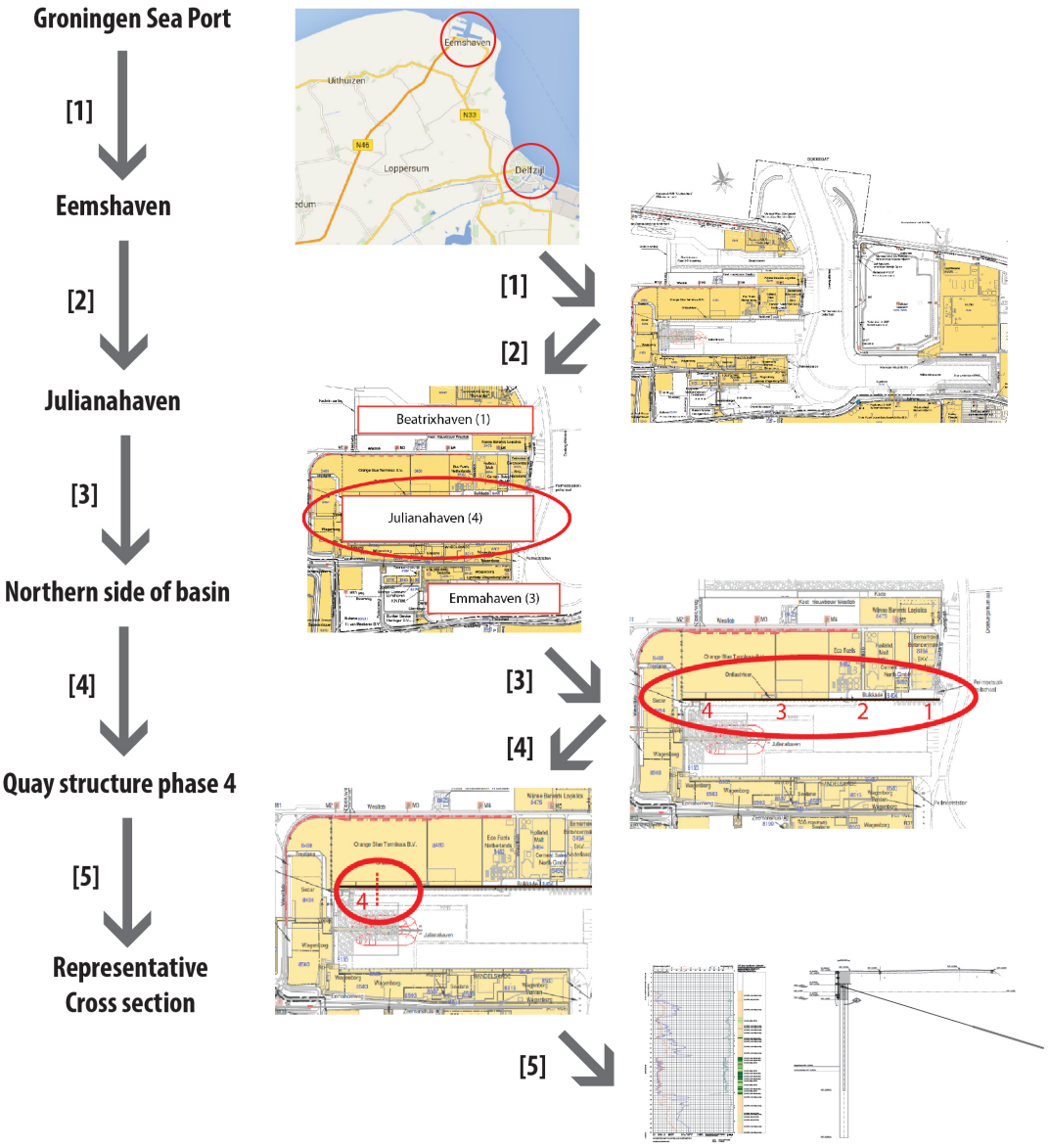

Figure 2.8: Decision scheme

Decision [1], [2] and [3]
The arguments behind decision [1], which makes distinction between the Eemshaven and the port of Delfzijl, decision [2], which basin to investigate in the Eemshaven and finally decision [3], which quay area to investigate are based on the availability of possible research subjects within TU Delft. Due to the fact that more research projects to quay structures in GSP are going on at the moment, a subdivision in different type of quay structures over different projects is made. In this research the focus will be on a combined wall with grout anchors located at the northern part of the Julianahaven basin.

Decision [4]
As earlier mentioned the basin of the Julianahaven has been build in different phases. This is presented in Figure 2.9. Phase one represents the oldest quay structures, with a made in 1994, followed by the second and third phase, from 2002 and 2007. The most recent build quay structures are from phase 4 designed in 2010.

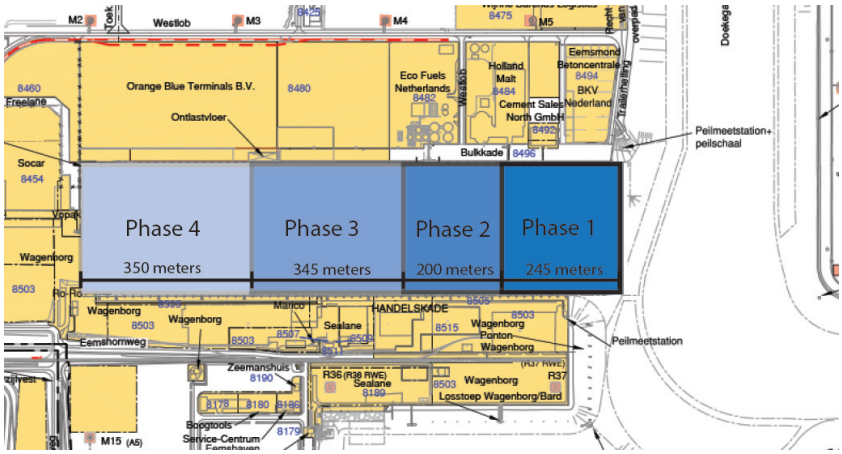

Figure 2.9: Building phases Julianahaven basin

In general the same type of quay wall is applied for all four phases of the northern quay of the Julianahaven. A combined wall with a capping beam on top with an anchorage system behind the wall is applied. Differences are present in the dimensions of the retaining wall, the sort and dimensions of the applied anchor and the way of connecting the structural parts together. The quay structure from phase one includes a crane track, but no crane is present and used during daily use. Phase two to four does not have a crane track, so over the entire quay length of the northern part of the Julianahaven basin no cranes are involved during operational hours. The listed arguments below clarify the decision on which location the focus of this research will be.

- Based on the available cone penetration tests from phase one and four a slight increase of weak layers becomes visible moving in the direction from phase one to four. From this result, is it assumed that phase four includes more sensible soil layers to cause failure of the structure during an earthquake.
- The grout anchors behind the structure are positioned at relatively shallow depths in phase four compared to the other phases. The high position of the anchors in the relatively weak soil are assumed to be unfavourable under seismic loading.
- The available information on the quay wall design of phase four is larger and better applicable compared to the other phases. Therefore, more reference material for the current project is available, which may result in more reliable conclusions from this research.

Combining the arguments from above result in a focus on the quay wall from phase four in this research.

Decision [5]
Cone penetration tests (CPT) from phase four are available. These tests provide information on the type of soil structure and some characteristics of the soil layers. In general the soil structure is relatively equal over the quay length. Small differences in cone resistance are visible, but the present soil layers are quite equal over the length of phase four. The sand layer in which the anchorage system is fixed is taken into account during the observations on the CTP. From the design report of N.Kraaijeveld the governing cross section causing the highest loads on the structure is located somewhere in the middle of the quay length, the so called section 5 of the quay area. The CPT available at this location is therefore taken as the reference soil structure and is presented in Section 2.4.2.

2.4. Reference case

To introduce the reference case for this research a subdivision in three parts is made. First the structure with associated structural elements is presented, whereafter the soil structure is given. Finally, an overview of the building stages is given which are important for the analysis. The water level in front and behind the quay differs over the building stages. Therefore, the levels are given in the last part of this section.

2.4.1. quay structure

The quay structure taken as a reference design from phase 4 is presented in 2.10. To create an overview of the important components, a brief decomposition of the important structure part elements are given in Table 2.1.

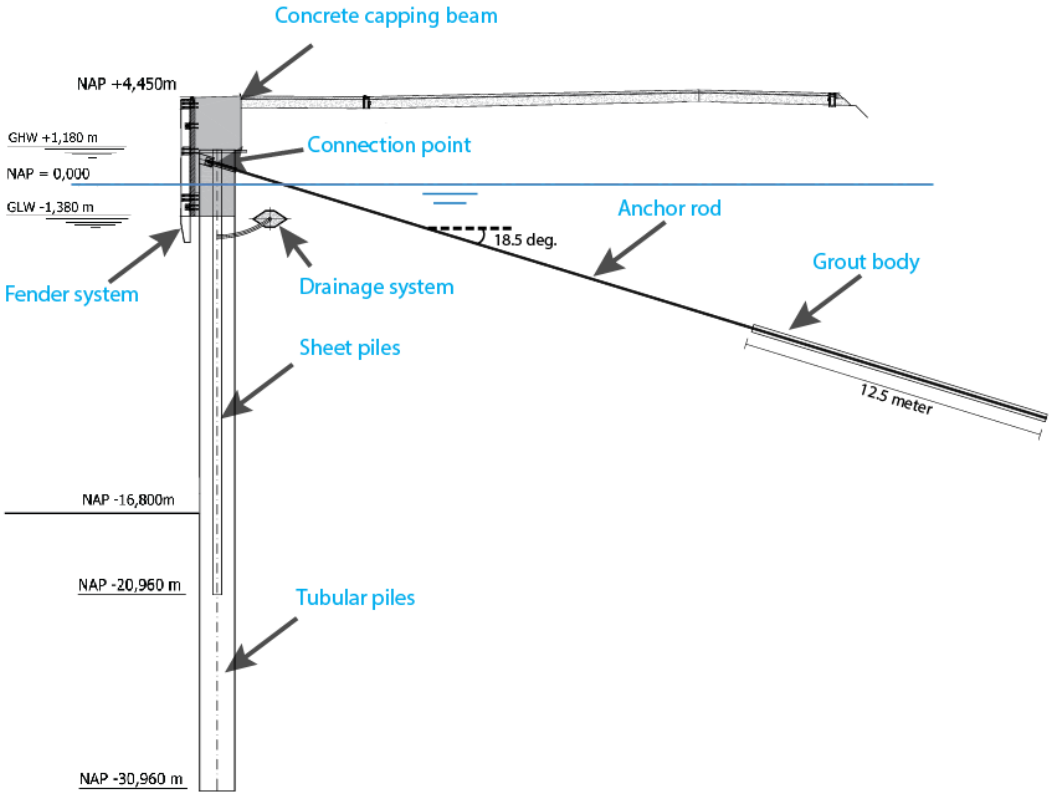

Figure 2.10: Cross section of quay structure phase 4

The most important parts of the structure are introduced below to provide an insight in the general lay-out.

Retaining element

The retaining element of the quay wall is carried out as a combined wall. Between each tubular pile, which reaches a depth of NAP -31 m, three sheet pile shelves are places reaching a depth of NAP -21 m. From Figure 2.11 the size ratio between the tubular piles and shelves is visible. The vertical black lines represent the two anchor rod connections in a tubular pile, every pile contains two anchor connections. The connections between pile and anchor are hinged. The horizontal lines represent the concrete capping beam on top of the combined wall.

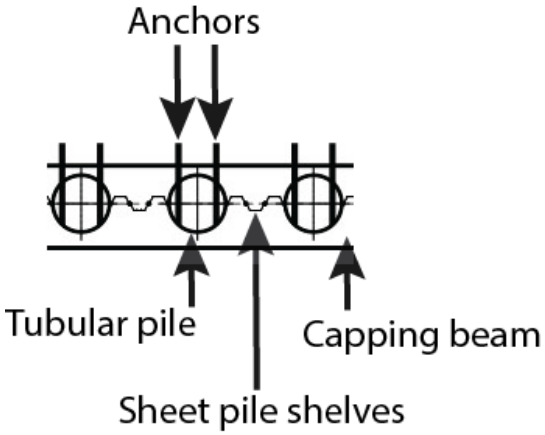

Figure 2.11: Top view of combined wall

Capping beam

The combined wall is covered with a capping beam. This capping beam is placed on top of the combined wall. Redistribution of the bollard loads from moored vessels over the spreading length of the wall is an important function of the capping beam. The capping beam is constructed with prefab elements which are filled with concrete after placement on top of the combined wall. No expansion joints are applied in the capping beam. It is therefore assumed that the structure behaves as one piece during loading.

Anchorage system

The quay structure is supplied with screw injection anchors behind the wall under an average angle of about 18.5 degrees with the horizontal. These anchors provide the required horizontal resistance for the wall. Each tubular pile is connected with two grout anchors, see the top view of Figure 2.12. The angle between the two anchors per pile is slightly different from each other, respectively 18 á 19 decrees. In this way, the depth between the tips of the anchors is not at the same level. The anchors are connected in the tubular piles at the same height of 1 meter above NAP.

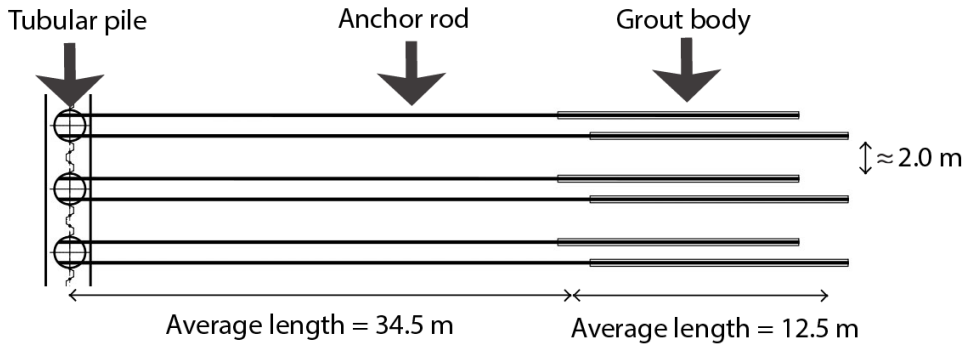

Figure 2.12: Schematic top view of applied anchor system

Drainage system

A drainage cover is positioned behind the structure at the level of NAP -1.82 m, which corresponds to the level of low low-water spring. Due to the drainage cover, the water can flow freely from inside the structure to the outside of the structure in case the water level at the inside is higher. Therefore, the ground water level at the inner side of the structure is able to follow the movement of the tide. In this way no large water level differences between both sides of wall will arise. A reduction of the water force behind the wall is accomplished in case a low water situation occurs.

Object characteristics

In Table 2.1 an overview of the structural element characteristics is given.

Object			
Tubular pile	$X70$	$\varnothing 1820 * 22.2$	mm
Top level		$+4.45$	m above NAP
Lowest level		-31.00	m below NAP
center-to-center		3.68	m
Sheet pile shelf	$PU22^{-1}$	S355GP	triple shelf application
Top level		$+1.27$	m above NAP
Lowest level		-21.00	m below NAP
Anchor	leeuwanker	101.6/28/M107	mm
Average total length		47	m
Average grout length		12.5	m
Average angle with the horizontal		18.5	degrees

Table 2.1: Structural element characteristics (N.Kraaijeveld, 2010)

* *The stiffness of the combined wall is taken as one average value. The sheet pile shelf elements are assumed to contain sufficient stiffness during an earthquake.*

Design values

The values from Table 2.2 are observed to be the limiting resistance values for the existing structure. These values are therefore assumed to present the maximum allowable loads on the structure during an earthquake before failure may appear. No additional safety factor will be applied, because the comparison between load and strength will be made in SLS, the Serviceability Limit State. If the appearing structural loads due to an earthquake exceed the values from the table, failure is assumed.

Parameter	Value	Unit	Reference
Bending moment resistance	6230	kNm/m	(N.Kraaijeveld, 2010)
Anchor rod resistance	3039	kN	(N.Kraaijeveld, 2010)
Grout body resistance	2356	kN	CUR166 [paragraph 4.9.6]

Table 2.2: Applied design values for strength of structure

The determined value for the grout body resistance from Table 2.2 is based on the selected CPT from the reference cross section. This value will be used to indicate the critical boundary of the installed anchors. A more reliable value, i.e. from a control test, should be gathered and used to indicate the pull-out force in Chapter 5.
For the allowable wall displacement difference should be made between the top and toe displacement and bending of wall at mid level. Also displacement of one single pile, which may indicate anchor failure, or displacement over a larger length influences the allowable displacement. The acceptable values should be determined in agreement with Groningen Seaport. For now an increase in displacement of several centimetres at mid level and 1/3 of that value at the top is presumed acceptable.

2.4.2. Soil structure of reference cross section

Section 2.3.1 explains the location of the cross section on which the focus of this research will be. The design report of the quay structure from N.Kraaijeveld present some soil parameters used during design. Unfortunately no CPT is available in the design report and therefore no reference behind the chosen and used values is given. Therefore, the decision is made to apply the available CPT from earlier investigations in this research and not the given values from the design report. From the CPT close to the reference cross section, the soil parameters are defined. The determination of the parameters is elaborated in Appendix **B**. Table 2.3 present the characteristic values and descriptions per layer. The complete described names per layer are given in Table B.3 of the appendix, but are simplified in the main report for practical reasons.

Layer	Soil type	γ/γ_{sat}	$q_c[MPa]$	$q_{c,100}[MPa]$	$\phi'[deg]$	$\delta'[deg]$	$c'[kPa]$
Layer 1	Fill	18/20	-	4	32.5	21.7	0
Layer 2	Sand 1	17/19	2.5	7.9	25	16.7	0
Layer 3	Sand 2	18/20	8.5	13	27	18	0
Layer 4	Clay 1	19/19	2	2	22.5	11.25	2
Layer 5	Sand 3	18/19	5.5	5.8	30	20	0
Layer 6	Sand 4	18/20	10	8.2	30	20	0
Layer 7	Clay 2	20/20	2.5	2.5	27.5	13.75	3
Layer 8	Sand 5	18/20	13	6.3	32.5	21.67	0

Table 2.3: Soil parameters

2.4.3. Building and design stage

The quay structure is build in different stages. The construction stages are given in the design report and elaborated in Appendix **C**. From this the water levels, soil levels and arising loads can be observed for every stage.
It is important to know the design stages, because the model output of every stage can create the insight in the governing design and users stage. This stage will form the static design state before an earthquake occurs. This is further elaborated in Chapter 3.

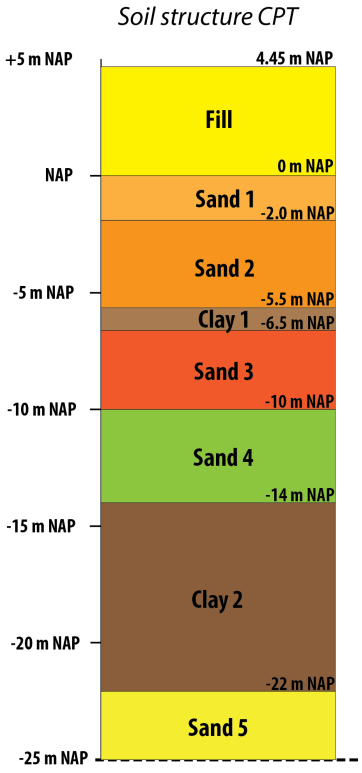

2.5. Failure mechanisms of retaining structures

History cases from all over the world proof the possibility of the devastating effects from an earthquake. In PIANC (2001) attention is paid to the failure mechanisms of different types of quay wall structures. For the sheet pile walls a subdivision is made between failure with respect to displacements, see Figure 2.13(a) and stresses (b). Failure by exceeding displacements or strengths are often the result of overloading the structure and/or a decreasing capacity of the soil.

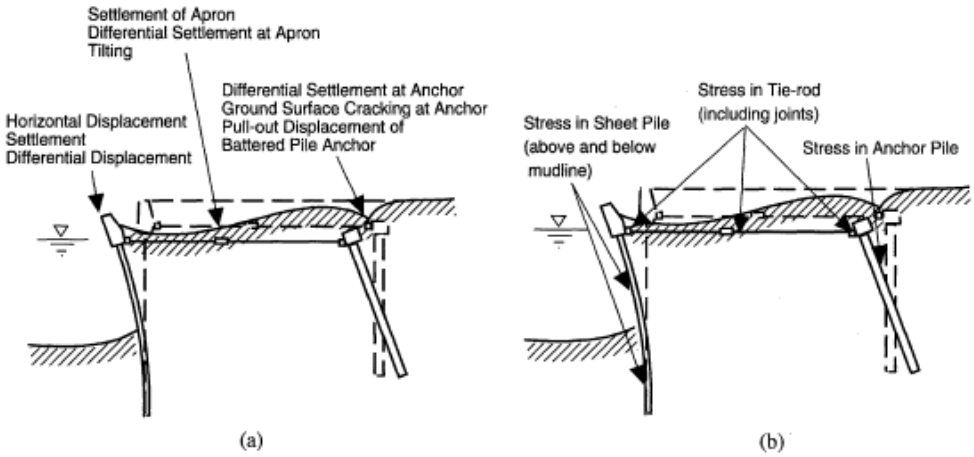

Figure 2.13: Possible exceeding locations of stress and displacement of anchored sheet pile wall (PIANC, 2001)

With the information from Figure 2.13 an overview of possible failure mechanisms for the quay structure from Figure 2.10 can be made. The marked areas in Figure 2.14 indicate the location for possible failure and are elaborated on the next page.

Area 1

- Exceeding bending moments at mid level of the wall
- Declutching of sheet pile elements

Area 2

- Displacement top of wall towards the water
- Vertical settlement of wall
- Breaking off capping beam
- Failure between connection of anchor with tubular piles

Area 3

- Pulling out or slipping of anchor system
- Yielding of anchor rod
- High perpendicular loads on anchor rod

Area 4

- (a) Horizontal toe displacement
- (b) Sliding of complete structure
- (c) Bearing capacity failure of soil beneath combined wall

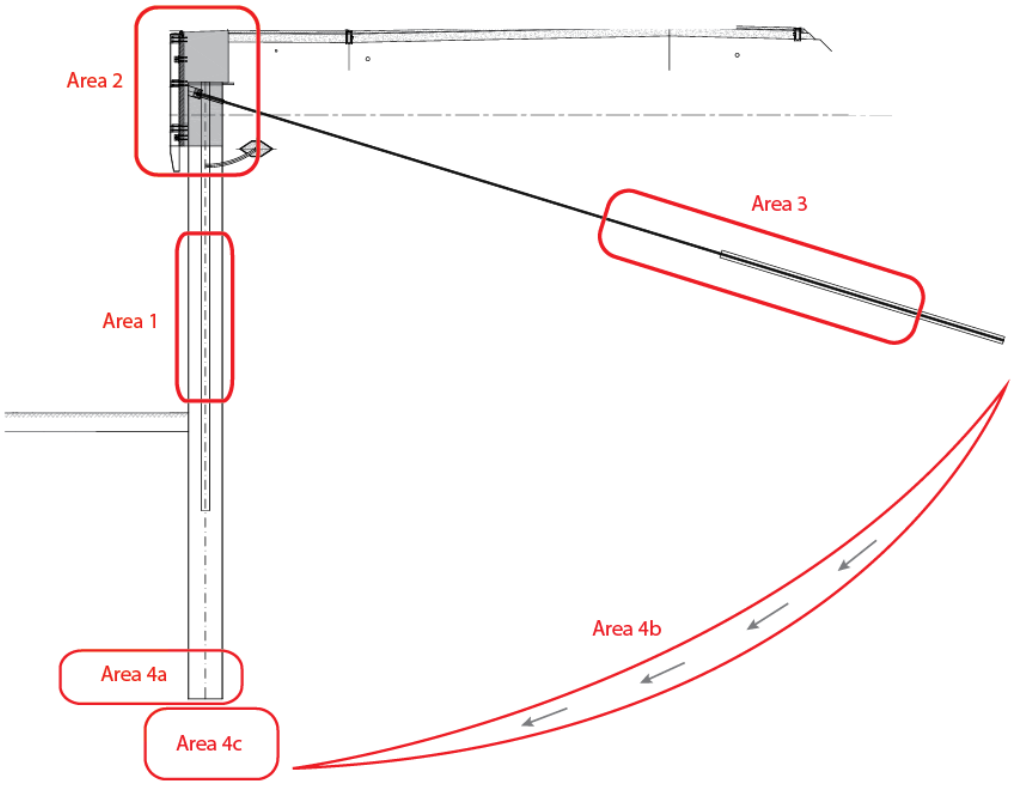

Figure 2.14: Possible failure areas regarding stress and displacement

The possible failure mechanisms for every area are schematically visualised in the Figures 2.15 to 2.18 and are briefly elaborated below.

Failure mechanisms area 1 (Figure 2.15)
In case the anchor connection and the toe of the wall enables sufficient strength, large bending moment develop around midspan. An increase of active forces and decrease of passive resistance during an earthquake is a possible scenario. Exceeding the bending moments resistance may results in interlocking failure or complete failure of the retaining wall.

Failure mechanisms area 2 (Figure 2.16)
Failure in area two refers to the top of the wall at surface level. An increase in horizontal force against the wall may result in displacement towards the water. High peak loads at the top of wall may cause failure of the anchor connection or capping beam. Buckling of the wall or insufficient bearing capacity may cause a vertical displacement at surface level.

Failure mechanisms area 3 (Figure 2.17)
Failure of the anchor system may cause complete or partial failure of the retaining structure. Exceeding the grout body resistance by overloading or decreasing resistance from the soil results in pulling out of the anchor system. If the grout body provides sufficient strength, yielding of the anchor rod may be the result of the increased pulling force. Bending of the anchor and increased tensions can be caused by increased soil weight above the anchor during an earthquake.

Failure mechanisms area 4 (Figure 2.18)
The soil strength at the passive side of the wall decrease, i.e. passive soil failure, the toe of the wall will move away from the backfill. In case the strength parameters of soil below the structure decrease, insufficient bearing capacity and settlement of the complete wall will appear. Failure of the macro stability, e.g. the complete structure and soil body slide along a plane of rupture, results in tilting of the complete structure.

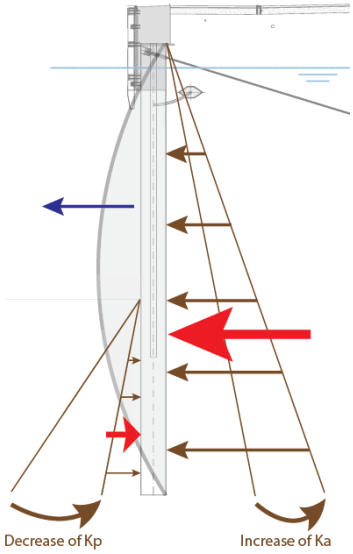

Figure 2.15: F.M. area 1

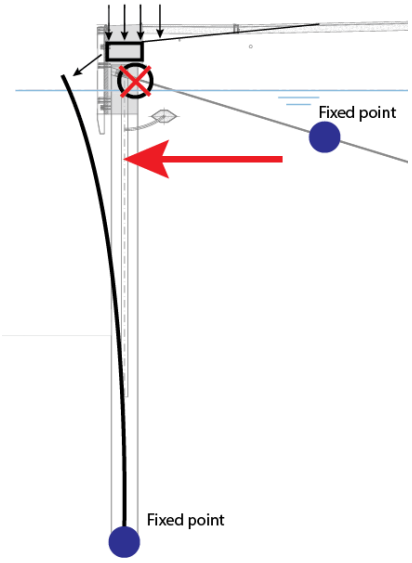

Figure 2.16: F.M. Area 2

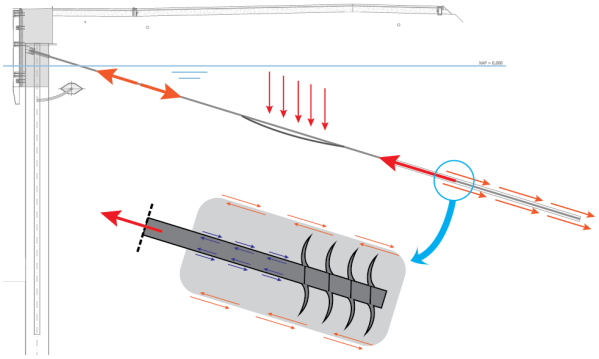

Figure 2.17: F.M. Area 3

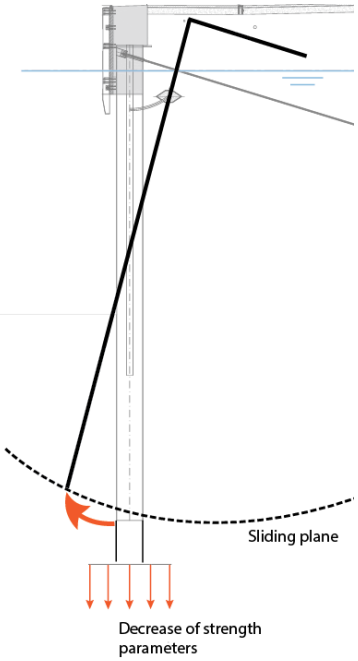

Figure 2.18: F.M. Area 4

In CUR166-2 (2012) attention is paid to the failure mechanisms of a static loaded anchored sheet pile wall. The resulting failure tree in Dutch is presented in Figure 2.19. From this figure failure can be caused in two ways, by exceeding the allowable movement of the wall or exceeding the strength capacity of the structural elements. From engineering judgement can be concluded that there is a strong interaction between the two aspects. Important to notice is the missing aspect of failure due to earthquakes. It may be useful to indicate where the influence of earthquakes can be positioned in the figure. This is depending on the results from the analysis to failure during and after dynamic loading of the anchored combined wall.

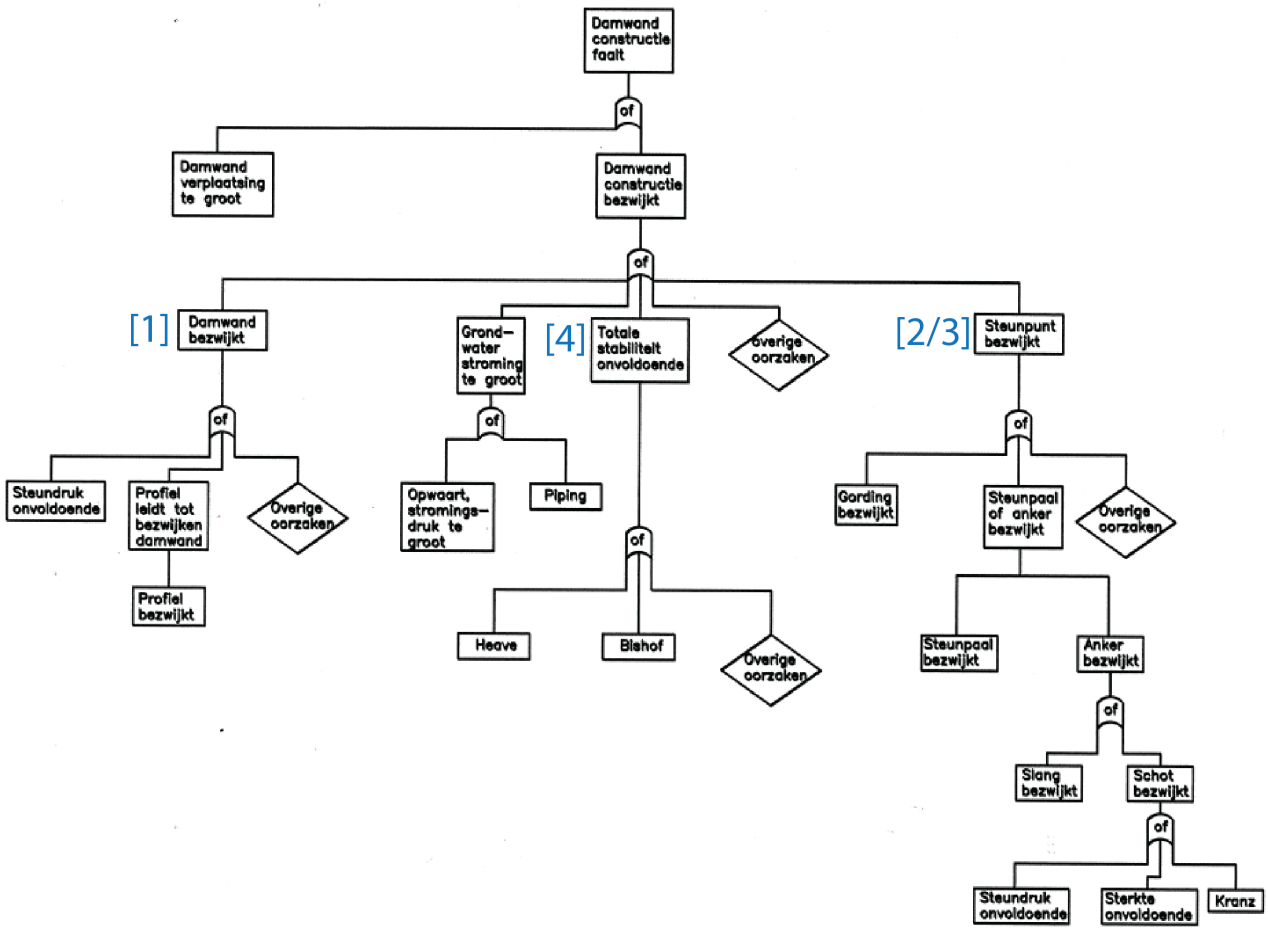

Figure 2.19: Fault tree of anchored sheet pile wall (CUR166-2, 2012)

The failure mechanisms from the Figure 2.15 to 2.18 can be related to certain aspects named in the failure tree. The failure tree designed for static state situations is not complete for failure due to dynamic loading. Different causes for failure, e.g. excess pore pressure, liquefaction and additional dynamic loads are not implemented.

2.6. Acting forces on the quay structure

Stationary soil creates static soil pressure on a wall. If the soil starts moving due to seismic activity also additional dynamic pressures starts acting on the wall. Determination of both static and dynamic forces will be introduced in this section. For further elaboration on the topics reference is made to Appendix **A.3**. information from (Kramer, 1996) is applied.

2.6.1. Static forces

Soil and wall movement have an influence on the static earth pressure. A subdivision in active and passive earth pressure can be made. If the wall moves away from the soil, active earth pressure can develop. Minimum active earth pressure acts on the wall in the case when the wall is moved away sufficiently so the strength of the soil can mobilize completely. Passive earth pressure develops in the case when the wall movement is in the direction of the soil. Maximum passive earth pressure will act on the wall in case the soil is completely mobilized. For a wall with an anchorage system, most displacements are constrained and therefore the maximum and minimum passive and active pressure is not able to develop.

To determine the static earth pressures, different methods can be applied. A common used method is the Coulomb theory. In this theory, force equilibrium is used for both minimum active and maximum passive to determine the soil forces acting on the wall. Additional information regarding this theory is presented in Appendix **A.3.1**.

2.6.2. Dynamic forces

The interaction between dynamic forces from earthquakes and the behaviour of the structure positioned in soil is complicated. This is caused by the interaction of the aspects schematically visualised below. To indicate the consequence of dynamic loads on a quay structure two applicable analysis are introduced, the pseudo static and dynamic analysis.

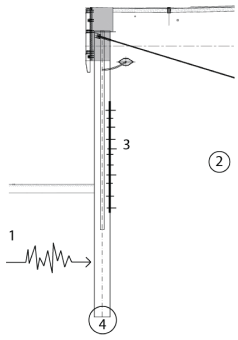

1. The characteristics of the seismic input signal
2. The response of the backfill to such a signal
3. The flexural response of the wall
4. The response of the soil under the wall

Pseudo static analysis
The complex interactions of these different processes have resulted in simplified models to determine the seismic influence on retaining structures. With a pseudo static analysis the dynamic loads from an earthquake can be schematised as a static force on a wall. In this way no difficult and complex dynamic calculations are required. The pseudo static analysis is further elaborated in Appendix **A.3.2**

Dynamic analysis
As earlier mentioned, the pseudo static analysis is a quick tool to investigate forces in structures. Due to the simplification of this method, the interaction between soil and structure during seismic loading is not taken into account. The important aspect is of great importance to provide a reliable forecast on the behaviour of a structure loaded by seismic forces. This interaction between soil and structure can be used in the dynamic analysis (PIANC, 2001). Different models in dynamic analyses are applicable, for example a Finite Element Method (FEM). The decision on what model to apply depends on the type of structure and the availability of soil characteristics and seismic motions.

Evaluation between pseudo static and dynamic analysis

To get insight in the limitations of the pseudo static method, a comparable design has been conducted in (Visschendijk et al., 2014b) with a dynamic approach using the Finite Element Method in PLAXIS. In Figure 2.20 the result of the calculated maximum bending moments in the reference case by the use of different methods is presented. The blue line represents the result of the maximum bending moment using the finite element method. The green line visualises the pseudo static method including a reduced PGA (NEN-EN:1998-5, 2005), with a value of 20%, which is assumed allowable for a walls larger than 10 meters (Visschendijk et al., 2014b).

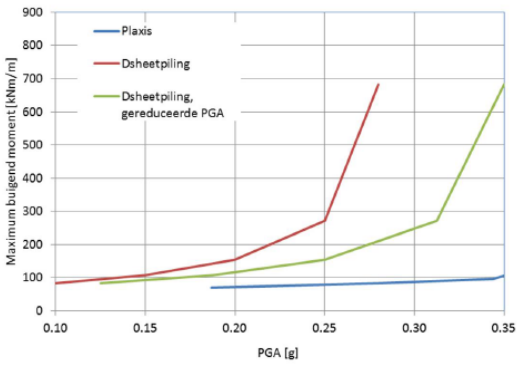

Figure 2.20: Bending moments (Visschendijk et al., 2014b)

The reduction is based on the fact that a constant acceleration in space and time is assumed in the pseudo static approach. Therefore, an average acceleration instead of a peak acceleration may be applied over the depth of the wall. The red line represents the expected bending moments from the pseudo static method with the original PGA. This example shows that the pseudo static method is more conservative, even with the reduced PGA, than the finite element method. With higher values for the PGA, above 0.25g, the difference in results increases.

Transforming the horizontal acceleration into a force by using a pseudo static approach is an oversimplification. This simplification results in this situation in a conservative approach on determining the loads. The fact that the lines are kinked and not smooth is caused by the limited number of calculation steps and therefore limit output values. Increasing the PGA values results in more conservative results and therefore larger deviation between the methods becomes visible. Due to the simplification, higher PGA values will be more conservative and therefore larger deviations between different methods arises. This causes the bending shape of the lines. No calculations values are produced above 0.35 g.

2.6.3. Applicable programs for determination of forces

The pseudo static and dynamic approach will be performed using two different software programs.

D-sheet Piling

The software from D-sheet Piling, from now on called 'D-sheet', is a tool for the design of statically loaded piles, diaphragm walls and sheet pile structures. In this program the soil is modelled as a foundation of uncoupled elasto-plastic springs and the sheet pile wall as an elasto-plastic beam. The stiffness of the soil is modelled as a series of discrete multi-linear springs, which act independently from each other. D-sheet is able to model load and anchor systems and includes water pressures. The software provides insight in the loading, strength and stability situation for structures in a static state positioned in soil bodies in a relatively quick and easy manner. For this reason the software is applied for the pseudo static analysis. (D-sheet, 2013)

Applying additional loads due to seismic activity in D-sheet provides insight in the resulting bending moments in the retaining wall, the pulling force in the simplified anchor system, the maximum displacement at one location and the overall stability. For those four aspects a failure mechanisms might be recognised during the analysis.

Remarks for application in this research:
Modelling the behaviour of grout bodies is not possible in D-sheet. The anchor tip will be applied as a fixed point. Soil behaviour will not always be modelled realistic. Settlement of soil during different stages is not taken into account and the soil-structure interaction is only limited captured in the software. Those aspects should be kept in mind during the analysis.

PLAXIS

PLAXIS is a tool to analyse the deformation and stability behaviour of geotechnical structures by using a finite element model. This means that the model is divided into a large number of small elements for which the behaviour of every element is taken into account. The two or three dimensional finite element models are based on a geometric model, containing these elements. These generated triangular elements are called a mesh. The soil can be approach by applying different types of models. The material input is related to stress and stiffness characteristics. Both the soil behaviour and the soil-structure interaction is included in the model. PLAXIS 2D is most common on modelling a quay structure and will therefore be applied. (PLAXIS-2, 2015)

Running a dynamic calculation with PLAXIS provides insight in the soil behaviour and the influence of the soil regarding the structure. Bending moments, anchor forces, displacements and stability of the structure at different locations in dynamic time can be determined. Including soil response behaviour regarding a seismic signal provides insight in the failure mechanisms for the named aspects above. The difference for these four aspects in PLAXIS regarding the mechanisms in D-sheet is that the results are determined more accurate and are visible at different location at different time steps during the earthquake. In this way a more advanced estimation to the response and therefore the failure mechanisms of the wall can be made.

Remarks for application in this research
Modelling the behaviour of a grout anchor is possible in PLAXIS 2D by applying an embedded beam row. Nevertheless, it is noted that the behaviour of a grout body in soil is a complex 3D problem and that the results from PLAXIS 2D regarding the behaviour of a grout body are not always modelled correctly. (PLAXIS-1, 2015)

2.7. Liquefaction

The effect of an earthquake can be described by two aspects, accelerations in the soil and the possible appearance of liquefaction (Visschendijk et al., 2014b). This section introduces the phenomenon of liquefaction. Additional information regarding liquefaction in presented in Appendix **A.4**

Liquefaction is the description for the phenomenon in which the shear stress between individual soil particles becomes absent and therefore the effective soil stress reaches a value of zero. This effect might be initiated if soil particles start moving to a more dense soil structure due to an earthquake. Commonly, with loosely deposited materials like silt, sand and fine gravel there is a high risk of liquefaction present in case of cyclic loading. Parameters of great influence on this phenomenon are the type of seismic signal, like duration and intensity, the substrata and the effective stress between the particles (de Gijt and Broeken, 2014). Port structures are generally constructed with and on man made or engineered soils, instead of naturally consolidated soils. It is therefore important to perform a check on the possible occurrence of this phenomenon.

Determination of liquefaction for Groningen

Different methods are applicable to determine the vulnerability to liquefaction. The NPR9998 applies a method based on the research of I. M. Idriss and R. W. Boulanger, referred as I-B method, and this is adjusted with a number of assumptions (de Jong et al., 2015). Another way to determine the vulnerability to liquefaction is with the method of Robertson (Robertson and Cabal, 2015).

Due to the relatively short time frame of the seismic activity by induced earthquakes, the number of load cycles on the soil is relatively low compared to tectonic earthquakes. Tectonic earthquakes have a higher number of significant vibrations and therefore more load changes than the induced earthquakes in the Groningen area. Until now, no major examples of liquefaction have been detected in the Groningen area. Nevertheless, a risk regarding the occurrene of liquefaction is definitely present for high PGA values(Visschendijk et al., 2014b). The liquefaction research from Deltares for the Groningen area indicates the complexity of the situation. For now the results from Figure A.15 in Appendix **A.4.3** are assumed applicable and complete liquefaction of the soil is assumed not to occur. Development of excess pore pressures, without complete liquefaction, will be taken into account.

2.8. Starting points from literature

Table 2.4 presents an overview of the most important findings during the literature review.

Input values for analyses		**(Section 2.2.1)**
Peak Ground Acceleration (PGA)	0.27 / 2.6	[g] / $[m/s^2]$
Return period	800	years
Acceptable individual risk	10^{-5}	per year
Structure		**(Section 2.3.1)**
Location of structure	Northern side of Julianahaven	
Type of structure	Combined wall with capping beam	
Anchorage system	Grout anchors (type: Leeuwankers)	
Maximum strength values in SLS		**(Section 2.4.1)**
Bending moment resistance	6230	kNm/m
Anchor force resistance	3039	kN
Grout body resistance	2356	kN
Wall displacement	$n.a.n^*$	m
Overall stability	$SF < 1$	[-]
Soil structure	presented in section 2.4.2	**(Section 2.4.2)**
Liquefaction	No further research will be applied regarding the vulnerability to liquefaction.	**(Section 2.7)**
Indicated failure areas and mechanisms		**(Section 2.5)**
Failure area 1	Regarding midspan of the wall	
Failure area 2	Regarding top of wall	
Failure area 3	Regarding anchorage system	
Failure area 4	Regarding toe / macro stability	
The analysis should provide insight:	Which failure area or combination of areas is governing during an earthquake	
Usable methods		**(Section 2.6)**
Pseudo static approach	Software: D-sheet	
- Additional dynamic soil forces	Mononobe-Okabe method	
- Additional dynamic water forces	Westergaard method	
Dynamic approach	Software: PLAXIS	
- Integral model of soil and water	Finite Element Method	

$n.a.n^*$ = not a number, should be determined in correspondence with Groningen Seaport.

Table 2.4: Design decisions and parameters from literature

3

Assessment on current quay structure state

To create insight regarding the effect of dynamic loads from induced earthquakes on the existing quay structure, an assessment on the current situation is required. The goal of this assessment is to provide insight in the structural response and to determine the effects of an induced earthquake. From the results, the critical aspects during an earthquake resulting in reduced structural safety can be indicated. In this way, a trial is made to provide insight in the possible failure areas during an earthquake.

The assessment contains an analysis of the structural state before, during and after an earthquake. To understand and observe the response of the structure to dynamic loading by an earthquake it is important to get insight in the static state situation, i.e. the state before the occurrence of an earthquake. This is from now on called the static state of the structure. By making a dynamic model, which will be elaborated later, insight regarding the influence of an earthquake can be obtained. The existing design report of the quay structure (N.Kraaijeveld, 2010), provides the information for the analysis regarding the static design state. The design report is therefore used as a reference document for the static state approach.

The influence of an earthquake on the quay structure will be investigated by evaluating the output of both static and dynamic state. The dynamic state of the structure refers to the static state combined with dynamic loading from an earthquake. The dynamic state will be assessed in two ways, with a pseudo static approach and subsequently through a dynamic approach. By comparing the results for the static and dynamic state, the influence of an earthquake on the existing quay structure can be determined.

This chapter is subdivided in four sections. Section 3.1 elaborates on the applied analysis to perform the assessment on the current quay structure situation. After the explanation of the performed steps in the analysis, the results of the static approach will be presented in Section 3.2. Following on the static approach, the pseudo static approach is explained in Section 3.3. In Section 3.4 the dynamic approach has been worked out. Every section ends with a conclusion on the most important aspects. Appendix **D** provides additional information to substantiate the elaborated aspects of this chapter.

3.1. Analysis to perform assessment

Figure 3.1 presents the approach for the assessment. The analysis is subdivided in a static and dynamic state. The static state of the quay structure includes no earthquake loads and is assessed with a static approach. The existing design report of the quay structure is used as input for this approach which will be explained in Section 3.1.1. The static approach is performed with the steps [1], [2], [3] and [5] which are explained in Section 3.1.2.

The dynamic state is subdivided with two approaches, i.e. a pseudo static and a dynamic approach, indicated with the colored areas in Figure 3.1. The pseudo static approach is indicated with step [4] and step [6] and [7] are applied for the dynamic approach. The performed steps are elaborated in Section 3.1.2 and worked out in more detail in Appendix **D**.

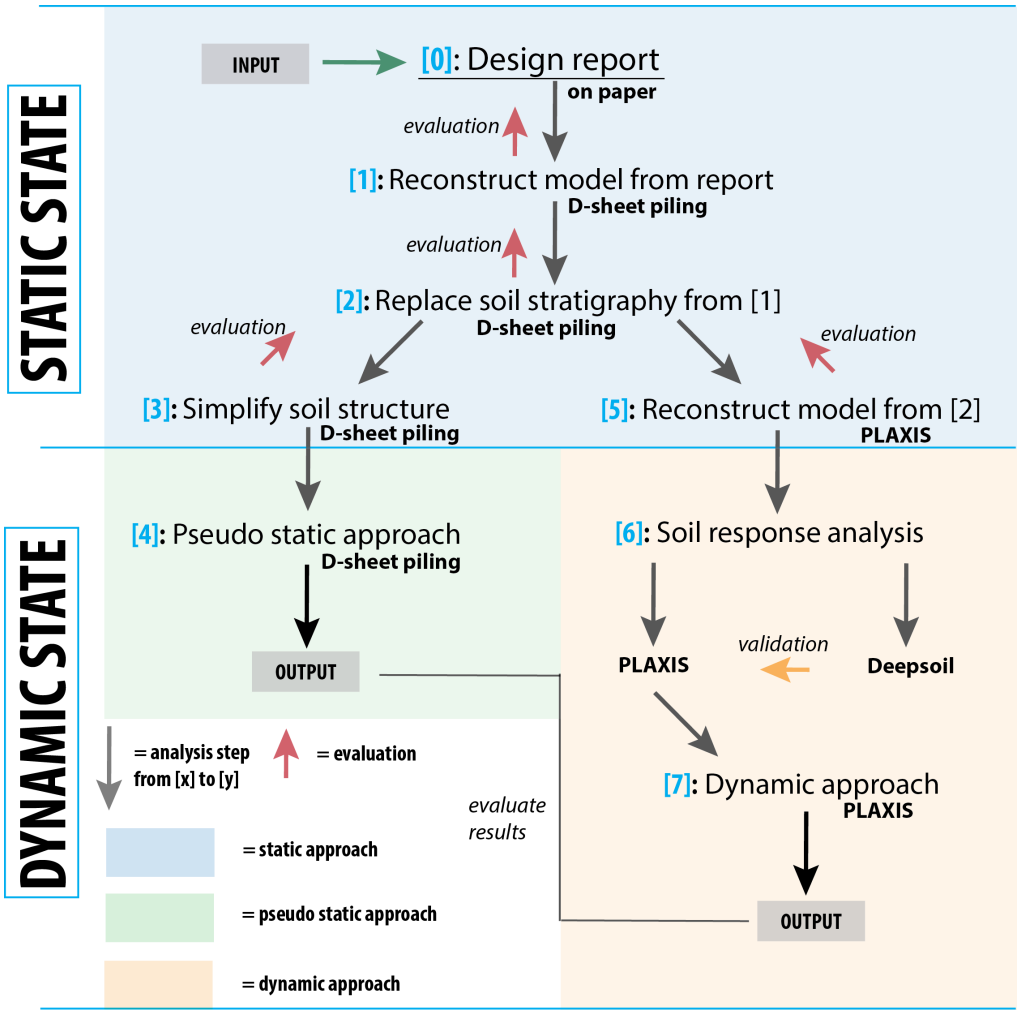

Figure 3.1: Performed analysis for assessment on current situation

3.1.1. Required evaluation of performed steps

Using software models for forecasting structural response requires precise judgement with regard to the provided output. The output is often highly dependent on the input. The input is often determined from measurements or empirical relationships which may contain inaccuracies or deviations. This may have influence on the provided output. It is therefore important to evaluate the output with reference models or reference cases.

Hardly any applicable and reliable historical reference cases or laboratory experiments with measurements of structural movements for this research could be found due to the following reasons:

- Due to the fact that the appearance of induced earthquakes is still relatively new in Groningen, no measurement results of the response of a quay structures during an induced earthquake are available.
- Up until now the maximum measured earthquake was a magnitude scale of 3.6. The models in this analysis are based on a magnitude scale of 5. No measurements of any kind are available in the Groningen area for this magnitude scale.
- There are reference cases with structural responses from large magnitude earthquakes in other countries. However, these measurements are not the result of induced earthquakes, but are caused by tectonic earthquakes. The differences between tectonic and induced earthquakes, for example the duration, the number of peaks in the signal and depth of source, are elaborated on in the literature study. Due to these differences a comparison between measurements from a tectonic earthquake and output from a model based on induced earthquake is questionable.
- Most measurements from case histories are from structures located in sandy soils with the source of the earthquake located in the bedrock. In this research the soil is partly sandy and the relatively shallow depth of the source is suggesting that the hypocenter is not located in bedrock. Both aspects are of influence on the soil response and therefore the soil-structure interaction. These differences make a validation not likely to fit.

It is decided that the original design report of the structure (N.Kraaijeveld, 2010) forms the basis for the static state of this analysis. After almost every step going downward in Figure 3.1 an evaluation of this performed step is applied. This is done by comparing the results of the performed step with the result from the step before. By investigating and judging the results of every step the changes are obtained and visualised. If the results are divergent and not in line with the expectations of the step made, a second judgement on the input and applied method should be carried out.

3.1.2. performed steps [1] to [7]

The performed steps from Figure 3.1 have been carried out to obtain insight in the response of the quay structure as a result of dynamic loading by an earthquake. The steps are briefly summed up below. For further elaboration and evaluation of the results reference is made to Appendix **D**.

Static approach

- **[1]** With the design report forming the basis of the analysis, the first step is to translate the existing results and model parameters from the design report on paper (N.Kraaijeveld, 2010) into a D-sheet model. All input values are copied from the report. The purpose of this step is to construct a model which contains the exact same output values as presented in the design report. In this way the model in D-sheet is equal to the original design model.
- **[2]** The created model in D-sheet from step [1] is based on the soil parameters as given in the design report. As explained in Section 2.4 the soil structure from the selected Cone Penetration Test (CPT) is used during the analysis. Therefore the determined soil parameters from Section 2.4 are implemented and replace the originally used soil parameters. By comparing the results caused by the new applied soil structure with the results from step [1] the influence of the changed soil parameters can be obtained and evaluated. Besides the soil stratigraphy no further changes will be made to the model from step [1].

- **[3]** The next step focusses on the pseudo static approach, as mentioned in Section 2.6.2, by simplifying the soil structure. The number of layers will be reduced. This is done for the following two reasons. The additional dynamic loads have to be determined for every single soil layer. The layers with generally corresponding characteristics have been merged together in one layer with average parameters for the practical reason of saving time. The determined additional dynamic loads will be implemented as line loads in D-sheet. D-sheet contains a maximum implementation of line loads. If every layer will contain additional dynamic loads, the number of loads is too large to implement in D-sheet. This forms the second and most important reason for merging a number of layers together.

- **[5]** This step contains the reconstruction of the model in D-sheet from step [2] into a PLAXIS model. It is aimed to construct the static state, without the occurrence of an earthquake, of the current structure. This static model will be evaluated to the model from step [2] and forms the basis for the dynamic analysis in step [7].

Pseudo static approach

- **[4]** The impact of an earthquake is determined by using a pseudo static approach, which is elaborated in the literature study. The determined additional dynamic loads will be implemented in the model from step [3].

Dynamic approach

- **[6]** After the evaluation of the static state model in PLAXIS, the dynamic soil response will be worked out. The response of the soil from a seismic signal in PLAXIS must be validated. This can be done regarding the 1-D software from Deepsoil. This software contains less input options and is therefore easier to understand regarding the soil response than the finite element software of PLAXIS. The soil response of PLAXIS will be validated regarding the response of Deepsoil. Besides the validation of the soil response also the seismic input signal will be determined.

- **[7]** Again the impact of an earthquake is determined, however this time in a fully dynamic approach. After the evaluation of the static state model and the validation of the soil response behaviour, the dynamic response of the structure regarding the seismic signal can be determined.

3.1.3. Overview of three approaches

In addition to Figure 3.1, the general characteristics from the three approaches are summarised. In this way a brief overview of the next three sections of this chapter is provided.

Static approach (Section 3.2)

- The goal is to provide the static state models forming the basis for the pseudo static and dynamic approach.
- The existing design report forms the basis for both static models [3] and [5]. Step [1] and [2] are sub steps between the design report on paper and the static models [3] and [5].
- The static model in D-sheet [3] includes a simplified soil stratigraphy from the selected cone penetration test (CPT).
- The static model in PLAXIS [5] includes the complete soil structure from the CPT.
- Evaluation between the sub steps is performed to create insight in the influence of the changed input for different steps.

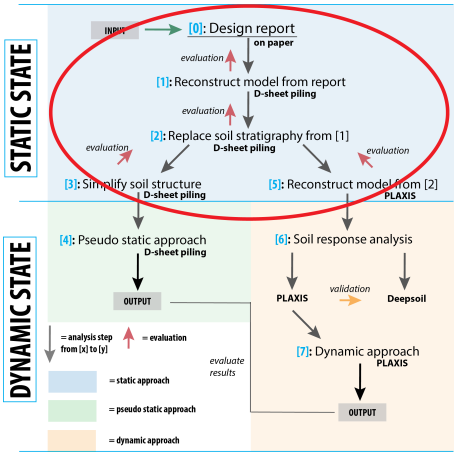

Pseudo static approach (Section 3.3)

- The goal is to provide insight to the impact of an earthquake loading an existing quay structure with the help of a simplified method.
- Horizontal loads are added to the static model [3] in D-sheet, determined with the M-O method (for soil) and Westergaard method (for water), based on the PGA value of 2.6 m/s^2 with a return period of once in 800 years.
- Subdivision will be made between loads from water, dry soil and saturated soil.
- By applying the simplified method in D-sheet is has been tried to find the failure mechanisms with respect to the bending moments, anchor force, horizontal displacements and overall stability.

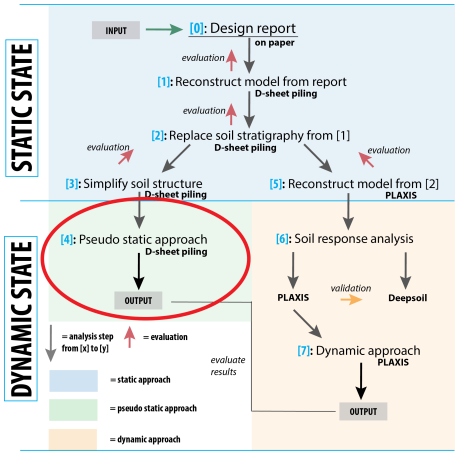

Dynamic approach (Section 3.4)

- The goal is to provide insight of the results of an earthquake regarding the quay structure by applying a more complex finite element model.
- The added dynamic phase with respect to the static model [5] in PLAXIS, contains an implemented seismic signal at the base of the model.
- Due to the dynamic soil behaviour as a result of the implemented signal insight is provided in the corresponding behaviour of the structure. The soil behaviour will be validated with the software Deepsoil.
- From the response of the structure possible failure mechanisms regarding the moments, anchor forces, displacements and overall stability become visible and can be observed in dynamic time.

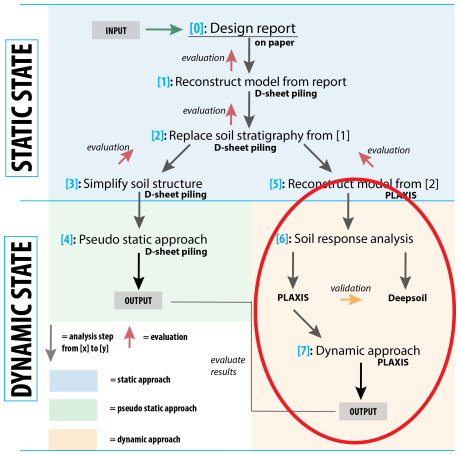

3.1.4. Summary of analysis set-up

This section elaborates the structure of the analysis as visualised in Figure 3.1. The analysis is used for the assessment on the current situation and is presented in the next sections. The static and dynamic state are observed with three approaches. In the static approach the model from the design report has been reconstructed in D-sheet and PLAXIS. The steps required and shown in Figure 3.1 are described briefly in this section and more detailed information is available in Appendix **D**. The pseudo static and dynamic approach are based on the models [3] and [5] from the static state, see Figure 3.1 By comparing the output results from static and dynamic state, the influence of an earthquake on the quay structure can be investigated. Important input parameters and decisions are presented in the summary table at the end of Chapter 2.

3.2. Static approach

As mentioned before it is important to evaluate the static state of a structure before looking to the dynamic state. For this reason, the static approach models have been constructed and evaluated regarding the existing design report of the quay structure (N.Kraaijeveld, 2010). The goal of this section is to create two static models [3] and [5], see Figure 3.1, which form the basis for the pseudo static and dynamic approach. To perform these models, the steps [0], [1] and [2] are required.

To evaluate the change in output from the performed steps, four parameters are observed (Visschendijk et al., 2014a). The parameters applied for this evaluation are:

- Maximum horizontal displacement of the wall
- Maximum acting bending moment in the wall
- Maximum acting anchor force
- Overall stability

These parameters are able to give some important insight in the response of the structure for every taken step. The displayed forces are presented in the serviceability limit state (SLS). In this state no safety factors are applied and the occurring forces are taken into account without any modification. This is done because in a later stage the comparison between D-sheet and PLAXIS is required, which is most reliable in the SLS state. For the input parameters and illustrations of the applied models reference is made to Appendix **D.2**.

3.2.1. Design report

As elaborated in Appendix C stages 5 to 8 form different load scenarios for the design model of the quay wall. To decide in which static load state an earthquake will arise, a brief explanation will be given.

- Stage 5 and 6 present the stage of daily use with and without a moored vessel at the quay. In these two stages the water level is positioned at low low water spring (LLWS), which is NAP -1.82 m. Due to the drainage cover the water level at the inner side of the wall is at NAP -1.50 m. The surface load behind the wall is 60 kN/m^2 which is determined as the maximum load during daily use. In stage 5 a vessels is moored at the quay and therefore a bollard load, presented as a horizontal line load, of 100 kN/m and a moment of 50 kN/m is included. In stage 6 these mooring loads are not taken into account.
- Stage 7 and 8 represent a load situation in which extreme low water has appeared. No frequency value is given in the report, but this situation is appointed as a special load scenario. The water level in front of the quay is at NAP -3.30 m and behind the structure -1.80 meter below NAP, which is extremely low. For this special water level situation a surface load of 20 kN/m^2 is accepted. The mooring loads are equal as stage 5 and 6.

The extreme low water case in combination with the low change occurrence of an earthquake does not seem to be a realistic scenario. Both frequencies of appearance are low and a multiplication of these frequencies is extremely low. For this reason stage 7 or 8 will not be seen as the design stage for an earthquake. The time at which an earthquake appears is not possible to forecast. It is therefore considered realistic that an earthquake occurs at the moment a vessel is moored at the quay, which is quite often the case. As a consequence stage 5 will be the governing static state before the appearance of an earthquake. The values from the design report in stage 5 are given in Table 3.1.

3.2.2. [1] Reconstruct model from report

The model that produces the output from the design report is reconstructed in D-sheet. Although the assumption is made that the design model of the real quay structure is applied correctly, the model layout should be judged accurate.

Evaluation

The output of the constructed model based on the design report is given in Table 3.1. The deviation per parameter regarding the earlier stage is given to get insight in the changed output.

Parameter	Design Report	D-sheet model	Unit	Deviation [%]
Horizontal displacement of wall	114	114	mm	1.7%
Maximum acting bending moment	4109	4111	kNm/m	0%
Maximum acting anchor force	972	975	kN/m	0.3%
Overall stability	1.60	1.60	[-]	0%

Table 3.1: Output from design report and D-sheet model (SLS values)

Remark on deviations:
The values of the deviations concluded that the D-sheet model corresponds correctly to the values from the design report. It seems very likely that the small deviations are caused by the different versions of the applied software from D-sheet.

3.2.3. [2] Replace soil stratigraphy from design report

The parameters from the CPT soil structure are determined in Appendix **B** and presented in Section 2.4. The soil applied in the design report is replaced with the determined soil layers and corresponding characteristics.

Evaluation

The output of the constructed model is given in Table 3.2. The deviation per parameters regarding the earlier stage is given to get insight in the changed output.

Parameter	Value	Unit	Deviation [%]
Horizontal displacement of wall	102	mm	-10%
Maximum acting bending moment	3838	kNm/m	-6.6%
Maximum acting anchor force	939	kN/m	-3.4%
Overall stability	1.66	[-]	3.8%

Table 3.2: Output D-sheet model with replaced soil structure (SLS values)

Remark on deviations:
It becomes clear from the output and the corresponding deviations that the soil structure from the CPT causes smaller load and deformation values. This can be caused by the type of soil in the modelled layers. It has been attempted to find a CPT as close as possible to the original location of the soil from the design report. A second reason for the less conservative values may be caused during the interpretation from the CPT. Although the parameters have been determined with the help of Table 2b from (NEN-EN:1997-1, 2012), the determination of soil parameters is always partly based on engineering judgement.

3.2.4. [3] Simplify soil structure

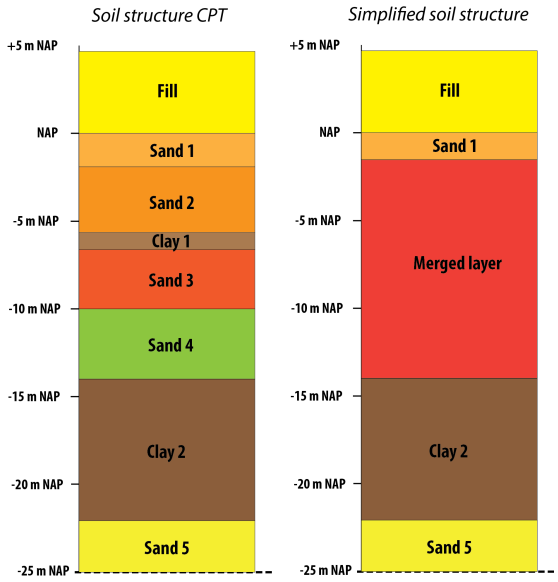

The argumentation behind the simplification of the soil layers is elaborated in Section 3.1.2 point **[3]**. The characteristics of the merged layer are presented in Table 3.3. The parameters are determined by averaging the values of the merged layers. The results from the simplified soil in D-sheet are given in the evaluation below.

Layer	Soil type	γ/γ_{sat}	$q_c[MPa]$	$q_{c,100}[MPa]$	$\phi'[deg]$	$\delta'[deg]$	$c'[kPa]$
Layer 1	Fill	18/20	-	4	32.5	21.7	0
Layer 2	Sand	17/19	2.5	7.9	25	16.7	0
Layer 3	**Merged layer**	**18/20**	**7.0**	**8.8**	**28**	**18.7**	**0**
Layer 7	Clay	20/20	2.5	2.5	27.5	13.75	3
Layer 8	Sand	18/20	13	6.3	32.5	21.67	0

Table 3.3: Soil parameters of simplified soil structure

Evaluation

The output of the constructed model with the simplified soil structure is given in Table 3.4. The deviation per parameters regarding the earlier stage is given to get insight in the changed output.

Parameter	Value	Unit	Deviation [%]
Horizontal displacement of wall	108	mm	6%
Maximum acting bending moment	4047	kNm	5.4%
Maximum acting anchor force	956	kN/m	1.8%
Overall stability	1.65	[-]	-0.6%

Table 3.4: Output D-sheet model with simplified soil structure (SLS values)

Remark on deviations:
Merging a number of soil layers together causes a slight increase, with a maximum of 6%, of the loads and deformations. This is considered acceptable for the pseudo static approach, because the output values are still lower than the values for the original design report.

3.2.5. [5] Reconstruct D-sheet model in PLAXIS

In this step the static state of the quay structure is build with the finite element software PLAXIS. This model will form the basis of the later developed dynamic model.

The applied model will be elaborated in Section 3.4.1 and further reference is made to Appendix **D.2**. The complete soil structure from the CPT, as discussed in step [2] for D-sheet, is applied in the PLAXIS model to ensure the most reliable results. The applied parameters are determined from empirical relations in literature and engineering judgement.

Evaluation

The output of the constructed model from PLAXIS is given in Table 3.5

Parameter	Value	Unit	Deviation regarding step [2]
Horizontal displacement of wall	126	mm	22%
Maximum acting bending moment	3740	kNm/m	-2.5%
Maximum acting anchor force	1175	kN/m	25%
Overall stability	1.73	[-]	4.2%

Table 3.5: Output PLAXIS model (SLS values)

Remark on deviations:
Comparing results between D-sheet and PLAXIS has been done for many times and therefore, also a lot of investigation has been done regarding the fixed output differences between both programs. Besides the different input parameters also the approach of the programs differ. For example, PLAXIS integrates the soil structure interaction in a more advanced manner and takes into account the settlement of the modelled soil while D-sheet does not include this aspects.

The output values from PLAXIS are compared with the values from D-sheet step [2], because the soil structure is equal for both models. Therefore the most optimal evaluation between the SLS values can be done.

The higher horizontal displacement of the quay structure in PLAXIS is explainable for multiple reasons. PLAXIS includes soil displacements of the modelled soil. From the output is observed that the soil behind the quay structure contains a horizontal displacement of several millimetres. A second clarification for the differences is related to the modelled soil stiffness parameters. D-sheet applies spring stiffness parameters, whereas E-moduli values are used in PLAXIS. This clarifies the difference in horizontal displacement of the wall.

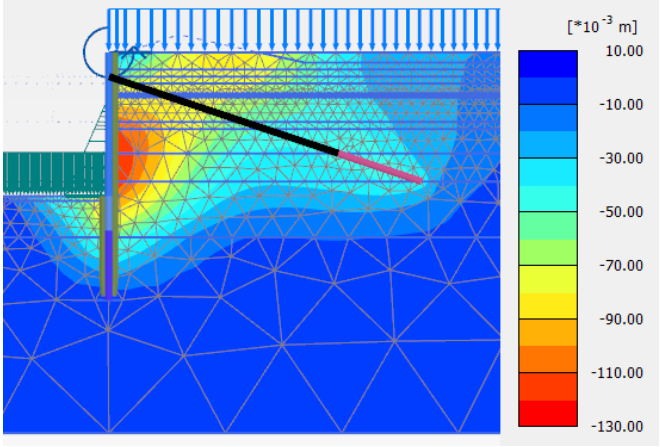

Figure 3.2: Horizontal displacement static state PLAXIS

To compensate the difference in soil movement between PLAXIS and D-sheet, it might be optional to reduce the anchor stiffness in D-sheet. However, PLAXIS includes the effect of arching, which refers to the phenomenon that higher stiffness attracts higher loads relative to materials with lower stiffness. For the retaining wall this effect occurs when the stiffness of structure and soil differ. The combined wall is stiffer than the surrounding soil and the load arches therefore to the structure, resulting in higher anchor forces. D-sheet does not include this effect and provides therefore lower anchor values. For this reason the compensation in anchor stiffness is not applied in the D-sheet model.

The maximum bending moment is presented in every stage by giving the maximum measured value. Plotting the development of the moments over depth for every static stage is a second method for a quick evaluation between the models. This is presented in Figure 3.3.

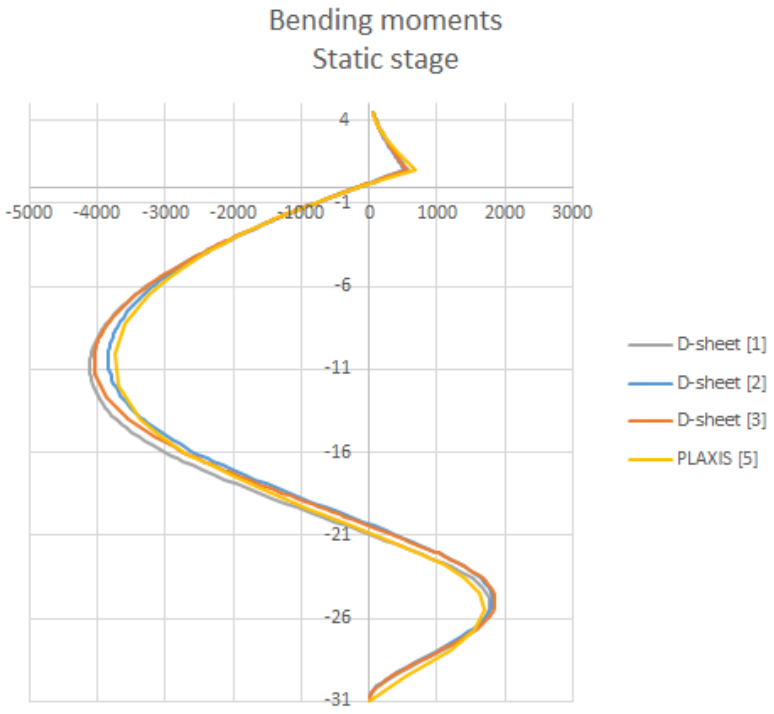

Figure 3.3: Development of bending moments for static state models

The maximum moments differ slightly between the static models, as was concluded above by the presented values. However, the locations of these maxima are corresponding well between the different models.

3.2.6. Conclusions of static approach

In this section attention is paid to the static state of the design models in D-sheet and PLAXIS, as a preparation for the pseudo static and dynamic analysis. Design stage 5 is determined as the reference load case in static state, before an earthquake appears, see Section 3.2.1. In every step done, as explained in Section 3.1, the output values have been evaluated to the previous stage. Some output differences between the steps have been observed, but the deviations are assessed as acceptable and in line with the expectation. Besides the determined maximum values, Figure 3.3 presents the development of the moments over depth. This evaluation step confirms that the static state models are applicable. Step [3] in D-sheet provides the static state for the pseudo static approach. Step [5] in PLAXIS provides the static state for the dynamic approach. Comparing the results after dynamic loading with those stages provides insight in the influence of the earthquake on the structure. For more information about the static state reference is made to Appendix **D.2**.

3.3. Pseudo static approach

In this approach the influence of the dynamic loads from an earthquake will be taken into account by adding additional horizontal loads to the static state model [3], from Section 3.2. The additional forces calculated by hand are based on the PGA value of 2.6 m/s^2. The behaviour of the structure after the implementation of the loads must provide insight regarding the named failure mechanisms. The calculations behind the presented results are elaborated in Appendix **D.3**. Several assumptions for this approach are made and are elaborated below. Before the results of the approach are presented, the required input and different loads aspects are elaborated.

Assumptions for the pseudo static approach

- Difference has been made between unsaturated and saturated soil in the backfill. For saturated soil the assumption is made that the water in the pores cannot dissipate quickly enough during an earthquake. This will result in the build up of excess pore pressures. Only in very open soil material the pore water can flow away freely during an earthquake, which is not likely for the applied soil structure.
- Dynamic water forces from the free standing water bodies will be approached with the Westergaard method, see Appendix **A.3.2.**
- The influence of the dynamic response of an vessel moored at the quay will be neglected.
- Dynamic soil forces will be determined with the M-O method, see Appendix **A.3.2.** for an elaboration of this method.
- The most unfavourable load combination will be applied. This is the case for the additional active and passive dynamic forces acting away from the backfill.
- Additional forces may be neglected in case their magnitude in negligible or if two forces are acting in opposite direction with equal magnitude.
- All soil at the left side of the wall is assumed to behave passive while the soil at the right side of the wall is assumed to behave active.
- The applied M-O method is valid for non-cohesive soil. The single present clay layer in the soil structure contains certain cohesive behaviour. This is neglected during this analysis.

For the determination of the additional loads a subdivision is made for water, dry soil and wet soil, see Figure 3.4. The additional loads due to the free water body in front of the quay will be determined with the Westergaard method. A distinction is made for the soil above and below the ground water level. Both dry and wet soil will be determined by using the M-O method, but an adjustment to the applied formulas is made for wet soil, by including the excess pore pressure rate, r_u (Kramer, 1996).

Dry soil is present at the backfill between the levels NAP +4.45 meter and NAP -1.5 meter. The saturated soil is present below a level of -1.5 regarding NAP, also visualised in Figure 3.4.

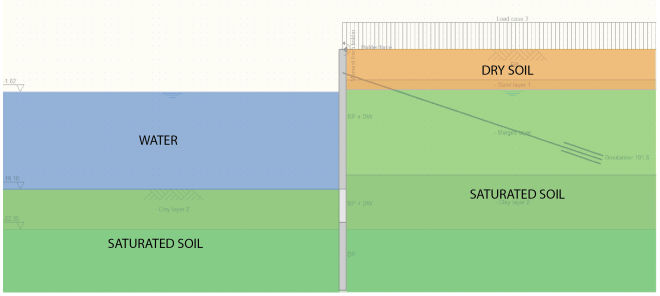

Figure 3.4: Overview of layers

3.3.1. Input

The applied value for the Peak Ground Acceleration is 2.6 m/s^2, determined in Chapter 2. The corresponding seismic coefficients in horizontal direction k_h and in vertical direction k_v are determined with Equation 3.1. These coefficients will be used for the determination of additional seismic loads (NEN-EN:1998-5, 2005):

$$k_v = \frac{PGA}{g} * \frac{s}{r} \tag{3.1}$$

With the input:

- PGA = 2.6 m/s^2
- g = 9.81 m/s^2
- s = 1 (Ontw.NPR9998, 2015) section 3.2.2.1
- r = 1 (NEN-EN:1998-5, 2005) section 7.3.2.2

The relation between the horizontal and vertical PGA is assumed to be: $PGA_v = 1.0 * PGA_h$ (Meijers and Steenbergen, 2015) and therefore (NEN-EN:1998-5, 2005):

$$k_h = +/- 0.5 * k_v \tag{3.2}$$

Resulting in $k_v = 0.265$ and $k_h = 0.133$

3.3.2. Loads from water

The water body in front of the quay and groundwater in the soil cause loads on the structure. A distinction between static and dynamic loads will be made. The dynamic load will only be present during an earthquake. Figure A.9 presents schematically the acting water forces. Forces [1] represent the forces from the static water pressure. The hydrodynamic water force [2] is only present during an earthquake and acts away from the backfill.

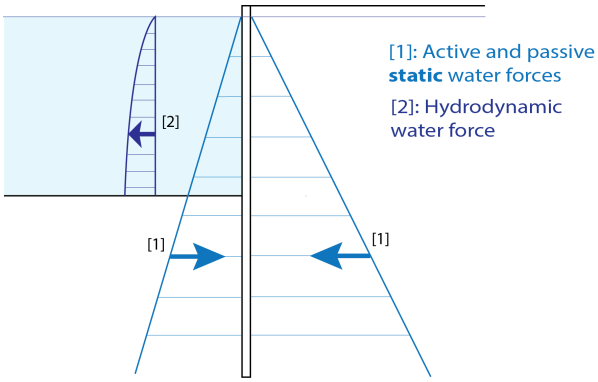

Figure 3.5: Additional hydrodynamic force from free water body

As explained above the ground water is assumed not to flow freely away during an earthquake. Therefore no additional dynamic water forces are taken into account for the ground water (Kramer, 1996). The effects of the present groundwater during an earthquake are taken into account in the additional dynamic soil forces. The additional dynamic load from the free standing water in front of the structure, also called the hydrodynamic force, is determined using the method of Westergaard. This force acts at a level of 0.4 times the water depth, see [2] in Figure A.9.

3.3.3. Loads from soil

The forces are schematically visualised by Figure 3.6 for one soil layer. Dry soil causes an additional dynamic force [4] to the wall. For saturated soil two additional forces are included. Besides the active and passive dynamic soil force [2] also an equivalent hydrostatic thrust [3] due to excess pore pressure must be added, which is done by including r_u. The relative excess pore pressure rate, r_u, is derived from the factor of safety against liquefaction (Meijers and Steenbergen, 2015). The active and passive static soil forces are presented by [1].

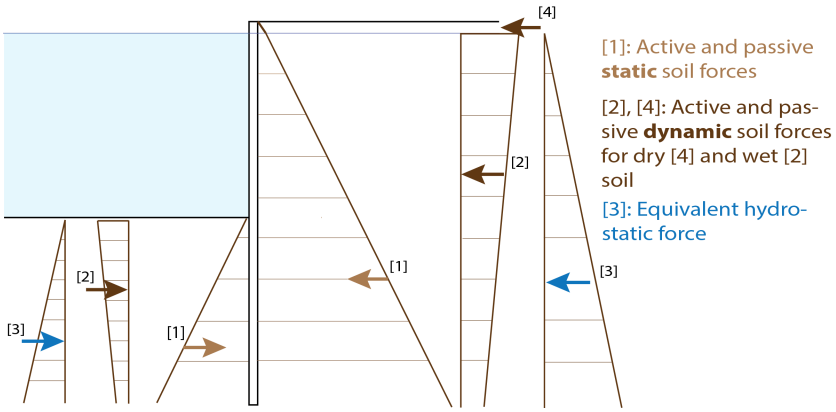

Figure 3.6: Additional forces from dynamic loading

The static model from D-sheet contains already the static forces on the structure, see force (1) in Figure 3.6. Therefore, only the additional dynamic loads (2) should be determined. By using the M-O method, the total active or passive force, meaning (1+2), on the wall is determined. After subtracting the static force (1), determined with the Coulomb theory, the additional dynamic force (2) is found. The direction of the dynamic components is therefore depending on the size of the total force. The equivalent hydrostatic thrust (3) is depending on the excess pore pressure rate. For elaboration of the presented forces in Table 3.6 reference is made to Appendix **D.3**.

All determined additional forces are presented in Table 3.6. These forces are the result of the assumed peak acceleration of 2.6 m/s^2.

Force	Value	Unit
WATER SIDE		
Dyn. free water force	450	kN/m
Dyn. passive force 1	513	kN/m
Eq. hydrost. passive force 1	21	kN/m
Dyn. passive force 2	2512	kN/m
Eq. hydrost. passive force 2	61	kN/m
LAND SIDE		
Dyn. active force 1	15	kN/m
Dyn. active force 2	2	kN/m
Dyn. active force 3	666	kN/m
Eq. hydrost. active force 1	141	kN/m
Dyn. active force 4	260	kN/m
Eq. hydrost. active force 2	38	kN/m
Dyn. active force 5	469	kN/m
Eq. hydrost. active force 3	61	kN/m

Table 3.6: Additional dynamic loads

3.3.4. Results of pseudo static approach

After implementing the additional forces from Table 3.6 in D-sheet, a recalculation can be performed. Including the additional loads, the output of D-sheet is stated as: 'sheetpile becomes unstable', which means that one or more failure mechanisms have occurred with respect to the programmed boundary conditions, elaborated in (D-sheet, 2013). D-sheet presents no output in case a assumed criteria for failure is exceeded within the program. Therefore, no insight in the response of the structure with a PGA value of 2.6 m/s^2 is provided.

For this reason a forecast on the development of the moments, anchor forces, displacements and overall stability related to lower acceleration values is made. The additional loads for lower PGA values than 2.6 m/s^2 are determined. This results in additional output values from D-sheet regarding the bending moments, anchor forces, displacements and overall stability. The changing return period corresponding to the lower PGA values is not taken into account in the extrapolation. The determined additional forces are based on the PGA values presented below.

- 20 % PGA value of 2.6 m/s^2: 0.52 m/s^2
- 30 % PGA value of 2.6 m/s^2: 0.78 m/s^2
- 40 % PGA value of 2.6 m/s^2: 1.04 m/s^2
- 50 % PGA value of 2.6 m/s^2: 1.30 m/s^2

The results from the incremental increase of the PGA value are plotted in different graphs, see Figure 3.7, and are based on the results from Appendix **D.3.5**. The input PGA values are presented on the X-axis and the dependent variable on the Y-axis. Output by D-sheet is given up to 1.3 m/s^2. PGA values exceeding 1.3 m/s^2 result in failure mechanisms and therefore no output is provided. For output values between 1.3 and 2.6 m/s^2 predictions based on extrapolation have to be made. From the gathered data points between 0 and 1.3 m/s^2, presented with the blue dots in Figure 3.7, a line is plotted to forecast the output for the PGA value of 2.6 m/s^2.

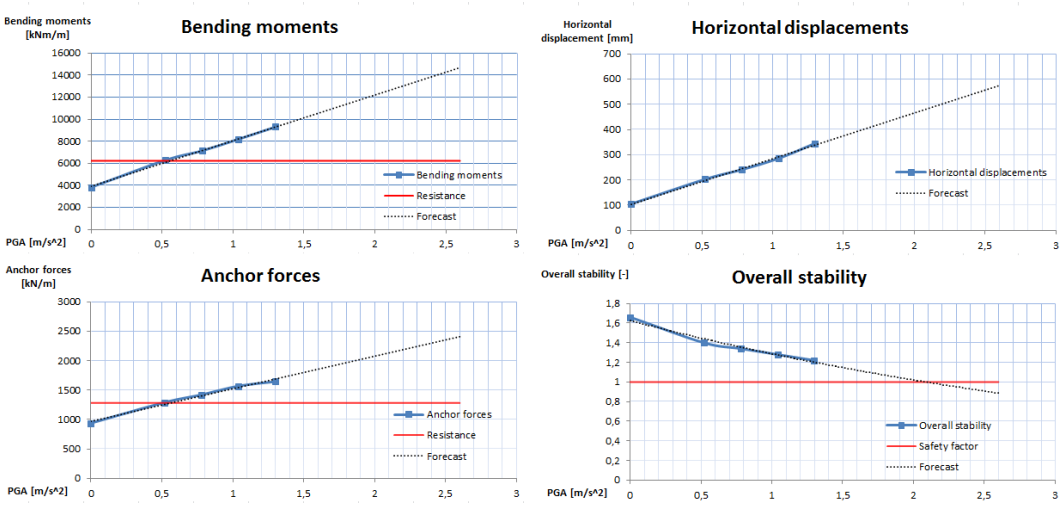

Figure 3.7: Forecast on developed forces and displacements

Based on the development lines it can be predicted at which PGA value a failure mechanism starts to occur. The allowable maximum forces of the structure are visualised with the horizontal red line (the resistance value of the structure). Values of the dependent variable above the red line correspond to a failure. For the bending moments and anchor forces, it becomes clear that the values exceed the resistance values quit fast, i.e. the blue line crosses the red resistance line for low PGA values. The point of crossing the lines for the moments and anchor forces corresponds to a PGA value of 0.5 m/s^2, which is about 20% of the original (2.6 m/s^2) PGA value. This suggest that the applied pseudo static method is conservative, as was in line with the expectation from (Visschendijk et al., 2014b) and will also be confirmed by comparing the results with the output from the dynamic approach.

Occurring failure mechanisms

For an estimation to the first appearing failure mechanism, the output values will be compared with the available resistance, as mentioned in Section 2.4.

- Exceeding bending moment resistance
  The applied design value for the maximum bending moment resistance of the wall without any safety factors is 6230 kNm/m. From the graph if Figure 3.7 becomes clear that this value is exceeded if 20% of the original PGA is applied to the structure.
- Insufficient overall stability
  The overall stability is expressed using a factor of safety and must be larger than 1 for a safe situation. Above 85 % of the original PGA value this is not any more the case , the situation becomes therefore unsafe.
- Displacements higher than 25% of structure length
  D-sheet assumes failure if the displacements are higher than 25 % of the structure length. This is certainly not the case because this would indicate a displacement of almost 9 meters. The allowable displacement value will be determined in a later stage.
- Exceeding anchor resistance
  The allowable grout body resistance is determined as $2356kN$ and corresponds to a maximum pulling force of 1280 kN/m, which is elaborated in the results for the dynamic analysis. This force will be exceeded if about 20% of the complete PGA is applied to the structure.
- Fully mobilised soil at the passive side of the structure.
  From D-sheet, not presented in this report, it becomes clear that the soil mobilisation is below 100% for 50% of the original PGA value.

From this brief and simplified comparison the expectation is that the bending moment resistance or the anchor resistance will be exceeded and therefore are likely to become the first appearing failure mechanisms. This initial presumption should be compared to the results from the dynamic approach.

3.3.5. Conclusions of pseudo static approach

The pseudo static approach is performed to gather initial insights in the consequence of an earthquake appearance. Additional horizontal loads are added in the static D-sheet model with simplified soil structure, as explained in Section 3.2. The additional load determination is elaborated in Appendix **D.3**. Adding the loads corresponding to a PGA of 2.6 m/s^2 to the static model of D-sheet results in multiple failure mechanisms and therefore no output values are given in D-sheet. To obtain insight in the internal forces and displacements, output for lower PGA values has been produced and presented in Figure 3.7. These figures contain trend lines which are extrapolated from lower PGA values to estimate the output for the PGA value of 2.6 m/s^2. High output values appear for the design PGA value of 2.6 m/s^2 which cause multiple failure mechanisms during dynamic loading. To create some insight in the first appearing failure mechanism, a brief comparison for different parameters between strength and force is performed. Exceeding the bending moment resistance of the wall or the allowable anchor force are tend to cause the first problems during an earthquake. Comment should be made on the reliability of the applied method in the following sentence. The conservative approach of simulating an earthquake by adding horizontal loads for a relatively high PGA value of 2.6 m/s^2 contains a large simplification of reality. Additional horizontal loads are added in most negative position to simulate the influence of an earthquake, without including the soil and structural response behaviour. To include possible excess pore pressure, large hydrostatic forces are added which are determined to be conservative. The proposed overall reduction for the pseudo static method from (Habets, 2015) is therefore a recommended possibility to apply if no dynamic calculations will be done. The pseudo static approach is therefore a good method for initial insights, but no decisions can be made based on the provided output. This statement will be substantiated in a later stage of the research.

3.4. Dynamic approach

The goal of this approach is to have insight in the response of the quay structure from seismic loading in a more advantaged manner than the performed pseudo static approach. From this measured response of the structure and soil the possible failure mechanisms can be determined.

The dynamic approach will be performed by making use of the finite element method in PLAXIS. In this way the soil-structure interaction and the soil response as a result of an implemented seismic signal will be taken into account. Both aspects where not included in the pseudo static approach. Therefore no additional horizontal loads based on a PGA value of 2.6 m/s^2 will be implemented. Instead of these loads an implemented seismic signal at the model base of the model will create vibrations for which the response of soil and structure to these accelerations can be simulated.

This dynamic approach is build up by performing the following steps, visualised with Figure 3.8:

1. Add a dynamic phase to the static model [5] from Section 3.2 (**Section 3.4.1**)
2. Modify the measured signal at surface level to a design input signal at the base of the PLAXIS model. This is performed by using Deepsoil. (**Section 3.4.2**)
3. Validate the soil response from PLAXIS with Deepsoil (**Section 3.4.3**)
4. Evaluate and comment on resulting output from PLAXIS model (**Section 3.4.4**)

Appendix **D.4** provides additional information with respect to the elaborated subject in this Section.

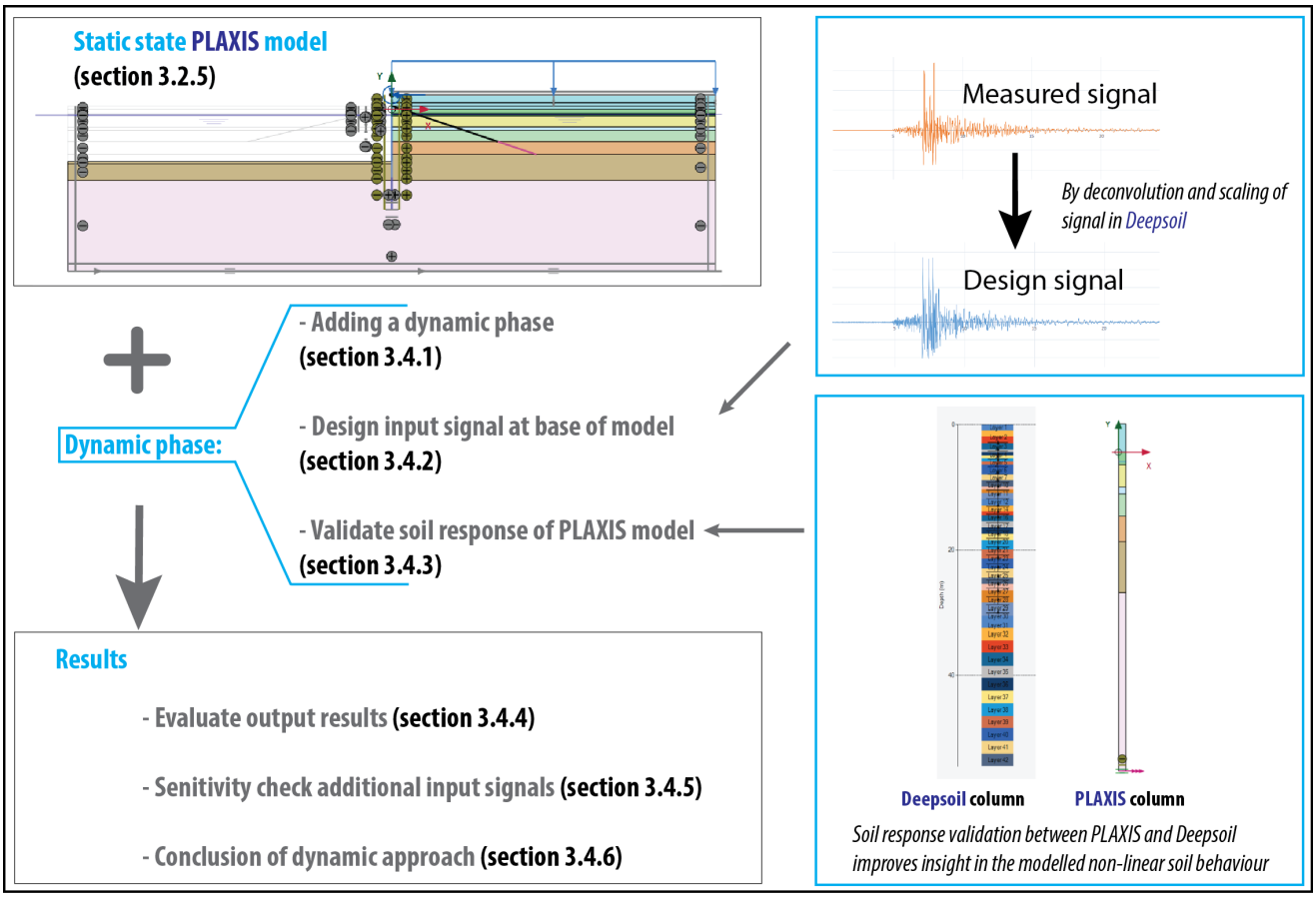

Figure 3.8: Schematic overview of performed dynamic approach

3.4.1. Adding a dynamic phase

The dynamic phase is added to the static PLAXIS model [5]. Deepsoil is applied for the soil response validation. Both software models are briefly introduced below.

Plaxis model

The applied parameters and decisions on the model set-up for the dynamic phase are summed up below. Appendixes **D.2.4** and **D.4** elaborate in more detail this set-up.

PLAXIS 2D (version 2015) applies triangular elements to generate the so called mesh. In this model 6-noded elements are applied (Visschendijk et al., 2014a). The default value for the generated mesh is 'medium'. In this stage of the research this is assumed acceptable from the observed target element mesh size (PLAXIS-2, 2015).

The reaction of the soil regarding stress and strains is determined by applying the correct soil model. For a dynamic analysis the Hardening Soil model with small-strain stiffness, also called HS small, is appropriate to use. This model includes the effect of non-linear stress-deformation behaviour in case of small stains. Hysteresis, which refers to the behaviour of loading and unloading of soil, is included. This is important during seismic activity in the soil (Visschendijk et al., 2014a).

No influence on the results may be noticed from the model boundaries. Therefore a relatively large model is applied, 200 m wide and 60 m high. X_{max} and X_{min} are therefore 100 and -100 meters. Y_{max} and Y_{min} are positioned at 10 and -50 meters.

Normally fixed, fully fixed and free boundary conditions are applied for the X-boundaries, Y-bottom boundary and Y-top boundary respectively. In the dynamic phase the X-boundaries become Free-field, the Y-bottom boundary becomes Compliant base and no Y-top boundary is applied.

Besides the damping already included in the HS small model also Rayleigh damping is applied. This damping is applied with a x% damping on the frequencies f_1 and f_2, corresponding to 1.1 and 12 Hz. The value of f_1 refers to the first natural frequency of the soil, which depends on the shear velocity V_s, and the value of f_2 relates to the seismic signal, see Appendix **D.4.1**. The percentage of damping may differs per soil layer to create the most reliable soil response which will be handled in Section 3.4.3.

Deepsoil

Deepsoil can be applied for non-linear and equivalent linear seismic site response of 1-dimensional soil columns. In this way a 1-dimensional non-linear time domain analysis can be performed. The software from Deepsoil (version 6.0.5.0) is applied for two aspects in this research: the determination of the input signal for the PLAXIS model and the validation of the soil response from PLAXIS. The software Deepsoil is practical to apply for the following reasons:

- A seismic signal can be easily transformed in depth by linear and non-linear soil response.
- The 1-dimensional software is relatively simple and contains a limited number of input variables.
- The software is generally accepted as a validation tool for more complex software programs like PLAXIS.

More detailed information about the applied software and calculations is given in Appendix **D.4**.

3.4.2. Adding an input signal

For the dynamic approach an input signal is required. The taken steps to construct a design signal for the reference case are presented in Figure 3.9 and elaborated below.

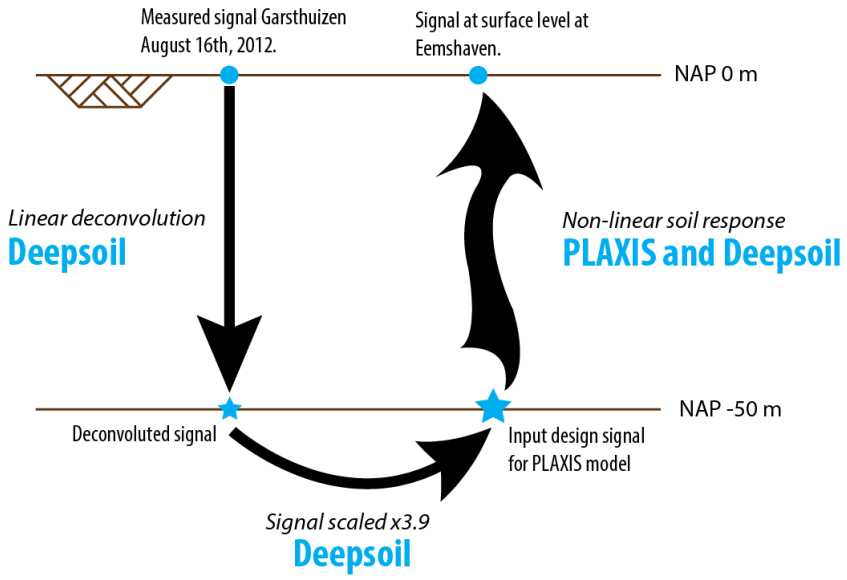

Figure 3.9: Performance regarding seismic signal

The earthquake signal used in the dynamic calculation was measured on 16^{th}, August 2012 in Huizinge, which is up to now the most heavy measured signal from induced activity in Groningen. During this event the KNMI has measured multiple signals at several measurement stations from different location. These signals are measured at surface level.

To simulate the structural response during an earthquake the signal will be implemented at a depth of 50 meters in the model. The measured signal at surface level must therefore be scaled to this depth. This so called deconvolution of the measured signal at surface level to 50 meters depth is done with the help of the software Deepsoil. The signal will be brought down to the required depth by assuming linear soil response, which can be done for relatively small accelerations. In this way it is tried to reproduce the original signal at 50 m depth.

As described in Chapter 2 weak soil layers are able to deform the original signal from the source. To find the most undisturbed signal at 50 meters depth, the deconvolution is done in a sand soil structure. For this research the measured signal from the measurement station in Garsthuizen is used. Gartshuizen contains a soil structure with the least weak soil layer and most sandy layers (Pater and Smeenge, 2015). Therefore, scaling of the signal will be most reliable at this location. The signal from Garsthuizen is presented in Figure 3.10, with the acceleration expressed in g on the y-axis plotted against the time in seconds on the x-axis. Data is measured for every time step of 0.005 seconds.

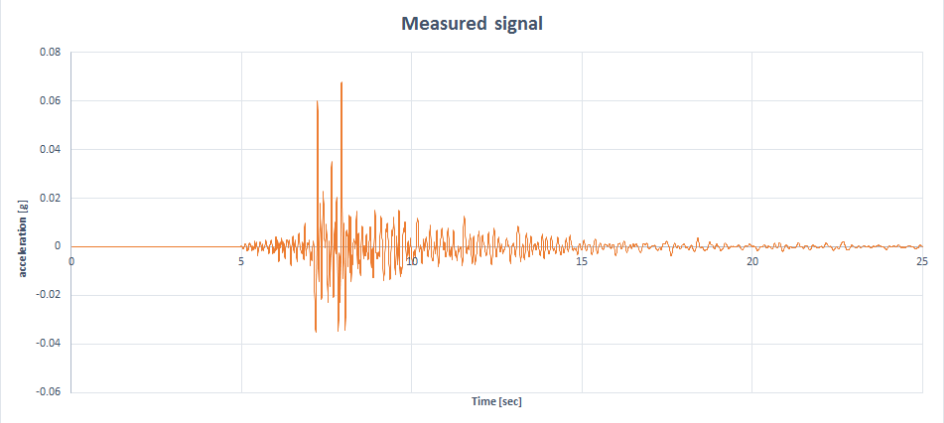

Figure 3.10: Measured signal Garsthuizen, earthquake Huizinge 2012

The maximum peak acceleration in the measured signal is 0.068 g which corresponds to 0.67 m/s^2. The design value for the maximum acceleration in the Eemshaven is assumed at 2.6 m/s^2 (Meijers and Steenbergen, 2015). For this reason a multiplier of $2.6/0.67 = 3.9$ is applied on the signal at 50 meters depth. The scaled input signal is presented in Figure 3.11, again the acceleration is expressed in g. It should be noted that at no time a step reduction is applied during scaling of the signal. For the induced earthquakes in Groningen this is still a point of discussion and should therefore be applied if more reliable information is available.

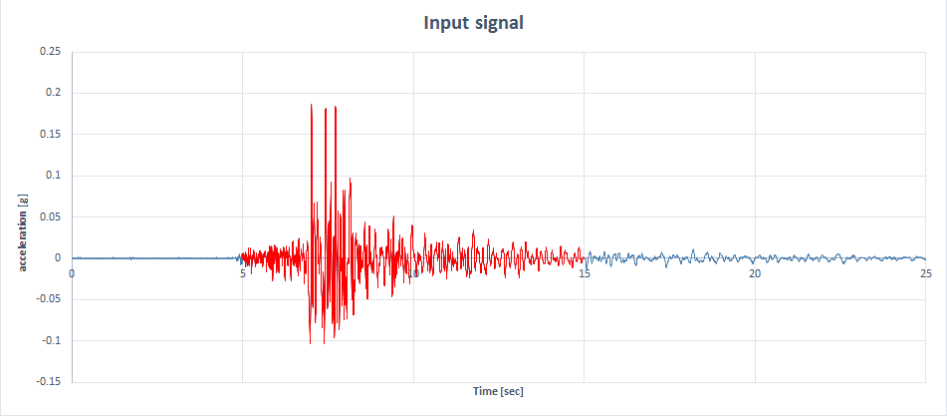

Figure 3.11: Input signal for model after deconvolution and scaling

The signal from Figure 3.11 will be applied as input signal for the dynamic calculation.

Shortening of signal

For practical reasons of saving calculation time the signal has been shortened from a 25 second signal to a 10 second signal. These 10 seconds contain the signal characteristics for the time domain between 5 and 15 seconds from the original signal. From a sensitivity check in PLAXIS, by comparing the response from both signal lengths, can be concluded that the influence of shortening the signal is negligible for a first impression to the response forces. Figure 3.12 presents the selected part for the shortened signal.

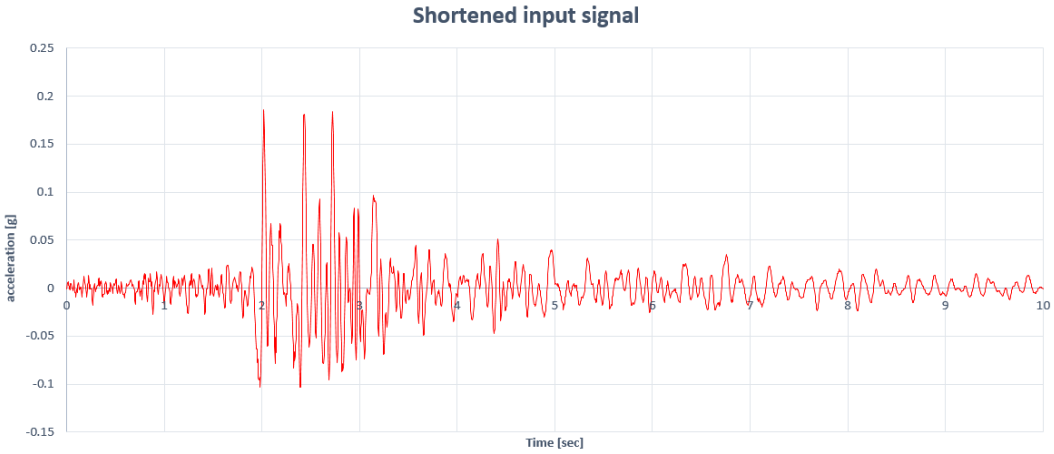

Figure 3.12: Shortened input signal for model after deconvolution and scaling

3.4.3. Required soil response analysis

The response and behaviour of the soil during seismic activity is a complex process (Kramer, 1996). At larger magnitudes the soil response behaviour becomes non-linear. This non-linearity makes it hard and complex to get insight in the correct behaviour of the model during seismic activity. To validate the soil response from the PLAXIS model, Deepsoil will be used to compare. The 1-D software from Deepsoil is relatively simple in comparison to the finite element software from PLAXIS. Therefore is has been tried to globally fit the results from PLAXIS to the response determined by Deepsoil. Due to the complexity of the soil behaviour no exact fit is expected between both models, nevertheless the results have to be in the same order of magnitude. For both PLAXIS and deepsoil the response will be observed with a 1-D soil column, see Figure 3.13. This simplifies the problem and makes the calculation more time efficient.

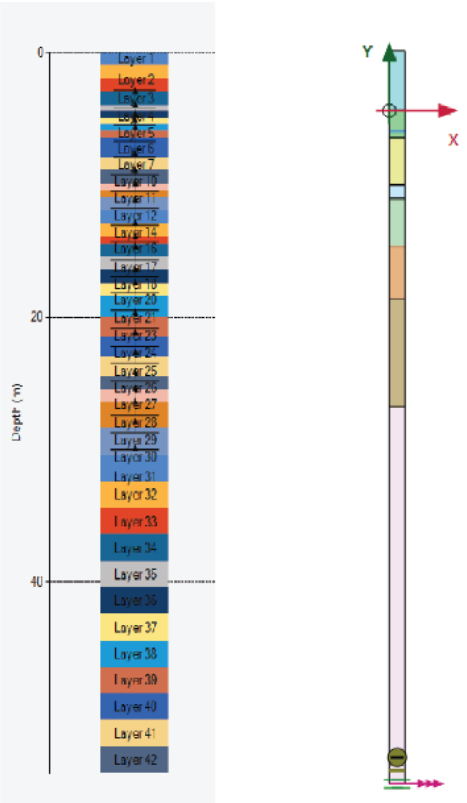

Figure 3.13: 1-D soil columns, Deepsoil at left and PLAXIS at right

The soil layers in Deepsoil are divided into smaller layers to provide a lower limit for the maximum frequency in the soil column in Deepsoil. The seismic signal is implemented at the base of the column for both programs. The boundaries of the PLAXIS soil column have been changed regarding the earlier mentioned boundaries in Section 3.4.1. The width of the PLAXIS column is based on the average element mesh size. For more information on the applied models from Figure 3.13 is referred to Appendix **D.4**.

For the validation between the soil response from PLAXIS with Deepsoil attention is paid regarding two aspects. Besides the development of the peak acceleration also the response spectra is important. Both aspects are briefly elaborated during the validation.

PGA development over depth

The Peak Ground Acceleration (PGA) refers to the maximum acceleration of the soil during an earthquake. Figure 3.14 presents the PGA development over the depth from bottom to surface level from soil columns of both PLAXIS and Deepsoil. It has been tried to reproduce the response from Deepsoil (orange line) with PLAXIS (blue line) by adjusting the Rayleigh damping parameters in PLAXIS.

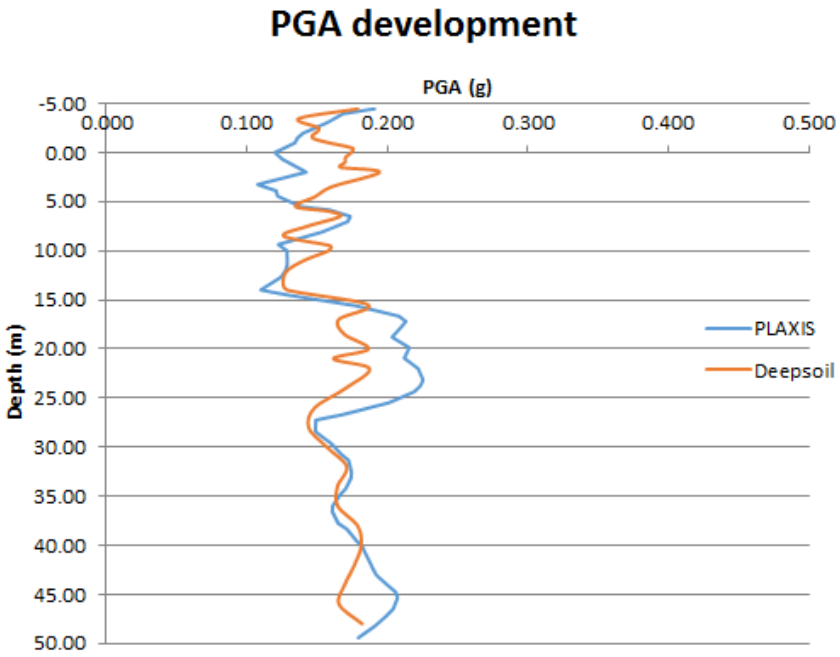

Figure 3.14: PGA development over depth

Remarks on validation
It can be stated that the clay layer, located between 14 and 22 meters, responds slightly different than expected from Deepsoil, which results in higher PGA values at this level. The two sand layers below 0 NAP underestimate the PGA value compared to the response from Deepsoil.

For this sand and clay layers a new model is made including only one of the two named soil materials. This results in a soil column of almost 55 meters containing only one type of clay or sand. In this way the behaviour of the two deviating material is further investigated. From these new models, presented in Appendix **D.4.3**, different PGA developments over depth for different Rayleigh damping values are visualised.

PGA development surface level

Besides the development of the PGA in depth it is also interesting to evaluate the maximum acceleration at surface level, this is presented in Figure 3.15. The global development of the acceleration from PLAXIS is in line with Deepsoil. The deviations between both graphs are assumed acceptable for this level of design.

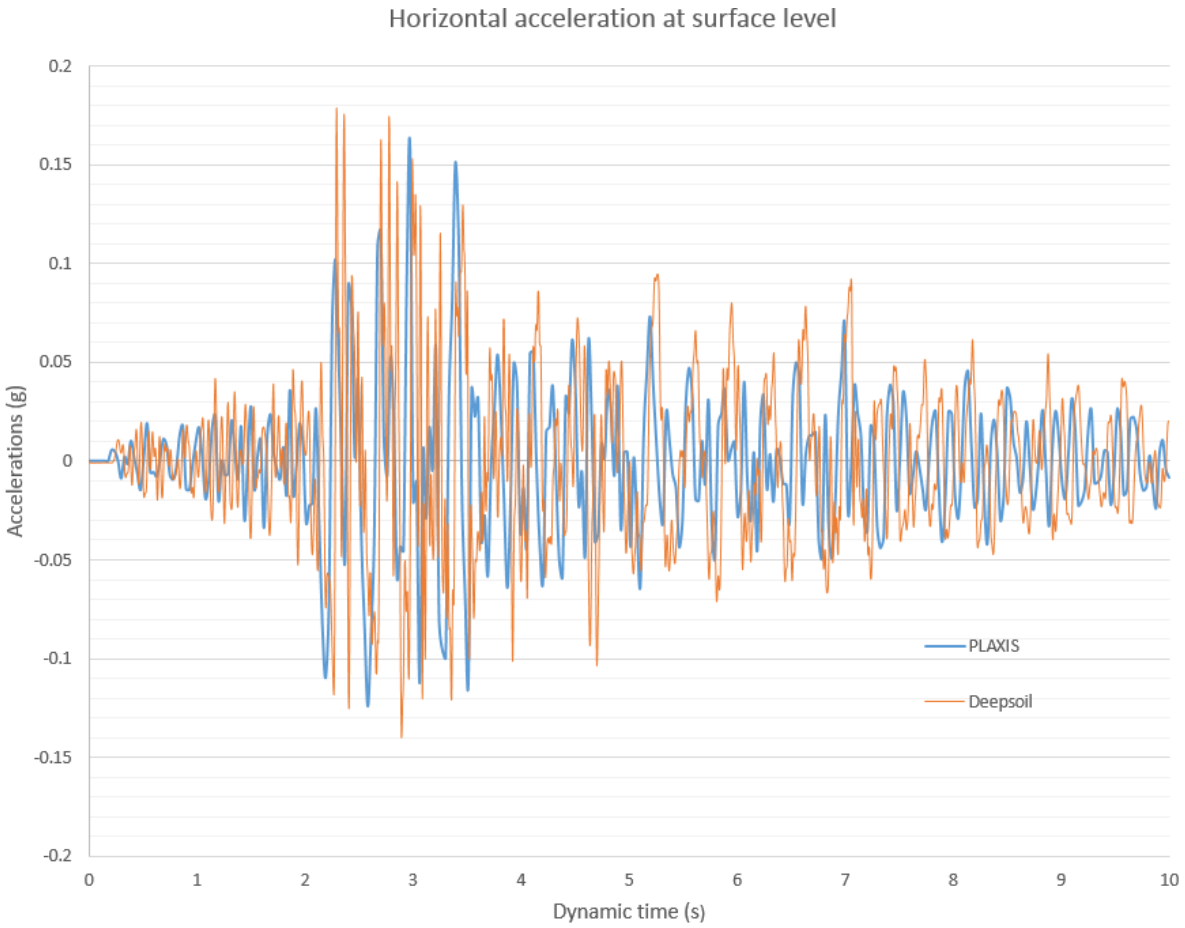

Figure 3.15: Horizontal acceleration at surface level during earthquake

Response spectra

In the response spectra the spectral acceleration versus the period is plotted. The spectral acceleration is described as the acceleration which is experienced by a structure or building, instead of what is experienced by a soil particle in a ground as described with the peak acceleration (USGS, 2014). The response spectra provides insight in which period range the acceleration is peaked. From the knowledge that a small period means a high frequency, a high frequency signal means a high acceleration at low periods. As visible from Figure 3.16 both acceleration peaks are in the period range of 0.10 seconds, which refers to the high frequency signal. A small phase shift of PLAXIS regarding Deepsoil is visible. The differences are assumed acceptable for this initial analysis.

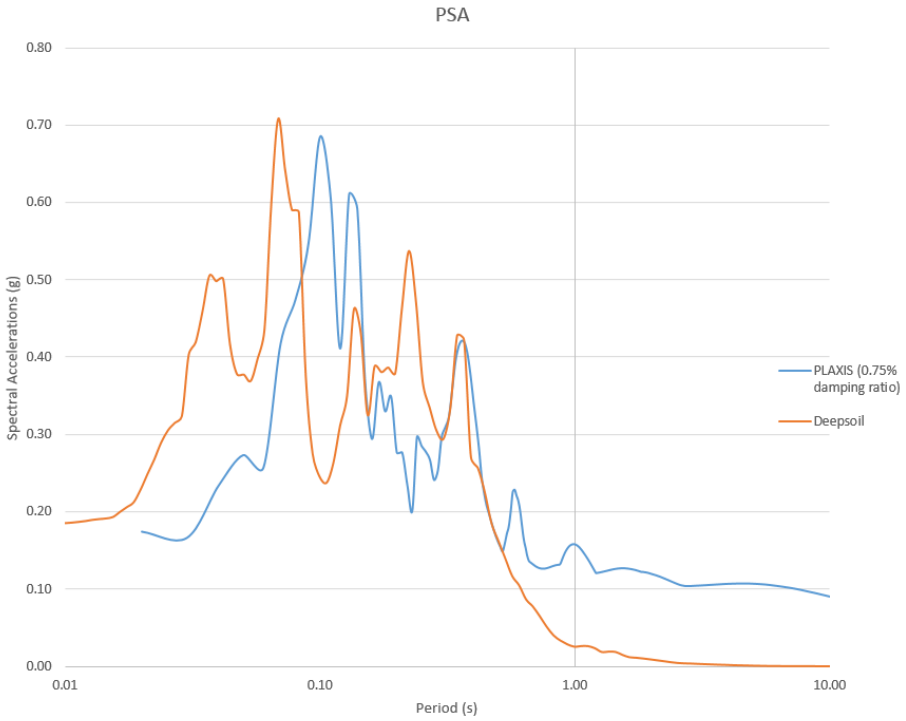

Figure 3.16: Response spectra

From the three figures presented above it can be stated that the soil response between PLAXIS and Deepsoil corresponds in orders of magnitude. A sensitivity check for different soil responses in PLAXIS should provide insight to the effect of the soil response regarding occurring internal forces. A comment regarding the improvement of the soil response is given below.

Soil response improvement

As seen in the figures above, an exact fit between Deepsoil and PLAXIS is not achieved. It has been tried to get more insight in two layers which present the largest deviation, see Figure 3.14. By adjusting the Rayleigh damping in PLAXIS the sensitivity of this parameter has been visualised for the sand and clay layer, presented in Appendix **D.4.4.3**. It becomes clear, as was already mentioned in the PLAXIS manual, that an exact fit by adjusting only the Rayleigh damping will not be reached.

More effective would be to fit the graphs of the shear modulus G/G_{max} and shear strain from PLAXIS to Deepsoil for each soil layer in particular. In this way the damping behaviour of the modelled soil layers is adjusted and a better fit will probably be achieved. Deviations between both responses are expectable due to the differences in soil models. The Hardening soil model with small strain stiffness (HS_{small}) from PLAXIS includes the Hardin-Drenevich relationship while the modelled soil in Deepsoil is mainly based on Seed & Idriss 1991. PLAXIS includes also a cut-off shear strain which bounds the small strain stiffness to a lower limit. This is not included in the shear strain curves from Deepsoil.

Fitting this curve from PLAXIS on Deepsoil is not easy due to the different software approaches between both programs and will not be performed further in this research than elaborated in Appendix **D.4.4.3**.

It should be kept in mind that an exact fit will probably not be reached. Comparing PLAXIS to Deepsoil provides an indication on the correctness of the response, but it should be noted that both programs contain different input parameters and different approaches to determine the soil behaviour. For this reason a certain deviation should be acceptable. For now the response as presented above is used in the model from PLAXIS.

3.4.4. Results from dynamic calculation

After the implementation of the input signal from Section 3.4.2 and the initial validation of the soil response from Section 3.4.3, the static model [5] is extended with a dynamic phase. The results from the dynamic phase are presented in this section. The conclusion regarding the dynamic approach is presented at the end.

Table 3.7 presents an overview of the values in Serviceability Limit State as a result after dynamic loading. From these values initial insights to the response of the structure can be gathered.

Parameter	Value [**static**]	Value [**dynamic**]	Unit	Increase
Horizontal displacement of wall	126	158	mm	26%
Maximum acting bending moment	3740	4120	kNm/m	11%
Maximum acting anchor force	1175	1342	kN/m	15%

Table 3.7: Output dynamic PLAXIS model (SLS values)

From the numerical results the behaviour of the structure regarding all three aspect will be elaborated below.

Horizontal displacement

Figure 3.17 visualises the response of horizontal soil displacement of the model. The largest displacement is located somewhere in the middle of the wall, because the wall performs the largest bending in this area. As a result of the soil displacement at midspan of the wall, the ground at surface level shows also a larger displacement. The figure indicates that the ground body behind the wall (the light blue area) performs a displacement towards the waterside.

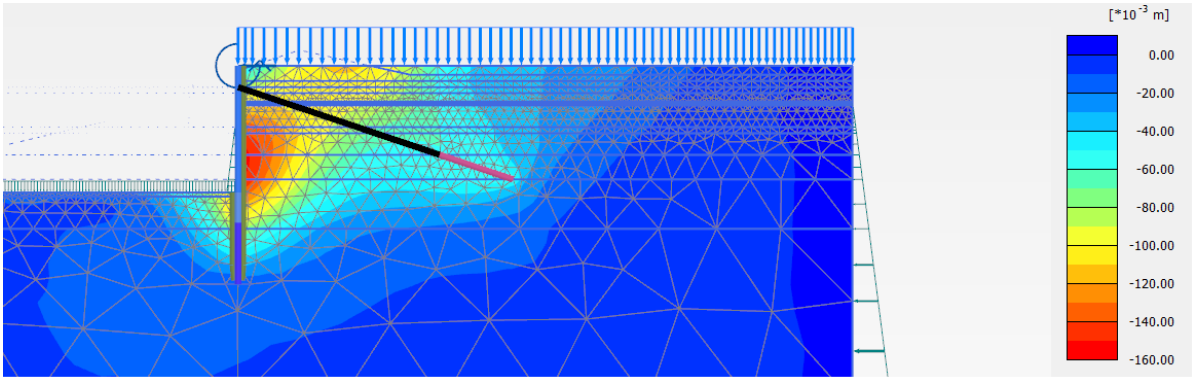

Figure 3.17: Horizontal soil displacement

To provide insight in the horizontal displacements of the wall Figure 3.18 presents the displacement development of the wall at different locations in dynamic time. In this way the development of the horizontal displacements of the wall during an earthquake is visible. The four lines present the displacement at the top and toe of the wall, at the connection point with the anchor and around midspan of the wall.

As visible from Figure 3.18 the horizontal displacement from the static phase is used as starting point. After a small decrease in the lines, which refers to a horizontal displacement towards the backfill, the complete wall starts to move away from the backfill towards the water. The largest increase is shown at midspan of the retaining height, as was already expected from the soil movement in Figure 3.17. A relatively small movement is visible at the toe of the wall compared to the other locations. The relatively higher top than toe displacement indicates tilting of the top towards the waterside. Besides the tilting effect over the full length, the midspan of the wall performs the highest bending deflection. The increase in vertical displacement is small and therefore not presented.

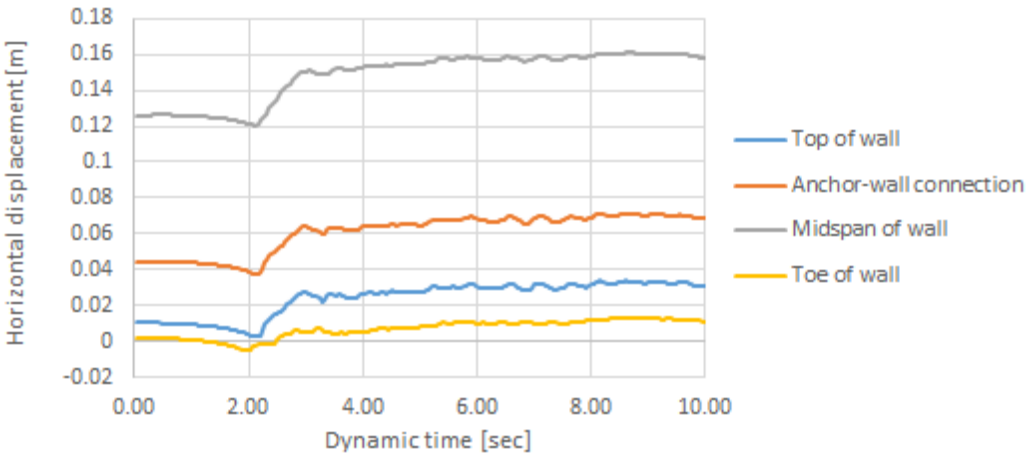

Figure 3.18: Development of horizontal displacement

Conclusion on displacement
The soil behind the wall presents an increase in horizontal displacement. The largest movement is located at midspan, likewise the wall contains the largest bending at this location. The complete wall will perform a small tilting effect with a higher top than toe displacement during the earthquake. For now this tilting effect is assumed acceptable from comments of GSP. A more detailed comment regarding the acceptability of the wall movement will be made in a later stage.

Maximum acting bending moment

During the earthquake the maximum bending moment in the wall will increase, as presented in Table 3.7. Figure 3.19 presents the moment in the wall with respect to the height. The highest moment occurs somewhere around midspan and is acting as a load on the structure, this is from now on called the (bending) field moment. The lower moment, around a height of -25 m is the resisting load for the structure, called the fixed moment. The values of these two moments before and during an earthquake are:

- Static state
  bending field moment: $3740 kNm/m$ and the fixed moment: $1686 kNm/m$
- Dynamic state
  bending field moment: $4120 kNm/m$ and the fixed moment: $1600 kNm/m$

It can be stated that during the earthquake the bending field moment increases and the fixed moment decreases. An explanation for this result is the increase of loading from the active soil body, positioned at the right side of the wall. A second explanation refers to the resistance reduction at the passive side of the soil, positioned at the left of the wall. If the soil resistance becomes less during an earthquake, e.g. due to excess pore pressure or reduced strength from the released energy, the fixed moment reduces and therefore the bending field moment increases. This process is visualised in Figure 3.19 with the line for the static state [5] and dynamic state [7].

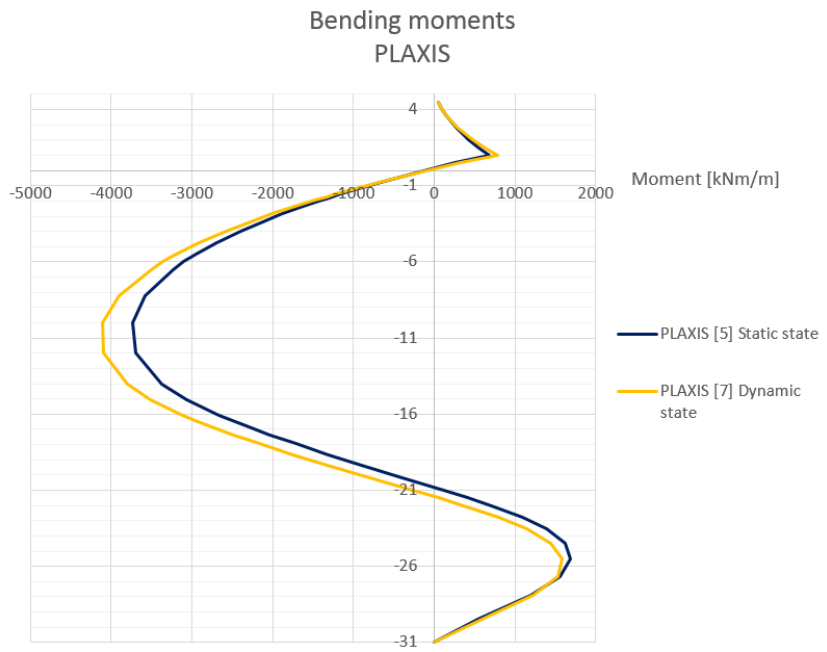

Figure 3.19: Development of bending moments for static [5] and [7] dynamic state

Conclusion on moments
During an earthquake the maximum bending field moment increases and the fixed moment decreases. This results in higher loads on the wall. The maximum resistance value without the use of safety factors for the structure in static state is 6230 kNm/m. The occurring bending field moment of 4120 kNm/m, also in the SLS state without including load factors, is lower than the resistance, which means that the structure contains sufficient resistance against the increased bending moment.

Maximum acting anchor force

The maximum acting anchor force refers to the normal force in the anchor system. The values presented in Table 3.5 are the acting pulling forces per meter. Taking into account the center to center distance and the presence of two anchors per pile, the anchor force without safety factors becomes:

- Static state
  (1175*3.68)/2 = 2162 kN
- Dynamic state
  (1342*3.68)/2 = 2469 kN

Two aspect of interest for the increased anchor forces are the yielding strength of the anchor rod and the sliding resistance of the grout body.

Resistance of anchor rod
The yielding resistance of the anchor rod is dependant on the size and material. For the applied anchor regarding the design report the resistance becomes:

$$F_r = A * f_{y,d}/\gamma = 6467 * 470/1.0 = 3039kN$$

with:

- A = cross section of the anchor
- $f_{y,d}$ = representing yielding stress of steel
- γ = safety factor

Resistance of grout body
The resistance of the grout body can be determined as (CUR166-2, 2012):

$$F_r = 0.015 * O * L * q_{gem} = 0.015 * (0.4 * \pi) * 12.5 * 10,000 = 2356kN$$

.

For:

- O = perimeter of the grout body
- L = length of the grout body
- q_{gem} = average cone resistance

Conclusion on anchor force
The pulling force in the anchor is increased as a result of dynamic loading. The influence of the increased force can be determined in a brief manner by comparing the occurring force from the analysis with the resistance strengths from both the anchor rod and grout body. The resistance against yielding of the anchor rod is not exceeded in both the static and dynamic state. The resistance of the grout body is however exceeded during the dynamic stage. Therefore the anchor with grout body may start slipping from the original position in the direction of the water, following the movement of the wall. The exact behaviour of the anchor rod and grout body relates to the manner of energy absorption and the resistance behaviour between soil and grout body.

A note should be made regarding the modelling of grout bodies in PLAXIS. For the exact movement of the grout body further investigation is required. PLAXIS 2D in not able to forecast the exact movement of grout body during dynamic loading (PLAXIS-1, 2015) and therefore only the occurring loads are observed and not the anchor movement.

3.4.5. Validation of performed analysis

Finding a reference case from case histories or laboratory test to validate the results is difficult. Arguments for this problem are explained in Section 3.1. For now, the best fitting reference case is from the article named: 'Evaluation of the seismic performance of dual anchored sheet pile wall' (Shunichi et al., 2012), as was also applied in Habets (2015). It is questionable if validation of the results regarding failure mechanisms with this laboratory test is possible due to the different conditions of soil, signal and structure. For this reason this validation step is not performed.

Without reliable validation material, a sensitivity check for the model in the dynamic phase might give insight in the sensitivity of the applied input parameters. The effect of changing the input parameters will become visible in the corresponding output. From the output results a conclusion can be drawn regarding the reliability of the model. This liability is checked for the applied input signal below. The input signal determines the magnitude of loading and a relevant influence on the output is therefore expected. For this reason, the impact of different input signals regarding the gathered output is presented below.

Sensitivity check of input signal

The output discussed above is based on one measured signal at the station located in Garsthuizen from the earthquake in 2012. To obtain insight in the influence of different input signal regarding the presented output, the model has been recalculated twice with measured signals from other locations during the earthquake of 2012. Apart from the results from Garsthuizen (GARST) also the bending moments and anchor forces of the other two input signals, measured in Middelstum (mid1) and Kantens (KANT), are presented in Figure 3.20. The red column at the right present in both figures the failure level. The failure level indicates an exceedance of the resisting bending moment or anchor capacity. The difference in output is caused by the different characteristics of the three signals. The magnitude and frequency do differ between the used signals. These differences are visualised in Appendix **D.4.4**.

It can be concluded that for all three signals, the bending moments are not exceeding the failure value, i.e. the orange middle column is lower than the red failure column. Though the failure value for the grout resistance in the anchor system is exceeded for all three signals. This indicates that the applied model behaves consistently for different input signals and the results from both signals are in line with the presented results from the signal of Garsthuizen.

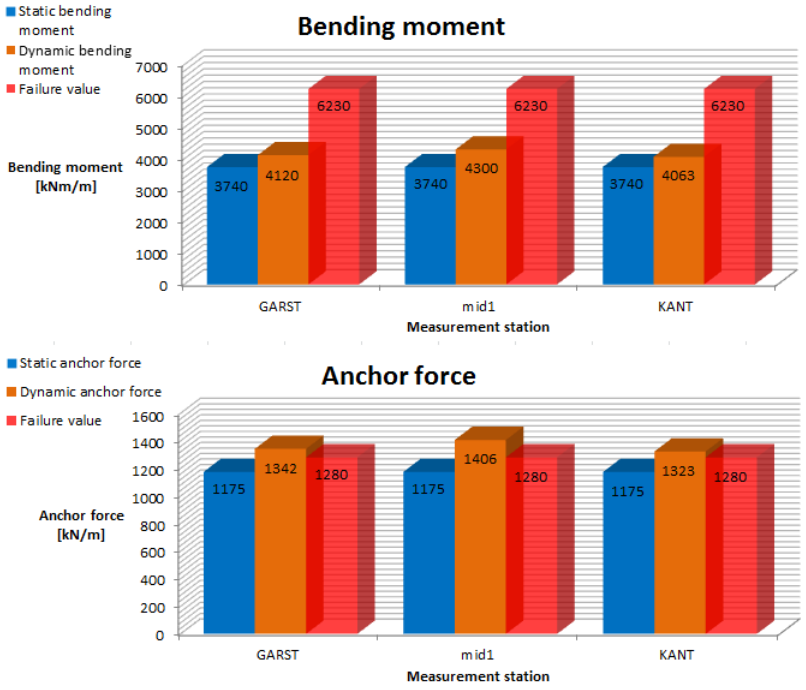

Figure 3.20: Output results for different input signals (SLS values)

3.4.6. Conclusions of dynamic approach

In the dynamic approach the influence of an earthquake on the existing quay structure is investigated by making use of the finite element method in PLAXIS 2D. A dynamic phase is added to the static model [5]. The measured signal from the station in Garsthuizen is modified with the help of Deepsoil and implemented as input signal at NAP -50 m. The soil response of PLAXIS is validated with Deepsoil. The results from both programs fit in order of magnitude, but further optimisation is preferable. In addition to the adjustment of the Rayleigh damping parameters for deviating soil layers, as presented in Appendix **D.4.4.3**, it is advised to fit the shear modules graphs from PLAXIS to the presented figures in Deepsoil. This has not been done in this research. The output values from the dynamic calculation are presented in Section 3.4.4. Increased bending moments, anchor forces and displacements are the result of seismic activity, which is in line with the expectations. The increases anchor forces exceed the grout resistance which may become the first failure mechanism. This result corresponds to the result from two other input signals.

3.5. Conclusion of assessment on current situation

In this chapter the influence of an earthquake on an existing quay structure is assessed. For this assessment an analysis as presented in Figure 3.1 is applied. This analysis is subdivided in a static and dynamic state. The static state includes the current existing state of the quay structure without dynamic loading from an earthquake. The dynamic state is observed using two approaches, a pseudo static and a dynamic approach, to gather insight of the influence of an earthquake to the existing quay structure.

From the pseudo static approach the initial appearing failure mechanisms are related to exceeding anchor resistance and bending moment resistance. The dynamic approach indicates that the anchor resistance will be exceeded, because the grout resistance seems not sufficient. It is concluded that both approaches indicate a critical situation with respect to the increased forces on the existing anchors. It should be noted that the output results from the pseudo static and dynamic approach differ considerably in magnitude. Several remarks for the higher and more conservative pseudo static results compared to the dynamic results are presented below.

Remarks regarding performed dynamic state approaches

To clarify the output differences between the simplified pseudo static and the dynamic approach, remarks regarding both approaches are summed up below.

Regarding the pseudo static approach:

- The pseudo static approach is a simplification of reality. Implementing horizontal loads in every soil layer to model the influence of an earthquake for the most unfavourable position with respect to the stability might is quite conservative.
- The horizontal loads are all based on one design PGA at surface level, or a value including 20% reduction. In this way the structure is loaded with a relatively high acceleration value, between 100% and 80% of the maximum peak acceleration, over the complete depth which is not likely the be the case in reality. For high acceleration values the soil is expected to behave non-linear.
- In the pseudo static approach excess pore pressure is taken into account by an equivalent hydrostatic force related to r_u. This simplification might be conservative, because the magnitude of appearance of excess pore pressure is questionable for induced earthquakes.
- No r_u values for a smaller PGA value than 2.6 m/s^2 are determined in the analysis. A assumed value for all PGA values smaller than 1.3 m/s^2 is applied for the pseudo static approach. This value is assumed conservative.
- By using the Westergaard method, a hydrodynamic water load is included. This additional force is based on the maximum acceleration value and assumed to be quite conservative. This value is not included in the dynamic approach. From the observed seismic magnitudes the negative contribution of the water mass in front of the quay with respect to the retaining wall is assumed to be small. Applying a small percentage, about 10%, of the determined force to the dynamic model is recommended during further research.

Regarding the dynamic approach:

- By taking into account the soil behaviour, the soil-structure interaction and a seismic signal at the base of the model, the dynamic approach is more realistic and has advantages over the pseudo static approach. The dynamic approach is less conservative in this research.
- The implemented signal in the dynamic approach contains smaller PGA values than the prescribes value in the pseudo static approach at surface level. This is the result of including non-linear soil behaviour and results in lower loads on the structure in the dynamic phase.

- For some first insights from the dynamic model, the sand is modelled as drained and the clay as undrained, as was advised by PLAXIS. In this way no excess pore pressure forces from sand are included in the model. From sensitivity checks made in different PLAXIS models, no major differences have been observed regarding the load increase during an earthquake. Due to the relatively short duration of the earthquake, dissipation of pore pressures in the sand layers are questionable. During further research, it is recommended to calculate the material in the static phase as drained and during the dynamic phase as undrained.

It is concluded that the pseudo static approach is conservative and less reliable due to the assumed simplifications in comparison to the dynamic approach. A comparison between results from both approaches confirms this statement. For example for a PGA value of 0.18 g at NAP 1 meter, which presents the connection point of the anchors with the combined wall, different anchor forces are observed from both approaches. From the pseudo static approach, an anchor force of 2000 kN/m is expected during an earthquake. The dynamic approach results however in a force of about 1350 kN/m. From the expected increase of anchor force due to an earthquake, a difference of 55 % between both approaches is observed. A conservative result for relatively high PGA values with the pseudo static approach was already expected from Meijers and Steenbergen (2015), Habets (2015), Kramer (1996) etc. The results from the dynamic approach are therefore assumed governing for further research.

4

Resistance investigation of a grout anchor under dynamic loading

The performed analysis from Chapter 3 points to the fact that the anchor forces increase during an earthquake and might therefore exceed the designed ultimate resistance. The applied resistance value of a grout anchor is based on an empirical determined formula in static state (CUR166-2, 2012). The question arises what happens with the resistance of a grout anchor during dynamic loading from an earthquake. No detailed information regarding the behaviour grout of anchors under dynamic loading has been found. Articles about reduction in pile shaft friction below offshore structures due to cyclic loading (Airey et al., 1992) and shaft friction reduction during installation of piles (Withe and Lehane, 2004) are collected. However, no research regarding the influence of earthquakes towards grout anchors is found. The investigation in this chapter introduces therefore an initial approach regarding this topic.

By determining the change of resistance during an earthquake, e.g. in dynamic state, a comment can be made regarding the capacity of the existing anchor if an earthquake arises. Under 'dynamic loading' two dynamic aspects are involved in this investigation. Due to an earthquake (1) the grout anchor moves dynamically as a result of structural movement. Simultaneously, (2) the soil surrounding this grout body will also move as a result of seismic waves in the subsoil. These dynamic movements are related to each other and determine the resistance behaviour of a grout anchor during an earthquake.

The goal of this chapter is to express first qualitatively what happens with the resistance of a grout body under dynamic loading followed by an initial quantitative estimation of the developed resistance. Based on the collected literature collected in this research, a hypothesis is defined as follows:

"*If a grout anchor is subjected to an earthquake, the resistance of the anchor regarding tensile forces decreases*"

In this investigation an attempt to formulate an initial verification for this hypothesis is put forward for consideration. A new approach is therefore introduced, elaborated in Section 4.3. The influence of an earthquake regarding anchor resistance is not included in present Dutch design guidelines (CUR236, 2011). By performing this investigation a trial to relate the new findings of this chapter with the existing resistance equation for the static state situation from (CUR166-2, 2012) is performed. Further studies into dynamic behaviour of grout anchors are strongly recommended, including scale tests and laboratory experiment, but are beyond the scope of this research.

This chapter is subdivided in three parts. First, information related to the static state of a grout anchor is presented in Section 4.1. After that, relevant geotechnical aspects are introduced combined with applicable reference cases to gather an insight in the possible dynamic behaviour of a grout anchor, which is presented in Section 4.2. From this point of knowledge an approach regarding the actual dynamic behaviour is elaborated in Section 4.3. Reflection and evaluation regarding the defined hypothesis is given in the conclusion of Section 4.4.

4.1. Static behaviour of grout anchors

Before any comments can be made regarding dynamic behaviour of a grout anchor, the static behaviour should be obtained. The general lay-out, force distribution and construction methods are introduced in the following two sections and further elaborated in Appendix E.1.

4.1.1. General description

A grout anchor consists of a cylindrical shaped body of grout at the end of a steel rod, see Figure 4.1 for a schematic illustration. The anchor system transfers the pulling force from the structure to the grout body via the anchor rod. Both the steel rod and the grout body should provide sufficient strength to resist the pulling force. The yielding resistance of the rod depends on the size and quality of the steel material of the anchor. The soil characteristics around the grout body and the quality of the grout itself determine the deliverable resistance of the grout body. The pressure from the soil on the grout body results in (sufficient) shear resistance. This soil pressure is the sum of the soil stress at a certain depth combined with a possible pretension due to the installed grout body under high pressure, elaborated on the next page. Stiff sand layers perform well in delivering resistance for a grout body to adapt the pulling force. In weak and unconsolidated clay layers however grout anchors will not behave well. The anchor should provide sufficient resistance against peak loads and the effect of creep on a longer period of time. One of these two criteria will form the design resistance value.

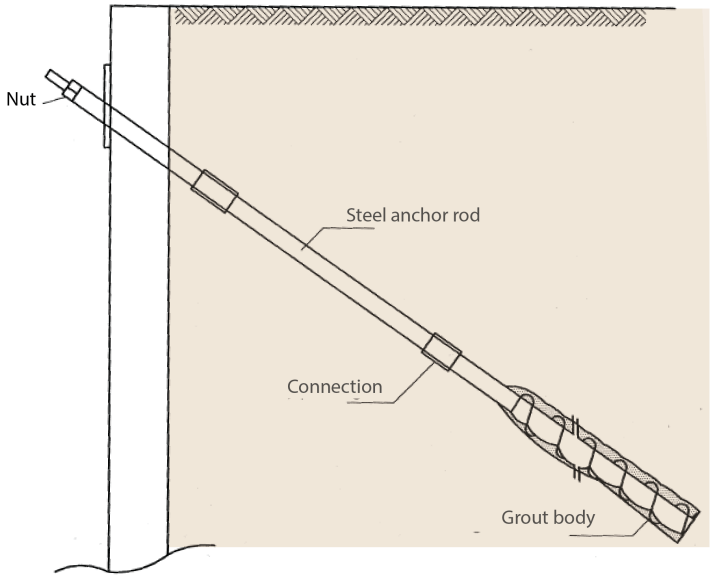

Figure 4.1: Illustration of grout anchor, (CUR166-2, 2012)

In general three main types of grout anchors are available. All three contain the same principle of providing resistance as described above, but the differences are mainly based on construction. The different construction principles result in different soil states after implementation of the anchor. Obtaining these differences might provide new insight in behaviour during loading. Therefore, all three types are briefly introduced below. (Productblad, 2012), (CUR236, 2011) and (CUR2001-4, 2003).

Traditional grout anchor

A pipe sleeve is applied during the construction of a traditional grout anchor. Within this sleeve a drill rod loosens the soil which will be transported to the surface level. This return flow of loose soil and water to surface level is positioned between the sleeve and the drill rod. At the correct anchor depth the drill is removed and the permanent anchor rod is implemented in the sleeve. After that the sleeve will be pulled out in phases while the grout in injected in a controlled manner under pressure to fill the free space. In this way a grout body is created around the anchor rod without disturbing the surrounded soil. A second method of construction is to use an outside return flow of soil and water to surface level instead of an inside flow in the sleeve. Overall this method is applied many times and with a correct execution it creates a grout anchor in a controlled manner.

Self drilling anchor

With a self drilling anchor, the permanent anchor rod which will provide the resisting pulling force after construction is not implemented in a later stage but is also used to reach the desirable depth during construction. Therefore no pipe sleeve and temporary drill is applied. The rod contains a rippled surface area, providing friction between the rod and the soil, and a drill head at the tip. During drilling grout is injected under high pressure which will blend with the surrounding soil. A return flow to the surface level of soil and water is appearing alongside of the rod. The shape of the resulting grout body, made under high pressure, is difficult to forecast. This depends highly on the quality of constructing and the response of the soil at a specific location, which might deviate largely over a certain area.

Screw injection anchor

The principle of a screw injection anchor is comparable with the self drilling anchor. Again the anchor rod is applied during implementation into the soil and no sleeve is applied. The rod of a screw injection anchor is not rippled like the self drilling anchor but has a flat surface and the end of the rod contains a thread. Therefore this type of anchor is screwed into the soil. At the thread a opening is present to inject the grout into the soil. The injection of grout is done during the spiral movement into the soil. The grout will mix with the surrounding soil. During injection no return flow is present, because this process is not executed under large pressures pushing the soil away.

4.1.2. Load resistance of grout anchor

The resistance of a grout anchor depends on several different aspects within the anchor system. The required pulling force is transferred from the connection point of the anchor and structure via the anchor rod toward the grout body. The grout body must transfer this pulling force to the surrounding soil, which contains a certain stress level σ', via friction between the soil and grout. The resistance between grout and soil depends on the way of execution as mentioned above, i.e. if grout is injected under high pressure a certain pretension is created in the soil, expressed with $\Delta\sigma'$. Load resistance of a grout anchor is schematically illustrated in Figure 4.2.

Several parts within the anchor system should therefore provide sufficient strength:

1. The connection point between structure and anchor
2. The yielding resistance of the anchor
3. Connection point between two anchor rod elements
4. The connection between anchor rod and grout body
5. The grout body itself
6. The resistance between soil and grout body

All named aspects are illustrated schematically in Figure 4.3.

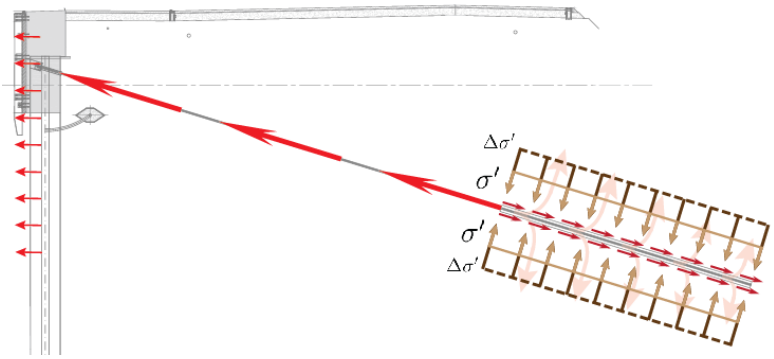

Figure 4.2: Force distribution of grout anchor

The parts [1,2 and 3] can be visually checked or tested before and during installation, therefore a certain safety regarding their deliverable resistance is guaranteed. The connection between the anchor rod and grout body [4] is assumed not to be governing in case a rippled rod or thread rod is applied. For a flat surface rod the connection strength must be proved with a test after installation (CUR236, 2011). The strength of the grout body [5] is depending on the grout quality, which should be applied conform the NEN-EN 14199 and is assumed not to be governing in the resistance aspect (CUR236, 2011).

The most interesting and complex part is the resistance between soil and grout [6]. The constructed grout body cannot be checked visually and the local appearance of soil can be highly variable within a small area. Therefore both aspects, i.e. the grout and soil, contain uncertainties. Although the existing anchor system is able to absorb a single anchor failure, the resistance between grout and soil determines to a large extend if anchor failure might occur. This aspect is therefore important regarding stability of the structure.

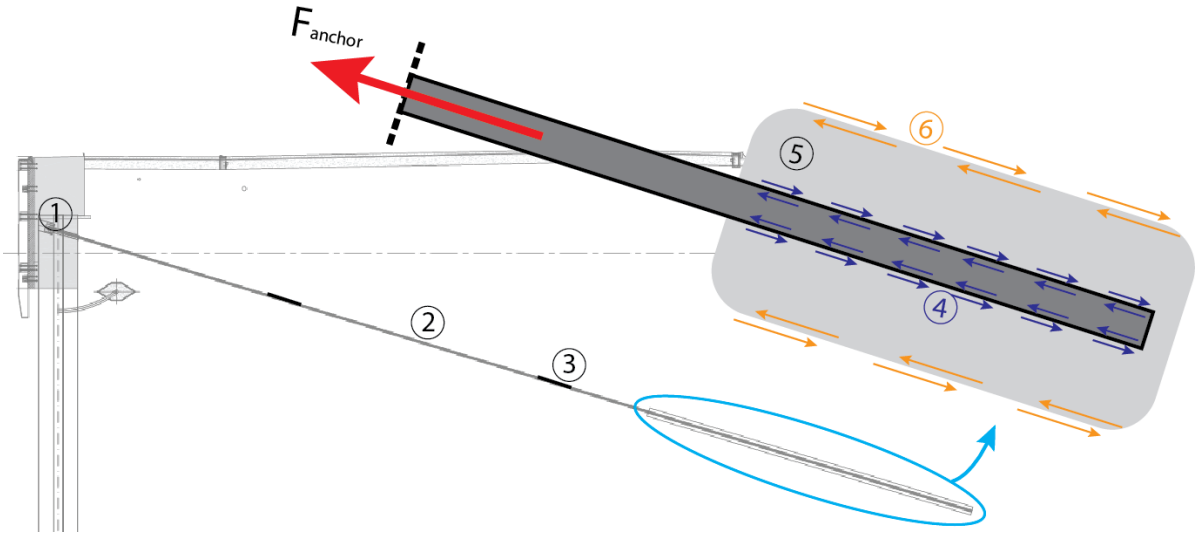

Figure 4.3: Schematic overview of grout body

To guarantee sufficient safety of the anchor resistance [6] after construction, a control test is performed, see Appendix **E.1**. Based on the test results the actual resistance of the anchor is measured and provides insight in the functionality of the anchor. The quality of construction and execution of the grout anchor has a large influence on the resistance capacity, therefore performing quality and structure control tests after construction are evident in many cases.

4.1.3. Theoretical pull-out resistance in static state

The friction between grout and soil is a complex and interesting part regarding the deliverable resistance of a grout anchor, presented with [6] in Figure 4.3. Under the assumption that the other named parts [1] to [5] contain sufficient strength, this section will focus on the theoretical determination of the pull-out resistance of the grout anchor under static conditions. From the knowledge of resistance in static state the focus can be shifted regarding the dynamic loading state in Section 4.2 and 4.3

Applied resistance formula

In general the pulling resistance of a grout body can be estimated with the following equation (CUR166-2, 2012):

$$F_r = \alpha * q_c * O * L \tag{4.1}$$

With:

- α = parameter for friction between soil and grout, assumed value: 0.015
- q_c = average cone resistance
- O = perimeter of the grout body
- L = length of the grout body

From this equation becomes clear that the pulling resistance is mainly depending on three aspects: *The dimensions of the grout body, the soil state and the friction resistance from interaction between soil and grout.* For further elaboration on these three aspects and the named parameter above reference is made to Appendix **E.1.**

Important remarks on resistance formula

The parameter α is completely empirical determined from earlier applied tests, as explained in Appendix **E.1**. Based on engineering judgement the value can be assumed to be higher or lower than the advised 1.5 % for a specific location. No theoretical equations are available for the determination of this value.

The complete formula $F_r = \alpha * q_c * O * L$ can be divided in two parts.

The part of the formula $\boxed{\alpha * q_c}$ describes the resisting force on a particular part of the grout body at a certain depth.
The second part $\boxed{O * L}$ includes the area on which this resisting stress is working. Under the assumption that the second part of the formula, the size of the grout body, does not change during an earthquake, it is interesting to zoom in on the first part.

From a research with tests of *Jelinek et al* (CUR166-2, 2012) the following relations between the static behaviour of a grout body and soil characteristics can be made.

- Higher soil density results in a higher pulling resistance due to the increased friction between soil and grout.
- The pulling resistance increases with an increasing length of the grout body. Though it is observed that the increase of resistance is not proportional with the increase of length. Besides this effect, a certain optimal maximum length of the grout body exists. Extending the anchor further than this length does not increase the resistance further.
- Increasing the diameter of the grout body results in a limited increasing effect regarding the pulling resistance.

These relationships are important to keep in mind during further research.

4.2. Involve dynamic aspects

To understand the development of the resistance between soil and grout during an earthquake two geotechnical aspects should be introduced, described as contraction and dilatation. Furthermore, reference subjects containing comparable behaviour as grout anchors are elaborated. From these reference subjects, e.g. cyclic loaded tension piles and traffic loaded piles, a general expectation can be formulated regarding the behaviour of dynamic loaded grout anchors.

4.2.1. Contraction and Dilatation

Under the assumption that the grout quality and body dimensions remains unchanged during an earthquake, the surrounding soil will influence pull-out resistance the most. Therefore, a brief introduction on two geotechnical processes is made.

The phenomena contraction and dilatation refer to the resettlement of the grains particles. In this case reference is made to a sand soil layer positioned below ground water level and the pore volumes are therefore filled with water.

- Contraction
  If loosely packed sand is (cyclic) loaded, resettlement of the grain particles may appear, which result in a more packed grain structure. The grain particles will move to a more dense position with less pore volumes. As a result the water originally positioned in the pore volumes will be forced to move. In case of low frequency cyclic loading the water has time to flow away from the pores and the stresses between the grain particles is constant. During high frequency loading the water can not flow away fast enough and will position around the grain particles for a short moment of time. In this way the interaction between the grains decreases. The overpressure of pore water is called excess pore pressure and causes a decrease of effective soil stresses (de Groot et al., 2007).

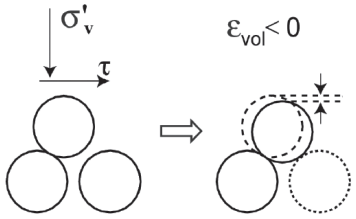

- Dilatation
  The opposite of contraction is named dilatation. A well packed set of sand grains moves due to loading to a more open structure. Larger pore volumes become available and the water will be attracted to these pores. The free space created between the soil particles become filled with the ground water. Therefore the effective grains stress between the grain particles increases. From several tests and numerical analysis it is concluded that the radial stress σ_{rad} on the pile, which is perpendicular directed, increases in case of dilatation (CUR2001-4, 2003).

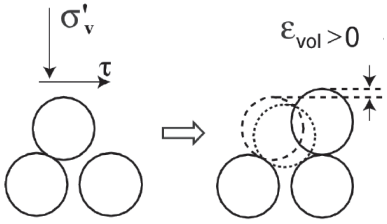

It can be concluded that the phenomena of contraction and dilatation are largely influenced by the packing density of the sand layer. Other influences are the frequency of cyclic loading, the sand structure and shape of the grains and the level of water pressure available in the soil.

4.2.2. Reference cases for dynamic grout anchor behaviour

In Section 4.3 the dynamic behaviour of a grout anchors will be investigated in addition to the know static resistance presented in Section 4.1.3. Less research has been performed regarding the behaviour of grout anchors under seismic loading. Therefore the process and development of the soil - grout interaction is still relatively unknown. Insight in this resistance development should therefore be gathered from other, related subjects which have been investigated in the past. A subdivision for a moving anchor in stationary subsoil and the soil loaded by seismic waves itself is made.

Reference material for moving anchor in stationary soil

- **Cyclic loading of tension piles in sand soil**
  Tension piles can be cyclic loaded by nature or during construction. This behaviour is comparable to the behaviour of a grout anchors under seismic loading. Both objects are dynamically loaded under static tension force which they resist from friction between pile and surrounded soil.

  The general conclusion from research towards the resistance behaviour of cyclic loaded tension piles is a reduction of the friction between pile shaft and surrounded soil (Withe and Lehane, 2004), (Airey et al., 1992) and (CUR236, 2011). This reduced shaft friction results in a decreased pulling resistance, which might result in partial or complete pull-out of the tension pile. The decrease in skin friction is associated with the decrease in normal stress. This is a result of the compressive strains in the soil around the pile. It is assumed that most soil deformation occurs in a narrow band close to the pile. Within this band the shear stress will probably mobilise and reduce (Airey et al., 1992).

  Conclusion: Due to cyclic loading of tension piles the shaft friction and therefore the shear stress between pile and soil reduces.

- **Cyclic load changes on piles by traffic**
  Tunnel structures may be cyclic loaded if heavy traffic is passing with high frequencies. These mobile loads cause both tension and compression loads in the foundation piles, which is called a load change. The changing load direction is partly comparable to the seismic loading of an anchor which is attached to a retaining structure. The response movement of the structure and anchor is in multiple directions.

  The reduction in bearing capacity of the surrounding soil is related to the number of load changes (CUR236, 2011). If the number of load changes exceeds a certain level, a reduction percentage of soil capacity should be used for the design. In this way the reduced soil resistance due to cyclic traffic loading is taken into account.

  Conclusion: Due to high frequency load changes between tension and compression the bearing capacity of the soil around the piles reduces.

Reference material for subsoil under seismic loading

- **Earthquake damage from the past**
  From observation of several earthquakes occurred in the past, it can be stated that in general the strength of the soil during an earthquake reduces, due to temporary excess pore pressures or even complete liquefaction of the soil. This temporary reduction of effective soil stress might reduce the resistance between soil and anchor.

  Two optional reference subject are named below. These subject are briefly investigated but are not further elaborated in detail.

  - *Cyclic DSS-tests*, cyclic direct simple shear tests, provide insight in the stress, strain and strength relationships of cyclic loaded soil.

  - *Cyclic triaxial tests* assess soil behaviour in the laboratory under both static and dynamic loadings.

4.3. Dynamic behaviour of grout anchors

As mentioned before, the behaviour of a grout anchor under dynamic loading is hard to forecast and has never been researched in depth. With the information regarding the existing static state behaviour from Section E.1 and the involved dynamic aspects from Section 4.2, it is tried in this section to forecast what might happen with the tensile resistance of a grout anchor during and after dynamic loading. This has been done by introducing an approach which relates the effective soil stress with the resistance force.

4.3.1. New alternative non-empirical approach

With this approach it has been tried to express first qualitatively the development of the resistance force during and after an earthquake. Therefore, the focus is on the first part of the resistance formula $\boxed{\alpha * q_c}$ from Equation E.1. As explained before the value α is empirical determined and q_c can be measured from a CPT (cone penetration test). Using this approach, the empirical parameter is replaced and determined in an alternative manner.

The force resistance part of a grout body expressed with $\alpha * q_c$ can be approached as the developed shear stress between soil and grout integrated over the grout body area, see Figure 4.4. In this way a relation between the soil stress state around a grout body and the resistance of the anchor has been made. The advantage of this relation is that the development of the soil stresses during an earthquake are predictable with a suitable PLAXIS model.

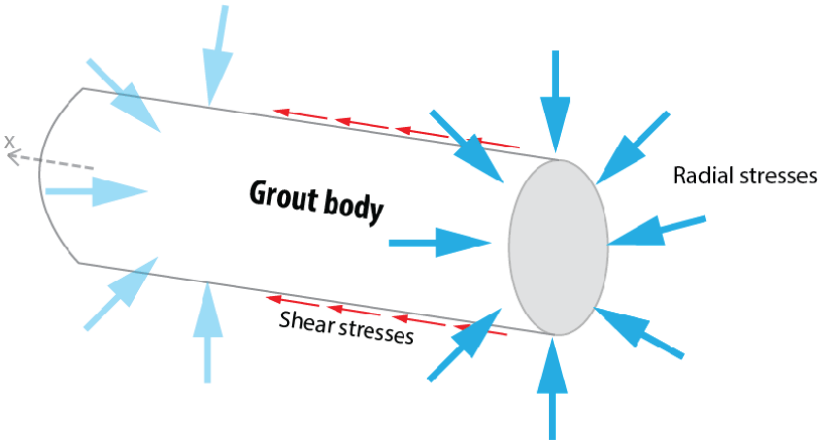

Figure 4.4: Stress distribution on grout body

The radial effective soil stress σ'_{rad} is the stress directed perpendicular on the grout body. The relation between the radial stress and the shear stress on a grout body can be approached with the wall friction angle parameter, determined as $tan(\delta)$. For the grout-soil interface it can be assumed that $\delta \approx \phi$ and therefore the wall friction angle can be approached as $tan(\phi)$, with ϕ expressing the internal friction angle of the soil. With this knowledge the resistance formula based on empirical values can be rewritten.

The original resistance formula:

$$F_r = \alpha * q_c * O * L \tag{4.2}$$

Can also be approached with an alternative new formula:

$$F_r = \int_0^L [(\sigma'_{rad} * tan(\phi)) * O] \, \mathrm{d}x \tag{4.3}$$

In this equation the integral over the length in x-direction times the perimeter of the grout body represents the part $\boxed{O * L}$. The resistance part $\boxed{\alpha * q_c}$ is now replaced and approached as the effective

radial stress σ'_{rad} times the wall friction angle ϕ. A deviation of about 30 % between the output values from both equations for the static state is observed. This is assumed acceptable and further elaborated in Appendix **E.1**. A lower and therefore a more conservative resistance value is observed from the new alternative Equation E.6. Reference to Appendix **E.1.** is made for additional information regarding the difference in output between both equations.

If from literature a prediction can be made for the development of both these variables, i.e. σ'_{rad} and ϕ, a comment can also be made regarding the development of the shear resistance during dynamic loading.

- **Friction angle ϕ**
  A decreasing internal friction angle ϕ results in lower shear resistance, given equation 4.3. The value of ϕ and therefore also the parameter δ is depending on the performed deformations. Increased deformations, e.g. from an earthquake or other dynamic loads, result often in decreasing magnitudes of these values (CUR2001-4, 2003). For this reason it is probable that an assumption of a reduction of the value ϕ during and after an earthquake is used.

  From research including traffic vibrations influencing the internal friction angle ϕ, the following relation to determine the reduction for ϕ, which should be subtracted from the static value value, is advised(Rotterdam, 2012).

$$\phi_{reduction} = arctan(\frac{a_{hor}}{a_{vert}}) \tag{4.4}$$

  Although the cause for the vibration is different, i.e. traffic or seismic activity, the qualitative effect is assumed to be equal in this research. A possible reduction for the internal friction angle is therefore assumed during an earthquake.

- **Radial effective stress σ'_{rad}**
  From literature and reference subjects, given in Section 4.2, the expectation is that the earthquake will cause a reduction of radial effective stress of the soil surrounding the grout body. A trial to confirm the expectation is carried out with the PLAXIS model introduced below and further elaborated in Appendix **E.2.1.**

4.3.2. Confirmation of literature with finite element model

A new 2D finite element model is used to investigate the named expectation regarding σ'_{rad} from literature. The goal of applying this model is to indicate first qualitatively what mechanisms occur around a grout body under seismic loading. From these results an initial quantitative estimation can be determined. The model zooms in on the grout anchor positioned in the sand layer as was earlier modelled in the analysis of Chapter 3, visualised in the Figure at the right. In this way, the resistance development corresponds to the reference case quay structure as determined in the literature study. After a brief explanation of the model set-up, the results will be presented including additional comments.

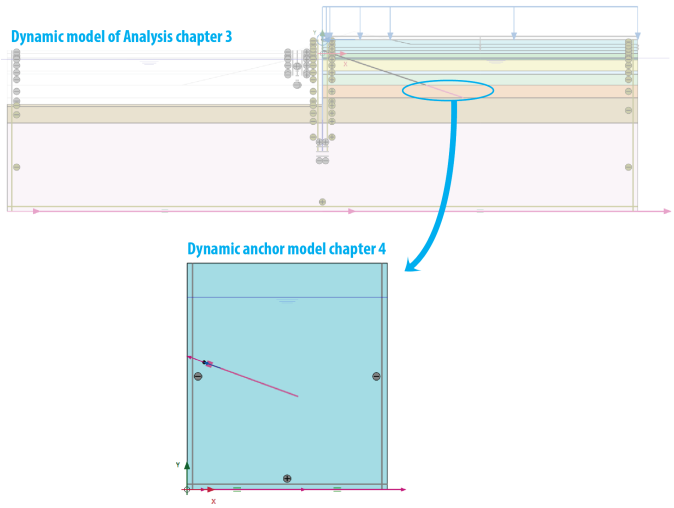

Set-up of PLAXIS model

The grout body is visualised as a straight line in a soil column as presented in Figure 4.5. The line is modelled as an embedded beam in an undrained sand column, to include excess pore pressures. The sand soil characteristics are equal to the earlier applied model in the analysis from chapter 3. For the most realistic simulation of the soil behaviour around a grout body under dynamic loading several load steps have been applied in the model. The depth of the embedded beam row is chosen in such way that the static soil and water stresses are equal to the stresses at anchor level from the PLAXIS model from Chapter 3. The simultaneously applied loading steps are presented below and visualised in Figure 4.5.

1. A static axial pulling force of 1175 kN/m is applied to the embedded beam. This static pulling force is equal to the normal force present in the anchors of the original model. In this way it is tried to create an equal soil stress state around the grout body as is present in the original model.
2. During an earthquake the anchor start to move, because the retaining wall which is attached to the anchor, responds dynamically towards to obtained seismic signal. This anchor movement can be measured in time from the analysis model from Chapter 3 and is plotted in a graph with dynamic time versus velocity, presented in Appendix **E.2.1**. This movement of the grout anchor is added to the embedded beam in axial direction. In this way the anchor performs equal movement in this new model as it did in the model from Chapter 3.
3. To simulate the soil response during an earthquake, an acceleration input signal is implemented at the base of the model simultaneously with the velocity movement of the grout anchor as described in step [2]. In this way the model includes the response behaviour of the grout body and simultaneously the soil movement around the grout body due to the earthquake signal at the base. The applied signal is presented in Appendix **E.2.1**.

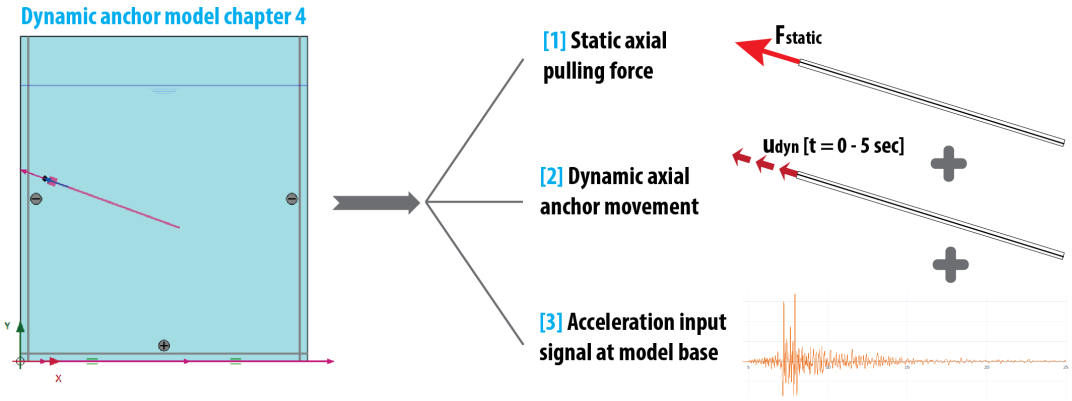

Figure 4.5: Applied loading stages in PLAXIS model

The dynamic X-boundaries are modelled as free-field and the Y-bottom boundary as compliant base. Besides the applied medium mesh grid size, a refined size of the mesh grid is applied around the embedded beam row. For further elaboration on the model set up and dynamic multipliers reference is made to Appendix **E.2.1.**

The goal of the applied model is to provide insight in the development of the effective radial soil stress σ'_{rad} along the grout body during dynamic loading. To provide this insight different aspect related to σ'_{rad} have been observed. After presenting the σ'_{rad} related results, a general conclusion can be formed regarding the development of the radial soil stress.

The presented graphs of the model results are measured at a stress point close to the grout body. A figure of the location of this measure point is presented in Appendix **E.2.2.**

Model results during dynamic loading

With the information from Section 4.2 the development of the following aspect will be elaborated: *volumetric strains, pore pressures, principal effective stresses and Cartesian effective stresses.* The development of the radial effective stress is qualitatively comparable to the Cartesian and principal effective stresses. The volumetric strains influence the development of excess pore pressures which determines the stress development in the soil. Observing these four aspects provide substantiated development of the radial stress.

- Volumetric strain development [ε_v]
  The volumetric strain represent the magnitude of pore volumes in the soil. An increase of ε_v, and therefore a positive value, relates to the process of *dilatation*. On the other hand a decrease of the volumetric strain, development with negative values, expresses *contraction* of the soil. Both phenomena are elaborated in Section 4.2.

  The development of the volumetric stain ε_v in dynamic time is presented in Figure 4.6.

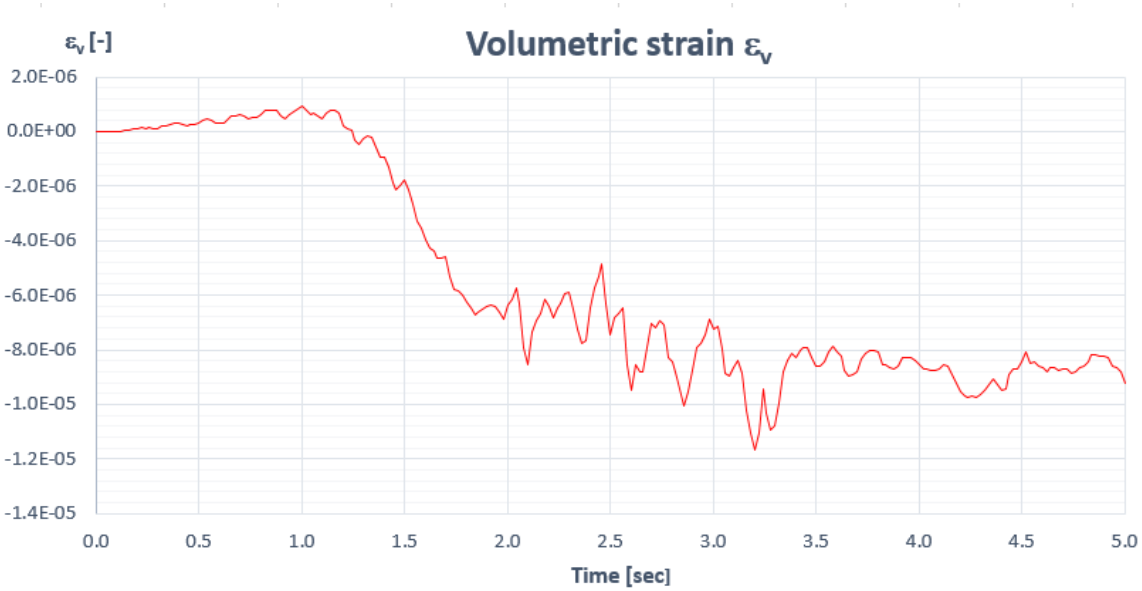

Figure 4.6: Volumetric strain development

Conclusion regarding ε_v
The volumetric strain ε_v increases negatively in dynamic time. This refers to a decrease of pore volumes which indicates contraction of the soil, as described in Section 4.2. The effect of contraction might be related to method of installation, i.e. grouting under high or low pressure. The existing anchors are installed without large grout pressures. The presented additional pretension $\Delta\sigma'$ from Figure 4.2 is therefore not expected after installation. Contraction of the soil during additional loading is therefore likely to appear for the existing anchors. The behaviour of soil around a grout body which is installed under high pressure is not investigated in this research. Whether contraction or dilatation in pretensioned soil will occur during an earthquakeis is therefore not known.

A note should be made regarding the PLAXIS calculation of the volumetric strain. The applied Hardening Soil model with small-strain stiffness is not intended to model the development of volumetric strains in soil. Though, better soil models are only available as User Defined Soil Model for PLAXIS, which have not been applied in this research. Further research regarding the exact development should therefore be done using more suitable software models for cyclic loaded soil.

- Excess pore pressure development [P_{excess}]
  If contraction of the soil appears, the present water in the pores must flow to other locations within the soil. If water is not able to flow away quick enough, excess pore pressures will develop. This additional water pressure, expressed in negative pressure values, influences the resistance between the grains. The development of the occurring excess pore pressure is presented in the graph in Figure 4.7. Below the graph a visualisation of the developed excess pore pressure around the grout body is given. The grout body is modelled as an embedded beam row, presented with the red line in the figure.

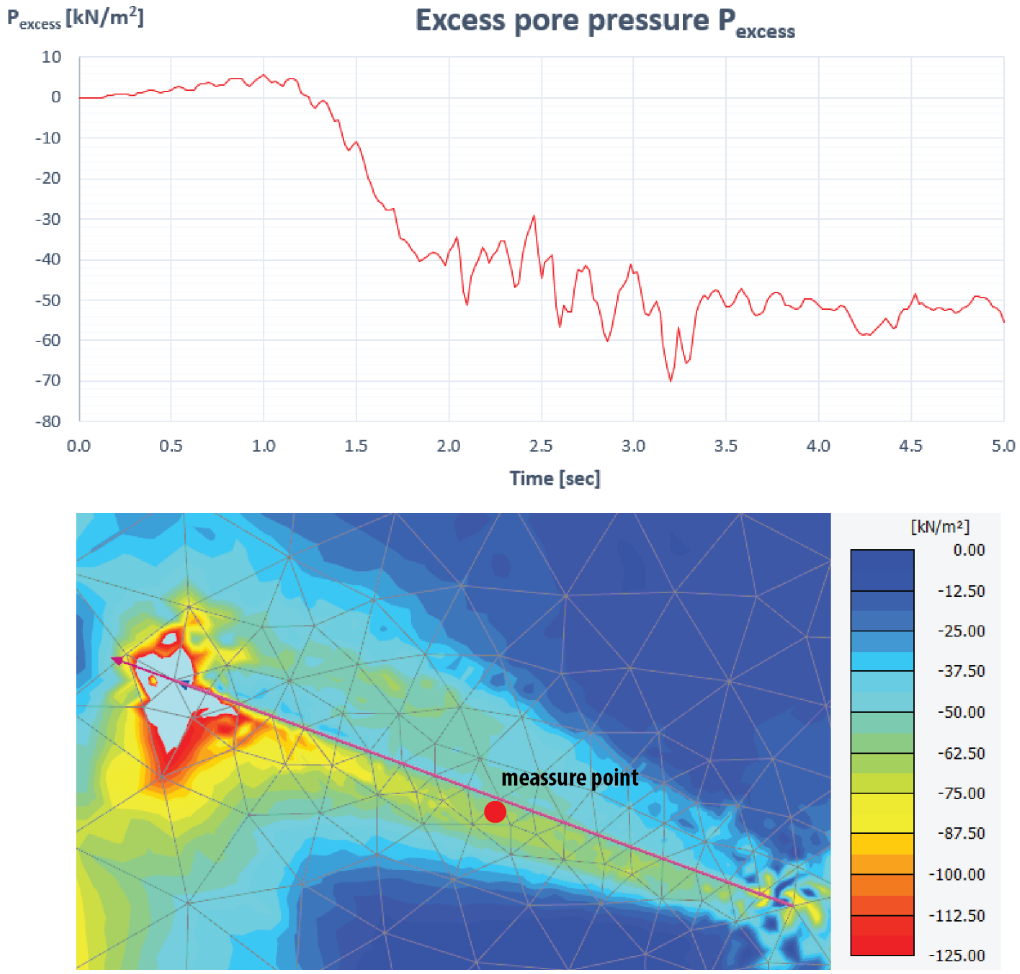

Figure 4.7: Excess pore pressure development

Conclusion regarding P_{excess}
The occurrence of the pore pressure becomes visible from the descending development in Figure 4.7. Pore pressures have been build up along the shaft during the dynamic phase. The developed pore pressure over the length of the grout body is shown in Figure 4.7. Pore pressures with a maximum of 10 kN/m^2 have been build up in the free field, further away from the anchor. The extreme pore pressure area indicated with the red circle at the tip of the anchor is caused by the dynamic pulling force in the axial direction. This situation will in reality not occur because the anchor is attached to the retaining wall and does not end in the soil in that way. It can be concluded that during dynamic loading excess pore pressures build up along the modelled anchor, which is in line with the volumetric strain development.

- Principal effective stress $[\sigma'_1]$
  The principal effective stress 1 $[\sigma'_1]$ presents the largest compressive principal stress in the soil (PLAXIS-4, 2015). The magnitude and direction of this stress may change during and after dynamic loading. Insight in the development of σ'_1 is provided by plotting this stress in dynamic time, see the graph in Figure 4.8. Below the graph two figures, before and after loading, visualise the change in stress direction.

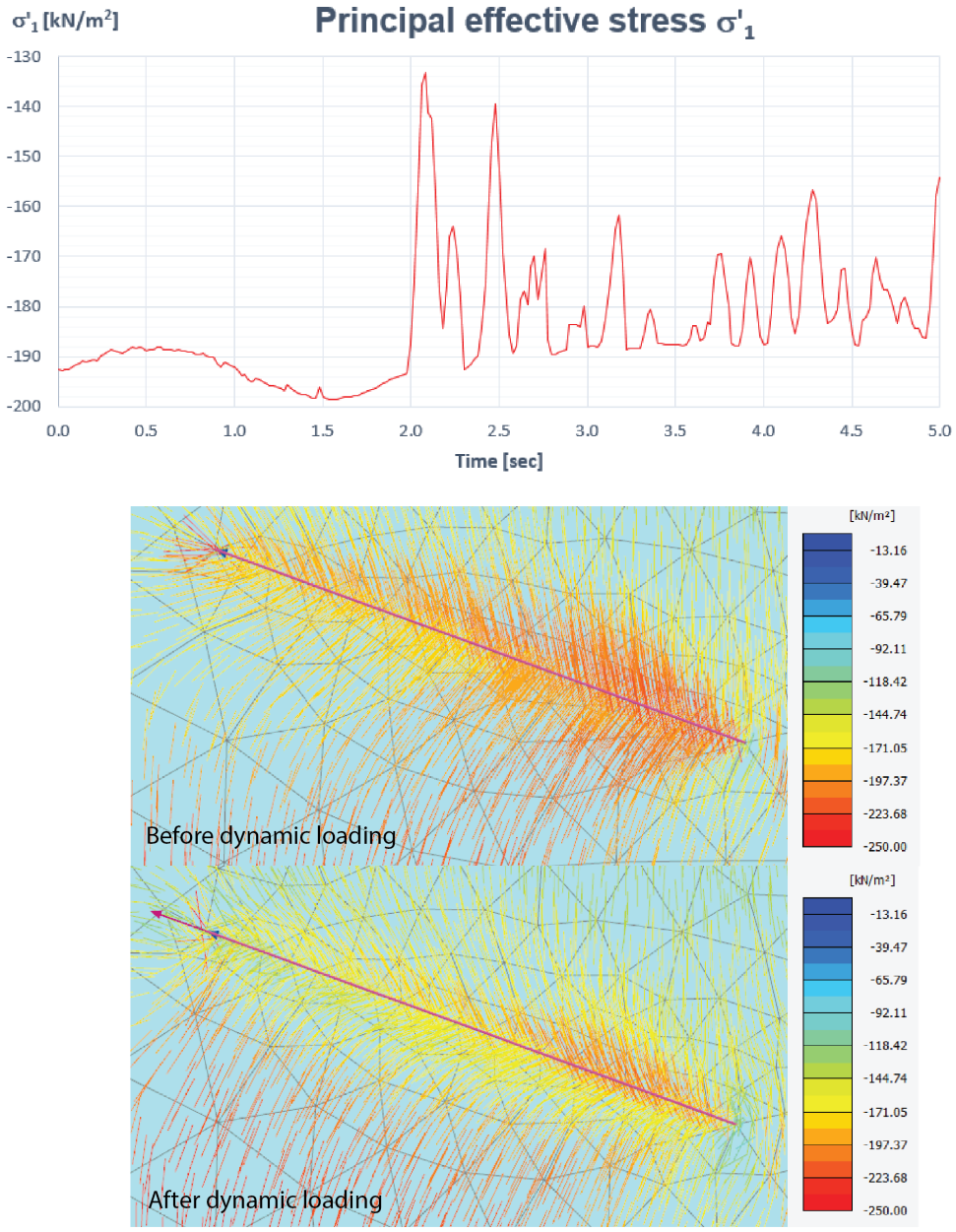

Figure 4.8: Principal effective stress development

Conclusion regarding σ'_1
During dynamic loading several drops in effective soil stress are visible resulting in an overall decrease of effective stress in dynamic time. This result corresponds to the increased excess pore pressure as observed earlier. Before loading, the stress direction is in a relatively straight line regarding the anchor. The stress line directions becomes more curved after the dynamic loading phase. The visible colors indicate the decreased stresses along the anchor shaft.

- Cartesian effective stress $[\sigma'_{yy}]$
  The Cartesian stress directions are based on a fixed coordinate system in the PLAXIS model. Stresses expressed in the Cartesian coordinate system do therefore not change in directions, but only in magnitude. Figure 4.9 visualises the direction of the Cartesian coordinate system. The direction of σ'_{yy} is vertical and due to the small angle of the anchor with the horizontal, σ'_{yy} is close to the direction of the radial stress σ'_{rad}. To determine qualitatively the development of σ'_{rad}, the development of σ'_{yy} is therefore observed.

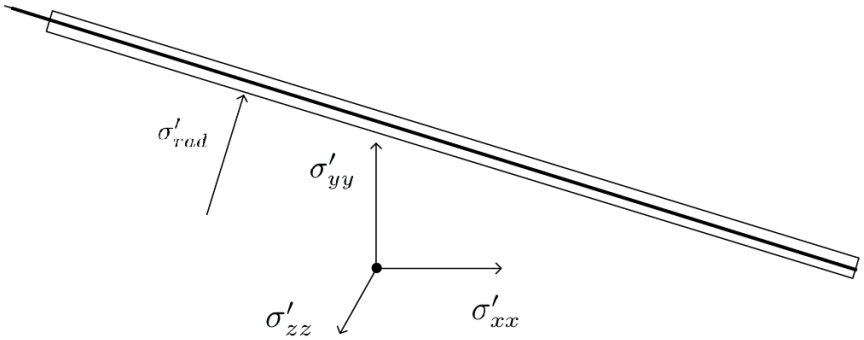

Figure 4.9: Stress direction visualisation

The development of σ'_{yy} in dynamic time is presented in Figure 4.10.

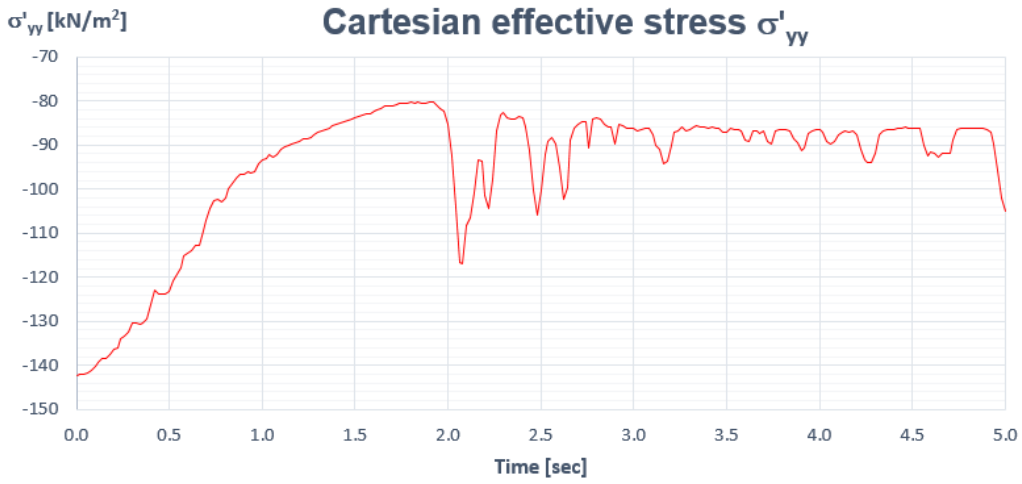

Figure 4.10: Development of cartesian effective stress in vertical yy direction

Conclusion regarding σ'_{yy}
It is assumed that the qualitative development of σ'_{yy} is representative for the development of σ'_{rad}. From the graph in Figure 4.10 a decrease in effective stress is visible after dynamic loading. This indicates a decreasing radial stress on the grout body during and after dynamic loading. A general decrease of σ'_{yy} and therefore the radial stress close to the anchor corresponds to the other results presented above, i.e. decreasing volumetric strains, occurring excess pore pressures and decreasing principal effective stresses. The development of σ'_{zz}, directed perpendicular to the grout body, is also observed. The effective stress level change in z-direction is in line with the presented results in y-direction.

Additional model results

The soil state after dynamic loading and insight in the contribution of each dynamic component are also obtained during the investigation. Conclusions regarding both aspects are presented below. Both aspects are further elaborated in Appendix **E.2.2.**

Consolidation period after dynamic loading
To model the soil behaviour after dynamic loading, a consolidation phase is added in which the pore pressures are able to dissipate. The results are based on a dynamic loading time of 5 seconds. The consolidation phase ends if the pore pressures are lower than 1 kN/m^2. It is observed that after the consolidation period of about 7 minutes the soil stress levels reach the initial values as was present before dynamic loading. It is therefore concluded that the reduced resistance is only present during the earthquake and the original strength is build up after the earthquake. The corresponding graphs are presented in Appendix **E.2.2**.

Contributions of individual dynamic components
The PLAXIS model contains two dynamic components, i.e. the dynamic movement of the anchor and the movement of the soil. The influence of both components is investigated. It is found that the dynamic movement of the anchor causes the general decrease of radial stress without large peak developments. As a result of the seismic input signal soil starts moving around the grout body. This results is a peaked development of the present stresses. The contribution of each load component is presented with several graphs in Appendix **E.2.2.**

4.3.3. Conclusion regarding qualitative resistance development

The influence of an earthquake regarding the radial effective soil stress σ'_{rad} and the internal friction angle ϕ is investigated. Literature indicates the expectation of a decrease of σ'_{rad} and ϕ during an earthquake. This expectation is confirmed with the applied model and can be substantiated with the presented figures. From Figure 4.6 and 4.7 is obtained that excess pore pressure occurs as a result of decreased volumetric strains. This results in drops of the effective stress which is visible in Figure 4.8. The qualitative development of σ'_{rad} can be expressed with the vertical Cartesian effective stress σ'_{yy}. This parameter presents a general decrease at the start of the seismic activity, see Figure 4.10. It is concluded that the results from the applied model are in line with the expectations from literature. The decreased values of σ'_{rad} and ϕ during an earthquake result in a decreased anchor resistance, which redevelop to the original values in about 7 minutes after the earthquake.

Recommendations

The applied model in PLAXIS is used for initial insights in the behaviour of soil surrounding a grout body. However, this model does include simplifications, as explained below and several recommendations should therefore be made.

- The applied seismic signal at the base of the model is not determined by taking into account non-linear soil response. This signal is applied to indicate the qualitative effect, but for an estimation of the quantitative effect a signal with the correct magnitudes should be applied. For the correct design signal the soil responses should be combined with the applied signal depth in the model.
- The applied soil model HS_{small} is basically not designed to model the exact behaviour of volumetric strains, but it is more suitable for modelling seismic damping behaviour. An alternative software model suitable for modelling of granular materials is a Hypoplastic model. This model describes the stress-strain behaviour of granular materials (Dung, 2009) and so, granular soils are modelled in a more reliable way.
- PLAXIS is a software tool based on a Finite Element Method and the elements are implemented as continuum element. No individual grain particles are modelled. Using a Material-Point Method (mpm) based on a Discrete Element Method, individual grain particles can be modelled (Database, 2016). Using this type of modelling provides more reliable output.
- The behaviour of a grout body is a 3-dimensional process, using a PLAXIS 3D model would certainly improve the model reliability.

4.3.4. Initial quantitative expression of decreased resistance

A value for the quantitative decrease of the anchor resistance provides insight in the magnitude of reduced safety. The graph presenting the qualitative development of the radial stress σ'_{rad}, can also provide an indication for the quantitative strength reduction during an earthquake. Assuming a decrease of the anchor resistance, the reduction of anchor resistance can be approached using the following relation:

$$\triangle F = F_{static} - F_{dynamic} \tag{4.5}$$

$$\triangle F = \int_0^L \left[(\sigma'_{rad,static} * tan(\phi)) * O\right] \, \mathrm{d}x - \int_0^L \left[(\sigma'_{rad,dynamic} * tan(\phi)) * O\right] \, \mathrm{d}x \tag{4.6}$$

For this equation, several simplifications are possible. It is assumed that the grout body does not change in size during an earthquake. The parameters L and O can therefore be neglected from the formula. Multiplying the vertical Cartesian effective σ'_{yy} stress with the cosine of the angle α, presenting the angle between the normal direction of the anchor and the horizontal, represents the radial effective stress. The presented relation is therefore written as:

$$\triangle F = (\sigma'_{yy,static} * cos(\alpha)) * tan(\phi) - (\sigma'_{yy,dynamic} * cos(\alpha)) * tan(\phi) \tag{4.7}$$

The exact development of the internal friction angel ϕ during an earthquake is not known in this research. A constant value is assumed for this initial quantitative approach. During further research the development of ϕ should taken into account. The reduction between static and dynamic anchor resistance is estimated as:

$$Reduction = \frac{(B - A)}{A} * 100\% \tag{4.8}$$

$$A = \sigma'_{yy,static} * cos(\alpha) * tan(\phi); B = \sigma'_{yy,dynamic} * cos(\alpha)) * tan(\phi)$$

The development of σ'_{yy} influences the reduction of the resistance mainly. A reliable value for σ'_{yy} should be determined. The presented figures for the qualitative determination of σ'_{yy} in Section 4.3.2 are based on a single measure point, presented in Figure E.10. For a more reliable value of σ'_{yy} additional calculation are performed. The development of σ'_{yy} is measured for eight measure points along the grout body for three different earthquake signals. Taking the average reduction of these 24 measure points provides a more reliable value for the reduced resistance. The output values corresponding to the measure points are presented in Appendix **E.2.3**. From this approach, a possible reduction of the anchor resistance of about 25% is determined during an earthquake.

The determined decrease of the anchor resistance corresponds to an average of three different seismic signals. All three signals do influence the development of σ'_{yy} and therefore the anchor resistance equal in the same order of magnitude, as presented in Appendix **E.2.3**. The measure points at the bottom of the modelled anchor do provide a larger decrease in comparison to the measure points positions at the upper side of the anchor. The dimensions of the model, which limit the waves from freely travelling from bottom to surface level, might cause this effect. The effect of an earthquake regarding the resistance is however clear and consistent from both the qualitative and quantitative approach. A reduction of the grout anchor resistance is observed during an earthquake as a result of developed excess pore pressures.

The quantitative determination of the reduced anchor force should be used carefully, because the expression is not validated with reference data from laboratory tests or measurements. Using the determined reduction value of about 25%, the following aspects should be kept in mind.

- As mentioned in the recommendations of Section 4.3.3, a 2D PLAXIS model is used for a complex three dimensional problem. The model is based on a finite element method using continuum elements instead of a discrete elements.
- Only one type of sand is applied using a HS_{small} model in this investigation. A change in soil characteristics might provide deviating results.
- The applied damping in the sand layer is modelled for initial indications, but should be optimised based on proper validation material.
- Three different seismic signals are applied at the base of the model. Although the magnitude and frequencies differ, more signals should be used for a proper average.
- The development of the effective stress is determined for eight stress points close to the grout body in the PLAXIS model. Additional measure points at the tip of the grout body will increase the reliability of the estimated value.
- The applied model is limited in size. A larger model with finer mesh elements is advisable to model in a more realistic way.
- The reduced anchor resistance is determined based on the parameters from equation E.6. In reality, additional aspects influence the reduction as well, for example the quality and condition of execution during construction of the anchor.
- Two parameters which are of importance for the soil compaction effect are the dilatancy angle and the poisson's ratio. Default values are applied, but more detailed research is advisable regarding the determination of more reliable values to model the soil behaviour.

4.4. Conclusion of resistance investigation

The analysis from Chapter 3 indicates an increase in anchor forces if the quay structure is subjected to the design earthquake. The goal of the investigation in this chapter was to express the development of the anchor resistance during an earthquake. The empirical determined resistance equation is therefore replaced for an equation including the radial stress σ'_{rad} and internal friction angle ϕ. By investigating the development of these two parameters, comment can be made regarding the resistance of a grout body during dynamic loading. From the results, an initial verification of the defined hypothesis can be given.

"*If a grout anchor is subjected to an earthquake, the resistance of the anchor regarding tensile forces decreases*"

It is stated that this hypothesis has be found to be correct under the applied model conditions within this investigation. A temporary reduction of anchor resistance during an earthquake of 25% seems to be possible. The estimation of this value is only applicable as a first indication regarding the magnitude of reduction. There are many variables of influence on the results, e.g. applied model, the parameters of the soil layer, seismic characteristics and the conditions of the soil-grout interface related to the quality of execution. The results from Section 4.3 confirm the initial expectations from the assumed hypothesis and these have been determined in this report to be correct.

The presented results in this chapter and Appendix E are based on literature and a finite element model. It should be kept in mind that these results form a starting point for further research regarding this topic, i.e. the dynamic behaviour of grout anchors. Additional model research and validation material are required to form a definitive and substantiated conclusion regarding the assumed hypothesis. The effect of installing grout anchor under large pressure, which results in pretensioned soil, is not jet taken into account. The execution of an experiment regarding behaviour of soil around a grout body under dynamic loading would be very informative. A test like this is therefore strongly recommended. Nevertheless, the gathered results from this investigation provide new insights and initial conclusions.

Combining the results from Chapter 3 and 4 brings up the following conclusion. If an earthquake with equal design conditions is applied to the model, the anchor loads increase and the resistance of the anchor decreases. Both effects influence the exiting quay structure negatively resulting in lower safety level. After the earthquake, the resistance redevelops to the initial values if sufficient consolidation time is available. It is therefore concluded that the most critical state regarding safety occurs during the earthquake.

5

Quay structure improvement

In this research, the influence of an induced earthquake for an existing quay structure in Groningen is obtained. From the assessment on the current situation is concluded that the quay structure undergoes a movement towards the water, combined with an increase of bending moments and anchor forces (Chapter 3). Comparing these increased loads with the static state resistance indicates that the most critical part of the existing quay structure is related to the ability to develop resistance of existing grout anchors. From this indication, the resistance of the grout anchors during an earthquake has been investigated (Chapter 4). Comparing the expectations from literature with a finite element model, an initial conclusion regarding the dynamic behaviour of grout anchors is made. The initial conclusion reveals a reduced anchor resistance during an earthquake compared to static behaviour.

The overall indication for the behaviour of the quay structure under dynamic loading is an increase in anchor force and a decrease in resistance ability during earthquake events. This results in a reduced safety rating for the existing quay structure of GSP. As a result of the expected safety decrease, improvement measures for the existing reference structure are proposed in this chapter. The goal of an improvement measure is to increase the safety of the structure during an earthquake with respect to the installed grout anchors. The proposed measures are subdivided into two categories. First, the structure will be improved by increasing the capacity of the anchor. The second category includes several measures to reduce the acting anchor force.

To understand the required safety increase, which should be achieved from the proposed improvement measures, an indication regarding the actual safety reduction for the reference structure is presented in Section 5.1 and Appendix F.1. This section includes also an initial estimation of anchor displacement, based on an energy balance between kinetic and work energy, which is further elaborated in Appendix F.2. Section 5.2 presents the proposed improvement measures to increase the safety regarding the existing anchor system. To select the two most suitable measures, a trade off matrix is applied and presented in Section 5.3. Replacement of soil for lightweight material is selected from the trade off matrix to improve the current situation. This measure is elaborated in Section 5.4 and Appendix F.3. Section 5.5 and Appendix F.4. describe the effect of the installation of a high and low position relieving structure, to improve the current situation. The findings from both measures are evaluated in the conclusion from Section 5.6.

5.1. Effect of results regarding quay structure GSP

Combining the results of Chapter 3 and 4, a comment regarding the safety of the observed quay structure in the Eemshaven from Groningen Seaport (GSP) can be made. The values of observed forces versus resistance for static and dynamic state provide insight in the actual reduced safety.

The increased anchor force due to an earthquake is determined in Chapter 3. The critical value of the anchor resistance as presented in Section 2.4 is based on the available CPT. This theoretical value should be replaced by a more reliable value based on results from a control test. Using a maximum resistance value based on a performed control test provides a more reliable value of the actual resistance of the installed anchors. For the reference cross-section in this research the control test indicates an average resistance of 2550 kN per anchor (Harmelen, 2010)*. However, the control test value is not equal to the actual failure value of the installed anchors, see Figure 5.1. A factor of 1.25 between the expected pull-out force and the control test value is assumed (Harmelen, 2010). Please note that this factor is not measured and depends on many variables in reality. As earlier mentioned in Section 2.2, the occurrence of an earthquake is defined as an extreme event or as a calamity and therefore no safety factors are used for the ultimate limit state design. The pull-out force for the installed anchors is therefore estimated to be approximately 3190 kN. This pull-out value is used to approach the actual safety in a more reliable manner during an earthquake.

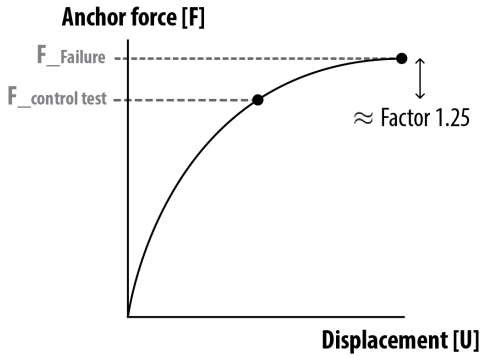

Figure 5.1: Estimated relation between resistance value and measured control test result

* *The report (Harmelen, 2010) was not available at the start of the research, but is received in a later stage. A resistance value from the CPT was therefore initially used instead of the control test values.*

Reduced safety during earthquake

To determine the actual safety of the existing reference quay structure from Groningen Seaport during an earthquake, a comment regarding the following four aspects should be made. Combining the results from these aspect provides an initial indication regarding the reduced safety of the quay structure, summarised in Figure 5.2.

- Increased anchor force during an earthquake.
  This value is estimated during the performed analysis from Chapter 3. Between the static anchor force of 2162 kN and dynamic value of 2469 kN, an increase of about 14% is observed. A reliable validation of the applied models is advised. Experimental data or further sensitivity checks should be applied during the validation.
- The pull-out resistance of the installed anchors in static state
  *The deliverable resistance of the installed grout anchors is determined with performed control tests after construction. During a control test the installed anchor is loaded to a design value which is assumed to be a factor 1.25 lower than the expected pull-out force. For the reference cross section, the pull-out resistance of the existing anchor is therefore an estimation and not a measured value from a failure test, as explained in appendix **E.1.** From (Harmelen, 2010), a control test value of 2550 kN is determined. The corresponding pull-out value of 3190 kN per anchor is therefore assumed*

- Reduced anchor resistance of grout anchor during earthquake
  An initial estimation regarding the reduced anchor resistance is made in Chapter 4. A temporary reduction due to an earthquake of 24% is observed. Combining the expected reduction of 24% with the estimated pull-out resistance of 3190 kN results in an upper limit regarding the possible anchor resistance during an earthquake of 2425 kN.

- A translation between the determined effect on one anchor regarding the complete anchor system
  The load and resistance effects are determined for a single anchor. It should be investigated whether the results can be applied for all anchors combined. Redistribution of the mutual anchor force in case of anchor failure plays a major role. This effect is not taken into account and assumed not to influence the presented output. It is advisable for future studies to take this into account by doing more detailed research.

Combining the quantitative effects of these aspects provides insight in the amount of reduced safety during an earthquake. The presented values are given without safety factors.

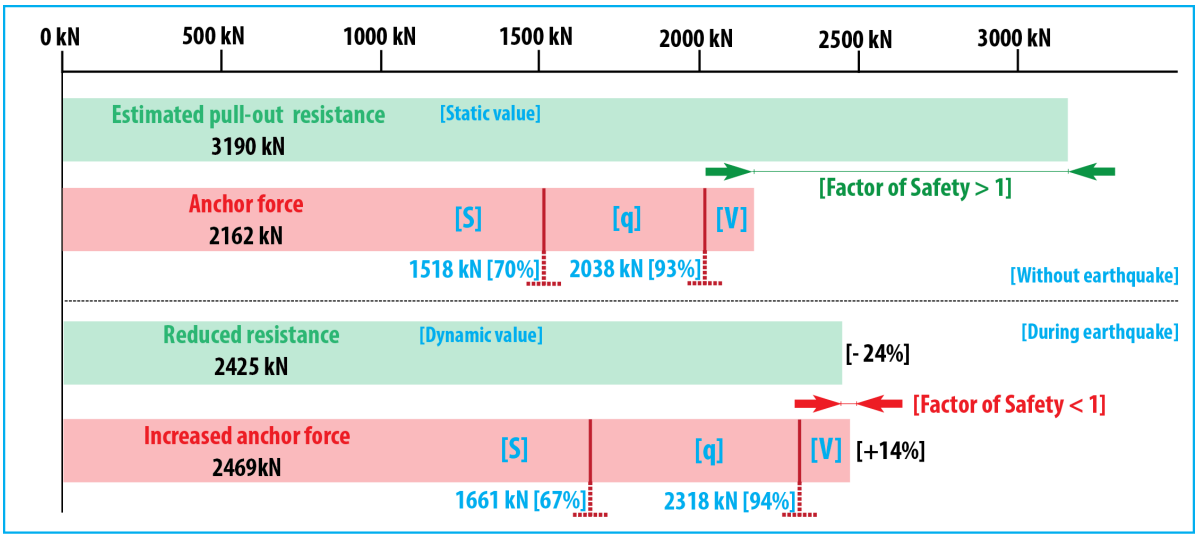

Figure 5.2: Overview of safety development regarding installed anchors due to an earthquake

From Figure 5.2 is concluded that a reduced safety rating for the reference cross-section of the quay structure in GSP is indeed fact. A temporary factor of safety lower than 1 is observed. This might result in movement of the anchors and quay wall. However, the increased force from Figure 5.2 is based on a design load combination, which might not often occur in reality. This load combination contains three main load aspects, i.e. soil and water loads [S], surface loads [q] and loads from the moored vessel [V]. The contribution of each load component is visualised in Figure 5.2 for static and dynamic state and is further elaborated in Appendix **F.1**. From the figure, a large influence of the design surface load [q] is observed. It is therefore important to evaluate how conservative the modelled surface load is with respect to the actual surface load from practice, before a reliable comment regarding the observed factor of safety can be made. If the modelled design surface load, for now assumed to act over the complete quay length, appears to be too conservative, a factor of safety larger than 1 might be maintained. However, existing design guidelines prescribe the use of load combinations including reduction factors to prevent the load combination from becoming too conservative. The use of different load components from (NEN-EN:1990NB, 2011) including the combination factors Ψ_1 from (BS-part2, 2010) Table A2 is therefore recommended to apply, which results in a significant reduction of the components [q] and [V]. From (de Gijt and Broeken, 2014) Table A2 is also recommended to apply, using the combination factors Ψ_2. The use of Ψ_2 include significant reductions which neglect almost the complete variable loads. The use of Ψ_1 is therefore recommended to apply during further research. The presented factor of safety during an earthquake indicates to a critical situation from the applied loading combination, but does not automatically refer to failure of the quay structure if the prescribed load combination are taken into account.

Initial estimation of anchor movement

After the visualisation of the reduced factor of safety from Figure 5.2, it is of interest to estimate the grout anchor displacement as a result of the earthquake. A rough and quick manner for an initial estimation is by using energy balances. Under the assumption that the additional energy from the moving active soil wedge should be absorbed by the grout anchors, the displacement of an anchor can be estimated. This approached is schematically visualised with the Figure below. A brief elaboration of the approach with the corresponding result is presented below. The applied parameters are given in Appendix **F.2**.

Due to movement of the soil area within the active soil wedge, kinetic energy E_{kin} will develop. To resist the additional energy on the wall, the existing anchors should adapt this energy by delivering so called 'work' E_{work}. If the kinetic energy and performed work energy are in balance, the structure is assumed stable. It should be noted that this approach contains large simplification, but might provide initial insight in the possible displacement. From the applied parameters elaborated in Appendix **F.2.** an anchor displacement of 1.25 cm is estimated. This value is relatively small and does not create great concern regarding the structure stability. However, the method used for this determination contains many simplifications and uncertainties, summed up below the figure. The reliability of the method is therefore assumed to be small.

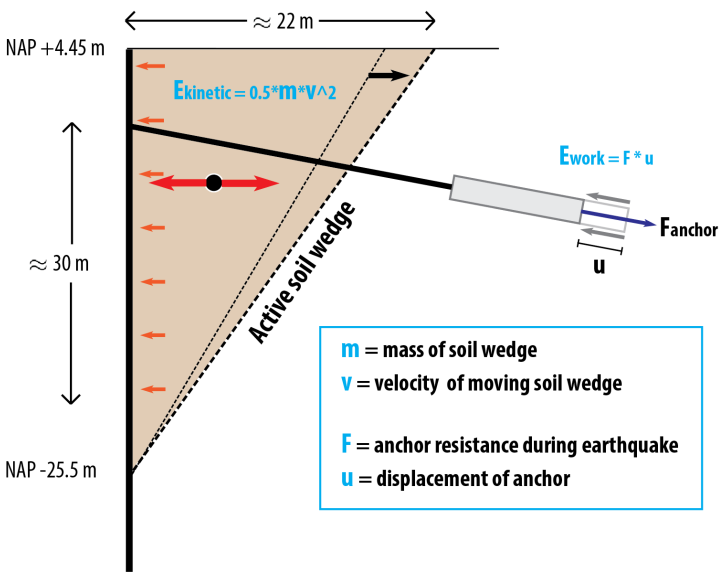

The most important simplifications and assumptions regarding the applied method are summed up below. These aspect should be kept in mind if the assumed displacement value is applied.

- The characteristic of the earthquake are only taken into account by implementing a peak velocity. The relationship between velocity and acceleration and its derivation includes the use of a reduced impact of the soil mass against the retaining wall.
- Surface loads are not included using this method.
- From the relation $E_{kin} = E_{work}$, the complete additional earthquake force is assumed to be adapted by the grout body. This is a large simplification or reality.
- The active soil wedge is assumed to be the only driving force during an earthquake. The dynamic behaviour from the wall and anchor are not included.
- The possible reduction from the passive soil during an earthquake is not taken into account. Only the force driven active soil wedge is included.
- A reduction of the angle between the horizontal and active wedge line during an earthquake is expected (Kramer, 1996). An additional 5 meters of active soil at surface level is estimated for this initial approach.
- The behaviour of the wall with respect to the effect of loading / reloading is not taken into account.

From the named restrictions it is concluded that the determined anchor movement is only applicable for an initial indication from which no conclusions will be drawn. Proposed improvements to the existing structure to increase the estimated safety during an earthquake are therefore desirable. Several improvement measures for the existing structure are elaborated in the next section. This provides an overview of possibilities to redevelop the safety.

5.2. Proposed improvements for existing quay structure

The goal of an improvement measure is to minimize the negative effects regarding the safety of the current anchor system during an earthquake. These (negative) effects are qualitative described in Chapter 3 and 4. From Chapter 3 is concluded that the anchor forces increase during and after an earthquake. Simultaneously, a decrease in resistance of the anchor is expected during dynamic loading, as described in Chapter 4. These two effects add up to produce reduction of safety of the installed anchor system. Therefore, several improvements have been proposed in this chapter. A subdivision with respect to capacity improvement measures and load reduction measures is made. Before these improvements are presented, two starting point should be noticed.

- The repetition time between multiple earthquakes is assumed extremely low, because this research is focussed on the near collapse state, see Section 2.2. The repetition value is interesting for the determination of acceptable damage regarding existing infrastructure, for example quay structures.
- Redistribution of loads after anchor failure should be kept in mind. A precise forecast regarding this redistribution is hard to provide and is not investigated in this research. The local soil conditions are variable and play a major role in local anchor failure.

The proposed improvement measures are presented in the following two subsections. As mentioned, the measures are divided into two categories, *capacity increasing measures* and *load decreasing measures*. The goal of all measures is to increase the reduced safety ratings regarding the grout anchors during dynamic loading. For all measures the most important advantages and disadvantages are given. After these comments, all measures are evaluated utilising a trade off matrix in Section 5.3.

5.2.1. Capacity increasing measures

- **Measure 1**: Add additional anchor [Figure 5.3]
  Adding an additional anchor may reduce the load on the existing anchor. Three possibilities, called [a], [b] and [c] are available based on the present sand layers. Option [a] refers to a horizontal anchor rod connected to a vertical plate, whereas option [b] a short and inclined anchor positioned into the shallow sand layer defines. Option [c] refers to an additional anchor positioned into the deep sand layer.

  Advantages: Adding anchors is a proven technology. Under correct installation and design conditions the load on the existing anchor can be reduced.

  Disadvantages: Besides the complex existing connection of the anchors within the tubular pile, all three options contain a major disadvantages. Option [a] requires large deformations before the passive soil is fully mobilised. After mobilisation the anchor will deliver complete resistance. This deformation is probably not possible from the stiffer grout anchor which is already installed and delivering resistance. Prestressing of the additional anchor might be a possibility, but requires information to the stresses from the existing anchor, which are very difficult to obtain. The anchor form option [b] is too short and is located in the kranz-stability zone. Option [c] contains a large vertical force component. This vertical force will act downwards on the wall during the earthquake. This influences the vertical bearing capacity of the complete structure and large vertical deformations may be expected.

- **Measure 2**: Apply spring connection [Figure 5.4]
  This measure replaces the stiff connection between anchor and pile for a ‘spring - dash pot’ connection system. This results in a more ductile structure which must adapt to the highest peak loads during an earthquake. With the proposed spring stiffness, see graph in Figure 5.4, almost no deformation during normal load situations occur. Only the extreme peak load should be adapted with the spring-dash pot system. For these peak loads the spring will elongate and thereby reduces the load on the grout body.

  Advantages: Only the most critical anchors, i.e. with the weakest sand layer, should be replaced with this connection type.

Disadvantages: This technique is not applied earlier and is based on theoretical insight. Adjusting the connection of existing anchors is hard and complex because of the existing high tensile forces. After elongation of the spring, the wall displacement is permanent due to repositioning of the soil.

- **Measure 3**: Increase soil stress [Figure 5.5]
  Increasing the weight of the upper soil results in higher effective stresses at the grout body. This results in a higher anchor resistance. The increase of effective soil stress should compensate the developed excess pore pressure.

  Advantages: Replacing several meters of existing soil for heavy material is a relatively simple technique, as long as the decreased soil pressure on the anchor during excavating is kept in mind.

  Disadvantages: After increasing the weight of the soil, the Kranz-stability is influenced and should be checked. The effect of increasing soil weight at surface level is strongly reduced at anchor depth, because the increased weight area will develop under an inclined angle due to stress spreading in the soil. During construction of the heavy weight layer, existing soil is excavated which reduces the anchor resistance temporary. This results in temporary decreased anchor resistance.

- **Measure 4**: Maintain passive soil resistance [Figure 5.6]
  During an earthquake a reduction of the resistance moment is observed. This may cause higher anchor forces. Maintaining the original resistance moment from static state results in lower anchor forces during an earthquake. This is achieved by improving the upper soil layer, e.g increasing the weight of the layer with heavy material or colloidal concrete, at the bottom in front of the quay.

  Advantages: With this measure there is no interference with the pavement area of the quay. Besides the effect of increasing vertical weight, the layer may function as a strut if sufficient width of colloidal concrete is applied.

  Disadvantages: Increase the weight of the soil by using large stones provides a limited effect under water. Before placing the large stones, a layer of existing soil should be dredged away which influences the stability negatively. If a colloidal concrete layer is constructed, pressures might build up under this layer.

- **Measure 5**: Install vertical drainage columns [Figure 5.7]
  To prevent the occurrence of excess pore pressures drainage columns can be installed close to the grout bodies. These drainage columns prevent the onset of factors which allow a developed decrease of the pulling resistance, as indicated in Chapter 4. The columns are constructed with geotextile and are filled with gravel material.

  Advantages: The occurring excess pore pressures will be drained during an earthquake if the drains are installed at the correct locations. The pull-out resistance of the grout body is therefore better maintained.

  Disadvantages: The vertical drainage columns are installed by vibrating a pile into the soil. These vibrations might influence the soil state. The effectiveness of draining the excess pore pressures is also questionable. From Chapter 4 it is seen that the pore pressures develop close to the grout body. It is therefore important to investigate the spacing of the columns and how close they can be installed to the grout body.

- **Measure 6**: Inject grout around existing grout body. [Figure 5.8]
  The resistance of the soil around the grout body that can be delivered in the event of an earthquake might be increased if grout is injected around the grout body.

  Advantages: Injecting grout around the existing anchor improves the soil characteristics with respect to the resistance.

  Disadvantages: During the injection of grout material under high pressure, the resistance of soil around the grout will be temporary lost due to the injected liquid grout. The acceptable percentage of temporary anchor lost should be known before grout can be injected at anchor depth. Otherwise a high risk of wall displacement is possible. In addition, the execution of injecting grout around the existing anchor is difficult at large depths. Injection of only grout above the existing anchor will not be sufficient.

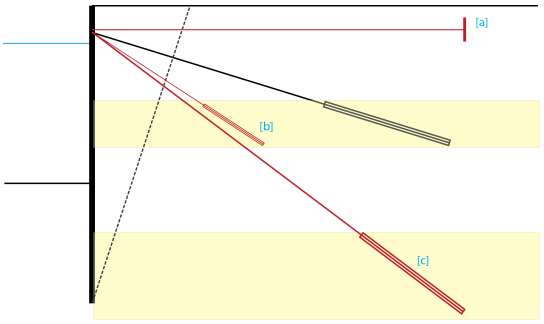

Figure 5.3: Apply additional anchor

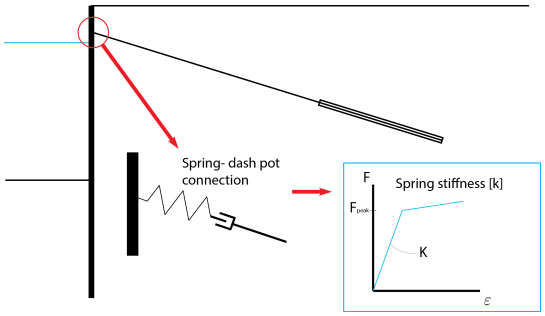

Figure 5.4: Apply spring connection

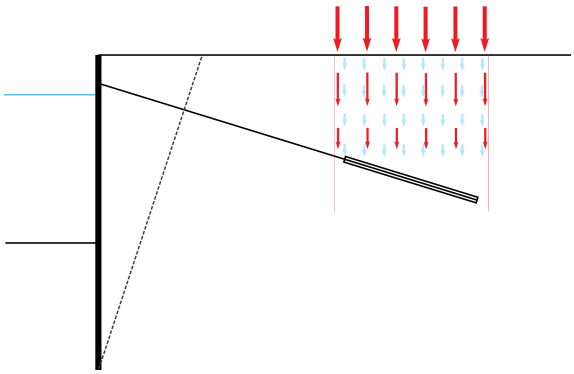

Figure 5.5: Increase soil stress

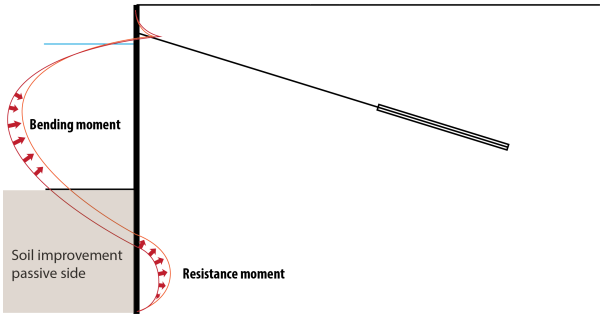

Figure 5.6: Increase resistance moment

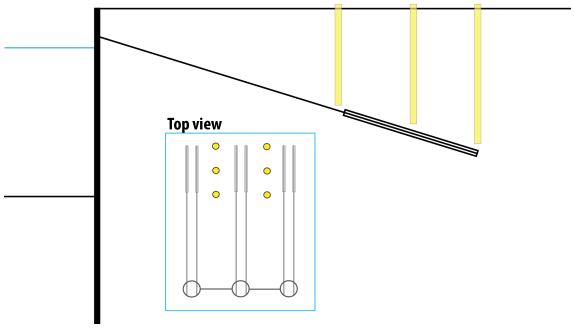

Figure 5.7: Provide drainage of pore pressures

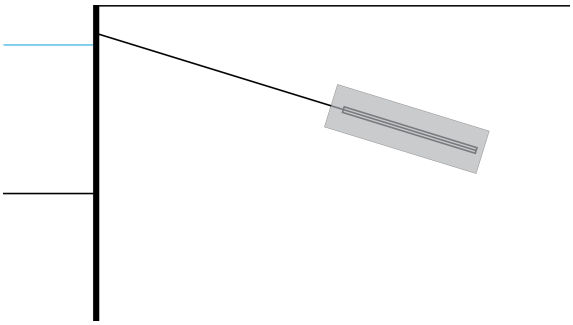

Figure 5.8: Improve soil state around grout body

5.2.2. Load decreasing measures

- **Measure 7**: Reduce acceptable surface load [Figure 5.9]
  A decreased surface load will reduce the horizontal soil force.

  Advantages: No structural measures are required, only a change in regulations regarding use of the quay.

  Disadvantages: The functionality of the quay reduces if the surface load is lower over a limited extent than the operational required load for daily use.

- **Measure 8**: Install relieving floor [Figure 5.10]
  If the top soil is replaced for a concrete floor with a foundation on concrete piles, a relieving floor is constructed. The surface loads are transferred via the concrete floor and vertical piles to the sand layer and do not act horizontally on the wall. Further optimisations regarding the exact design should be made in a later stage.

Advantages: Reduction of active horizontal soil loads on the wall from a relatively simple structure.

Disadvantages: A foundation with limited width, as visualised in Figure 5.10 is only possible if no large horizontal loads from machinery at the pavement area are present.

- **Measure 9**: Replace soil for lightweight material [Figure 5.11]
  Decreasing the soil mass by replacing the existing soil for lightweight materials results in lower horizontal soil pressure. This reduced horizontal force on the wall causes lower anchor forces. If the volumetric weight of the material is lower than the water weight, this material can only be applied above spring tide level. The material should contain sufficient pressure strength.

  Advantages: Relatively simple technique. Many optimisations are possible, e.g. lightweight materials or open structure elements from materials like concrete.

  Disadvantages: Sufficient strength of the installed materials must be guaranteed for long period of time. During construction, the existing quay area is temporary out of use.

- **Measure 10**:Improve soil characteristics in active soil wedge [Figure 5.12]
  If the internal friction angle ϕ can be increased, the inclination of the active wedge becomes steeper and the soil mass acting on the wall decreases. Increasing the internal friction is possible by installing several grout columns. The grout column size determines if bending moments can be withstood. The distance of the column from the wall determines the effectiveness of the measure. Further investigation should provide insight in the application of more economical materials.

  Advantages: Installing grout columns is a proven technology and decreases the acting soil mass behind the wall. The active wedge line becomes steeper.

  Disadvantages: A sufficient column size should be applied to prevent the columns from breaking at midspan due to horizontal loads and bending moments.

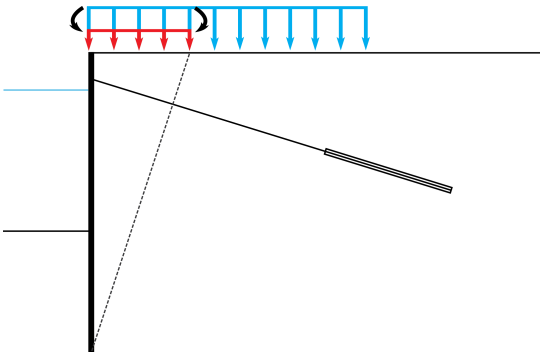

Figure 5.9: Reduce acceptable surface load

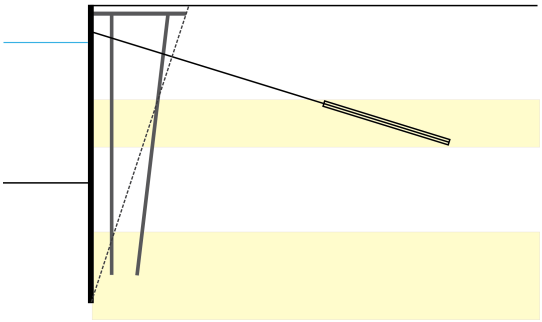

Figure 5.10: Install relieving floor

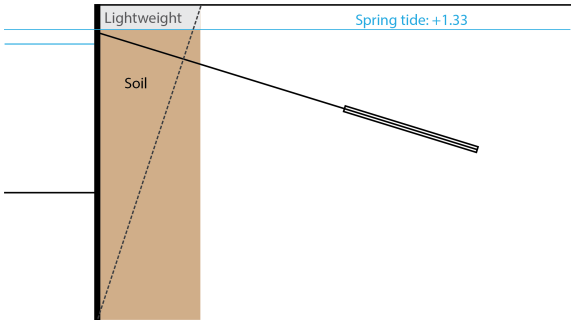

Figure 5.11: Replace soil for lightweight material

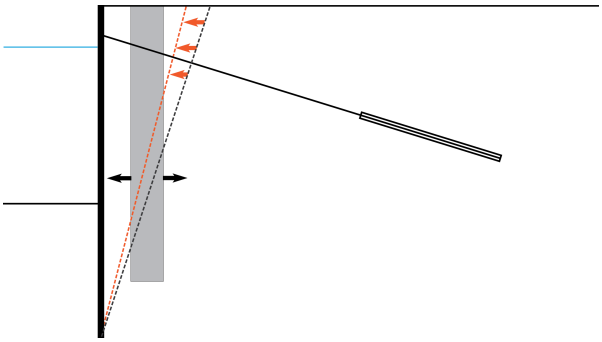

Figure 5.12: Improve soil in active soil wig

5.3. Selection of most suitable improvement measures

From the ten proposed measures in Section 5.2, the most suitable improvements are selected in this section. The goal of the applied selection is to filter out two of the best solutions in a quick way based on the present information. This is done by applying a trade-off matrix. Using this method, the proposed improvements are qualitatively evaluated based on five criteria. The chosen criteria are further elaborated below. The goal of this assessment is finding the most suitable improvement measures for the existing quay structure.

Applied criteria for trade-off matrix

To asses the suitability of the proposed measures in a qualitative manner, five criteria are used. A description of each criteria is presented below.

- **Technical risks**
  The technical risk expresses the degree of innovation and complexity of the measure. A **high** technical risk refers to a innovative or complex measure, whereas a **low** technical risk refers to a simple and proven technology. [*Applied qualitative expressions: Low - medium - high*]
- **Constructibility**
  With the constructibility the risk of failure of the structure during construction is expressed. If the execution causes an increased risk for the existing quay structure, the constructibility is mentioned as **difficult**. If the execution is relatively simple and without risks for the quay structure, the constructibility is determined as **easy**. [*Applied qualitative expressions: easy - medium - difficult*]
- **Effectiveness**
  The objective of the proposed measures is to increase the safety of the structure during an earthquake with respect to the installed anchors. The effectiveness refers to the degree of achieving this objective. If the effectiveness is **large** the degree of reaching the objective is high. The opposite expression is occurring if the effect of the proposed measure regarding the objective is relatively **small**. [*Applied qualitative expressions: small - medium - large*]
- **Influence on functionality**
  The influence of the measure during and after construction on the functionality of the quay is important. If the exiting quay has to be rebuild completely the functionality is temporary lost and the influence on functionality is therefore **high**. If the quay stays operational and functional during of after the implementation of the improvement, the influence is **low**. [*Applied qualitative expressions: low - medium - high*]
- **Costs**
  For the proposed measures an initial estimation of costs is performed. The cost estimation is expressed qualitative for this level of design and is therefore very rough. Difference between **high** and **low** costs are made relatively to each improvement measure. [*Applied qualitative expressions: low - medium - large*]

5.3.1. Assessment on suitability of measures

The proposed improvement measures are rated with a qualitative expression to indicate the governing positive and negative aspects of every measure. The governing drawbacks of a measure determine if the measure will be excluded for further research. The related criteria regarding the governing drawbacks are circled in the trade off matrix and are clarified below. It should be noted that the determination of a suitable measure is not based on the amount of positive or negative scores. Adding up the amount of green or red boxes is therefore not suitable. The coloured boxes are applied to provide a quick overview regarding the positive and negative aspects of every measure.

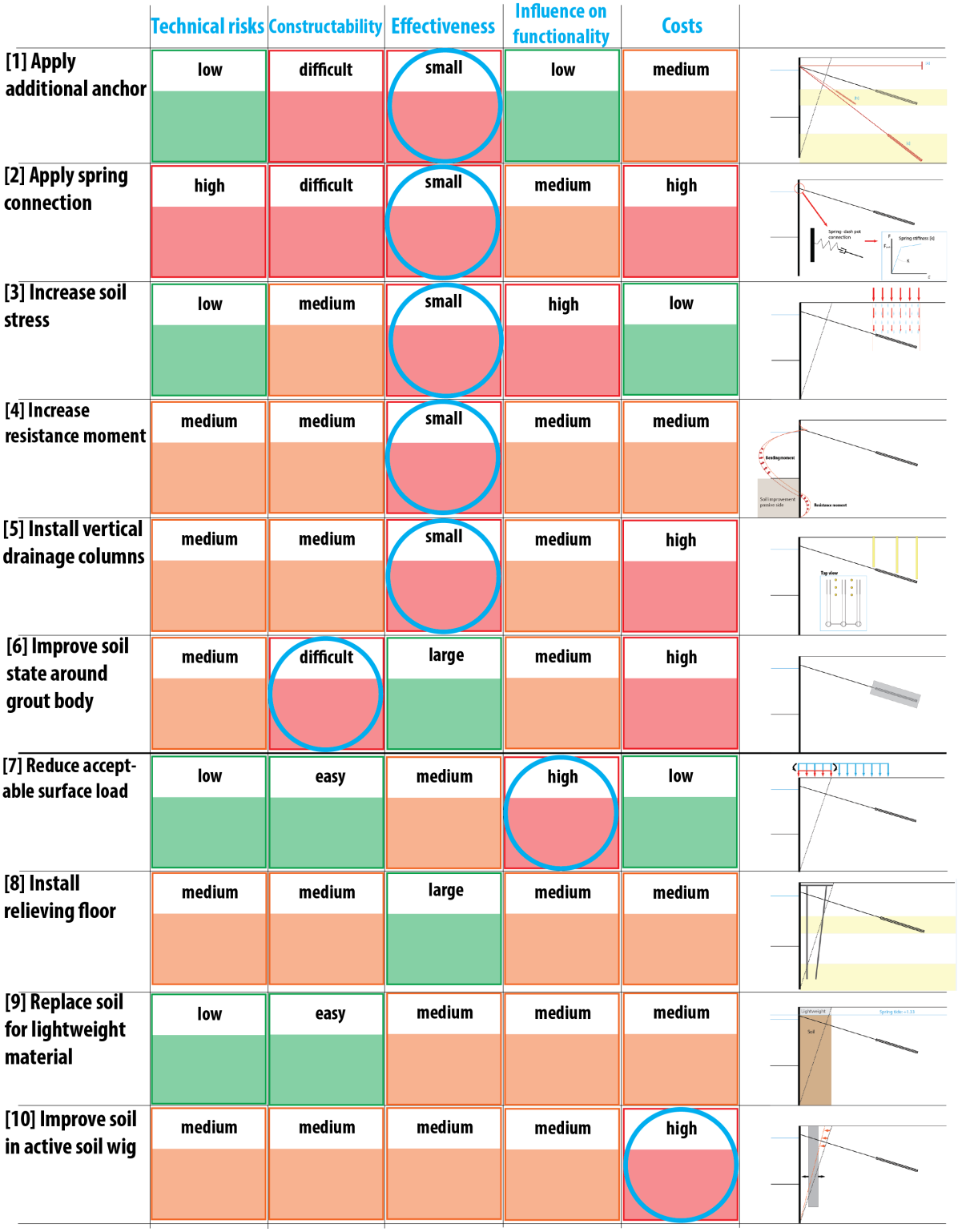

Figure 5.13: Trade off matrix for proposed improvement measures

Substantiate judgement of criteria in trade-off matrix

The arguments regarding the governing drawbacks as indicated in the trade off matrix, will be elaborated for the eight measures marked with a circle. These measures are not further elaborated in this research. Further research is required to indicate if these eight measures are applicable. No major drawbacks for the two remaining measures [8] and [9] are indicated in the initial evaluation regarding the suitability.

The decisive drawbacks of the eight measures are summed up below.

- Measure 1:
  The connection between the existing tubular pile and the additional anchor is difficult to realise, because the capping beam closes the entrance to the tubular pile. More importantly, the effectiveness of an additional anchor is low or not even possible due to the limited sand layers, elaborated in '*disadvantages*' Section 5.2.1.
- Measure 2:
  The peak loads of an earthquake are adapted with the new connection, but the wall will permanently displace as a result of the new connection. Installation of the spring connection within the tubular piles will be extremely difficult, time consuming and expensive. During further investigation of this measure results from (Por, 2010) are recommended to use.
- Measure 3:
  The increased weight at surface level will spread over an inclined line in depth. The effect at anchor depth is therefore relatively low. The increase of weight is limited regarding the towards the required Kranz-stability.
- Measure 4:
  More research towards the development of the fixed and bending moments during an earthquake is required. In addition, the relation between these two moments and the anchor force should be determined. This indicates the effectiveness of the improvement. More research is therefore required to form a statement about the efficiency of this measure.
- Measure 5:
  The observed excess pore pressure is positioned close to the grout body. Installing the drainage columns between the anchor will therefore not be efficient. It is difficult to place the columns close to the installed grout bodies, because of the uncertain location of the installed anchor.
- Measure 6:
  Injecting grout around existing grout anchors is difficult and uncertain, because the exact locations of the grout bodies are not known. The injection of grout causes a temporary loss of soil resistance at the installed anchor bodies.
- Measure 7:
  Reducing the quay functionality by lowering the acceptable surface load is assumed to be undesired.
- Measure 10:
  A large amount of grout is required to influence the present internal friction angle with individual grout columns which cross the active soil wedge line. This will involve high costs. Proving the efficiency of this measure is associated with complicated geotechnical aspects.

Conclusion from trade-off matrix

From the initial assessment on the proposed improvements, measures [8] and [9] are assessed without major drawbacks during this research. Please note that other proposed measures might also be suitable to improve the current state of the structure against earthquakes. More investigation regarding the named drawbacks of these measures should however be performed, before a more substantiated opinion is possible. Both measures [8] and [9] are further elaborated in a the two sections below.

5.4. Replace soil for lightweight material

This section present the initial results regarding the effect of soil replacement for lightweight material, indicated as measure [9] in the trade off matrix. Expanded Polystyrene, from now on described as EPS, is used worldwide as lightweight soil replacement material (Elragi, 2006) (Aaboe). EPS is extremely light and therefore often applied as fill material below road constructions. As a result, the vertical weight reduces resulting in less settlements and a shorter settlement process (Alliance).

From this initial observation regarding the positive EPS characteristics, this type of material will be used to improve the safety of the existing quay structure. The weight of the soil within the active wedge behind the quay structure determines the acting loads against the structure. By replacing the upper soil layer within the active wedge for lightweight material, less force is acting on the wall which results in a reduced anchor force. During evaluation of the proposed measure, the main focus will be on the development of anchor force during an earthquake. The goal of applying lightweight material is to reduce the anchor force during an earthquake to increase the observed safety.

During the elaboration of lightweight material in this section, the main goal is to determine whether the applied measure is effective. The effectiveness is measured with the magnitude of anchor force reduction, which is elaborated below. If a positive effect is obtained, the applicability of the improvement is elaborated. Under the applicability the three criteria 'technical risk', 'constructibility' and 'influence on functionality' are further introduced. This section will be concluded with an initial cost estimate of the proposed measure. In this way, a comment regarding all five criteria from the trade off matrix is made. Corresponding to the estimated costs, a trial to optimise the applied width of EPS is performed.

Effect of improvement

The effect of applying lightweight material depends mainly on the amount of replaced soil. To determine the boundaries for the placement of lightweight material, two starting point are used. The application of EPS should always be positioned above the ground water level. In this way, floatation of the lightweight material is prevented. A corresponding depth of NAP +1.50 m is therefore possible for EPS application.

Secondly, the lightweight material should be applied only in the active wedge area to ensure a positive effect on the anchor force. To estimate the width of the active wedge at surface level, an average angle of internal friction ϕ is determined. A width for the active wedge of 17 meters is determined. An initial width of 15 meters EPS is therefore applied.

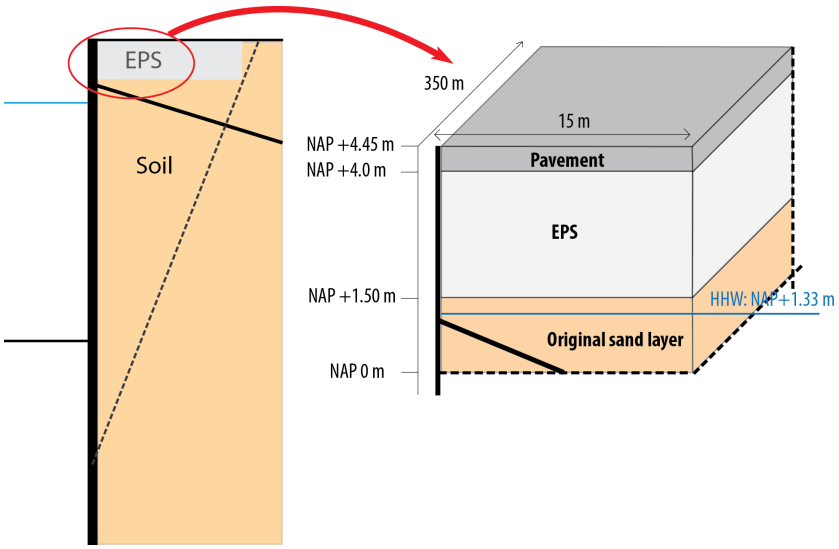

Figure 5.14: Application of EPS light weight material

To investigate the effectiveness of replacing existing soil for lightweight material, the PLAXIS model from Chapter 3 is used. As presented in Figure 5.14, 2.5 meters of soil over a width of 15 meters is replaced for EPS material. For information about the applied model parameters, a reference to Appendix **F.3.1.** is made.

It is of interest to know the effectiveness of EPS for weaker and stronger earthquakes in addition to the determined design signal. The resulting anchor force is therefore determined for 4 seismic intensities, presented in Figure 5.15. The original design signal for this research is presented with the 100% value on the x-axis. Three additional signal intensities are used as input, i.e. 33%, 67% and 133% of the magnitude of the original seismic signal. The corresponding anchor force as a result of those seismic signals is determined for all four signals intensities, presented with the bullets in every line.

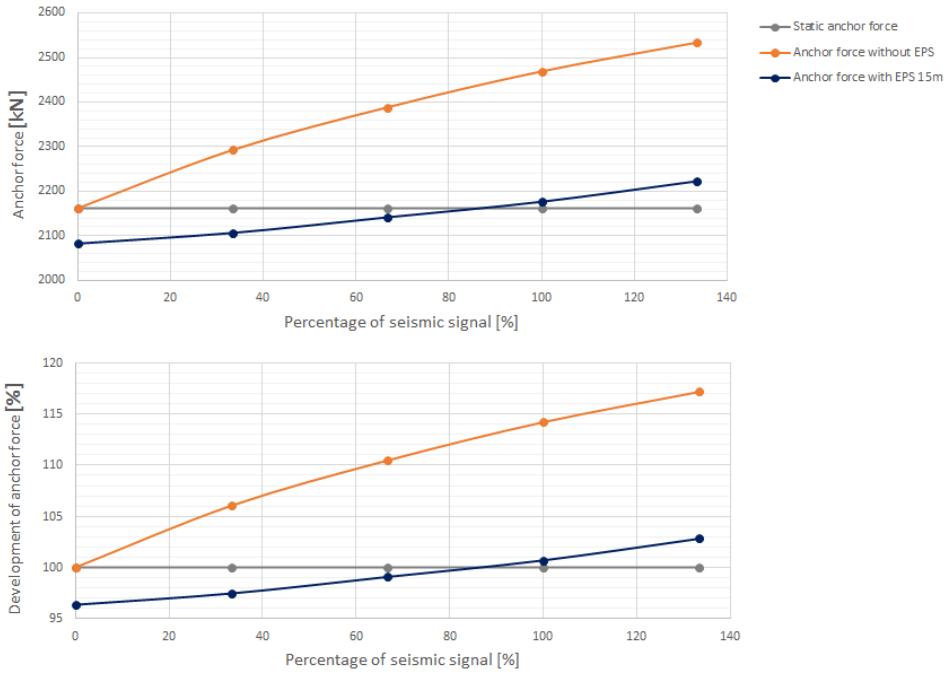

Figure 5.15: Development of anchor force with applied improvement measure

Three lines are visible from the presented graphs in Figure 5.15. On the x-axis a percentage of magnitude related to the design signal is given. The original magnitude of the design signal is described as the 100% value. The upper graph presents the anchor force in [kN] on the y-axis whereas the lower graph a percentage of anchor force development presents for different seismic magnitudes. The horizontal grey line represents the static anchor force without an earthquake. The orange line presents the increase of anchor force in case no improvement measure is applied. The 100% value of the orange line is equal to the earlier presented dynamic anchor force in Section 3.3.4. To prevent the anchor force to develop as presented with the orange line, lightweight material like EPS is used. As a result of using EPS with the dimensions from above, the anchor force develops as presented with the blue line. A reduction of anchor forces due to lightweight material is observed during an earthquake. The original increase of 14% is reduced to an increase of 1% for the design earthquake which is quite effective.

Applicability of improvement

From the results regarding the effectiveness of the measure, it is important to briefly observe other criteria which influence the applicability. A comment is made using three criteria from the trade off matrix, i.e. technical risk, constructibility and maintenance of functions.

The *technical risk* of installing EPS is low because of the relatively simple technique. The position of cables and pipes within three meters below surface level should be know and damage should be avoided during construction. Applying EPS is a proven technology as foundation for roads. The most critical

component of applying EPS is to ensure sufficient bearing capacity. A unity check regarding the pressure strength of EPS is presented in Appendix **F.3.3.** and indicates sufficient safety. The durability of EPS should be determined before installation, to prevent damage at a later stage. The *constructibility* of applying EPS is straight forward. Installation of the material requires an excavation of the existing pavement area which is seen as the major drawback of this measure. After construction, the initial *functions* of the quay area are still present if sufficient pressure capacity of EPS is guaranteed. During construction, a temporary lost of quay functions is expected. This can however be minimized in case of strategic construction planning.

Cost estimation and optimisation

The reduction percentage of anchor force during an earthquake due to 15 meters soil replacement for EPS material is presented in Figure 5.15. It is of interest to investigate the influence between the applied EPS width and the corresponding anchor force development, because this might influence the construction costs significantly. The thickness of 2.5 meters EPS is assumed constant due to the expected high ground water level. Figure 5.16 presents the corresponding anchor force developments for different width applications of EPS, i.e. 5, 10 and 15 meters of EPS.

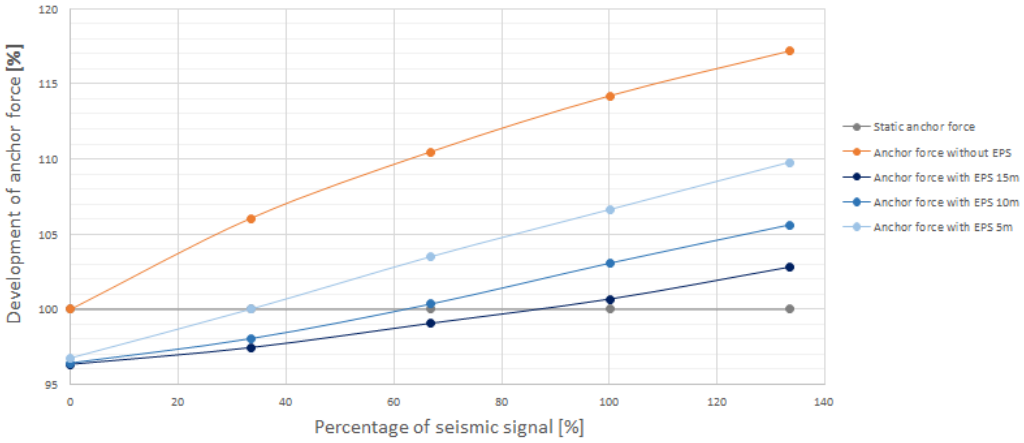

Figure 5.16: Development of anchor force for different application volumes of EPS

From Figure 5.16 the relation between the amount of EPS and the reduction of anchor forces becomes visible. Less EPS results in higher anchor forces. Optimisation of the applied EPS width should be related to an estimation of corresponding construction costs. The estimation of the costs for the different dimensions of EPS is given in Table 5.1. The presented costs are further elaborated in Appendix **F.3.4**. The volume of EPS influences the construction costs significantly. Applying a larger width results therefore directly to higher construction costs.

Applied EPS width	Total construction costs	Total construction costs/m quay
EPS 5 meters	1,106,806 *euro*	3162 *euro/m*
EPS 10 meters	2,184,902 *euro*	6243 *euro/m*
EPS 15 meters	3,262,998 *euro*	9323 *euro/m*

Table 5.1: Cost estimation of lightweight material (EPS) improvement

In addition to the estimated costs, the determination of sufficient EPS width is also depending on the desirable Factor of Safety (FS) for the existing anchor. The factors of safety regarding the existing anchors are approached as the factor between the serviceability resistance and load during a design earthquake. The values are presented in Figure 5.17. In this figure, the anchor force is presented on the y-axis. In this way, the force development can be compared with the assumed anchor resistance during an earthquake as described in Section 5.1.

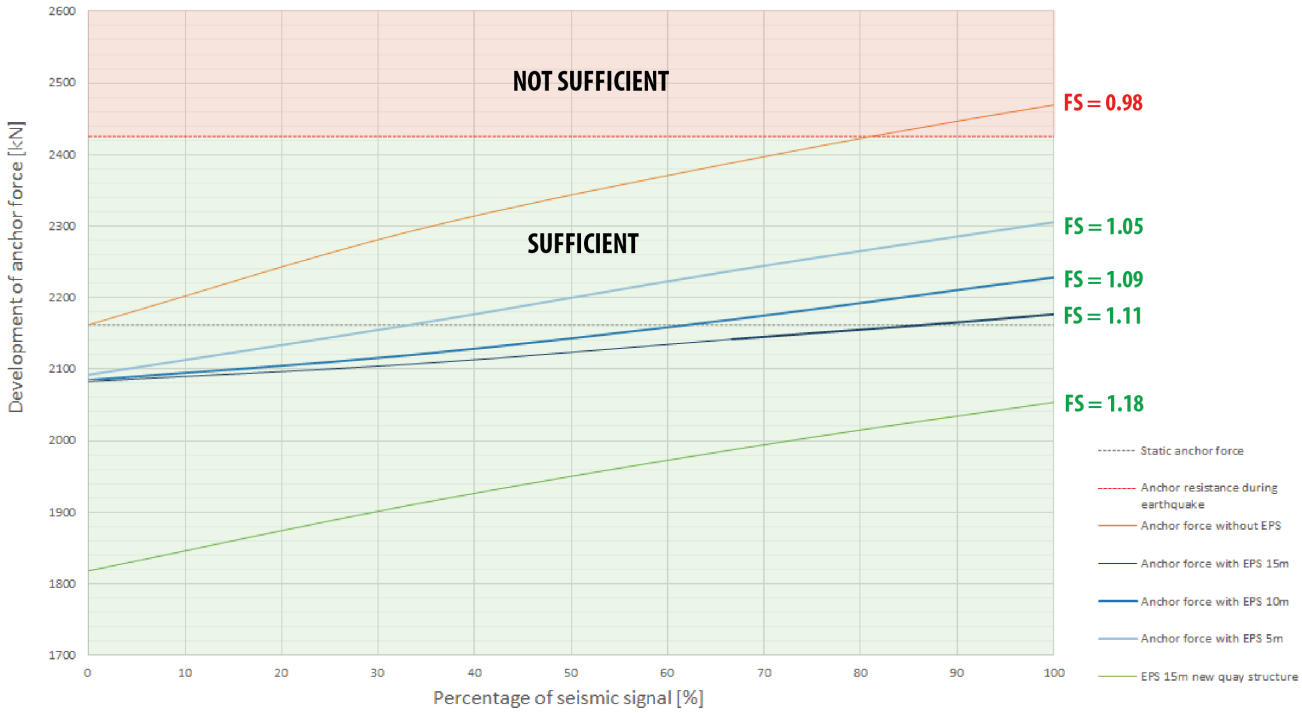

Figure 5.17: Development of anchor force including factors of safety

Equally to Figure 5.16, the orange line presents the force development without the use of EPS. The three blue lines visualise this development for different EPS volumes. The reduced resistance of the grout anchor from Figure 5.2 is presented with the horizontal red line. This line will in reality not be straight but curved. The quantitative reduction value for the grout resistance is only determined for the design earthquake magnitude, i.e. the 100% value, and no values for lower magnitudes are know. A straight line is therefore initially assumed for the resistance.

It can be concluded that that all three EPS volumes have a positive effect regarding the estimated factor of safety. The FS value of 0.98, which indicates possible failure is increased to a value larger than 1 as a result of applying EPS. Please note the factors of safety are based on the Serviceability Limit State (SLS), so without the use of load and resistance factors.

In addition to the investigation of applying EPS to the existing structure, also the effect of lightweight material for a new retaining structure is briefly observed. The anchor development for a new structure combined with EPS, as a result of different earthquake magnitudes, is presented with the green line in Figure 5.17. The governing difference between the green and blue lines contains the static anchor force before an earthquake has appeared. Lower deformations and internal forces are observed due to a reduced mass behind the structure. For a new quay structure this results in lower static anchor forces. For an existing structure, deformations and internal forces from the past are of influence. Less effect of EPS on the static state is therefore observed.

5.5. Install relieving floor behind existing wall

In addition to the improvement with lightweight material from Section 5.4, the suitability of installing a relieving floor behind the existing quay structure is obtained. Multiple different lay-outs and dimensions of relieving structures do exist. To improve the existing structure, two types, i.e. a high and low relieving floor, will be observed. A high relieving structure consists of a horizontal concrete floor at surface level and is founded on piles. The low relieving structure is positioned three meters below surface level and is build in the shape of an L-wall, illustrated in Figure 5.18. Again, the concrete floor is founded on piles to bear the vertical loads from the floor and soil above the wall. The goal of installing a relieving structure is to reduce the acting horizontal loads on the wall. Transfer of vertical surface and soil loads to the deeper positioned sand layers through the piles below the floor contribute to realisation of this goal. A reduction in horizontal loads results in lower anchor forces.

Again, the main focus during elaboration of this measure is to determine whether the applied method is effective. The effect is measured with the magnitude of anchor force reduction. This is obtained for both the low and high relieving floor.

The applicability elaborates the criteria technical risk, constructibility and influence on functionality. This section will be concluded with an initial cost estimation of the proposed measure. The suitability of the improvement can be initially determined by comparing the construction costs to the corresponding effectiveness of the improvement.

Effect of improvement

The effect of the installed relieving floor depends on the amount of vertical load transferred to lower sand layers. The low position relieving floor from Figure 5.18 transfers both the surface load and three meters of soil mass to the subsoil below the active wedge. The high position floor at surface level transfers only the surface loads at the quay to the sub soil. The effectiveness of a low position relieving floor is therefore assumed to be larger than the high position floor.

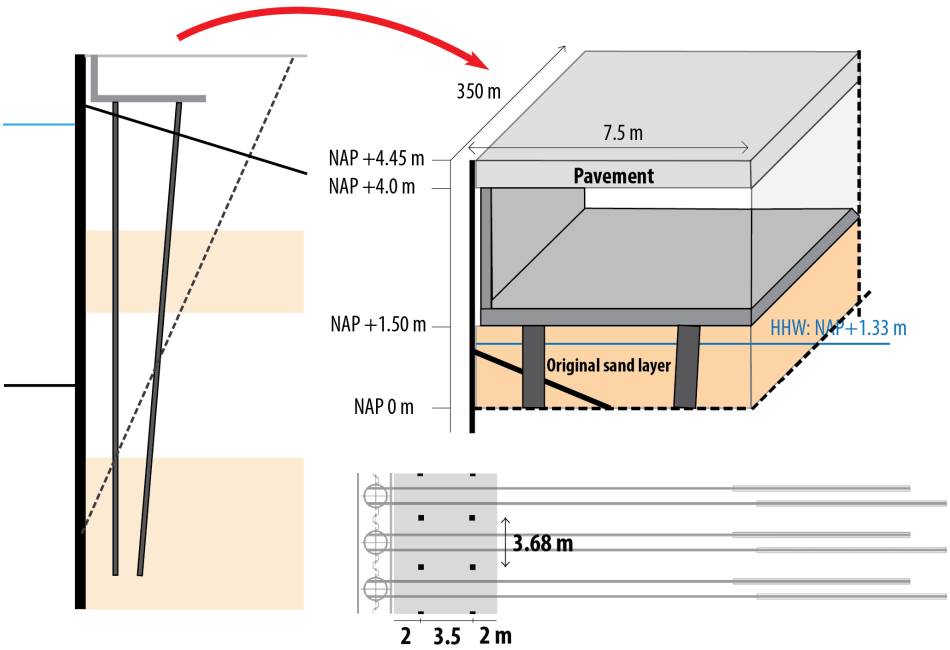

Figure 5.18: Visualisation of relieving floor

As a starting point, the floor width is assumed to be 7.5 meters. The floor of the L-shaped structure is positioned at a depth of NAP +1.50 m. This level is higher than the ground water, which prevents drainage during construction.

To investigate the effectiveness of the measure, the relieving structures are again modelled in the PLAXIS model from Chapter 3. For information about the applied parameters, a reference to Appendix **F.4.1.** is made. The results regarding the anchor force and development of this force are presented in Figure 5.19. The x- and y-axis are equal to Figure 5.15 from the results of EPS in Section 5.4. On the x-axis a percentage of magnitude related to the design signal is given. The original magnitude of the design signal is described as the 100% value. The upper graph presents the anchor force in [kN] on the y-axis whereas the lower graph a percentage of anchor force development presents for different seismic magnitudes.

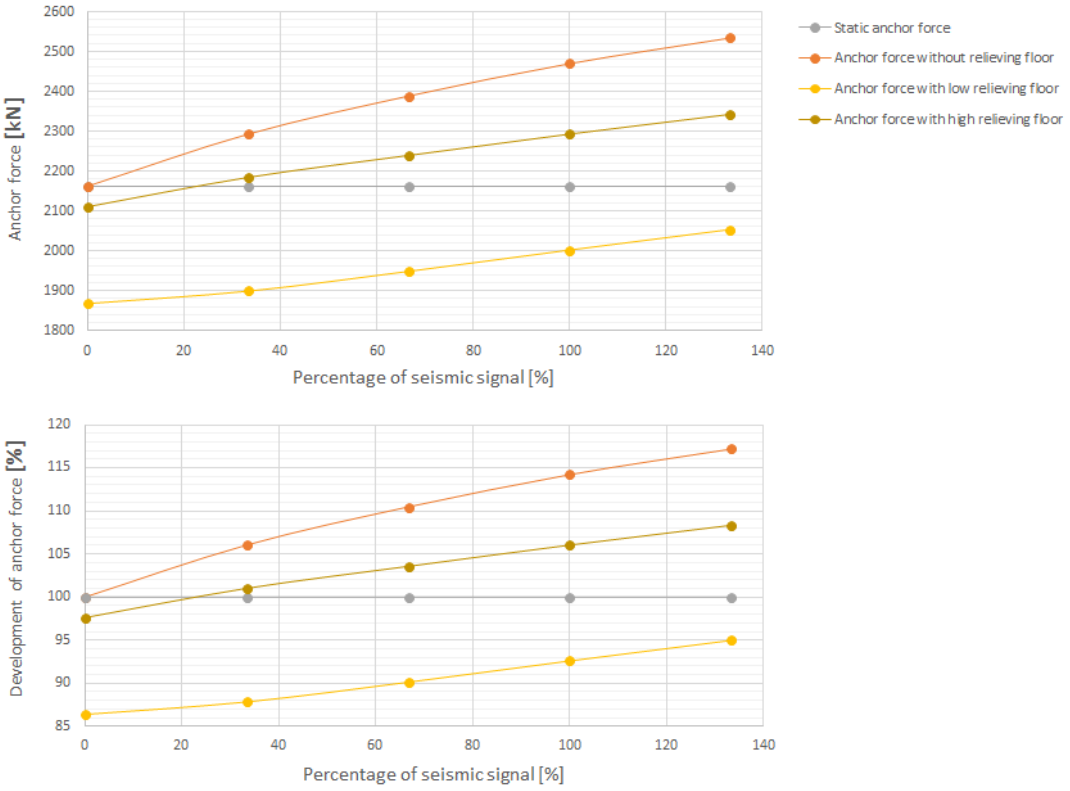

Figure 5.19: Application of relieving floor

The horizontal grey line represents again the static anchor force without an earthquake. If no improvement measure is applied, the anchor force will develop as expressed with the orange line. The influence of the relieving structure during an earthquake is visualised with the two yellow lines. The effectiveness of the low position relieving floor, presented with the light yellow line, is significant compared to the effect of the high position floor, defined with the darker yellow line. It is concluded that both structures contribute positively to the anchor force development for different seismic intensities. The original anchor force increase of 14% with respect to the static anchor value is reduced to an increase of 6% and even a reduction of 7% for the design earthquake.

Applicability of improvement

From the results regarding the effectiveness of the relieving floor, it is again important to briefly observe other criteria which influence the suitability of the improvement. A comment is made using three criteria from the trade off matrix, i.e. technical risk, constructibility and maintenance of functions.

The *technical risk* of constructing a relieving floor is relatively low, because it is a proven technology. The piles below the structure should contain sufficient strength capacity to transfer the vertical loads acting on the floor outside the active wedge. The relieving floor will not be attached to the existing vertical wall. A small space between wall and relieving structure will be filled with elastic material, e.g. rubber or EPS with low stiffness, causing additional damping during the earthquake. The connection

between piles and concrete floor is assumed sufficient to withstand the dynamic forces. Engineering of the concrete structure and connections is not included in this research.

Installation of the piles is an important aspect regarding the *constructibility* of the improvement. The concrete relieving floor will be placed on two piles as schematically visualised in Figure 5.18. The right pile will be installed under a small angle to enlarge the horizontal capacity of the relieving structure. The piles are installed close to the existing wall. Two types of piles are therefore proposed during this initial design stage. Both pile types, i.e. concrete prefab pile and a fundex pile, will be installed using a different installation method. The prefab concrete pile will be brought to the required depth due to piling, causing vibrations in the surrounding soil. Vibration free installation is achieved using fundex piles. The type of pile and possible installation method should be further optimised in a more detailed design stage. From initial calculations regarding the bearing capacity using the software D-foundations, the prefab concrete pile with dimensions 0.45*0.45 m should be installed to NAP -28 meter to guarantee sufficient bearing capacity. If vibration free installation is required, a fundex pile with a base diameter of 0.56 meter should be installed to NAP -28.5 meter. Reference to Appendix **F.4.2.** is made for performed calculations behind the proposed dimensions.

Equal to the EPS improvement, a temporary lost of quay *function* is present during construction of the relieving floor. A significant advantages of the relieving floor improvement relates to added functions after construction. Higher surface loads are possible if the existing structure is combined with a relieving structure. In addition to the increased allowable surface loads, it is also possible to deepen the bottom level to allow larger vessels at the quay.

Cost estimation

The difference between a high and low position relieving floor is made, to determine the difference regarding the effectiveness. To substantiate a comment on the suitability of both relieving floors, the corresponding construction costs should be included. Table 5.2 presents the results from an initial cost estimation and distinguishes the high and low positions floor in combination with prefab concrete piles and fundex piles. The total construction costs refer to the complete quay length of 350 meters from phase four, elaborated in Section 2.3.1.

Type of floor	Total construction costs	Total construction costs/m quay
HF,PP*	1,091,525 *euro*	3118 $euro/m$
HF,FP**	1,478,203 *euro*	4223 $euro/m$
LF,PP***	1,563,742 *euro*	4468 $euro/m$
LF,FP****	1,910,383 *euro*	5458 $euro/m$

Table 5.2: Cost estimation of relieving floor improvement

* High relieving Floor, Prefab concrete Piles
** High relieving Floor, Fundex Piles
*** Low relieving Floor, Prefab concrete Piles
**** Low relieving Floor, Fundex Piles

The presented costs from Table 5.2 are elaborated in Appendix **F.4.3**. Costs for the different type of piles do influence the construction costs. A low position relieving floor becomes more expensive due to additional excavation and the required concrete wall.

The corresponding Factors of Safety (FS) of the improvement for both floors should be obtained and compared to the estimated construction costs. This can be observed from Figure 5.20. The effectiveness of the EPS improvement is also presented on the background to visualise a comparison between both improvement measures.

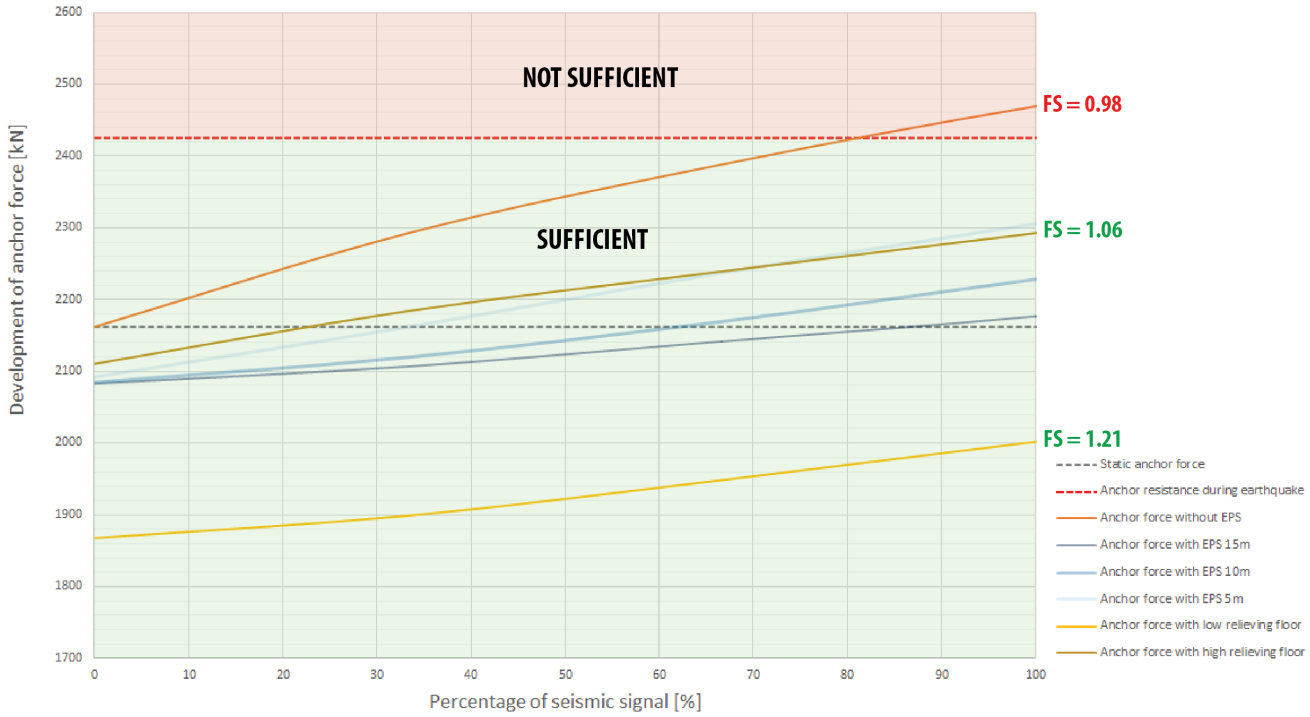

Figure 5.20: Development of anchor force with relieving floor

The effectiveness of the high position relieving floor is comparable to the EPS improvement of 5 meters width. The low position relieving floor provides however significantly more safety regarding the installed anchors.

5.6. Conclusion of quay structure improvement

This chapter elaborates on possible quay structure improvements, as a result of the initial conclusion regarding a reduced safety rating. The goal of an improvement measure is to increase the safety of the existing structure during an earthquake with respect to the installed grout anchors. Ten different improvement measures have been proposed in Section 5.2. To determine the most suitable improvements from the knowledge in this design stage, a trade off matrix is applied. Using five criteria to evaluate the improvement measures qualitatively, two proposed measures have been assessed without a major drawback. These two measures, i.e. applying lightweight material and installing a relieving structure behind the existing quay, have been worked out to provide insight in the effectiveness and corresponding construction costs. The remaining eight measures might be applicable as well, but require more research regarding a specific criteria, elaborated in Section 5.3, to comment on the possible suitability. These eight measures are therefore not further observed in this research.

Insight regarding the reduced safety during an earthquake is required to comment on the effectiveness of the proposed measures. Section 5.1 elaborates therefore on the reduced safety of the existing quay structure by taking into account the result from Chapter 3 and 4. This effect is visualised in Figure 5.2. From the determined factor of safety in static and dynamic state, expressed as the ratio between the anchor resistance and force, a significant safety reduction is observed during an earthquake. To prevent this reduction, improvement measures have been proposed. It is concluded that both measures from Section 5.4 and 5.5 contribute positive towards the anchor force development during an earthquake. A reduction of anchor force development results in a higher factor of safety, which is a desirable effect. To conclude on the suitability of the two measures from Section 5.4 and 5.5, a brief evaluation of the results is presented below.

Evaluate results of both improvement measures

To evaluate on the suitability of the two selected improvement measures, the criteria from the trade off matrix have been used in Section 5.4 and 5.5. To compare the results from both improvements, the effectiveness and corresponding costs to achieve the effect have been evaluated, presented in Figure 5.21.

The effectiveness of 5 meter soil replacement behind the existing quay for EPS material is quite comparable to the effectiveness of a high position relieving floor. Also the costs between these two different measures are in the same order of magnitude. The costs for larger EPS volumes do however influence the construction costs significantly. The high price per volume for high quality EPS material, which is required to withstand the surface loads, results in significantly higher cost. Applying EPS material over a width larger than 5 metes is therefore observed not be economical due to the relatively small additional effectiveness for these larger EPS widths. Comparing the effectiveness and corresponding costs of a low position relieving floor, i.e. 3 meters below surface level, indicates the favourable effect of decreased loads from a relieving structure. Lower construction costs and the possibility for additional quay functions are the result of a low position relieving floor in comparison to 10 or 15 EPS application. If a high position floor or comparably 5 meters of EPS do not deliver sufficient reduction in anchor force, a low position relieving floor is advisable.

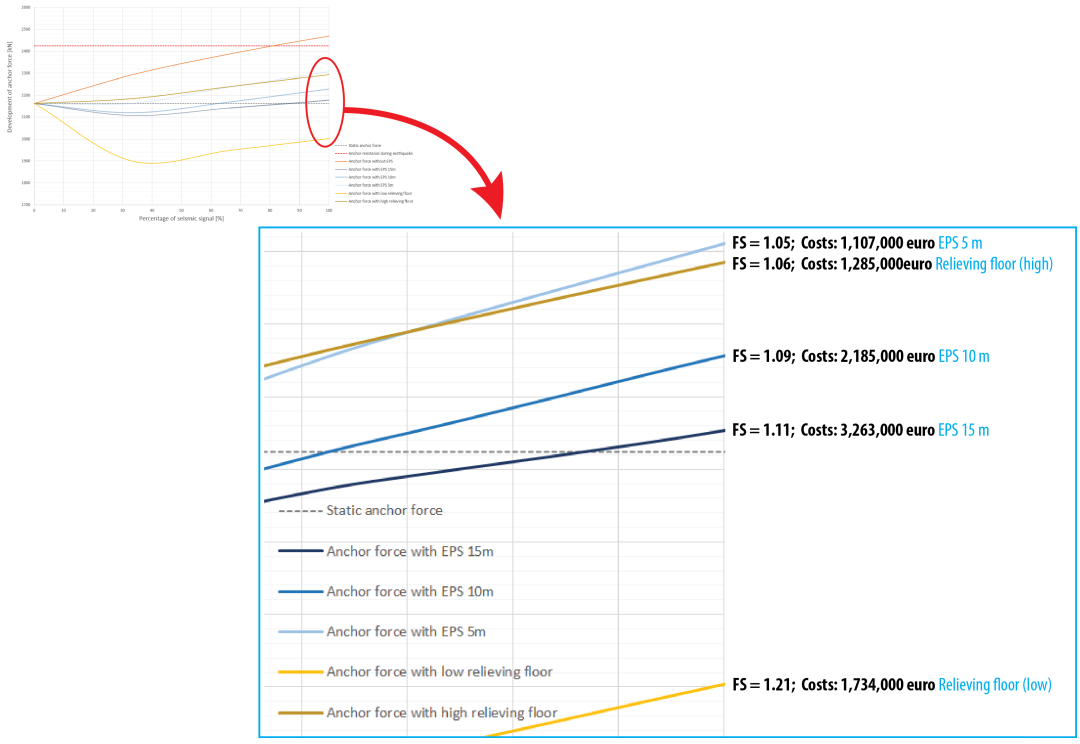

Figure 5.21: Overview of improvement measures including effectiveness and corresponding costs

To comment on which improvement measure is the most suitable application, several aspects should be taken into account. The most important decision is to decide whether quay improvement is required at all. The reduced safety from Figure 5.2 provides an indication to formulate an answer to this initial question. A more reliable visualisation of the reduced safety might be found from a probabilistic method, instead of the applied deterministic method. In this way, the reduced safety can be coupled to a certain desired exceedance probability. The required safety increase from an improvement measure could than be selected to guarantee sufficient safety for an acceptable exceedance probability. In addition to the attainable effectiveness and corresponding construction costs of a measure, the applicability, which refers to the technical risk, constructibility and functionalility of the measure, should also be taken into account.

6

Conclusions and recommendations

At the start of this research the following research question was defined:

"Are modifications to the existing combined walls in the Groningen Seaport required and applicable to resist seismic loading from induced earthquakes?"

To gain sufficient understanding to answer this question, the defined sub-questions are elaborated during this research. This chapter will reflect upon the research question by providing the conclusions and recommendations, presented in the sections 6.1 and 6.2.

6.1. Conclusions

Insight regarding the research question and proposed sub-questions is gathered from the preceding chapters of this report. Four main conclusions from this research are summed up and elaborated in the paragraphs below. The final paragraph reflects on the main research question.

- *Conclusion [1]*
  From the observed aspects during the assessment on current state, in which the influence of an induced earthquake towards an existing combined wall is investigated, the increased anchor forces appear to be most critical during an earthquake.
- *Conclusion [2]*
  An initial investigation of the grout anchor resistance during an earthquake is performed. A qualitative reduction of shear stress between soil and grout body is observed during an earthquake. This effect is quantitatively expressed with a possible anchor resistance reduction of about 25 %. A decrease of anchor resistance during an earthquake is observed, which redevelops afterwards due to dissipation of excess pore pressures.
- *Conclusion [3]*
  A reduced safety rating for the existing quay structure of Groningen Seaport is observed. The corresponding factor of safety, defined as the ratio between anchor resistance and anchor force, becomes temporary lower than 1 for the assumed load combination during an earthquake. The question whether failure of the existing quay structure due to an earthquake appears, depends on the present load components which are acting on the structure simultaneously with the earthquake. The assumed combination during this research is assumed to be quite conservative. Including proper reduction factors or a probabilistic approach for the governing load combination would provide a more realistic view regarding the possible failure.
- *Conclusion [4]*
  Due to the uncertainty regarding possible failure of the existing structure, two of ten proposed improvement measures have been elaborated and assessed on their effectiveness. Applying lightweight material and installing a relieving floor behind the existing wall are determined to be effective

and applicable. If a large effectiveness and increase of the factor of safety is required, the low position relieving floor is recommended. For a cheaper, but less effective measure the high position relieving floor or 5 meters of EPS is a possible solution to install behind the wall

Elaboration of conclusion [1]
The effect of an induced earthquake regarding the existing combined quay wall structure was observed using a pseudo static and dynamic approach. The pseudo static approach is performed as a simplified method. Horizontal loads, representing the earthquake force with an acceleration of 2.6 m/s^2 and a return period of 800 years, are added to the static D-sheet model. The increase of bending moments and anchor forces in the existing structure tend to create the first appearing failure mechanism. This approach is considered to be conservative due to the large simplifications. Initial insight is gathered from this approach, but no decisions can be made from the output values.

A more reliable method is performed using a dynamic approach. In this approach a finite element method is applied using PLAXIS, which includes a seismic design signal and the soil-structure behaviour in a more realistic manner. From the results regarding non-linear soil response, a more reliable model for loading on the existing structure is made. Due to an earthquake, the bending moments increase with 11% and the anchor force becomes 15% higher. From a brief comparison with the resistance values of the structural elements, the increased anchor force reveals to be critical, specifically the grout body resistance. This result is observed for three different seismic signals.

Please note that the occurrence of liquefaction is assumed not to occur and not taken into account during the assessment. This assumption is made during literature and based on the determined factor of safety using the Robertson method. If liquefaction does occur, the influence regarding the stability is large. Major quay damage as observed in the past is often the result of liquefied soil behind the quay. The effective soil stresses decrease significantly which results in a lower resistance force of the anchors, as explained in Chapter 4. The influence of liquefaction should therefore be kept in mind and further elaborated during additional research.

Elaboration of conclusion [2]
To determine the first occurring failure mechanism, the indication regarding the critical state of the anchors is further investigated. The analysis points to fact of an increased anchor force, but excludes the development of anchor resistance during an earthquake. An initial investigation of anchor resistance during an earthquake is therefore performed. The comparison between findings from literature and results from a finite element model did correspond and confirmed the initial investigation assumptions. A qualitative reduction of shear stress between soil and grout body is observed during an earthquake. This effect is quantitatively expressed with a maximum anchor resistance reduction of 25 %. This value can only be considered as an initial indication. Many assumptions and variables are used for the determination of this value. The original anchor resistance will redevelop within about 7 minutes after the appearance of an earthquake. The observed excess pore pressures, which cause the temporary anchor reduction, disappear in time without seismic activity. The observed reduction in anchor resistance during an earthquake could be added to the fault tree in Figure 2.19 under the points [2/3]. Additional research is required to define the exact location in the existing fault tree.

Elaboration of conclusion [3]
The expected behaviour of the quay structure under dynamic loading can be summarised as an increase in anchor force and a decrease in resistance ability during earthquake events. This results in a reduced safety rating for the existing quay structure of GSP. The corresponding factor of safety, defined as the ratio between anchor resistance and anchor force, becomes lower than 1. This might lead to failure of the quay structure, due to failure of the anchor system. The factor of safety is however based on a design load conditions, which includes a combination of multiple load components. Generally, this design combination includes loads from presents soil and water behind the quay, surface loads over the complete quay width and loads from a moored vessel. The influence from the design surface load of 60 kN/m^2 regarding the anchor force appears to be large. The question whether failure of the existing quay structure appears is therefore depending on the present load components during an earthquake. In case a vessel is moored at the quay in combination with the design surface load, local anchor failure occurs if the design earthquake appears. If the design earthquake force is combined with a reduced surface load or without a moored vessel, the factor of safety remains larger than 1 and no failure of existing anchors seems to appear. The appearance of an earthquake with the assumed design

magnitude is also questionable. Including proper reduction factors for the governing load combination would provide a more realistic view regarding the possible failure. An initial estimation of anchor movement is made using an energy balance with kinetic energy and work energy. Each velocity peak creates an impulse towards the wall which should be absorbed by the grout anchor. Including all simplifications of this method, an anchor displacement of 12.5 mm is determined. The findings from this research with respect to the anchor resistance is also applicable towards other quay structures, if comparable boundary conditions are taken into account.

Elaboration of conclusion [4]
Due to the uncertainty regarding possible failure of the existing structure, several improvement measures have been proposed. The goal of an improvement measure is to increase the safety of the existing structure during an earthquake with respect to the installed grout anchors. Two of the ten proposed measures have been elaborated in more detail. This selection is performed using a trade off matrix. Applying lightweight material by using Expanded Polystyrene (EPS), seems to be effective during an earthquake but includes high construction costs due to a high price of EPS per cubic meter. The second proposed improvement measure relates to anchor force reduction from a high or low position relieving floor. A high position relieving floor is comparable in costs and effectiveness with 5 meters of EPS. The effectiveness of a low position relieving floor is large and cheaper than 10 or 15 meters EPS width. If a large effectiveness and increase of the factor of safety is required, the low position relieving floor is recommended. For a cheaper, but less effective measure the high position relieving floor is a recommended solution. Applying EPS includes uncertainty regarding the deliverable pressure strength of the material if a surface load of 60 kN/m^2 is acting on the quay for a longer period of time. A relieving floor does not include this uncertainty due to the pile foundation and might even introduce additional functions to the quay, e.g. higher surface loads during daily use or enlargement of the quay depth for larger vessels. The installed relieving structure itself is assumed to be able to resist the occurring dynamic loads.

An initial answer regarding the research question can be substantiated from the presented results. The question whether modifications are required depends on the assumed acceptable load scenario. If the combination of the design load scenario, i.e. *maximum surface load* and a *moored vessel*, with a *design earthquake* for the near collapse state are observed as representative, failure of existing anchors might occur. This load combination seems to be conservative compared to daily use of the quay. If reduction factors are included for the surface load, the anchors will probably be affected by the earthquake but will not fail. The decision for modification of the existing quay depends therefore mainly on the assumed representable load combination. The assumed earthquake magnitude for the near collapse state corresponds to a return period of 800 years. Assuming the existing quay structure to stay operational for another 40 years, the probability of occurrence of the design earthquake during lifetime is about 5%. Including the suggested load combinations from Section 5.1 decrease the acting loads and might prevent the proposed investment between 1 and 3 million Euro. The decision to modify the existing quay is also depending on economical aspects and should be made by Groningen Seaports.
The applicability of the proposed measures do not indicate large uncertainties. The pressure strength, both short and long term, of EPS includes however some assumptions regarding the performed unity check. Installing a relieving floor is therefore observed to be preferable for this level of engineering.

6.2. Recommendations

As mentioned in the introduction, the occurrence of seismic events in the Groningen area is relatively new. As we speak, the influence of induced earthquakes on existing houses and buildings is broadly being investigated. The effects of these induced earthquakes with respect to existing quay structures are still unknown. The presented study has provided initial insights in the potential failure mechanisms. However, many new uncertainties and questions arised during this research. Including the recommendations for future research as presented below create more insight in these uncertainties and questions.

- *Validate results from dynamic approach*
  In this study, a finite element model in PLAXIS has been used to visualise the influence of an earthquake. The applied seismic signals at the base, which are gathered from measurements during the earthquake in Huizinge, should be compared with the published design signals for the induced earthquakes in Groningen. These signal have only been published just recently. Measurement results from the soil response of the upper soil layer during an earthquake are required to validate the modelled soil response. This validation is strongly advised, because the soil response from an earthquake was found to have a large influence on the output. If no measurement data can be gathered, additional sensitivity checks regarding the applied input parameters are recommended. Measure equipment on the existing quay wall, might provide the most valuable data. Validation between the results of the model and the real behaviour of the existing quay wall during a future earthquake can then be performed.

- *Investigate the influence of an induced earthquake for the 'Serious damage state'*
  This research is based on the 'Near collapse state', which is the state in the current NPR guideline, presented in Section 2.2.1. A return period of 800 years corresponds to the applied PGA values from the assumed CC1B class. The probability of occurrence of this design earthquake is therefore about 5% for the lifetime of the existing structure. Applying the 'Serious damage' state, instead of the 'Near collapse state', provides insight regarding the damage effect during daily use of the quay without assuming complete collapse of the structure after an earthquake has occurred. For the 'serious damage state', lower load values with a higher occurrence probability will be used. The values for the serious damage state are however not yet published for existing structure in Ontw.NPR9998 (2015). Recalculation with this design state may lead to lower effects and makes the approach more applicable regarding the effects for daily use of the quay. Using the 'serious damage state' besides the 'Near collapse state' corresponds to the design earthquake levels 1 and 2 as recommended in PIANC (2001).

- *Gain insight in reduced quay wall safety from a probabilistic approach*
  The determined factor of safety in this research is gathered from a combination of observed deterministic loads. Including the probability of occurrences from the assumed loads, a corresponding exceedence probability for the assumed factor of safety will be obtained. If the reduced safety is coupled to an exceedance probability, the decision whether to invest in the proposed improvements can be better substantiated.

- *Investigate the influence of an induced earthquake for other type of quay wall structures within GSP*
  During this research one existing quay structure is investigated towards the vulnerability of an induced earthquake. The grout anchors are defined to be the most critical part during an earthquake. The findings from this research with respect to the critical anchor resistance is also applicable to other quay structures. It is however the question, if the other existing structures do find their stability only from their anchors, as is the case for the combined wall. To indicate the possible danger of an induced earthquake for the complete port, additional quay structures should be investigated including the findings from this research.

- *Perform additional research on the liquefaction vulnerability*
  The occurrence of liquefaction may be of great influence regarding the determined safety. The quick check regarding the vulnerability should be substantiated with additional research. After that, a more reliable conclusion regarding the possible occurrence of liquefaction can be made.

- *Improve reliability of determined loads and combination of loads for the Pseudo Static approach*
  The Pseudo Static approach is observed to be quite conservative. Additional calculations should be performed including a more realistic PGA value from the most recent NPR publication. Research regarding the applied M-O method for the pseudo static approach is performed by a master student at the TU Delft at this moment. In this research, it is tried to find a less conservative way of including hydrostatic forces due to excess pore pressure. If a more accurate method is found to include the phenomenon of possible excess pore pressure, the results from the pseudo static method will be less conservative. This will reduce the difference between the output from the pseudo static and dynamic approach.
- *Validate initial results from anchor resistance under dynamic loading*
  More realistic model results regarding the anchor resistance during an earthquake will be gained by using a more advanced model. A 3-dimensional PLAXIS model or a discrete element model are recommended to apply. Performing model tests regarding the resistance behaviour of a grout body during dynamic loading of soil and anchor is highly recommended. This can be executed by laboratory test on smaller scale, or during a failure test of an existing anchor. A laboratory test is considered to be most realistic, because dynamic loading of soil at real anchor depths is complicated and expensive to realise.
- *Investigate compressive strength of EPS*
  The assumption regarding the compressive strength of EPS (Expanded Polystyrene) should be investigated in more detail, to assure sufficient stability of the pavement area during daily use after installation. The loading conditions, e.g. magnitude and duration, of the existing quay can be tested using a scaled model test. If the compressive strength of EPS is not sufficient, application of XPS (Extruded Polystyrene) which contains higher strengths is recommended.

Bibliography

Het ontwerpen van grondconstructies met geavanceerde modellen, syllabus, PAO, 2002.

Analysis of seawal concepts using yielding soil anchors, powerpoint presentation, ASCE, 2010.

Aaboe, R. 40 years of experience with the use of eps geofoam blocks in road construction. Technical report.

Airey, D.W.; Al-Douri, R. H., and Poulos, H.G. Estimation of pile friction degradation from shearbox tests. *American Society for Testing and materials*, 1992.

Alliance, EPS Industry. Expanded polstyrene (eps) geofoam applications and technical data. Technical report.

Boulanger, R.W. and Idriss, I.M. Liquefaction susceptibility criteria for silts and clays. *Geotechnical and Geoenvironmetal Engineering*, 2006.

BS-part2, . Bs 6349-2:2010 maritime works - part 2: Code of practice for the design of quay walls, jetties and dolphins. Technical report, 2010.

CUR166-1, . *CUR 166 Damwandconstructies part 1,* 6^{th} *editon.* CUR Bouw & Infra, 2012.

CUR166-2, . *CUR 166 Damwandconstructies part 2,* 6^{th} *editon.* CUR Bouw & Infra, 2012.

CUR2001-4, . *Ontwerpregels voor trekpalen.* Civieltechnisch Centrum Uitvoering Research en Regelgeving, 2003.

CUR236, . *Ankerpalen.* CUR Bouw & Infra, 2011.

D-sheet, . Design of diaphragm and sheet pile walls, d-sheet piling user manual 9.3. Technical report, December 2013.

Database, DEM Literature. Discrete and continuum modelling of soil cutting, 2016. URL `http://www.dem-solutions.com/papers/discrete-and-continuum-modelling-of-soil-cutting/`.

de Gijt, J.G. and Broeken, M.L. *Quay walls, second edtion.* SBRCURnet Publication 211E, 2014.

de Groot, M.B.; Stoutjesdijk, T.P.; Meijers, P., and Schweckendiek, T. Verwekingsvloeiing in zand. *Geotechniek*, 2007.

de Jong, K.; Kaspers, E.; Hartmann, D., and van der Stoel, A. Praktische overwegingen bij de npr9998, jaargang 19 nummer 3. Technical report, July 2015.

Dost, B.; Caccavale, M.; van Eck, T., and Kraaijpoel, D. Report on the expected pgv and pga values for induced earthquakes in the groningen area. *KNMI*, December 2013.

Dung, P.H. Modelling of installation efect of driven piles by hypoplasitcity. Master's thesis, Delft University of Technology, 2009.

Elragi, A.F. *Selected Engineering Properties and Applications of EPS Geofoam.* PhD thesis, 2006.

GEOblock, Productblad. Geoblock sterktecijfers, versie 17082009. Technical report.

GSP, . Website groningen seaport. URL `http://www.groningen-seaports.com/DeHavens/Eemshaven/tabid/2154/language/en-US/Default.aspx`.

Habets, C.J.W. Performance-based seismic analysis of an anchored sheet pile quay wall. Master's thesis, Delft University of Technology, 2015.

Harmelen, Ingenieursburea. Ankerberekening tbv project julianahaven fase 4, groningen. Technical report, 2010.

Hashash, Y.M.A. User manual deepsoil 6.0. Technical report, July 2015.

Kramer, S.L. *Geotechnical Earthquake Engineering.* Prentice-Hall, 1996.

Lunne, T. and H.P., Christoffersen. Interpretation of cone penetrometer data for offshore sands, otc 4464. 1983.

Meijers, P. and Steenbergen, R.D.J.M. Handreiking voor het uitvoeren van studies naar het effect van aardbevingen voor bedrijven in de industriegebieden delfzijl en eemshaven in groningen, versie 4 juli. Technical report, 2015.

NEN-EN:14933-2007, . European standard, thermal insulation and light weight fill products for civil engineering applications- factory made products of expanded polystyrene (eps) - specification. Technical report, 2007.

NEN-EN:1990NB, . Nationale bijlage bij nen-en 1990+a1+a1/c2: Euro: Grondslagen van het constructief ontwerp. Technical report, 2011.

NEN-EN:1991-1-1, . Nederlandse norm, eurocode 1: Belastingen op constructies - deel 1-1: Algemene belastingen - volumieke gewichten, eigengewicht en opgelegde belastingen voor gebouwen. Technical report, 2011.

NEN-EN:1997-1, . Nederlandse norm, eurocode 7: Geotechnisch ontwerp - deel 1: Algemene regels. Technical report, 2012.

NEN-EN:1998-5, . Nederlandse norm, eurocode 8: Ontwerp en bereking van aardbevingsbestendige constructies - deel 5: Funderingen, grondkerende constructies en geotechnische aspecten. Technical report, 2005.

N.Kraaijeveld, . Constructieberekening, alternatief combiwand julianahaven fase 4, groningen. Technical report, 2010.

Ontw.NPR9998, . Nederlandse praktijkrichtlijn, grondslagen voor aardbevingsbelasting: geinduceerde aardbevingen. Technical report, Feb 2015.

Pater, R. and Smeenge, D.J. Aardbevingbestindigheid van onderdoorgangen. Technical report, 2015.

PIANC, . Seismic design guidelines for port structures. Technical report, 2001.

PLAXIS-1, . Tutorial manual plaxis 2d. Technical report, 2015.

PLAXIS-2, . Reference manual plaxis 2d, anniversary edition. Technical report, 2015.

PLAXIS-3, . Scientific manual plaxis 2d, anniversary edition. Technical report, 2015.

PLAXIS-4, . Material models plaxis 2d. Technical report, 2015.

Productblad, BAM. Groutankers, bam speciale technieken: Bst4-300. Technical report, 2012.

Robertson, P.K. Robertson's remarks evaluation of cyclic softening in clays. May 2008.

Robertson, P.k. and Cabal, K.L. *Guide to Cone Penetration Testing for Geotechnical Engineering, 6th edition.* 2015.

Rotterdam, Gemeente. Waalbrug nijmegen, referentieontwerp. Technical report, 2012.

Scientias, . Interview met geofysicus rob govers, 2013. URL `http://www.scientias.nl/aardbevingen-door-gaswinning-wat-is-het-probleem-nu-eigenlijk/`.

Shunichi, H.; Kenichi, M.; Yasushi, N.; Yoshiyuki, M.; Takahiro, S.; Yoshiaki, K.; Masami, H., and Kazuhiro, H. Evaluation of the seismic performance of dual anchored sheet pile wall. 2012.

Sorensen, K.K and Okkels, N. Liquefaction susceptibility criteria for silts and clays. *Geotechnical and Geoenvironmetal Engineering*, 2013.

Stybenex, . Rekenvoorbeelden constructieve toepassing eps. Technical report.

TNO, . Tno bouw en ondergrond, geïnduceerde aardtrillingen groningen veld. *Geotechnical and Geoenvironmetal Engineering*, October 2009.

USGS, . Earthquake hazards 201, technical q and a, 2014. URL http://earthquake.usgs.gov/hazards/about/technical.php.

van den Ham, G.A.; de Groot, M.B., and van der Ruyt, M. Handreiking toetsen voorland zettingsvloeiing t.b.v. het opstellen van het beheerdersoordeel (bo) in de verlengde derde toetsronde. Technical report, 2012.

Visschendijk, M.; Meijers, P.; van der Meij, R.; Coelho, B.Z., and de Bruijn, H. Aardbevingsbestendigheid kades noordzijde eemskanaal, bijlage 2. Technical report, 2014a.

Visschendijk, M.; Meijers, P.; van der Meij, R.; Coelho, B.Z., and de Bruijn, H. Aardbevingsbestendigheid kades noordzijde eemskanaal, bijlage 1. Technical report, 2014b.

Withe, D.J. and Lehane, M.B. Friction fatigue on displacement piles in sand. *Geotechnique*, 2004.

A

Information from Literature study

This appendix elaborates additional information which is gathered during the literature study. The reference projects used for background information are summed up in Section 1.1. The different quay structures from the Eemshaven are presented in Section 1.2. Methods to determine the static and dynamic forces acting on a quay structure are given in Section 1.3. To conclude, Section 1.4 provides information regarding the phenomenon of liquefaction.

A.1. Reference projects for background information

It is important and practical to know what researches have been conducted in the past. Besides the fact that it may increase the level of knowledge, it is of importance to know the similarities with a new planned research. For this reason, a number of earlier performed researches are presented below.

Camille Habets, 2015:

Type of report: Master Thesis, TU Delft

Title: *Performance-Based Seismic Analysis of an Anchored Sheet Pile Quay Wall*

The main focus of this research lies on the improvement of seismic design methodologies for anchored sheet pile quay walls by considering deformation behaviour.

Rens Pater & David-Jan Smeenge, 2015:

Type of report: Final assignment, Windesheim

Title: *Aarbevingsbestendigheid van onderdoorgangen*

The resistance of 'spoorse onderdoorgangen'(Dutch) against earthquakes in the Groningen area is investigated. Central in this research is the question which method is applicable for measuring the resistance.

Juan Pablo Lopez Gumucio, 2013:

Type of report: Master Thesis, TU Delft

Title: *Design of Quay Walls using the Finite Element Method. The importance of relieving structures in quay walls*

Main objective of this research was to figure out the importance of a relieving structure compared to a normal sheet pile retaining structure. The relieving structure is investigated by means of two calculation methods. First a beam on elastic foundation method followed by a Finite element method was obtained.

Floris Besseling, 2012:

Type of report: Master Thesis, TU Delft

Title: *Soil-structure interaction modelling in performance based seismic jetty design*

In this study, three different design approaches are found suitable for jetty structures. These approaches are the simplified dynamic analysis, uncoupled dynamic analysis and coupled dynamic analysis. The results of the seismic jetty responds from different methods formed a basis for recommendation to the account of soil-structure interaction.

Jaw Wah Liang, 2011:

Type of report: Master Thesis, TU Delft

Title: *Earthquake analysis of quay walls*

The impact of an earthquake on both a diaphragm quay wall with relieving structure and a caisson type of quay wall is investigated. This behaviour is compared to a seismic analysis which contains regional seismicity, geologic hazards and soil-structure interaction.

Dong-Shan Yang, 1999:

Type of report: Master Thesis, TU Delft

Title: *Deformation-Based Seismic Design Models for Waterfront Structures*

In this research an investigation to seismic performance of gravity retaining walls and pile supported wharves is done by using a pseudo static analyses followed by a dynamic analysis. Besides this, a parametric study for gravity walls in improved and unimproved soils is conducted.

A.2. Quay structures from Eemshaven

The Eemshaven, as elaborated in Section 2.3, is subdivided in four basins. Each basin includes different quay structures, which are briefly introduced in this section. Information and figures are gathered from conversations with Groningen Seaport. The given figures from quay structures below are technical drawings. They are visualised to indicate the type of structure. There is no intention to present detailed information about the structures from the figures.

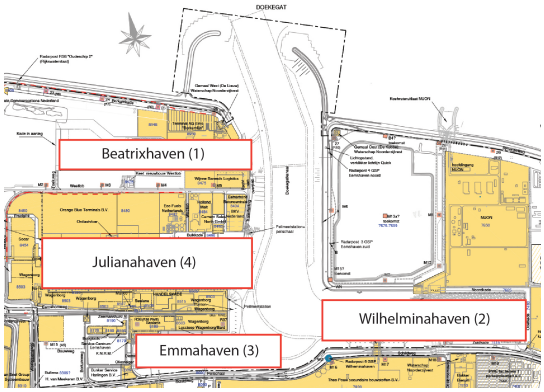

Figure A.1: Overview of Eemshaven

Beatrixhaven

This basin is recently developed and facilitates mainly the offshore wind industry. The quay structure is build in different phases with different contractors. Therefore the layout of the quay may differ at the locations of the phases. A cross section of the quay structure build in phase 5 (most recent phase) is given in Figure A.2. This combined wall with on top a capping beam is anchored with a grout anchor under an angle of about 45°. The retaining height of the wall is about 15 meters. Behind the capping beam a concrete floor on vertical piles is placed. This quay is build to withstand very high vertical loads at the quay front.

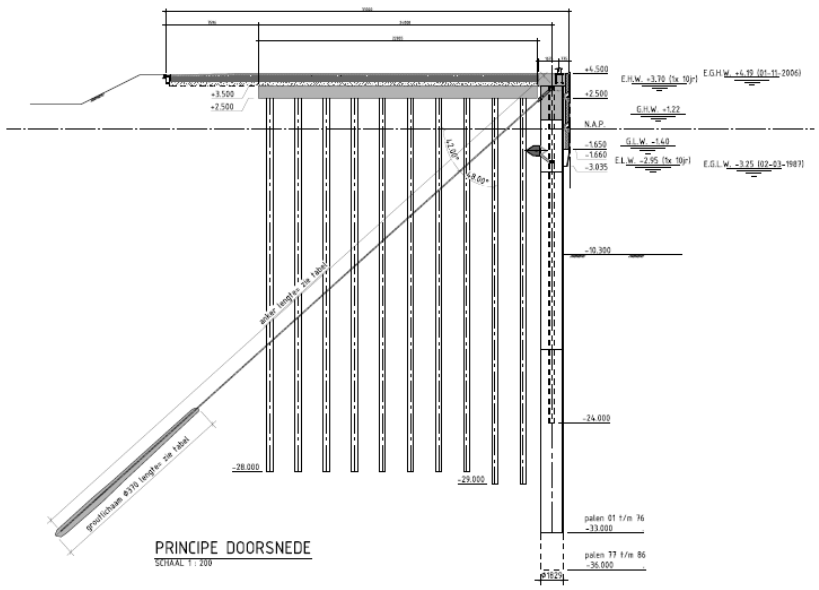

Figure A.2: Cross section quay wall Beatrixhaven

Wilhelminahaven

This section of the Eemshaven facilitates mainly biomass and coal transshipments, project cargo and general goods. The lay-out of the quay structure is presented in Figure A.3. The relieving floor is anchored with MV-piles to resist the pulling forces and supported by vibro-piles to ensure sufficient bearing capacity. The retaining height of this quay wall is about 23 meters.

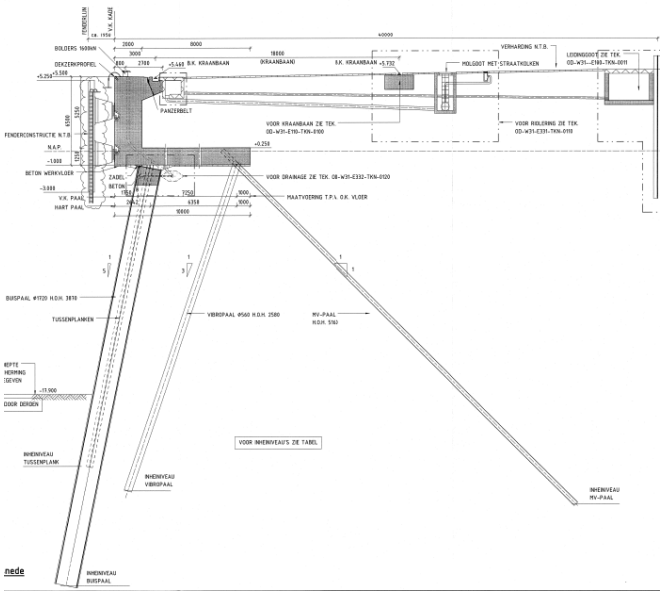

Figure A.3: Cross section quay wall Wilhelminahaven

Emmahaven

The basin of the Emmahaven provides space for maintenance and service vessels. Next to that offers the basis transshipment possibilities for general cargo, project cargo and oil. A cross section of the quay is given in Figure A.4. This sheet pile wall has an almost horizontal anchorage behind the wall. The black triangle in the figure represents a plastic filter cloth in reality. The reason behind this design decision is not known. The retaining height of this wall is about 14 meters.

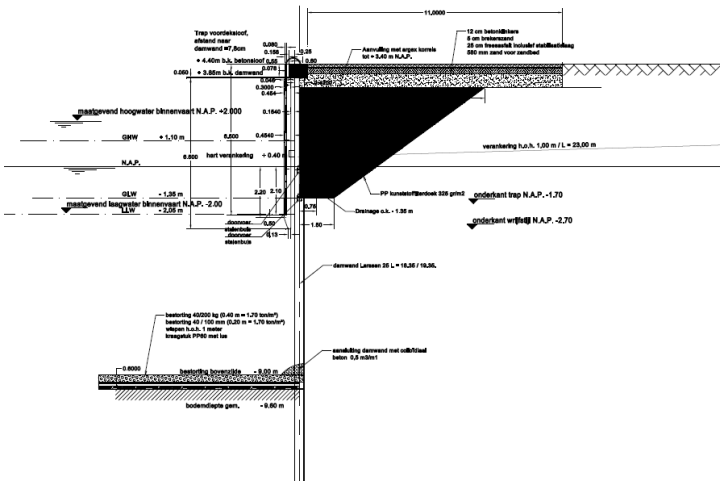

Figure A.4: Cross section quay wall Emmahaven

Julianahaven

The Julianahaven provides storage and transhipment facilities for rolling material, bulk products, oil material and general cargo. At this moment the quay at the northern side of the basin is mainly used for transshipment and storage of windmill parts. The basin of the Julianahaven is also developed in different phases. In Figure A.5 the cross section of the quay structure from phase 4 is presented. More information about this structure is given in the next section.

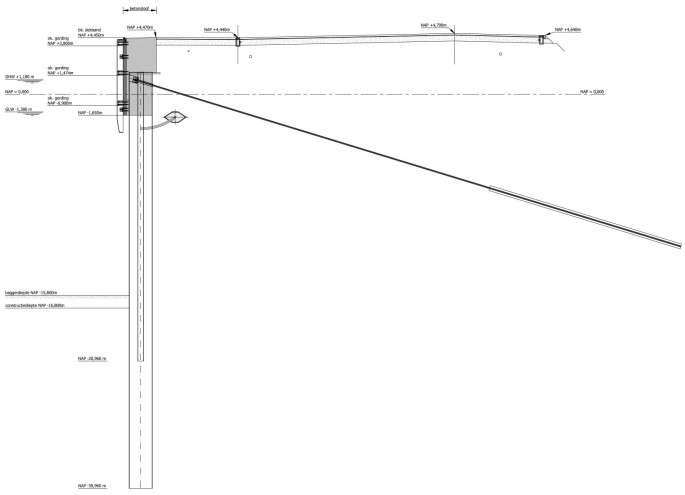

Figure A.5: Cross section quay wall Julianahaven

A.3. Determination of acting forces on quay structure

The acting forces on the quay structure are divided into static and dynamic loads, which are both elaborated below in addition to the information from Chapter 2.6.

A.3.1. Determination of static forces

To determine the static earth pressures, different methods can be applied. A common used method is the Coulomb theory. In this theory, force equilibrium is used for both minimum active and maximum passive to determine the soil forces acting on the wall. The governing soil force is assumed to be the weight of a wedge of soil which is located above a planar failure surface. This principle is shown in Figure A.6 and A.7. This method is originally designed for gravity walls, but is used for retaining walls in this research. For the initial investigations, no negative effects of this application are assumed.

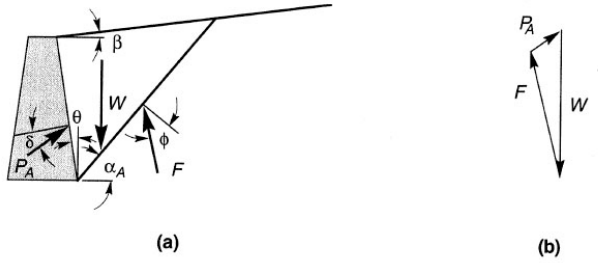

Figure A.6: Active force with Coulomb theory (Kramer, 1996)

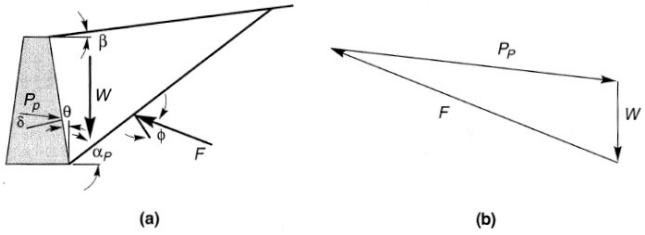

Figure A.7: Passive force with Coulomb theory (Kramer, 1996)

A.3.2. Determination of dynamic forces [pseudo static analysis]

With a pseudo static analysis the dynamic loads from an earthquake can be schematised as a static force on a wall. In this way no difficult and complex dynamic calculations are required. A subdivision between soil and water forces is required.

Soil forces

One of the widely accepted methods for the determination of soil forces due to earthquakes in a pseudo static analysis is the Mononobe-Okabe method, developed by Okabe (1926) and Mononobe and Matsuo (1929), also called the M-O method. The method is based on the principle of the Coulomb theory which they extended with earthquake loads by including horizontal en vertical inertia forces. The thought behind this is that the active and passive soil sides are exposed to accelerations which result in an additional force on the wall. As a result, the active soil pressure will increase and the passive side will reduced. The parameter γ will represent the earthquake force in the pseudo static calculation. The value of this parameter is determined by the horizontal and vertical acceleration and the presence of water. A difference should be made between dry and wet soil. For the wet soil a subdivision between permeable and impermeable soil should be applied, because the level of permeability is related to the possible movement of soil particles with respect to the water particles. The magnitude of the added

earthquake force can be determined as the mass times the acceleration. From force equilibrium the pseudo static soil thrust can be obtained. Figure A.8 illustrates the approach of the M-O method for the determination of the active force. Comparing this figure with A.6, the additional loads due to the earthquake become visible. The presented method is originally developed for gravity walls, but is also accepted for other type of retaining walls.

It is important to realise the limitations a simplified method. From Kramer (1996) and Visschendijk et al. (2014b) limitations of the M-O method are summed up. These should be kept in mind during design.

- The method assumes a cohesionless backfill
- In practice failure sliding plans are curved, but this method assumes straight Coulomb sliding planes
- Overestimation of the passive earth pressure for values of $\delta > \phi/2$.
- Complete mobilisation of the ground pressure is assumed
- Soil cracks, which may increase the active soil pressure, are not taken into account
- Undrained behaviour of soil during an earthquake is not taken into account
- The acceleration is determined at a fixed point and no variation in magnitude or acceleration over the height of the wall is taken into account
- The translation from an acceleration of the soil to an additional force on the wall is a simplified way of including an earthquake load

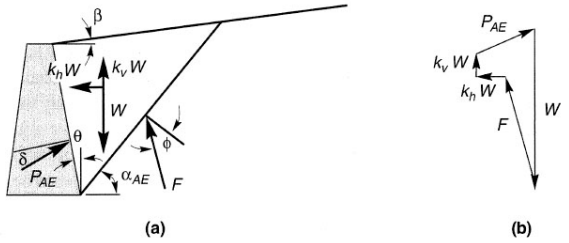

Figure A.8: Active force with M-O method (Kramer, 1996)

Water forces

With most quay structures, water forces are present in the backfill and in front of the wall. Different approaches are developed for determining the forces in front and behind the wall. The determination of water forces during an earthquake can also be subdivided. The hydrostatic water pressure, which is present before, during and after the earthquake, is proportionally linear in depth. The hydrodynamic water pressure is only present during the seismic loading and is the result of the dynamic response of the water on the earthquake.

- water in front of quay

The hydrostatic pressure can be determined linearly over the underwater quay height. Due to the dynamic response of the water body in front of the quay, hydrodynamic pressures develop which can be estimated with the Westergaard method. With his theory the hydrodynamic force can be determined with Equation A.1, under the assumption that the fundamental frequency of the water basis is higher than the frequency of the induced seismic motion.

$$F_{dyn,water} = \int_0^y \left[\frac{7}{8} * k_h * y_w * \sqrt{y * h} \right] \mathrm{d}y. \tag{A.1}$$

The development of the hydrodynamic water pressures is presented at the right of Figure A.9. The total dynamic water force in front of the quay is the sum of the hydrostatic and hydrodynamic water forces.

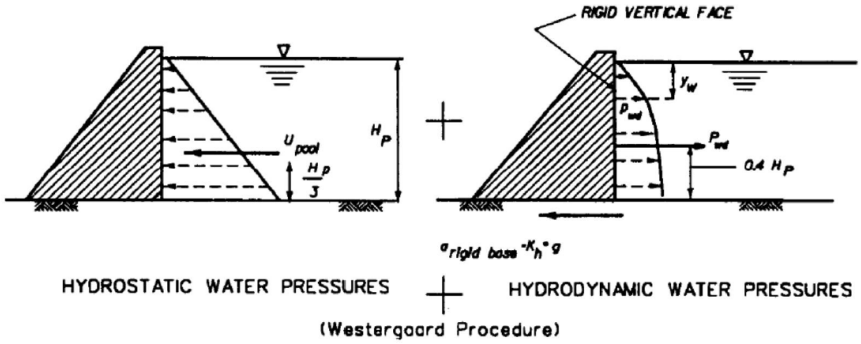

Figure A.9: Development of additional hydrodynamic water pressure (Meijers and Steenbergen, 2015)

- water in the backfill

Besides the possible development of hydrodynamic water pressures in the soil at the backfill, also excess pore pressure can be generated due to cyclic loading of the backfill. Pore water pressure can be included by a modification of the M-O method, as described above, after implementing the pore pressure ratio, r_u. For the hydrostatic force, an equivalent unit weight factor should be used (Kramer, 1996).

A.4. Liquefaction

During the literature study, information regarding the phenomenon of liquefaction is gathered. In addition to the different types of liquefaction, the vulnerability of the soil to liquefy is observed in general and after that for the Groningen case in specific.

A.4.1. Types of liquefaction

Different forms of liquefaction are known to exist. Two general types are flow liquefaction and cyclic mobility. The relation between most sorts of liquefaction is the phenomenon of excess pore pressure under undrained loading conditions.

Flow liquefaction occurs if the steady-state strength of the soil is smaller than the static shear stress. During or after an earthquake landslides may arise which are driven by the static shear stress. The development of flow liquefaction can be divided in two stages. In the first stage, sufficient excess pore pressure is built up by monotonic or cyclic loading until instability of the soil is reached. In the second stage additional pore pressure can be built up and the soil is inherently unstable. According to Robertson and Cabal (2015) this form of liquefaction can occur in sand, clay and silt deposits.

Cyclic mobility occurs when the cyclic shear stress exceeds the steady state strength momentarily, for example in case of cyclic loading due to an earthquake. The deformations are therefore driven by cyclic and static shear stresses. Deformations develop incrementally and can therefore become substantial during a longer period of time. If the cyclic loading is sufficiently long and strong, this type of liquefaction can occur in most saturated sand soils. In case of a clay soil deposit, influence will be noticeable if the cyclic shear stress due to the earthquake is close to the undrained shear strength of the clay (Kramer, 1996).

A.4.2. Liquefaction vulnerability

To judge on the vulnerability of liquefaction at a certain location, the following aspects should be observed:

- Susceptibility of soil to liquefactions

- Initiation of the expected liquefaction
- Level of damage (the effect) created by liquefaction

The aspects are elaborated below.

Susceptibility

To make a judgement concerning the susceptibility of liquefaction at certain locations different criteria can play a role.

Historical criteria, with information from postearthquake field investigations, can describe general conditions with a high susceptibility to future earthquakes.

Geologic criteria with characteristics about the soil deposit can clarify the liquefaction susceptibility of the soil. Deposits of loose states and uniform grain size are more susceptible to liquefaction. This also applies for relatively new soil deposits in comparison to older soil deposits and therefore soils from the Holocene age are more susceptible compared to the Pleistocene soil layers. Due to the fact that liquefaction only occurs in saturated soils, the groundwater level plays also an important role. Liquefaction is observed mostly at depths within a few meters from the ground surface.

The *compositional criteria* for susceptibility to liquefaction is related to the particle size and shape, gradation and plasticity of the soil and therefore also the potential of changing the intern volume. Changing volume behaviour is related to the development of excess pore water, which is the main requirement for liquefaction. The general particle size of sand, rounded particle shapes and poorly graded soils are in general more susceptible to liquefaction.

At the moment an earthquake arises, the density and stress characteristics of the soil at that particular moment influence the occurrence of liquefaction. The density and stress conditions of soil determine if excess pore pressure can be generated. Therefore, the *state criterion*, which indicates the initial state of the soil, is of great influence.

Initiation

To initiate liquefaction, a disturbance with a strong enough influence, is necessary to trigger the process. Without the generation of excess pore pressure, no decrease in effective soil stress will occur and therefore no liquefaction will take place. The amount of excess pore pressure is related to the characteristics of the earthquake, specifically the amplitude and duration of the induced cyclic loading. In general liquefaction can be expected where the loading exceeds the resistance, see Figure A.10.

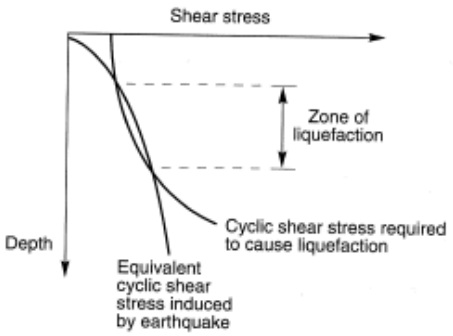

Figure A.10: Liquefaction identification area (Kramer, 1996)

Effect

Both flow liquefaction and cyclic mobility can create heavy damage to quay structures. Induced loading by earthquakes can change the internal structure of the soil and therefore create stability problems which may result in sliding planes and settlements of soil layers.

Liquefaction can alter the characteristics, frequency and amplitude, of a seismic signal at surface level. Due to the generation of excess pore pressures the soil can change from being stiff in the initial state to softer by the end of the motion. The possibility arises that, due to the softening of the soil by liquefaction, high frequency components of the motion will be filtered out and therefore only low frequencies will influence the structure. Figure A.11 indicates the change in frequency due to liquefaction.

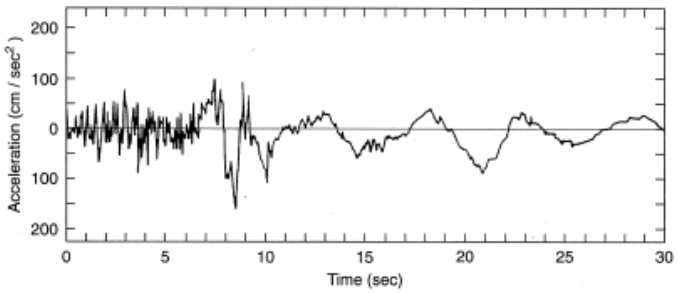

Figure A.11: Accelerogram of liquefied soil (Kramer, 1996)

Approach of sand and clay

In (Robertson and Cabal, 2015), page 102 is stated: 'The transition from more sand-like to more clay-like behaviour has a direct correspondence to the types of engineering procedures that are best suited to evaluate their seismic behaviour'. It is therefore important to have an understanding in the approach of sand-like and clay-like behaviour.

In the past the relation between liquefaction and soils was limited to sandy soils. Soils with other characteristics than sand where not seen vulnerable to the phenomena of liquefaction. For fine-grained soils like clay the assumption was made that excess pore pressure could not be built up. In contrast to the fine-grained soils, coarser grains where considered to be permeable to built up pressure (Kramer, 1996). In research done by R.W. Boulanger and I.M. Idriss and also Robertson the difference between sand and clay behaviour in relation to liquefaction is more elucidated.

The behaviour of soil response to seismic activity is highly dependant on the type of soil. A subdivision in the fine-grained soils between sand soil and clay soil can be made, due to the different behaviour and characteristics of the material. Ground failure due to earthquakes is observed more frequently in sands than in clay. For soils behaving in a sandy-like manner the term 'liquefaction' should be applied. For soils which behave in a clay-like manner the term 'cyclic softening' is appropriate. Different theories exist on how to distinguish sand-like and clay-like behaviour. Boulanger and Idriss (Boulanger and Idriss, 2006) made the distinction between the two types of soil with the plasticity indices (PI). For PI-values higher than 6 or 7 clay-like behaviour can be expected, see Figure A.12.

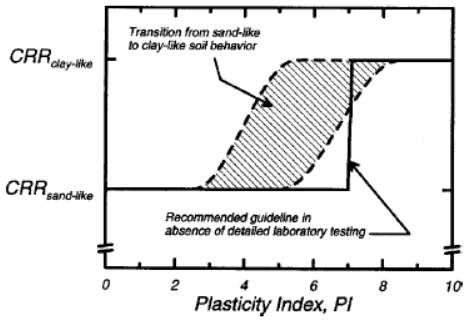

Figure A.12: PI index Boulanger and Idriss 2006 (Boulanger and Idriss, 2006)

The advice is given to use a slightly more conservative approach of Bray and Sancio, 2006 (Robertson and Cabal, 2015). The transition from sand-like to clay-like behaviour can be found between 12 to 18 PI values, see Figure A.13. Clay-like soils tend to have a better resistance against cyclic loading than sand-like soils. A higher transition value indicates therefore a more conservative approach.

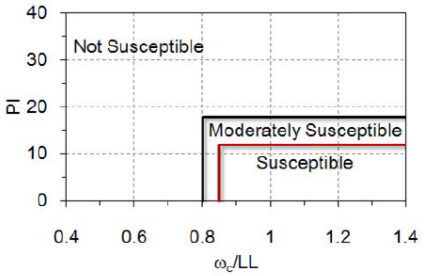

Figure A.13: PI index Bray and Sancio 2006 (Robertson and Cabal, 2015)

The theory of Robertson gives a second possible approach on the transition between sand and clay like behaviour by using the Soil Behaviour Type index, Ic, with a boundary value of 2.6 (Robertson, 2008), see Figure A.14

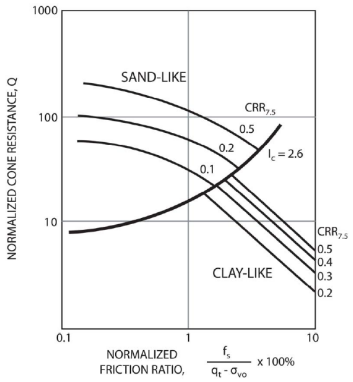

Figure A.14: Ic values Robertson method 2008 (Robertson, 2008)

Cyclic softening of clayey soils is mainly dependant on the number of load changes caused by induced loads from earthquakes. The number of load changes is dependant on the duration of an earthquake signal. The governing cause for liquefaction of sandy soil is the generation of excess pore pressure.

A.4.3. Determination of liquefaction potential for Eemshaven

Different methods are applicable to determine the vulnerability to liquefaction. The NPR9998 applies a method based on the research of I. M. Idriss and R. W. Boulanger, referred as I-B method. This method is adjusted with a number of assumptions (de Jong et al., 2015). Another way to determine the vulnerability to liquefaction is with the method of Robertson (Robertson and Cabal, 2015).

Due to the relatively short time frame of the seismic activity by induced earthquakes, the number of load changes on the soil is relatively low compared to tectonic earthquakes. Tectonic earthquakes have a higher number of significant vibrations and therefore more load changes than the induced earthquakes in the Groningen area. Until now, no major examples of liquefaction have been detected in the Groningen area. Nevertheless, in the determination to liquefaction in the soils of the Groningen area by Deltares a risk is obtained for PGA values of 0.15 or higher (Visschendijk et al., 2014b).

In de Jong et al. (2015) comments are made on the used method in the NPR9998. From the use of the I-B method, the assumptions made in the NPR9998 increase the level of safety. This results in a more conservative way of determining liquefaction hazard de Jong et al. (2015). Whether the I-B method is conservative is still a point of discussion worldwide and will therefore not be further discussed in this research. It is assumed practical to apply the Roberson method in the determination of the vulnerability of liquefaction in the Groningen area. In this research the determination regarding the factor of safety against liquefaction is done by applying the Roberson method with the software Geoligismiki, further elaborated in Appendix **D.3**. The resulting factor of safety over depth is almost always larger than 1, see Figure A.15. Therefore the safety against liquefaction is assumed acceptable and no further research to this phenomena will be done.

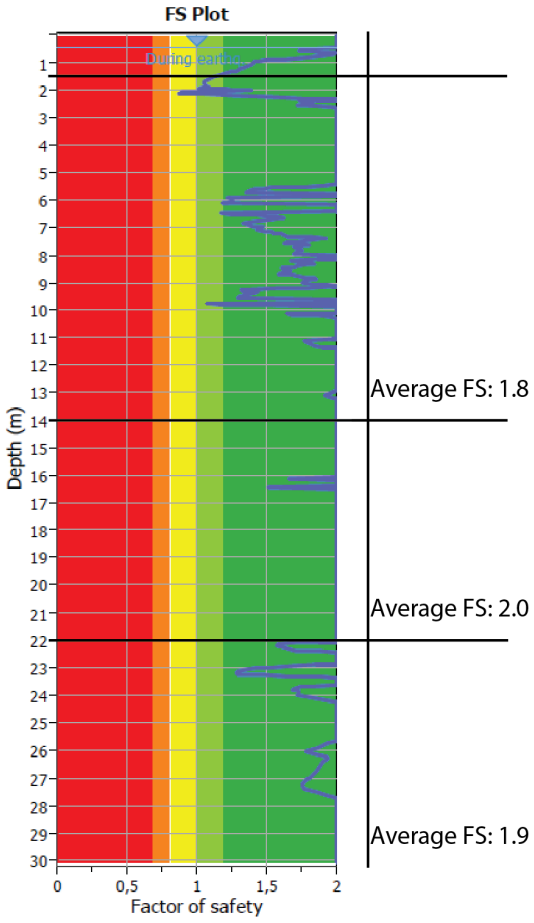

Figure A.15: Factor of safety against liquefaction

Remark regarding applied method: The methods available regarding the determination of liquefaction are based on tectonic earthquakes. It should be kept in mind that the applied check to the vulnerability is a first approximation and includes no detailed research. The liquefaction research from Deltares for the Groningen area indicates the complexity of the situation. For now the results from Figure A.15 are assumed applicable, because no additional suitable methods are available for the specific case in Groningen.

B

Soil interpretation

To find the soil parameters for the reference cross section, which is determined in Section 2.3.1, the following manner steps should be worked out:

- Determine the soil layers from the CPT (Cone Penetration Test)
- Determine q_c (Cone resistance) per layer
- Define soil layer parameters
- Define the layer characteristics

The original CPT of the reference location is presented in Figure B.1. In this figure the cone resistance (q_c) is given over depth at the left side. At the right side the friction ratio over depth is given. From an interpretation of the cone resistance and friction ratio, a subdivision of soil layers can be extracted over the depth. This is presented in Figure B.2. Note that the first layer in the CPT is called 'Soil layer 2'. The fill layer above 0 NAP after constructing of the quay structure, is called 'Soil layer 1'. The soil characteristics should be determined without the added fill layer to find original strength parameters of the soil.

The combination of the mean cone resistance, the layer depth and the friction ratio supplies an indication of the soil type. At the right of each soil layer the average cone resistance is presented. This determination is done by pulling a vertical line between the layer boundaries in a way that the cone resistance area is approximately equal left and right of the vertical line. It should be noted that the interpretation of a soil layers and parameters is no fixed theory and therefore more output possibilities are possible.

With help of Table 2b (NEN-EN:1997-1, 2012), the specifications of the soil parameters in each layer are determined using the measured q_c value, presented in Table B.3. The q_c values from table 2b are normed from a vertical effective soil stress of 100 kPa. The measured values from the CPT should therefore be converted to a level of 100 kPa for the vertical effective soil stress. This conversion is only required for sand layers. Applying the following equations with respect to the cone resistance result in the normed values for q_c (NEN-EN:1997-1, 2012).

$$q_{c,100} = q_{c,measured} * C_{qc} \tag{B.1}$$

with

$$C_{qc} = \left[\frac{100}{\sigma_{eff}}\right]^{0.67} \tag{B.2}$$

By implementing the effective soil stress, the normed cone resistance can be determined. The results of this determination for each layer are presented in Table B.2. Table B.3 presents more information about the interpretation of the determined layers. The name description and associated soil characteristics of eacht layer are according Table 2b from (NEN-EN:1997-1, 2012).

The parameter δ (delta) is related to ϕ by a certain factor. The relation between these parameters can be approached as (NEN-EN:1997-1, 2012):

- sand : $\delta = 2/3 * \phi$
- clay/loam : $\delta = 1/2 * \phi$

To create some first insights regarding the package density of the sand layers, a value for the relative density can be estimated by using the following equation (van den Ham et al., 2012):

$$Re = 0.34 * ln \frac{q_c}{0.61 * \sigma_{eff}} \tag{B.3}$$

From equation B.3 the relative density Re of a sand layer can be estimated based on the measured cone resistance. The effective soil stress is determined for every soil layer between the fill layer and NAP -31 m, which represents approximately the toe of the structure. Table B.1 presents the calculated values of Re for the naturally presented sand layer in the ground. The fill layer will be placed and packed by human action and characteristics are therefore known and estimated.

Layer	$q_c[MPa]$	$\sigma_{eff}[kPa]$	Re [-]
Layer 2	2.5	18	0.56
Layer 3	8.5	53	0.72
Layer 5	5.5	93.5	0.43
Layer 6	10	133.5	0.55
Layer 8	13	393.5	0.45

Table B.1: Relative density of sand layers

The combination of the estimated packing density, the layer depth and soil parameters from Table B.2 provide the information to give an initial description of the soil type. Note that the described soil type names from Table B.3 are simplified in other tables for practical reasons.

Layer	Soil type	γ/γ_{sat}	$q_c[MPa]$	$q_{c,100}[MPa]$	$\phi'[deg]$	$\delta'[deg]$	$c'[kPa]$
Layer 1	Fill	18/20	-	4	32.5	21.7	0
Layer 2	Sand 1	17/19	2.5	7.9	25	16.7	0
Layer 3	Sand 2	18/20	8.5	13	27	18	0
Layer 4	Clay 1	19/19	2	2	22.5	11.25	2
Layer 5	Sand 3	18/19	5.5	5.8	30	20	0
Layer 6	Sand 4	18/20	10	8.2	30	20	0
Layer 7	Clay 2	20/20	2.5	2.5	27.5	13.75	3
Layer 8	Sand 5	18/20	13	6.3	32.5	21.67	0

Table B.2: Soil parameters

Layer	Depth [m] relative to NAP	Soil type	Description
Layer 1	+4.45 ; 0	Fill, sand	Clean sand is used as fill material during the construction phases of the quay. From the design report becomes clear this layer is a moderate packed sand layer. The cone resistance is estimated on engineering judgement.
Layer 2	0 ; -2	Sand, very silty	The relatively low cone resistance and the ripples in the friction ratio indicate a loosely packed and very silty sand layer.
Layer 3	-2 ; -5.5	Sand, very silty	The cone resistance and ripples in the friction ratio indicate a moderate packing density of a very silty sand layer.
Layer 4	-5.5 ; -6.5	Clay, slightly sandy	This small clay layer is slightly sandy and is moderate to dense packed.
Layer 5	-6.5 ; -10	Sand, slightly silty	The cone resistance and ripples in the friction ratio indicate a loosely packed and slightly silty sand layer.
Layer 6	-10 ; -14	Sand, very silty	The cone resistance and ripples in the friction ratio indicate a loosely to moderate packed very silty sand layer
Layer 7	-14 ; -22	Boulder clay	Boulder clay (Dutch: keileem) is the description of the slightly sandy layer of loam which is in this case moderate to densely packed
Layer 8	-22 ; –	Sand	This relatively clean sand has a moderate packing.

Table B.3: Description of soil layers

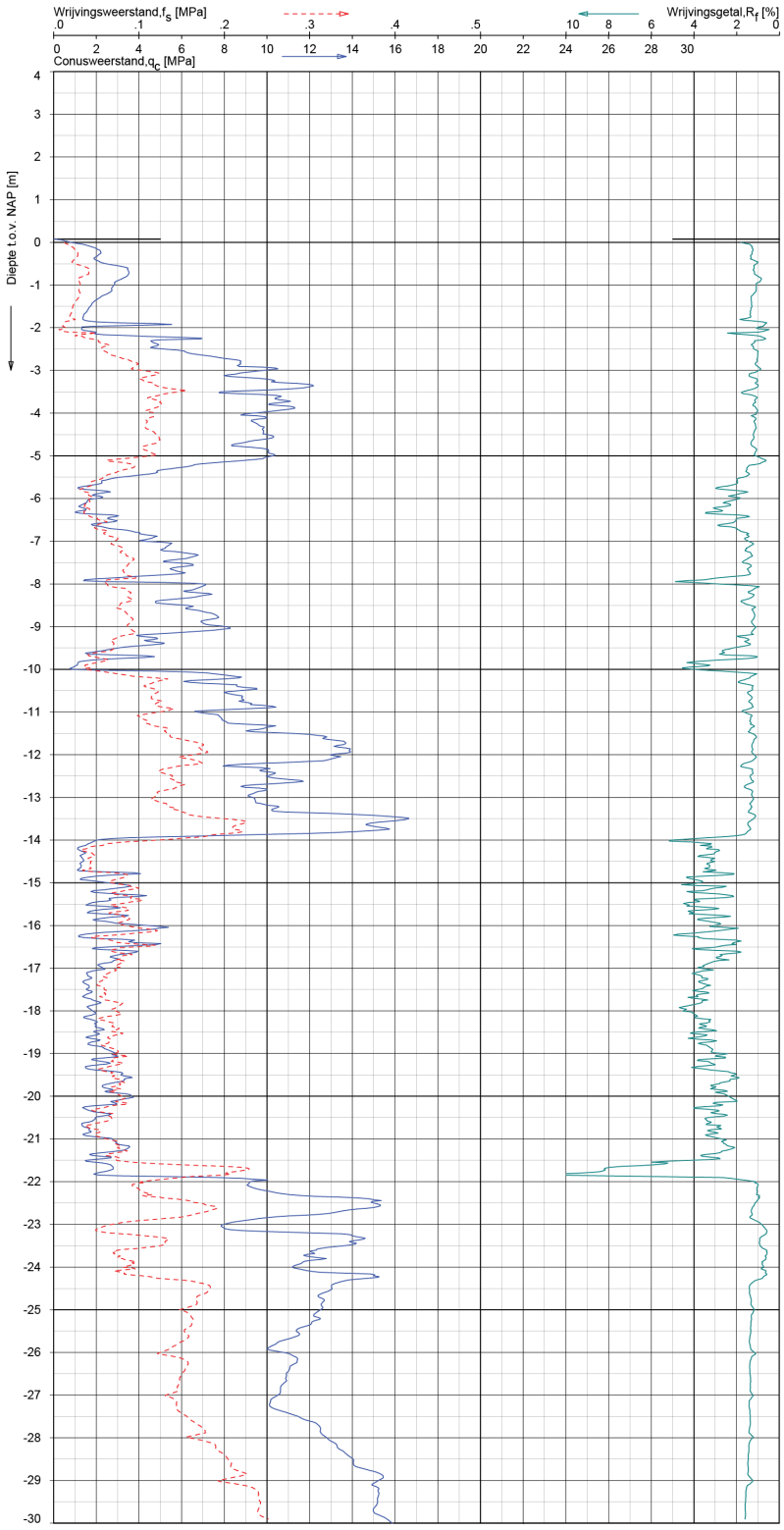

Figure B.1: Cone penetration test

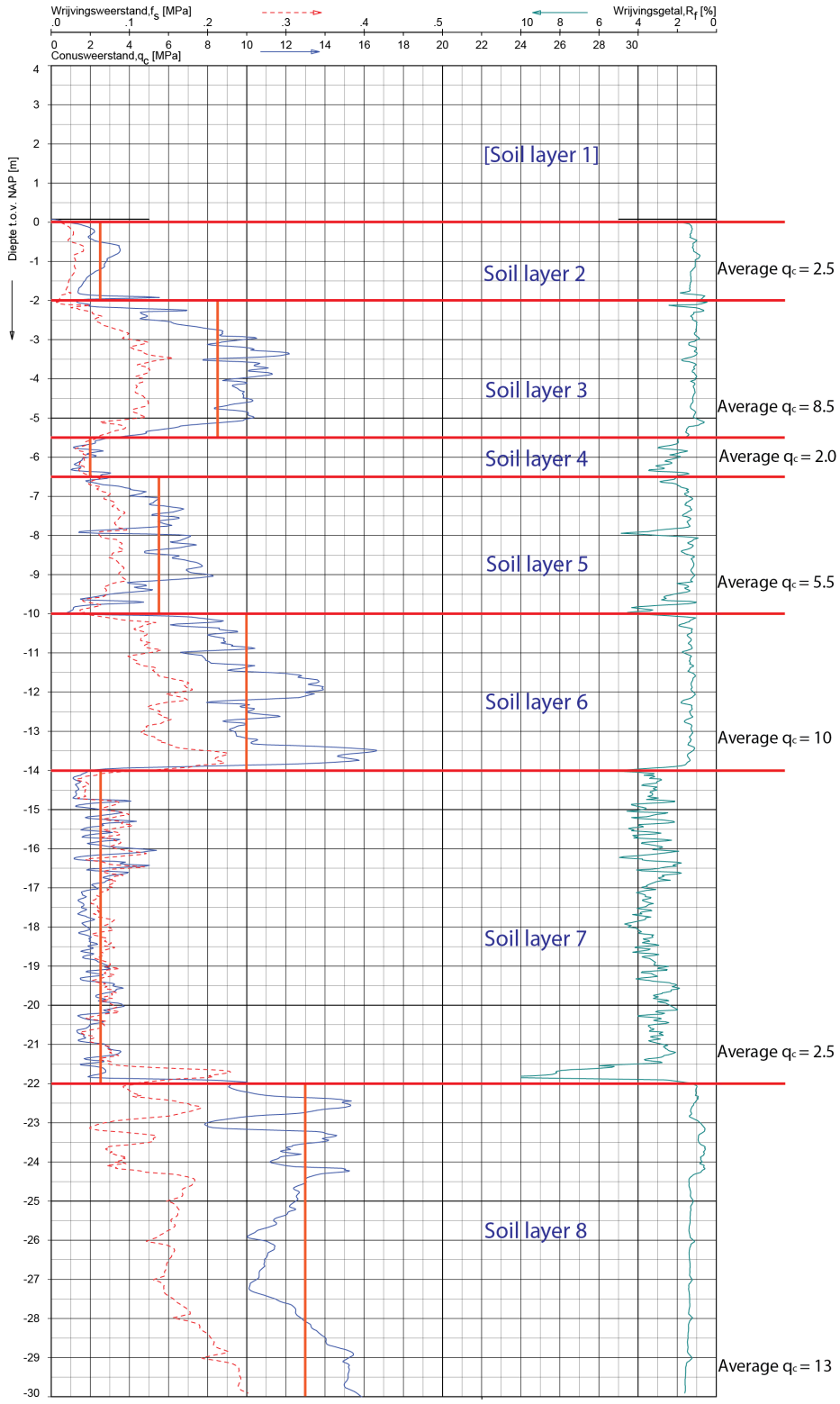

Figure B.2: Subdivision of soil layers

Grondsoort			Karakteristieke waarde[a] van grondeigenschap																					
Hoofd-naam	Bijmengsel	Consis-tentie [b]	γ [c] kN/m^3		γ_{sat} kN/m^3		q_c [d g] MPa		C'_p [g]		C'_s		$C_c/(1+e_0)$ [g] [-]		C_α [f] [-]		$C_{sw}/(1+e_0)$ [g] [-]		E_{100} [g h] MPa		φ' [g] Graden		c' kPa		c_u kPa	
Grind	Zwak siltig	Los	17		19		15		500		∞		0,0046		0		0,0015		45		32,5		0			
		Matig	18		20		25		1000		∞		0,0023		0		0,0008		75		35,0		0		n.v.t.	
		Vast	19	20	21	22	30		1200	1400	∞		0,0019	0,0016	0		0,0006	0,0005	90	105	37,5	40,0	0			
	Sterk siltig	Los	18		20		10		400		∞		0,0058		0		0,0019		30		30,0		0			
		Matig	19		21		15		600		∞		0,0038		0		0,0013		45		32,5		0		n.v.t.	
		Vast	20	21	22	22,5	25		1000	1500	∞		0,0023	0,0015	0		0,0008	0,0005	75	110	35,0	40,0	0			
Zand	Schoon	Los	17		19		5		200		∞		0,0115		0		0,0038		15		30,0		0			
		Matig	18		20		15		600		∞		0,0038		0		0,0013		45		32,5		0		n.v.t.	
		Vast	19	20	21	22	25		1000	1500	∞		0,0023	0,0015	0		0,0008	0,0005	75	110	35,0	40,0	0			
	Zwak siltig, kleiig		18	19	20	21	12		450	650	∞		0,0051	0,0035	0		0,0017	0,0012	35	50	27,0	32,5	0		n.v.t.	
	Sterk siltig, kleiig		18	19	20	21	8		200	400	∞		0,0115	0,0058	0		0,0038	0,0019	15	30	25,0	30,0	0		n.v.t.	
Leem [e]	Zwak zandig	Slap	19		19		1		25		650		0,0920		0,0037		0,0307		2		27,5	30,0	0		50	
		Matig	20		20		2		45		1300		0,0511		0,0020		0,0170		3		27,5	32,5	1		100	
		Vast	21	22	21	22	3		70	100	1900	2500	0,0329	0,0230	0,0013	0,0009	0,0110	0,0077	5	7	27,5	35,0	2,5	3,8	200	300
	Sterk zandig		19	20	19	20	2		45	70	1300	2000	0.0511	0,0329	0,0020	0,0013	0,0170	0,0110	3	5	27,5	35,0	0	1	50	100
Klei	Schoon	Slap	14		14		0,5		7		80		0,3286		0,0131		0,1095		1		17,5		0		25	
		Matig	17		17		1,0		15		160		0,1533		0,0061		0,0511		2		17,5		5		50	
		Vast	19	20	19	20	2,0		25	30	320	500	0,0920	0,0767	0,0037	0,0031	0,0307	0,0256	4	10	17,5	25,0	13	15	100	200
	Zwak zandig	Slap	15		15		0,7		10		110		0,2300		0,0092		0,0767		1,5		22,5		0		40	
		Matig	18		18		1,5		20		240		0,1150		0,0046		0,0383		3		22,5		5		80	
		Vast	20	21	20	21	2,5		30	50	400	600	0,0767	0,0460	0,0031	0,0018	0,0256	0,0153	5	10	22,5	27,5	13	15	120	170
	Sterk zandig	-	18	20	18	20	1,0		25	140	320	1680	0,0920	0,0164	0,0037	0,0007	0,0307	0,0055	2	5	27,5	32,5	0	1	0	10
	Organisch	Slap	13		13		0,2		7,5		30		0,3067		0,0153		0,1022		0,5		15,0		0	1	10	
		Matig	15	16	15	16	0,5		10	15	40	60	0,2300	0,1533	0,0115	0,0077	0,0767	0,0511	1,0	2,0	15,0		0	1	25	30
Veen	Niet voorbelast	Slap	10	12	10	12	0,1		5	7,5	20	30	0,4600	0,3067	0,0230	0,0153	0,1533	0,1022	0,2	0,5	15,0		1	2,5	10	20
	Matig voorbelast	Matig	12	13	12	13	0,2		7,5	10	30	40	0,3067	0,2300	0,0153	0,0115	0,1022	0,0767	0,5	1,0	15,0		2,5	5	20	30
Variatiecoëfficiënt v			0,05				–		0,25										0,10				0,20			

Figure B.3: Table 2b (Dutch) (NEN-EN:1997-1, 2012)

C

Building stages

The quay structure is build in several stages. The calculations to strength and stability during engineering of the structure are done using the software D-sheet piling. The design stages become visible from the design report (N.Kraaijeveld, 2010). The information regarding the engineering phases is presented below. The first four stages belong to the construction phases of the structure. Stages five to eight are different load combination scenarios and are applied to discover the governing load combination during design. The goal of this appendix is to discover which design stage should be used in combination with an earthquake.

Design stages

- *Stage 1:* Construction of the building pit followed by the installation of the combined sheet pile wall
- *Stage 2:* Installation and prestressing of the anchor system.
- *Stage 3:* Partly excavation in front of the wall combined with a partial fill behind the wall. Installation of the concrete capping beam.
- *Stage 4:* Complete excavation to reach the design depth in front of the wall. Final fill behind the wall to reach the quay design surface level.

Table C.1 presents an overview of the used levels and surface loads during the design stages. All levels are in meters regarding NAP level and the surface loads in kN/m^2. The terms [land] and [water] refer to the land- or waterside with respect to the quay structure.

Stage	Surface level [land]	Surface level [water]	Water level [land]	Water level [water]	Surface load [land]
Stage 1	1.00	1.00	0.50	0.50	0
Stage 2	1.00	1.00	0.50	0.50	20
Stage 3	2.00	-1.70	1.50	-2.00	20
Stage 4	4.45	-16.80	0.10	-0.10	20

Table C.1: Construction stages

Used load combinations during engineering of the quay structure

- *Stage 5:* Stage of daily use including bollard force and additional moment due to bollard force
- *Stage 6:* Stage of daily use without bollard force
- *Stage 7:* Extreme low water including bollard force and additional moment due to bollard force
- *Stage 8:* Extreme low water without bollard force

Table C.2 presents an overview of the used levels, loads and moments during the different load stages. All levels are in meters regarding NAP level and the surface loads in kN/m^2. The horizontal bollard force is given in kN/m and the additional moment due to eccentricity of this bollard force is expressed in kNm/m. The terms [land] and [water] refer to the land- or waterside regarding the quay structure.

Stage	Surface level [land]	Surface level [water]	Water level [land]	Water level [water]	Surface load [land]	Bolder force	Bolder moment
Stage 5	4.45	-16.10	-1.50	-1.82	60	100	50
Stage 6	4.45	-16.10	-1.50	-1.82	60	0	0
Stage 7	4.45	-16.10	-1.80	-3.30	20	100	50
Stage 8	4.45	-16.10	-1.80	-3.30	20	0	0

Table C.2: Load stages

Stage 5 and 6 represent the conditions of daily use with and without a vessel. Stage 7 and 8 represent the case including extreme low water in front of the quay. The probability of occurrence of extreme low water is not given. The bolder force en corresponding moment represent the loads from a moored vessel at the quay.

D

Analysis

Information regarding the assessment on the current situation, presented in Chapter 3, is presented in this Appendix. Information with respect to the input, model parameters and output from the performed analysis is mainly elaborated. The sequence of the topics in this appendix corresponds to Chapter 3.

D.1. Input and validation

Figure D.1 presents the structure of the analysis. The performed steps, the input and the associated evaluation are further elaborated in this Section. The static, pseudo static and dynamic approaches will be elaborated in additional sections D2, D3 and D4.

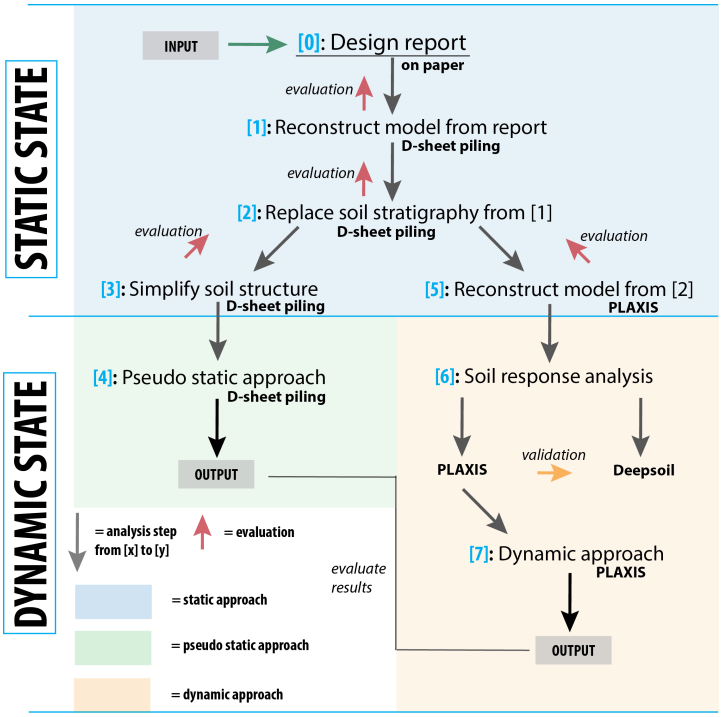

Figure D.1: Performed analysis

D.2. Static approach

This appendix elaborates the input of the applied models during the analysis for the static approach. The output from these models is presented in Chapter 3. For every step of the analysis the most important input values are presented.

D.2.1. Step [1]: Reconstruct model from report

The layout of the D-sheet model from stage 5 is presented in Figure D.2. This model is a reconstruction from the design report.

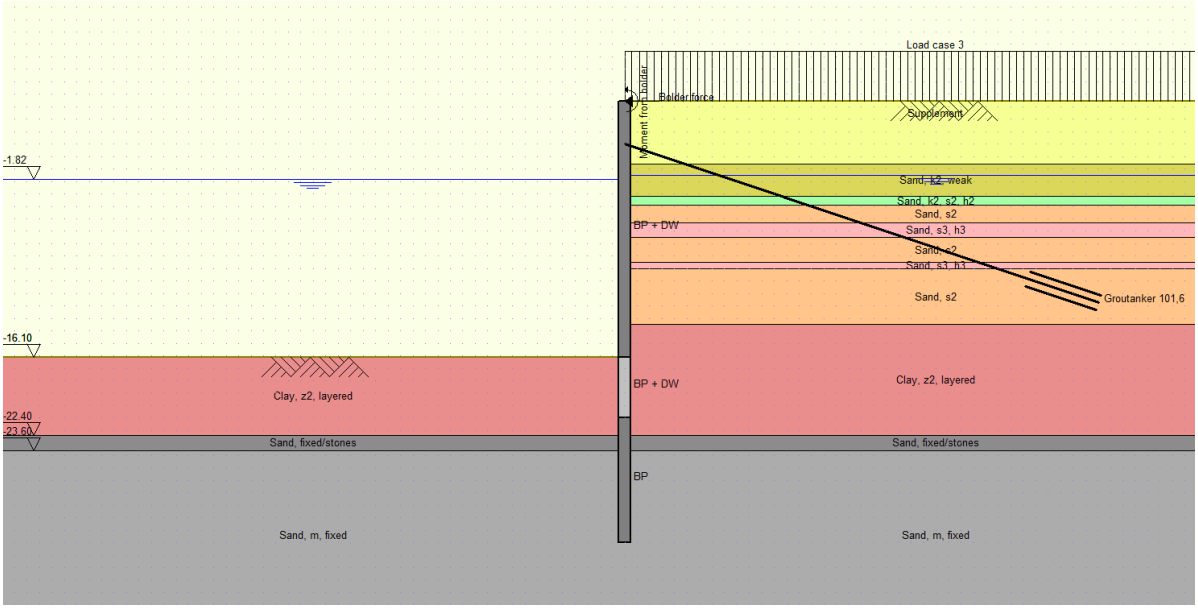

Figure D.2: D-sheet model reconstructed from design report

Some important aspects of the model are described below.

- **Soil**
  The layered horizontal areas present the different soil layers which are given in the design report. The corresponding parameter values are given in Table D.1. The subscriptions k, s, h and z in the soil type column are presenting the rate of additional soils present in the named main soil type. k represents clay, s presents silt, h is organic clay and z stands for sand.

Soil type	$\gamma/\gamma_{sat}[kN/m^3]$	$\phi'[deg]$	$\delta'[deg]$	$c'[kPa]$	$K_1[kN/m^3]$
Fill	18/20	32.5	21.7	0	40,000
Sand, k2, weak	17/19	25	16.7	0	6,000
Sand, k2, s2, h2	16/18	25	16.7	0	4,000
Sand, s2	18/20	30	20	0	15,000
Sand, s3, h3	17/19	27	18	0	12,000
Clay, z2, layered	18/19	25	16.7	3	6,000
Sand, fixed/stones	19/21	35	23.3	0	30,000
Sand, m fixed	18/20	32.5	21.7	0	20,000

Table D.1: Soil parameters design report

- **Anchor**
  In reality two screw anchors per pile are present, as explained in Chapter 2.4. In D-sheet this is modelled as one anchor with the strength values of a double set of anchors. It is important that the acting anchor force will be divided by two during the strength calculation. D-sheet is not able to model a grout body. The tip of the anchor is therefore modelled as a fixed point with a length: *Length anchor rod + 0.5*grout body length.* This is a common used method of modelling which is also applied in the design report (N.Kraaijeveld, 2010).

  The input parameters with respect to the anchor are given in Table D.2.

Parameter	Value	Unit
Attachment level	1	m
E-modules	2.1E+08	kN/m^2
Cross section	3.52E-03	m^2/m
Length	40.15	m
Angle	18.5	deg
Design Yield force	1644	kN/m

Table D.2: Anchor parameters design report

- **Combined wall**
  The effect of corrosion is taken into account in the strength parameters of the combined wall. This is visible in the different values for the bending stiffness, EI. The given values of EI represent the stiffness of the complete combined wall, which is a combination of sheet pile shelf elements and tubular piles, expressed per running meter. More information on the combined wall is described in section 2.4. Table D.3 describes the input values for the D-sheet model.

Section of combined wall	Bottom level $[m]$	Stiffness EI $[kNm^2/m]$	Acting width $[m]$	Maximum moment ULS $[kNm]$
Upper part	-16.10	2.60E+06	1.0	6272
Middle part	-21.00	2.86E+06	1.0	7272
lower part	-31.00	2.82E+06	1.0	7170

Table D.3: Combined wall parameters design report

- **Loads**
  The applied loads are those caused by the moored vessel, i.e. the bolder force plus a corresponding moment and the surface load behind the wall. Table D.4 describes the used input values. The direction of the load in D-sheet determines if the load is positive or negative.

Type of load	Value	Unit
Horizontal line load	-100	kN/m
Moment	50	kNm/m
Surface load	60	kN/m^2

Table D.4: Load parameters design report

The output from D-sheet regarding the bending moments, shear forces and displacements is given in Figure D.3

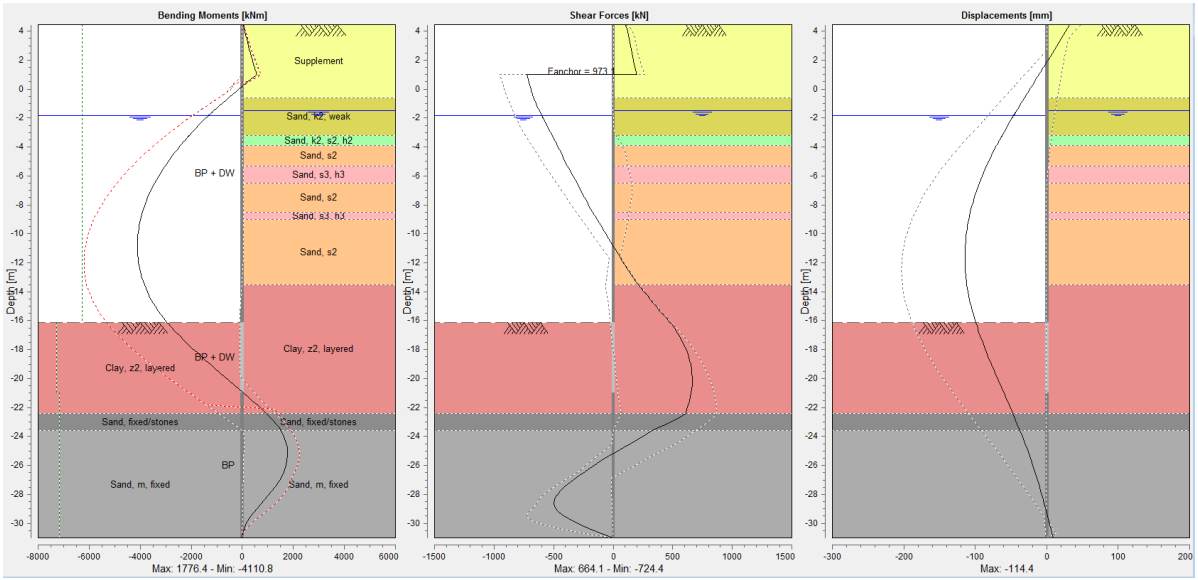

Figure D.3: D-sheet output from reconstructed model design report

D.2.2. Step [2]: Replace soil stratigraphy

The layout of the D-sheet model including replaced soil from the CPT is presented in Figure D.4.

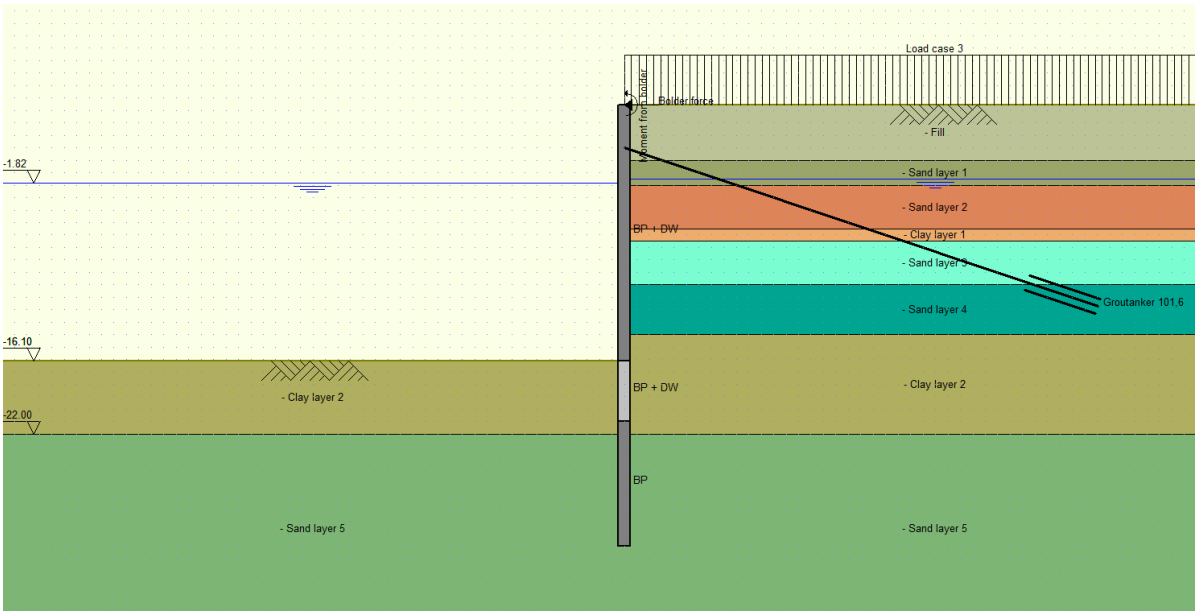

Figure D.4: D-sheet model with soil structure from CPT

Except for the soil structure, all other aspects named in the previous section, e.g. the anchor, combined wall and loads parameters stay equal. Therefore, only the soil input will be elaborated.

- **Soil**
  The layered horizontal areas present the different soil layers which are given in appendix **B** and Section 2.4. The input parameters for the D-sheet model from Figure D.4 are given in Table D.5. The values for the modulus of subgrade reaction, K_1, are derived from Table 3.3 from CUR166-1 (2012).

Soil type	$\gamma/\gamma_{sat}[kN/m^3]$	$\phi'[deg]$	$\delta'[deg]$	$c'[kPa]$	$K_1[kN/m^3]$
Fill	18/20	32.5	21.7	0	30,000
Sand 1	17/19	25	16.7	0	12,000
Sand 2	18/20	27	18	0	18,000
Clay 1	19/19	22.5	11.25	2	5,000
Sand 3	18/19	30	20	0	12,000
Sand 4	18/20	30	20	0	15,000
Clay 2	20/20	27.5	13.75	3	6,000
Sand 5	18/20	32.5	21.67	0	20,000

Table D.5: Soil parameters

The output from D-sheet regarding the bending moments, shear forces and displacements is given in Figure D.5

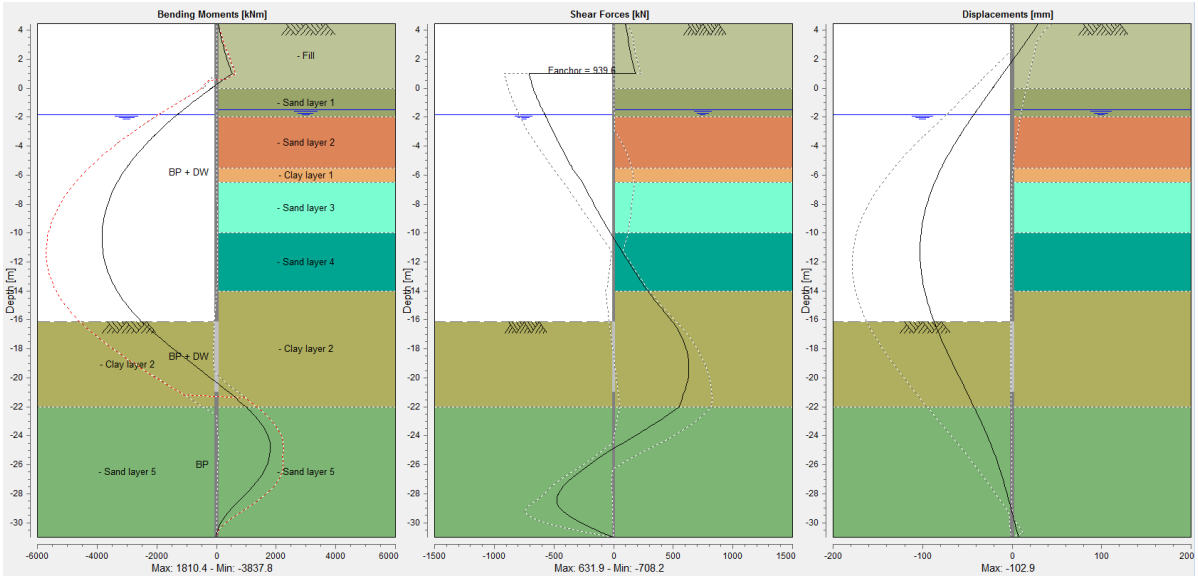

Figure D.5: D-sheet output from model with CPT soil

D.2.3. Step [3]: Simplify soil structure

The layout of the D-sheet model with the simplified soil layer structure is presented in Figure D.6.

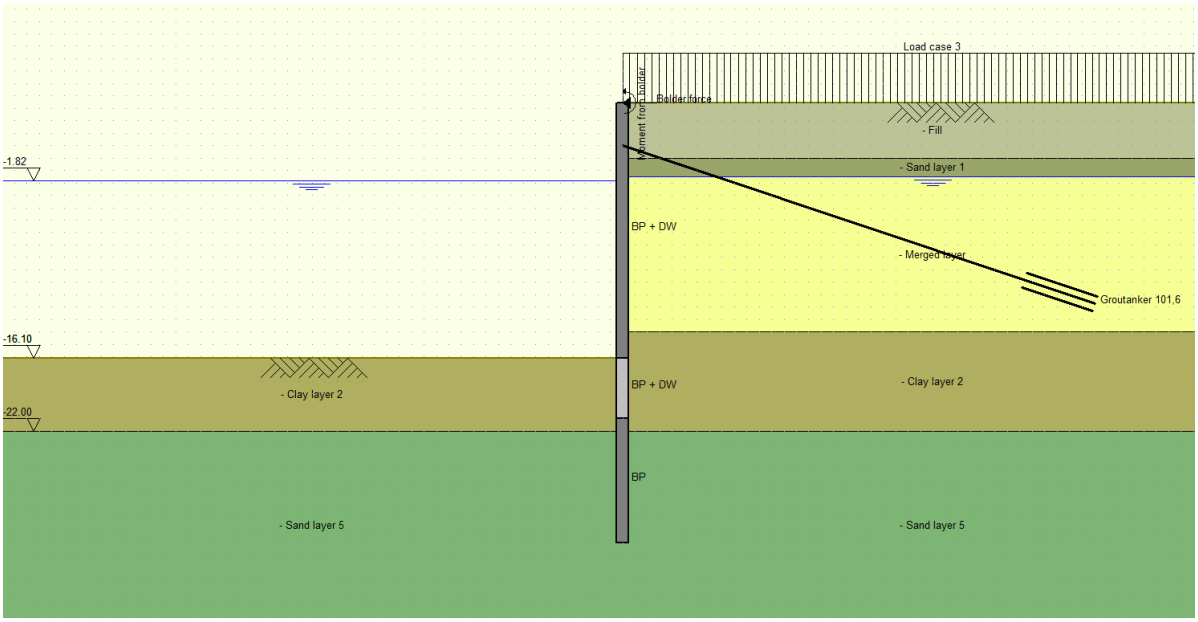

Figure D.6: D-sheet model with simplified soil structure from CPT

Except for the soil structure all other aspect named in the previous sections, e.g. the anchor, combined wall and loads parameters stay equal. Therefore, only the soil input will be elaborated.

- **Soil**
  The layered horizontal areas present the different soil layers which are elaborated in Section 3.2. The input parameters for the D-sheet model from Figure D.6 are given in Table D.6.

Soil type	$\gamma/\gamma_{sat}[kN/m^3]$	$\phi'[deg]$	$\delta'[deg]$	$c'[kPa]$	$K_1[kN/m^3]$
Fill	18/20	32.5	21.7	0	30,000
Sand 1	17/19	25	16.7	0	12,000
Merged layer	18/20	28	18.67	0	15,000
Clay 2	20/20	27.5	13.75	3	6,000
Sand 5	18/20	32.5	21.67	0	20,000

Table D.6: Soil parameters simplified soil structure

The output from D-sheet regarding the bending moments, shear forces and displacements is given in Figure D.7

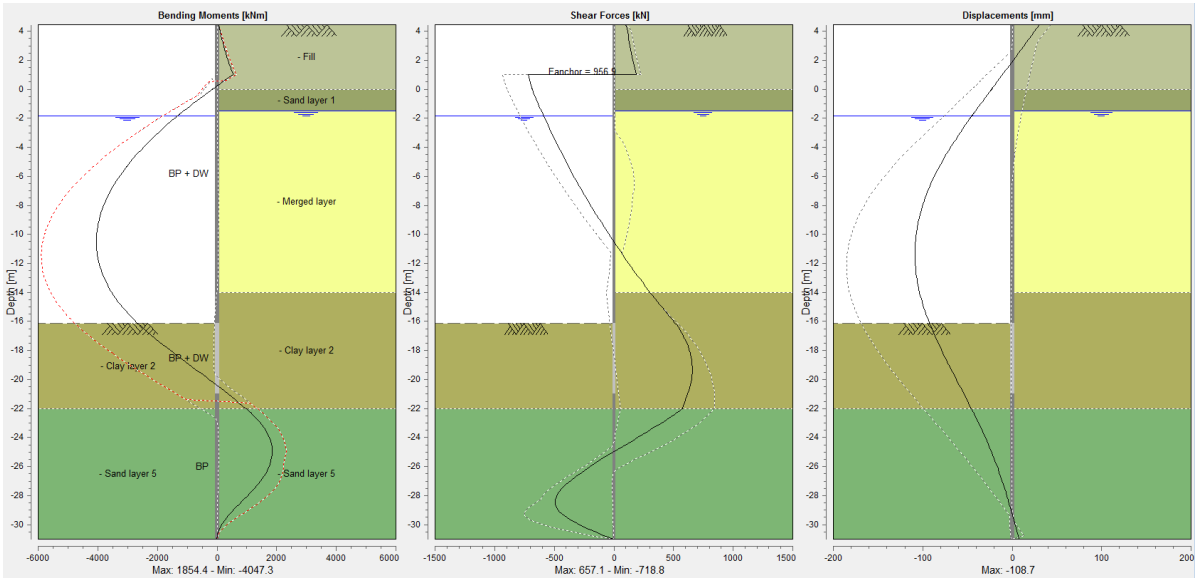

Figure D.7: D-sheet output from model with simplified soil structure

D.2.4. Step [5]: Reconstruct model from [2]

The layout of the PLAXIS model is presented in Figure D.8

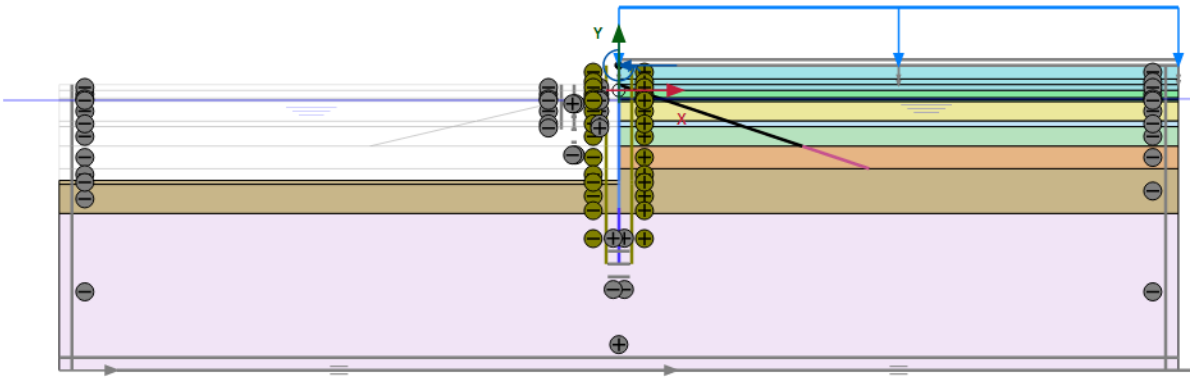

Figure D.8: Plaxis model stage 5

The presented model layout is reconstructed from the D-sheet model from step [2]. From this static state model the dynamic state will be modelled in Appendix D.4. The applied model and soil parameters for the static state are presented below.

- **Model parameters**

Input aspect	applied input	Unit
Model type	Plane strain	[-]
Elements	6-Noded	[-]
Contour, Xmin	-100	m
Contour, Xmax	100	m
Contour, Ymin	-50	m
Contour, Ymax	10	m
Constants	default values	[-]
Material model	HS small	[-]
Drainage type, sand	Drained	[-]
Drainage type, clay	Undrained (A)	[-]
BoundaryXmin	Normally fixed	[-]
BoundaryXmax	Normally fixed	[-]
BoundaryYmin	Fully fixed	[-]
BoundaryYmax	Free	[-]

Table D.7: Model parameters Plaxis model

The PLAXIS 2D model is generated with the model parameters presented in Table D.7.

- **Soil parameters**
  Except for the K_1 value, the values from Table D.5 are applied as input for PLAXIS. Additional values are presented in Table D.8.

Soil type	m	E_{50}^{ref}	E_{oed}^{ref}	E_{ur}^{ref}	G_0^{ref}	$Y_{0.7}$	R_{inter}
Fill	0.5	32,000	32,000	128,000	192,000	3.07E-05	0.7
Sand 1	0.5	20,000	20,000	80,000	120,000	2.55E-05	0.7
Sand 2	0.5	57,000	57,000	228,000	342,000	1.47E-05	0.7
Clay 1	0.9	18,000	13,000	72,000	108,000	7.60E-05	0.6
Sand 3	0.5	25,000	25,000	100,000	150,000	8.08E-05	0.7
Sand 4	0.5	37,000	37,000	148,000	222,000	7.98E-05	0.7
Clay 2	0.9	12,600	9,000	50,000	76,000	3.303E-04	0.6
Sand 5	0.5	39,000	39,000	156,000	234,000	1.948E-04	0.7

Table D.8: Soil parameters of PLAXIS model

For a precise estimation of the parameters a triaxial test should be available. This is not the case and therefore empirical relations regarding the required parameters have been made. Multiple documents containing different empirical relations are available. The applied parameters required for the HS small model are given in Table D.8.

The power for stress-level dependency of stiffness, 'm', for sand and clay is applied a 0.5 and 0.9 (PAO, 2002). The reference secant stiffness E_{50}^{ref} is scaled as a reference stress of 100 kPa. The original value is based on the measured cone resistance (Lunne and H.P., 1983) of sand and clay. The relation between E_{50}^{ref} and the tangent stiffness E_{oed}^{ref} for sand and clay is applied as 1 and 1.4 (PLAXIS-4, 2015) and (PAO, 2002). The unloading / reloading stiffness, E_{ur}^{ref}, is applied as $4{*}E_{50}^{ref}$. The reference shear modulus at small shear strains, G_0^{ref} is estimated as $1.5{*}E_{ur}^{ref}$. The soil response of this simplified estimation has been compared to a more advantaged determination. From the comparison is concluded that the simplified estimation has no large influence on the soil response. For this level of design, the applied values are assumed acceptable. The threshold shear strain, $\gamma_{0.7}$, is determined as $\frac{1}{9G_0^{ref}}\left[2c(1+cos(2\phi)) - \sigma_{eff}(1+K_0)sin(2\phi)\right]$ from (PLAXIS-4, 2015). The interface strength, R_{inter}, may be assumed to be approximately 2/3 in absence of detailed information (PLAXIS-4, 2015).

A note should be made regarding the two lowest soil layers. From engineering judgement became visible that the stiffness parameters of these layers was relatively low. Therefore, these parameters have been multiplied with a factor 1.5. In this way a better fit regarding the original design report was reached.
In general an upper limit of the soil parameters regarding the stiffness is applied. The soil contains low damping values which is expectable for the Groningen soil structure. The upper limit of stiffness parameters should be kept in mind and should be further optimised if a more detailed research phase.

D.3. Pseudo static approach

The pseudo static approach will be performed with reference to (Kramer, 1996).

D.3.1. Free water body

Under the assumption that the fundamental frequency of the water basis is higher than the frequency of the induced seismic motion, the Westergaard method is applied to determine the dynamic water force, see Section 2.6. For the water body in front of the structure this force becomes:

$$F_{dyn,water} = \int_0^{14.28} \left[\frac{7}{8} * k_h * \gamma_w * \sqrt{y * 29.18} \right] \mathrm{d}y. \tag{D.1}$$

and therefore:

$$F_{dyn,water} = \frac{7}{8} * 0.265 * 10 * \frac{1}{1.5} * \sqrt{29.18} * 14.28^{1.5} = 450 kN/m$$

With the input:

- k_h : horizontal earthquake coefficient = 0.265
- γ_w : Density of water = 10 kN/m^3
- y : vertical downward coordinate regarding water level = 29.18 m
- h : free water height = 14.28 m

D.3.2. Dry soil

Only the land side of the structure contains dry soil in the two upper layers. Under the assumption that the land side soil delivers active soil pressure, only active forces have to be determined for the dry soil. The following steps have been performed for the additional dynamic forces in the dry soil layers.

1. determine the seismic inertia angel Ψ_e
2. determine the active dynamic earth pressure coefficient k_{ae}
3. determine the total dynamic force P_{ae}
4. determine the static component P_a
5. determine the additional dynamic force ΔP_{ae}

The steps from above will be explained with the parameters for the upper soil layer. For the second dry layer only the output will be given.

Parameters:

Parameter	value	unit
Layer thickness H	4.45	m
γ_{dry}	18	kN/m^3
ϕ	32.5	degrees
δ	21.6	degrees

Table D.9: Soil parameter dry upper layer on active side

the seismic inertia angle Ψ_e can be determined using Equation D.2:

$$\Psi_a = tan^{-1}\left[\frac{k_h}{1-k_v}\right] \tag{D.2}$$

Which becomes:

$$\Psi_a = tan^{-1}\left[\frac{0.265}{1-0.133}\right] = 17$$

By knowing the inertia angle the dynamic active earth pressure coefficient can be determined with Equation D.3.

$$k_{ae} = \frac{cos^2(\phi-\beta-\Psi)}{cos(\Psi)*cos^2(\beta)*cos(\delta+\beta+\Psi)\left[1+\sqrt{\frac{sin(\delta+\phi)*sin(\phi+\alpha-\Psi)}{cos(\delta+\beta+\Psi)*cos(\alpha-\beta)}}\right]^2} \tag{D.3}$$

For a vertical wall with horizontal backfill β and α will become zero. k_{ae} therefore becomes:

$$k_{ae} = \frac{cos^2(32.5-0-17)}{cos(17)*cos^2(0)*cos(21.6+0+17)\left[1+\sqrt{\frac{sin(21.6+32.5)*sin(32.5+0-17)}{cos(21.6+0+17)*cos(0-0)}}\right]^2} = 0.53$$

The total dynamic active force can be determined with Equation D.4:

$$P_{ae} = \frac{1}{2}*k_{ae}*\gamma_{eff}*H^2*(1-k_v) \tag{D.4}$$

and becomes:

$$P_{ae} = \frac{1}{2}*0.53*(18-10)*4.45^2*(1-0.133) = 36kN/m$$

To find the additional dynamic load component, the static force component should be subtracted from P_{ae}. The static component can be found using the method from Coulomb, presented below. After the determination of the active earth pressure coefficient using Equation D.5, the static load component can be determined applying Equation D.6.

$$k_a = \frac{cos^2(\phi-\beta)}{cos^2(\beta)*cos(\delta+\beta)\left[1+\sqrt{\frac{sin(\delta+\phi)*sin(\phi-\alpha)}{cos(\delta+\beta)*cos(\alpha-\beta)}}\right]^2} \tag{D.5}$$

$$k_a = \frac{cos^2(32.5-0)}{*cos^2(0)*cos(21.6+0)\left[1+\sqrt{\frac{sin(21.6+32.5)*sin(32.5-0)}{cos(21.6+0)*cos(0-0)}}\right]^2} = 0.27$$

The static active force becomes:

$$P_a = \frac{1}{2}*k_a*\gamma_{eff}*H^2 \tag{D.6}$$

$$P_a = \frac{1}{2}*0.53*(18-10)*4.45^2 = 21kN/m$$

The additional dynamic force from the upper soil layer is therefore:

$$\triangle P_{ae} = P_{ae} - P_a = 36 - 21 = 15kN/m$$

This force will act approximately at a level of $0.6 * H$ regarding the base of the wall.

D.3.3. Saturated soil

For saturated soil the applied method from dry soil will be modified to include the presence of excess pore pressures. This is done by a modification of the parameters γ and Ψ and by adding an equivalent hydrostatic force. The determination of the relative excess pore pressure rate R_u is elaborated below.

- Modification of γ
  In the determination of P_{ea} the effective soil density, γ_{eff} is included. Taking excess pore pressure into account by implementing the parameter R_u, the effective soil density becomes:

$$\gamma_{eff,R} = (\gamma - \gamma_w)(1 - R_u)$$

- Modification of Ψ
  Taken into account the modified γ parameter, Ψ will be approached as:

$$\Psi_{a,r} = tan^{-1}\left[\frac{k_h}{1 - k_v}\frac{\gamma}{\gamma_{eff,R}}\right]$$

- Adding an equivalent hydrostatic force
  The additional hydrostatic force can be calculated with Equation D.7 by applying $\gamma_{eq} = R_u * (\gamma - \gamma_w)$.

$$P_{hydrst.epwp} = \frac{1}{2} * \gamma_{eq} * H^2 \tag{D.7}$$

R_u determination

The relative excess pore pressure rate, R_u, describes the rate between the excess pore pressure and the vertical effective stress before an earthquake appears. $R_u = 1$ refers to the state of liquefaction.

For a first estimation R_u can be determined with the factor of safety against liquefaction. The relation between these two parameters is presented in Table D.10 (Meijers and Steenbergen, 2015).

The factor of safety is estimated with the geotechnical software from 'GeoLogismiki' with the method of Robertson, as discussed in Chapter 2. GeoLogismiki is a quick tool to estimate the factor of safety for a certain soil profile during an earthquake. The average value for each soil layer is presented in Figure D.9. From this figure the assumption is made that no liquefaction will appear during an earthquake.

FS	R_{ud}
1.1	1
1.2	1
1.25	1
1.3	0.67
1.4	0.46
1.5	0.35
1.6	0.27
1.7	0.22
1.8	0.18
2.0	0.12

Table D.10: relation between FS against liquefaction and excess pore pressure

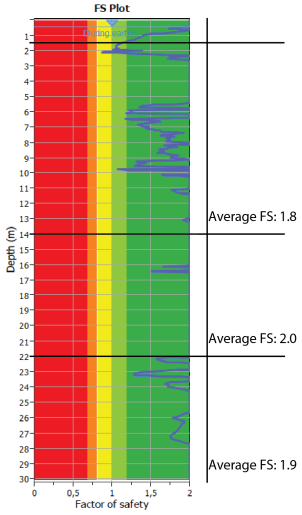

Figure D.9: Factor of safety against liquefaction

Combining the results of Figure D.9 and Table D.10 provides for every soil layer a value for R_u, summarised in Table D.11.

Layer	FS_{layer}	R_u
-1.5; -14	1,80	0,18
-14; -22	1,99	0,12
-22; -31	1,89	0,15

Table D.11: Estimated R_u values per soil layer

The additional dynamic force for the active side can be estimated with the same formulas as where elaborated in Section D.3.2, but now including the modified parameters and by adding the equivalent hydrostatic trust. The steps and equations for the determination of an additional force regarding to the passive side are presented below.

For the determination of the additional forces on the passive side the following steps should be conducted.

1. determine the seismic inertia angel Ψ_e
2. determine the passive dynamic earth pressure coefficient k_{pe}
3. determine the total dynamic force P_{pe}
4. determine the static component P_p
5. determine the additional dynamic force ΔP_{pe}
6. determine the equivalent hydrostatic force $P_{hydrst.epwp}$

By applying the following formulas:

$$\Psi_{a,r} = tan^{-1}\left[\frac{k_h}{1-k_v}\frac{\gamma}{\gamma_{eff,R}}\right] \tag{D.8}$$

with:

$$\gamma_{eff,R} = (\gamma - \gamma_w)(1 - R_u)$$

The passive dynamic earth pressure coefficient can be determined with:

$$k_{pe} = \frac{cos^2(\phi + \beta - \Psi)}{cos(\Psi) * cos^2(\beta) * cos(\delta - \beta + \Psi)\left[1 - \sqrt{\frac{sin(\delta+\phi) * sin(\phi+\alpha-\Psi)}{cos(\delta-\beta+\Psi) * cos(\alpha-\beta)}}\right]^2} \tag{D.9}$$

Resulting in a total dynamic active force:

$$P_{ae} = \frac{1}{2} * k_{pe} * \gamma_{eff} * H^2 * (1 - k_v) \tag{D.10}$$

The static passive component can be determined with:

$$P_a = \frac{1}{2} * k_p * \gamma_{eff} * H^2 \tag{D.11}$$

with:

$$k_p = \frac{cos^2(\phi + \beta)}{cos^2(\beta) * cos(\delta - \beta)\left[1 - \sqrt{\frac{sin(\delta+\phi) * sin(\phi+\alpha)}{cos(\delta-\beta) * cos(\alpha-\beta)}}\right]^2} \tag{D.12}$$

Resulting in an additional dynamic component:

$$\triangle P_{pe} = P_{pe} - P_p \tag{D.13}$$

By applying the method as described above the additional active or passive forces are determined for every soil layer.

D.3.4. Result of pseudo static approach

The resulting additional forces for a assumed PGA of 2.6 m/s^2 are given in Table D.12. Figure D.10 presents the implemented forces in D-sheet. As mentioned in the assumptions from Chapter 3 some forces may be neglected.

Force	Value	Unit
WATER SIDE		
Dyn. free water force	450	kN/m
Dyn. passive force 1	513	kN/m
Eq. hydrost. passive force 1	21	kN/m
Dyn. passive force 2	2512	kN/m
Eq. hydrost. passive force 2	61	kN/m
LAND SIDE		
Dyn. active force 1	15	kN/m
Dyn. active force 2	2	kN/m
Dyn. active force 3	666	kN/m
Eq. hydrost. active force 1	141	kN/m
Dyn. active force 4	260	kN/m
Eq. hydrost. active force 2	38	kN/m
Dyn. active force 5	469	kN/m
Eq. hydrost. active force 3	61	kN/m

Table D.12: Additional dynamic loads for PGA = 2.6 m/s^2

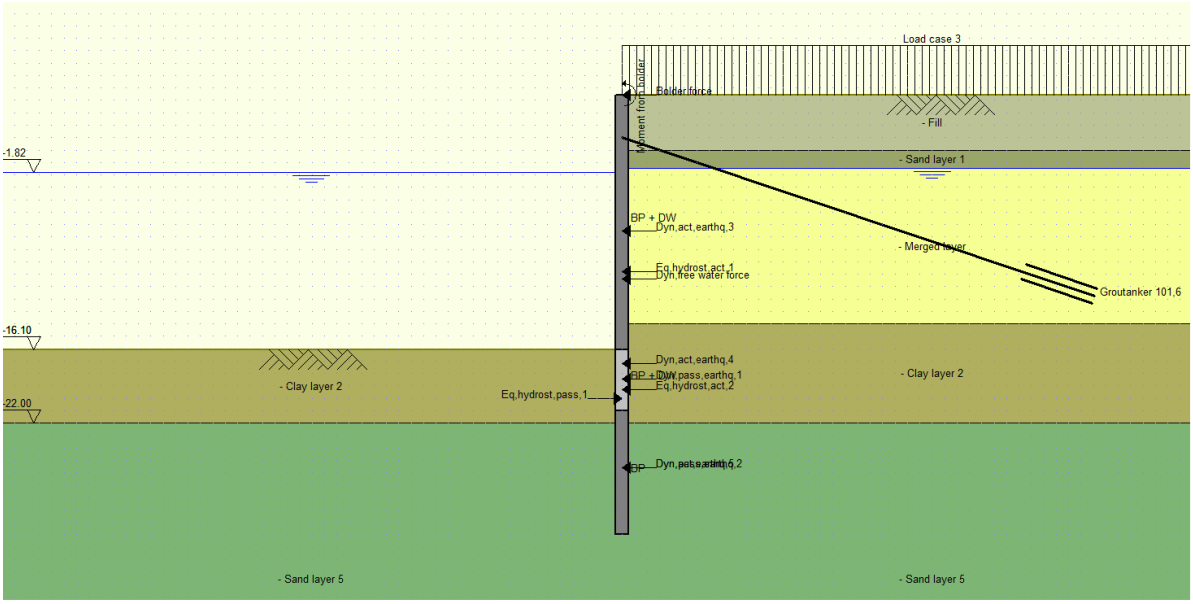

Figure D.10: Additional loads implemented in D-sheet

D.3.5. Forecast for lower PGA values

After implementation of the determined additional forces in D-sheet, no output will be provided due to the occurrence of one or more failure mechanisms. For this reason all forces are recalculated from lower PGA values. The resulting forces for different PGA values are presented in the tables below. From these output values a forecast on the development of the internal response forces from the structure can be made. For lower PGA values no R_u is determined, therefore a value of 0.12 is assumed for all PGA values smaller then 50% of the original value of 2.6 m/s^2.

A PGA value higher than 50% of the original results in failure in D-sheet and therefore no output will be produced. The trend lines from Figure 3.7 of the main report are therefore based on the output between 0 and 50% of the PGA value.

20 % PGA value

Force	Value	Unit
WATER SIDE		
Dyn. free water force	90	kN/m
Dyn. passive force 1	168	kN/m
Eq. hydrost. passive force 1	21	kN/m
Dyn. passive force 2	739	kN/m
Eq. hydrost. passive force 2	49	kN/m
LAND SIDE		
Dyn. active force 1	2	kN/m
Dyn. active force 2	0	kN/m
Dyn. active force 3	25	kN/m
Eq. hydrost. active force 1	94	kN/m
Dyn. active force 4	9	kN/m
Eq. hydrost. active force 2	38	kN/m
Dyn. active force 5	13	kN/m
Eq. hydrost. active force 3	49	kN/m

Table D.13: Additional dynamic loads for PGA = 0.52 m/s^2

The output from D-sheet after the implementation of the forces is presented in Table D.14. Also the static state without additional loads is given. The displacement is presented in mm, the maximum moment in kNm/m and the anchor force in kN/m.

PGA	Hor. displacement	Max. moment	Anchor Force	Overall stability
0%	105,2	3838	940	1,66
20%	202,5	6276	1290	1,40

Table D.14: Output from D-sheet

30 % PGA value

Force	Value	Unit
WATER SIDE		
Dyn. free water force	135	kN/m
Dyn. passive force 1	211	kN/m
Eq. hydrost. passive force 1	21	kN/m
Dyn. passive force 2	926	kN/m
Eq. hydrost. passive force 2	49	kN/m
LAND SIDE		
Dyn. active force 1	3	kN/m
Dyn. active force 2	0	kN/m
Dyn. active force 3	62	kN/m
Eq. hydrost. active force 1	94	kN/m
Dyn. active force 4	24	kN/m
Eq. hydrost. active force 2	38	kN/m
Dyn. active force 5	30	kN/m
Eq. hydrost. active force 3	49	kN/m

Table D.15: Additional dynamic loads for PGA = 0.78 m/s^2

The output from D-sheet after the implementation of the forces is presented in Table D.16. The displacement is presented in mm, the maximum moment in kNm/m and the anchor force in kN/m.

PGA	Hor. displacement	Max. moment	Anchor Force	Overall stability
0%	105,2	3838	940	1,66
20%	202,5	6276	1290	1,40
30%	240,9	7132	1421	1,34

Table D.16: Output from D-sheet

40 % PGA value

Force	Value	Unit
WATER SIDE		
Dyn. free water force	180	kN/m
Dyn. passive force 1	256	kN/m
Eq. hydrost. passive force 1	21	kN/m
Dyn. passive force 2	1116	kN/m
Eq. hydrost. passive force 2	49	kN/m
LAND SIDE		
Dyn. active force 1	4	kN/m
Dyn. active force 2	1	kN/m
Dyn. active force 3	107	kN/m
Eq. hydrost. active force 1	94	kN/m
Dyn. active force 4	41	kN/m
Eq. hydrost. active force 2	38	kN/m
Dyn. active force 5	50	kN/m
Eq. hydrost. active force 3	49	kN/m

Table D.17: Additional dynamic loads for PGA = 1.04 m/s^2

The output from D-sheet after the implementation of the forces is presented in Table D.18. The displacement is presented in mm, the maximum moment in kNm/m and the anchor force in kN/m.

PGA	Hor. displacement	Max. moment	Anchor Force	Overall stability
0%	105,2	3838	940	1,66
20%	202,5	6276	1290	1,40
30%	240,9	7132	1421	1,34
40%	285,4	8197	1568	1,28

Table D.18: Output from D-sheet

50% PGA value

Force	Value	Unit
WATER SIDE		
Dyn. free water force	225	kN/m
Dyn. passive force 1	304	kN/m
Eq. hydrost. passive force 1	21	kN/m
Dyn. passive force 2	1311	kN/m
Eq. hydrost. passive force 2	49	kN/m
LAND SIDE		
Dyn. active force 1	6	kN/m
Dyn. active force 2	1	kN/m
Dyn. active force 3	156	kN/m
Eq. hydrost. active force 1	94	kN/m
Dyn. active force 4	64	kN/m
Eq. hydrost. active force 2	38	kN/m
Dyn. active force 5	76	kN/m
Eq. hydrost. active force 3	49	kN/m

Table D.19: Additional dynamic loads for PGA = 1.30 m/s^2

The output from D-sheet after the implementation of the forces is presented in Table D.20. The displacement is presented in mm, the maximum moment in kNm/m and the anchor force in kN/m.

PGA	Hor. displacement	Max. moment	Anchor Force	Overall stability
0	105,2	3838	940	1,66
0.52	202,5	6276	1290	1,40
0.78	240,9	7132	1421	1,34
1.04	285,4	8197	1568	1,28
1.30	345,4	9305	1644	1,22

Table D.20: Output from D-sheet

The results from the tables presented above can be summarised by plotting a graph. From the known data points a forecast can be made for the forces at a 100 % (2.6 m/s^2) PGA value. This is presented in Section 3.3.4 of the main report.

D.4. Dynamic approach

Information regarding the dynamic models is presented in this section. In addition to the dynamic phase models, the soil response analysis is also elaborated in more detail.

D.4.1. Model parameters of added dynamic phase in PLAXIS

Information regarding the mesh, model boundaries, seismic signal and model damping is presented below.

Generated mesh

As mentioned before, the applied mesh in the model is 'coarse' for the first indications and will be 'medium' for the final calculations in this research. Smaller mesh sizes result in more accurate results, but require longer calculation times. Two tests have been performed regarding the output differences from a medium and course mesh size. Both tests provided small output differences between coarse and medium mesh sizes. The first models will therefore be calculated with a coarse mesh size to prevent long calculation times. The final design models in this research are calculated with a finer mesh size.

Applied boundaries

The boundary conditions for the dynamic phase are given in Table D.21. To avoid that the created edges of the model disturb the soil response, the X-boundaries are modelled as free-field. The bottom boundary, Ymin, is modelled as a compliant base boundary. In this way the signal will be damped at the boundaries and reflection is avoided.

Input aspect	applied input	Unit
BoundaryXmin	Free-field	[-]
BoundaryXmax	Free-field	[-]
BoundaryYmin	Compliant base	[-]
BoundaryYmax	None	[-]

Table D.21: Boundary parameters dynamic Plaxis model

The size of the model is based on an estimation in which the edges have no or minimal influence on the results. The width of the model is 200 meters and the hight 60 meters.

Implementing of signal

As explained in Section 1.4.2 the applied input signal is a measured at surface level in Gartshuizen during the earthquake in August 2012. With the help of Deepsoil this signal is deconvoluted linearly, which is assumed acceptable for relatively low seismic waves. The resulting signal at -50 meters is scaled based on the design PGA from the NPR9998. After scaling, the signal can be applied as input signal in Deepsoil or PLAXIS.

Attention should be paid regarding the different types of input signals applied in the software programs. Three types which are common to apply are briefly introduced below and visualised with Figure D.11.

- Incoming signal
  This signal is measured between the boundary of rock level and the start of the soil layer. The propagating seismic waves from the epicentre in rock are travelling upwards through the rock towards the rock boundary. The 'incoming signal' reflects to the seismic wave measured at this rock boundary.
- Outcrop signal
  The summation of the incoming wave from the epicentre trough the rock and the reflection at the rock boundary represents the outcrop signal. This effect can be compared to an incoming

water wave reflecting against a vertical wall. The amplitude of the reflected wave will be twice the incoming wave amplitude. It is concluded that the outcrop signal is about twice the incoming signal.

- Within signal
  A within signal contains the summation of the incoming signal from rock and the reflecting signal travelling downwards from the soil surface level to the rock. The different stiffness magnitudes between rock and soil cause different signal response. Therefore, a difference between the within signal and outcrop signal arises.

All three signal are schematically illustrated in Figure D.11.

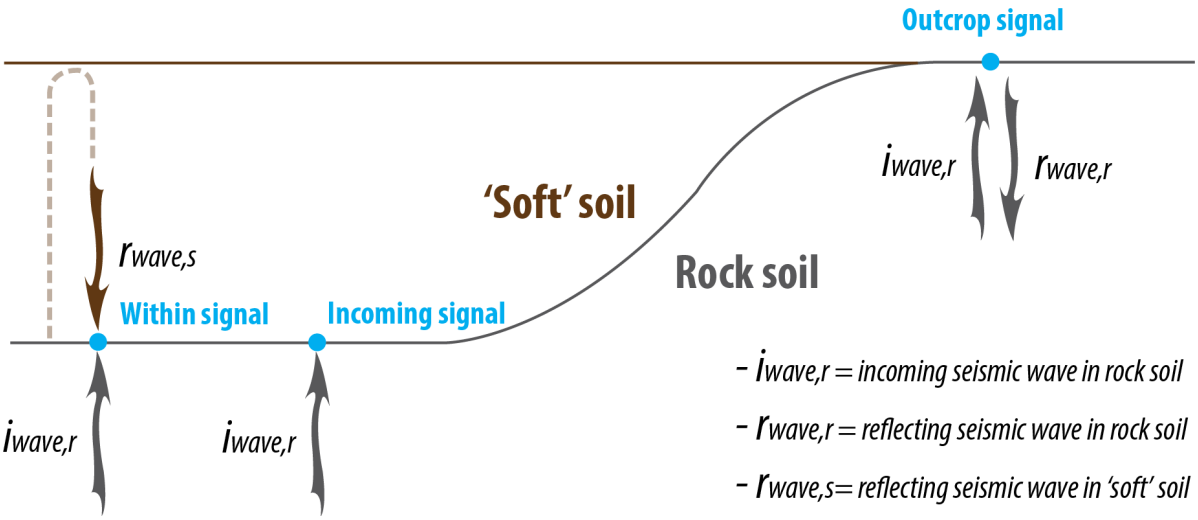

Figure D.11: Schematic overview of different signal types

The y-boundary in PLAXIS is modelled as compliant base. This boundary option is a combination of a line prescribed displacement and a viscous boundary. The viscous boundary consists of series of dash-pots in shear and normal direction to absorb the downward propagating waves (PLAXIS-2, 2015). The input signal for this model boundary should be an 'incoming signal'. It is not clear which type of signal deepsoil produces after the deconvolution. This is not given in the manual or in the software program itself. From a number of test running with different types of signal in deepsoil, the presumption is that the produced signal after the deconvolution is a 'within signal'.

Theoretically it is therefore incorrect to implement the signal from deepsoil as input signal in PLAXIS. Still a quite good fit is achieved as presented in the next section. An explanation for this might be related to the equal soil stiffness below and above the bottom of the model at -50 meter. Further research to improve the results regarding this subject is required, but is not taken further into account in this research.

The best fit from PLAXIS regarding Deepsoil is achieved if the base of the model is modelled as sand. Therefore no rock layer of one meter at the base of the PLAXIS model is applied.

Damping

Hardening Soil model with small-strain stiffness (HS small) is applied for the soil models. With this type of model, taking into account damping in PLAXIS is possible in several ways:

- *Numerical damping using the method of time integration* is mostly applied in elastic materials to filter the high frequencies. The elasto-plastic behaviour of soils contains damping on itself and numerical damping in not applied in this case (Visschendijk et al., 2014a).

- *Damping from the constitutive model* is included in the HS small model by hysteresis.

- *Rayleigh damping* can be added to all soil layers in PLAXIS. No laboratory tests with specific characteristics are available, therefore the advised Rayleigh damping from Visschendijk et al. (2014a) will be partly applied. The rayleigh damping is described as a % of damping for certain frequencies f_1 and f_2, resulting in two damping parameters α and β. The parameter α determines the influence of the mass in the damping. A higher value for α results in more damping of lower frequencies. The parameter β includes the effect of stiffness regarding the damping. A higher value of β results in more damping of high frequencies.

  The value of f_1 refers to the natural frequency of vibrations of the soil layer with thickness H. The first natural frequency can be determined with (PLAXIS-3, 2015) and (Kramer, 1996):

$$f_1 = \frac{V_s}{4H} \tag{D.14}$$

  and f_2 depends on the applied seismic signal.

  From Visschendijk et al. (2014a) a 1% damping on the frequencies 2 and 12 Hertz is applied. The value for f_1 is relatively easy to determine and also required for the validation with Deepsoil. This value is therefore determined below. For the value of f_2 no proper information has yet been found. Therefore the given value from Visschendijk et al. (2014a) is applied.

  Determination of f_1

  The value for the shear velocity, V_s, can be determined with (Robertson and Cabal, 2015):

$$V_s = [\alpha_{vs} * (q_c - \sigma_v)/100]^{0.5} \tag{D.15}$$

  with: $\alpha_{vs} = 10^{0.55*Ic+1.68}$

  The values for I_c, the soil behaviour type index, are gathered from the geotechnical software from 'GeoLogismiki' with the method of Robertson. The applied parameters, the resulting shear velocity V_s per layer and the resulting frequency f_1 are presented in Table D.22. The weighted average of the total soil body is 1.1 Hz.

Soil layer	$\sigma_v[kPa]$	I_c	α_{vs}	$q_c[kPa]$	$V_s[m/s]$	$f_1[Hz]$
Fill	40.1	2.00	603	4000	154	8.1
Sand 1	99.1	2.32	905	1500	113	14.1
Sand 2	153.1	1.87	510	8500	206	14.7
Clay 1	197.6	2.55	1211	2000	148	36.9
Sand 3	240.4	2.25	832	5500	209	14.9
Sand 4	313.6	2.08	665	10000	254	15.9
Clay 2	433.6	3.00	2129	2500	210	6.6
Sand 5	693.6	2.11	695	13000	292	2.6

Table D.22: Determination of frequency f_1

D.4.2. Soil response validation

As mentioned in Section 3.4, the soil response from PLAXIS requires validation. A commonly used method for the validation of PLAXIS is by making use of Deepsoil. The dynamic calculation of the complete PLAXIS model is time consuming and therefore a soil column is applied for the validation in PLAXIS. Information about the applied Deepsoil and PLAXIS validation is elaborated below.

Deepsoil

The soil column is designed by implementing several soil layers. The existing layers are subdivided in smaller layer between 0.5 and 2 meters. In this way the maximum frequency has a minimum value of 30 Hz, as advised in the manual (Hashash, 2015). The unit weight and shear velocity are applied as input. Additional input parameters are determined by the implemented models from Deepsoil. For sand the upper limit reference curves of Seed & Idriss, 1991 are applied. For clay the curves from Vucetic & Dobry, 1991 are used. For the plasticity index a value between 10 to 15 is applied (Sorensen and Okkels, 2013). The first natural frequency of the complete soil column is given by Deepsoil with a value of 1.06 Hz. This is almost equal to the determined value of 1.1 Hz by hand.

Deepsoil does not include a Rayleigh damping for every soil layer, but for the whole soil column. The implemented Rayleigh damping is therefore on the frequencies of $f_1 = 1.1Hz$ and $f_2 = 12Hz$. The base is modelled as 'rigid halfspace' which should be applied in case of a 'within signal'.

The non-linear soil response is plotted as presented in Section 3.4.

PLAXIS

To prevent the validation of the complete PLAXIS model to become a large time consuming process, a soil column with equal soil properties as the model is created, see Figure D.12. The boundary conditions are presented in Table D.23. These boundary conditions are applied on advise from PLAXIS.

Input aspect	Applied input	Unit
BoundaryXmin	Tied degrees of freedom	[-]
BoundaryXmax	Tied degrees of freedom	[-]
BoundaryYmin	Compliant base	[-]
BoundaryYmax	None	[-]

Table D.23: Boundary parameters soil column

From PLAXIS the advice is given to model the width of the column based on the average element size. The mesh size can be controlled better in case of one element in horizontal direction. The average element size can be estimated as:

$$Size = \frac{V_{s,minimal}}{8 * f_{max}} \tag{D.16}$$

With $V_{s,minimal}$ as the minimum shear velocity in the present soil layers. From Table D.22 this is assumed to be 113 m/s. f_{max} is the maximum significant frequency of the input signal. This value is assumed to be 12 Hz for a first estimation Visschendijk et al. (2014a).

This results in an average element size and therefore column width of 1.17 m.

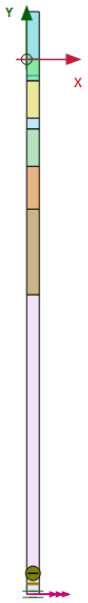

Figure D.12: Soil column PLAXIS

The base of the soil column is again modelled as a compliant base boundary. This boundary is implemented in the available sand layer. The best fit with deepsoil is gathered by using a sand material at the base instead of rock.

To validate the response from PLAXIS with Deepsoil the output values are compared by plotting the PGA development in depth, see Figure D.13, and the PGA development in time at surface level and finally by presenting the response spectra of both soil columns. All figures are presented in Section 3.4 of the main report.

To achieve the validation as presented in these graphs, the Rayleigh damping has been modified for certain soil layers in PLAXIS. As a starting point all layers had the same values as implemented in Deepsoil. To optimise this first output, the Rayleigh damping parameters from Table D.24 are applied in the PLAXIS model.

Soil layer	damping [%]	f_1 [Hz]	f_2 [Hz]
Fill	2	1.1	12
Sand 1	0	1.1	12
Sand 2	0	1.1	12
Clay 1	1	1.1	12
Sand 3	1	1.1	12
Sand 4	1	1.1	12
Clay 2	3	1.1	12
Sand 5	1	1.1	12

Table D.24: Modified Rayleigh damping parameters

D.4.3. Improvement of soil response

To improve the fit of the soil response between PLAXIS and Deepsoil further research has been done regarding two specific soil layers which present the largest deviation in Figure D.13. The development as presented in this figure depends on the applied damping in the soil. The applied damping in PLAXIS is based on the constitutive model of HS small with hysteresis and additional Rayleigh damping. For Deepsoil the damping curves for sand soil are based on the upper limit of Seed & Idriss 1991. The curves for clay are based on Vucetic & Dobry, 1991 using a PI value between 10 and 15.

Sand layer 2, present between 2 and 5.5 meters, and clay 2, located between 14 and 22 meters have been investigated in more detail.

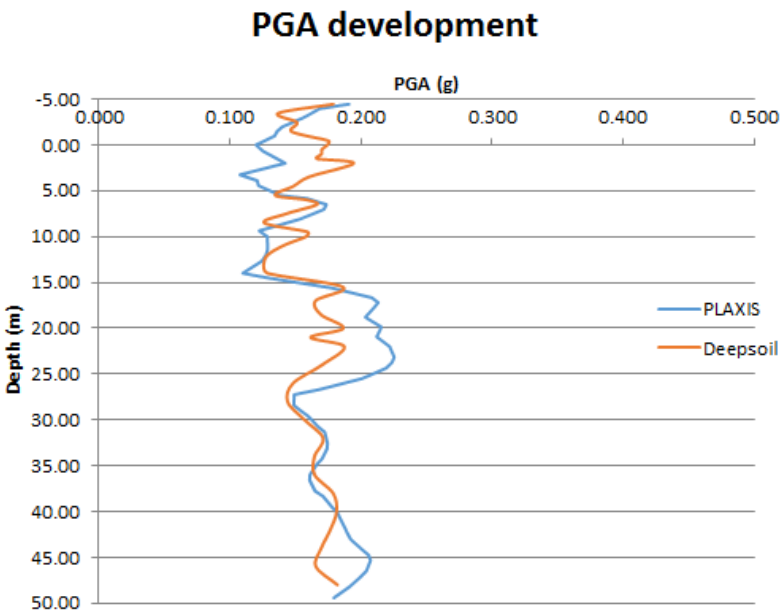

Figure D.13: PGA development over depth

Two models in both PLAXIS and Deepsoil have been made with only one soil material layer, respectively sand 2 or clay 2. These two layer have been selected because they contain the largest deviation between PLAXIS and deepsoil. In this way, more insight in the behaviour of this specific soil layer is provided. It has been tried to fit the soil behaviour from PLAXIS for this specific soil material to the soil response from deepsoil. This has been done by adjusting the Rayleigh damping parameters. For both soil materials the modelled PGA development has been presented in the figures below for different damping and frequency values. The influence of the Rayleigh damping parameters becomes visible in this way.

Comments regarding Figure D.14
By applying different values for the Rayleigh damping it has been tried to fit the response from PLAXIS to the black line from Deepsoil. The PGA values at 50 meters depth are not explainable and might be the result from a numerical error in PLAXIS. It can be concluded that the response from PLAXIS does not fit well regarding Deepsoil for this sand layer.

Comments regarding Figure D.15
Again different values for the Rayleigh damping are applied in PLAXIS to provide a fit regarding Deepsoil. It is obtained that the response from 4% damping combined with frequencies of 1 and 6 Hz fit quite well between PLAXIS and Deepsoil.

A better option of response improvement is achieved by fitting the curves from the shear modulus G/G_{max} and the cyclic shear strain between PLAXIS and Deepsoil. This is not further elaborated in this research, but is strongly recommended for further detailed research.

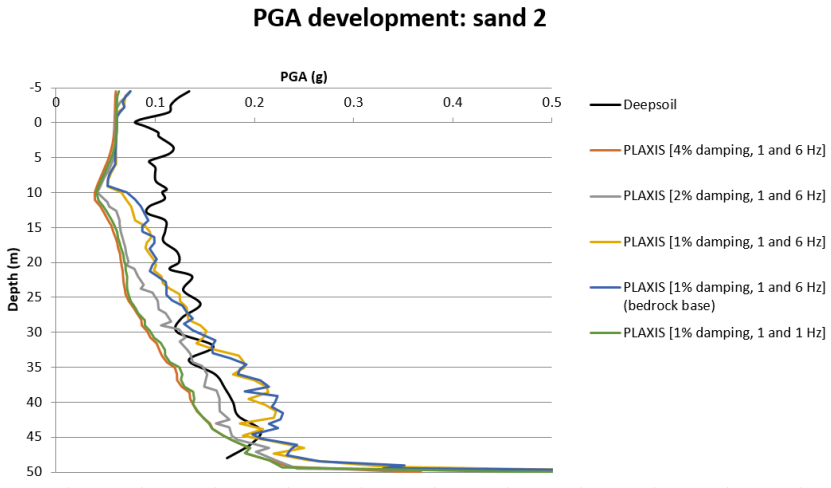

Figure D.14: PGA development of sand 2 material

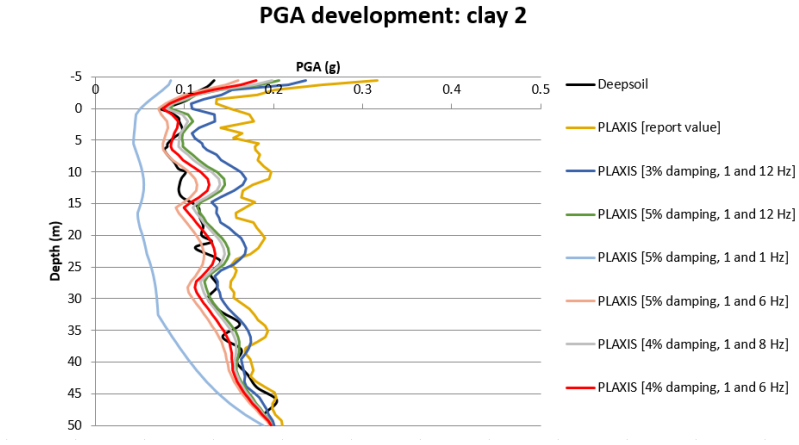

Figure D.15: PGA development of clay 2 material

D.4.4. Sensitivity analysis for different input signals

For the sensitivity analysis, the response of the structure regarding two other signals is obtained, elaborated in Section 3.4.5. All three signals are measured during the earthquake in 2012, as mentioned in Chapter 2. The shape and magnitude of the signals differ for the different measure locations. The corresponding output is presented in Table D.25. The influence from the presented seismic signals becomes visible from the output values.

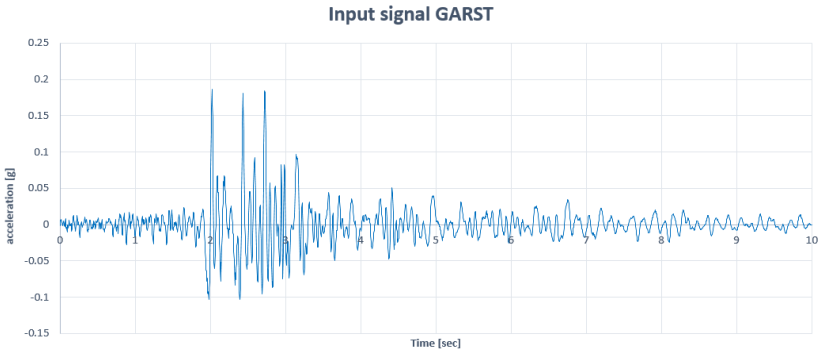

Figure D.16: Applied input signal Garsthuizen (GARST)

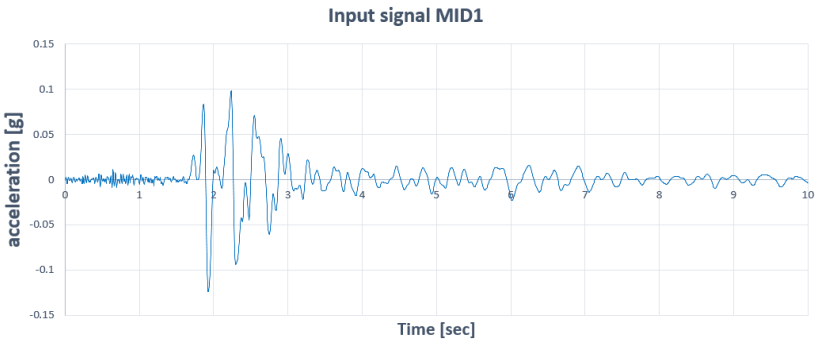

Figure D.17: Applied input signal Middelstum (mid1)

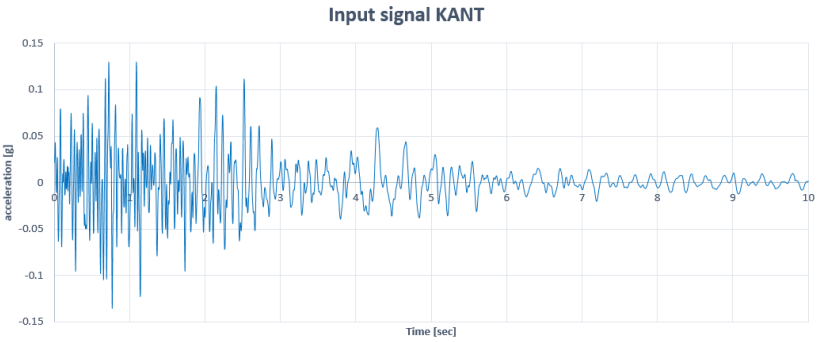

Figure D.18: Applied input signal Kantens (KANT)

Parameter	Value [**dynamic**]	Unit
GARST		
Horizontal displacement of wall	158.2	mm
Maximum acting bending moment	4155	kNm/m
Maximum acting anchor force	1342	kN/m
mid1		
Horizontal displacement of wall	170.6	mm
Maximum acting bending moment	4300	kNm/m
Maximum acting anchor force	1406	kN/m
KANT		
Horizontal displacement of wall	141.5	mm
Maximum acting bending moment	4063	kNm/m
Maximum acting anchor force	1323	kN/m

Table D.25: Output overview different input signals

The output values from the table are schematically visualised in Figure 3.20 of Section 3.4.5 from the main report.

E

Grout anchor resistance

This appendix presents additional information regarding the static and dynamic behaviour of grout anchors and is related to Chapter 4 of the main report. Background information regarding the named subjects in both static and dynamic state from Chapter 4 will be elaborated in more detail.

Section E.1 contains additional information regarding the static state behaviour of grout anchors. Resistance quality and determination related aspects are elaborated. Section E.2 starts with the PLAXIS model set-up followed by the elaboration of additional results. The conclusions of these results from Section 4.4.2. are further elaborated in this appendix.

E.1. Static related information regarding grout anchors

This section elaborates additional information regarding the static state resistance of grout anchors.

Control resistance quality

The deliverable resistance of a grout anchor is highly depended on the construction and execution quality. Also the soil characteristics close to the grout body play an important role. Several aspects are summed up below.

Construction related aspects

- The scale of disturbed soil around the grout body due to construction. This is mainly depending on: drilling speed, grout injection pressure, movement during drilling and the position of injection point
- Application of high pressure during injection
- The amount and quality of used grout during injection
- Pollution of sand/grout mix with clay and peat during injection

Soil related aspects

- Shape of sand particles
- Size of sand particles
- Density of the soil layer
- Presence of excess pore pressure or over-consolidated layers

The named aspects create uncertainty regarding the constructed grout anchor. Due to these uncertainties in construction and in soil stratigraphy, tests are available to perform before or after the anchor is produced. Three types of tests are available to provide insight in the possible resistance of an anchor.

- Failure test
  The failure test will be executed *before* any construction work had been performed. The goal of this test is to gather insight in the extreme resistance value, e.g. the friction parameters between soil and anchor α_t. This is achieved by an incremental increase of the pulling force, until the test anchor is pulled out of the soil. In this way the friction factor α_t can be determined. Also the behaviour of creep can be obtained from this test. The failure test is interesting to perform in new or unknown soil layers, which might be used as a resisting layer for the grout anchor.
- Suitability and control test
  The suitability and control test are both applied *after* the installation of the anchor. These tests are performed as a verification regarding the assumed resistance on forehand. If no failure test is applied in the area of construction, the assumed resistance of the anchors must be verified by performing suitability en control tests on the installed anchors. The design pulling force is simulated by increasing the loading steps incremental to that specific design load. Also the creep behaviour is obtained during such a test. Higher creep values than 2 mm are generally not allowed.

Resistance determination

In general the pulling resistance of a grout body can be estimated by the following equation (CUR166-2, 2012):

$$F_r = \alpha * q_c * O * L \tag{E.1}$$

With:

- α = parameter for friction between soil and grout, assumed value: 0.015
- q_c = average cone resistance
- O = perimeter of the grout body
- L = length of the grout body

From this equation, it becomes clear that the pulling resistance is mainly depending on three aspects: *The dimensions of the grout body, the soil state and the friction resistance from interaction between soil and grout.*

The quality and therefore the deliverable resistance of a grout anchor is highly depended on the construction and execution quality. Also the soil characteristics play an important role. The construction and soil related aspects which influence the resistance quality are summed below.

- *The dimensions of the grout body*
  The perimeter (O) and length (L) of the grout body relate the deliverable resistance to the dimensions of the grout anchor. It should be kept in mind that the constructed grout body will never contain the exact values as determined on paper during design. As mentioned above, the quality of construction determines in a large way the formed shape, dimensions and quality of the grout body in the soil.
- *The soil state*
  The soil characteristics are expressed in the average cone resistance, q_{gem}. From the cone resistance an indication can be provided regarding the density and quality of the sand. This forms an input value for the design of the grout body.
- *The friction resistance from interaction between soil and grout*
  The friction between soil and grout is expressed with a factor α. The estimation of this factor is based on empirical relations from tests in the field and from the laboratory. No validated equation for the determination of this parameter is available. From (CUR166-2, 2012) a value of 1.5% is suggested to apply for the determination of grout body resistance. This empirical value is determined in static state and does not include dynamic soil behaviour. From (CUR236, 2011) a value of 0.9% is suggested for α.

The empirical determination of this friction parameter α is done by taking the following steps (CUR236, 2011):

1. Determine the maximum net test pulling load on an anchor without exceeding the creep value of 2 mm. The net load is subtracted from the real test load measured by extracting several losses, further elaborated in (CUR236, 2011).
2. Determine the maximum mobilised shear stress $\tau_{mob,max}$ along the surface of the grout body by using the following equation:

$$\tau_{mob,max} = \frac{F_{test,max,net}}{\Pi * \varnothing * Ł} \tag{E.2}$$

3. Determine the average cone resistance $q_{c,average}$
4. Determine the friction parameter per anchor and average this value if multiple tests are performed.

$$\alpha_i = \frac{\tau_{mob,max}}{q_{c,average}} \tag{E.3}$$

$$\alpha_{gem} = \frac{\alpha_i}{N} \tag{E.4}$$

Depending on the tests and results a certain reduction may be applied on the determined value of α_{gem}. This results in the design value of α determined in an empirical way.

Evaluate output of new resistance formula

Before Equation 4.3 from the main report will be used to gather insight towards the dynamic resistance behaviour, the difference in output between both, the original and new equation for static states should be obtained.

Assuming equal values as applied in Chapter 2 the anchor resistance is estimated to be:

$$F_r = \alpha * q_c * O * L \tag{E.5}$$

$$F_r = 0.015 * 10,000 * 0.4 * \pi * 12.5 = 2356kN$$

For the alternative new formula a value for σ'_{rad} should be estimated. The magnitude of this value is depth dependent. An average value over the complete anchor length of 175 kN/m^2 for σ'_{yy} is estimated from the PLAXIS model. Including the angle of the anchor with the horizontal results in an average value for σ'_{rad} of about 185 kN/m^2. The anchor resistance is therefore assumed to be:

$$F_r = \int_0^L [(\sigma'_{rad} * tan(\phi)) * O] \, \mathrm{d}x \tag{E.6}$$

$$F_r = 185 * tan(30) * 0.4 * \pi * 12.5 = 1680kN$$

A deviation of about 30% between both equations is observed. The proposed alternative approach expects a lower anchor resistance which results in a more conservative approach. The original Equation E.5 assumes equal resistance over the complete soil layer by taking an average cone resistance per layer. The new formula defines a certain resistance based on a specific soil stress state a at certain location. Average values for the soil stress state of Equation E.6 should therefore be applied to compare the output results. The deviation of 30 % is assumed to be acceptable in order of magnitude. The assumed value for α might also be 0.009 instead of 0.015 (CUR236, 2011) which makes the deviation already

smaller. In general, the output from Equation E.5 is based on an empirical value including the effect of installing the anchors. The alternative new approach from Equation E.6 does include the specific soil stress state, without including the installation effects. It is concluded that the new introduced formula does correspond in order of magnitude towards the original resistance equation.

E.2. Dynamic related information of grout anchor

The dynamic behaviour of a grout anchor is modelled by using a PLAXIS model, elaborated in Section 4.3 of the main report. Section E.2.1 and further present the applied input and additional results with respect to the model.

E.2.1. Information related to model set-up

An overview of the model input parameters is presented in Table E.1. Additional information regarding related aspects of the model are elaborated below the table.

Input aspect	Applied input	Unit
Model type	Plane strain	[-]
Elements	15-Noded	[-]
Contour, Xmin/max	0/25	m
Contour, Ymin/max	0/28.25	m
Water level	24	m
Constants	default values	[-]
Material model, sand	HS small, Undrained (A)	[-]
Stat.BoundaryXmin/max	Normally fixed	[-]
Stat.BoundaryYmin	Fully fixed	[-]
Stat.BoundaryYmax	Free	[-]
Dyn.BoundaryXmin/max	Free-field	[-]
Dyn.BoundaryYmin	Compliant base	[-]
Dyn.BoundaryYmax	None	[-]

Table E.1: Model parameters PLAXIS model

Size and model mesh
The dimensions of the model have been chosen in such way that the vertical soil and water stresses correspond to the original model from Chapter 3. The midpoint of the anchor is positioned around +13.5 m NAP. To model an effective soil stress of about 190 kPa and a water stress of 105 kPa, the top of the soil layer should be positioned at +28.25 m NAP and the water level at +24 m. For saturated sand the assumed volumetric weight is 20 kN/m^3 and dry sand 18 kN/m^3. The X-boundary is estimated on engineering judgement keeping in mind that the seismic waves should travel around the modelled anchor. The mesh size is chosen as 'medium' and around the grout body the element size is four times smaller, to calculate the behaviour more accurately.

Soil parameters
The soil parameters of the modelled sand layer are copied from the model applied in the analysis. This is presented in Appendix **D.2.2** and **D.2.4**. Rayleigh damping is not included in this initial model. For a more advantaged model indicating quantitative effects, a proper value for the damping should be used.

Dynamic multipliers

The responding anchor movement on the design earthquake is measured from the model in the analysis and presented in Figure E.1. This movement is implemented as prescribed displacement in the model from Chapter 4 to simulate the anchor response.

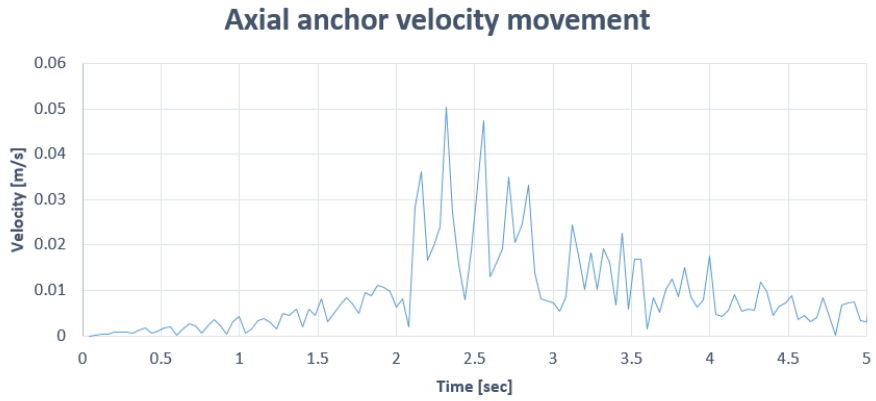

Figure E.1: Applied dynamic multiplier for anchor movement

Simultaneously with the anchor movement, the soil starts moving as a response on the implemented seismic signal at the base of the model. As mentioned in Chapter 4, the applied input signal at the base is not scaled at the correct magnitude regarding the implemented depth. This requires a non-linear soil response analysis which is advised to apply for further application. To indicate the qualitative effect of moving soil around a grout body, the input signal from the analysis model from Chapter 3 is applied, presented in Figure E.2

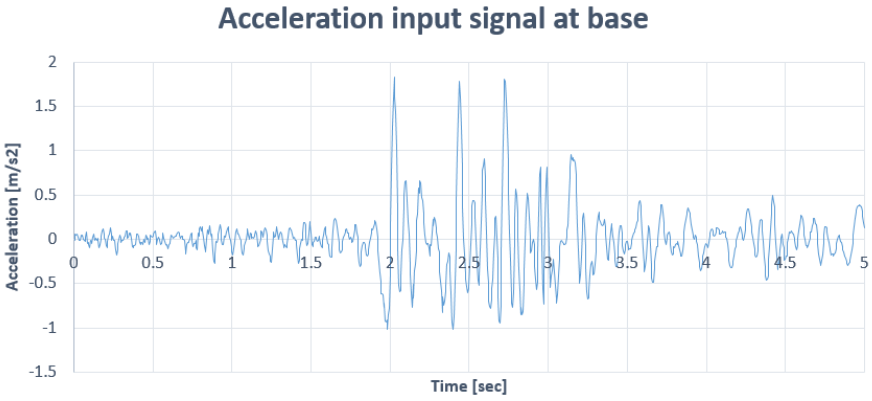

Figure E.2: Applied acceleration input signal at base of model

E.2.2. Additional results

The soil state after dynamic loading is of interest to investigate, to comment on the redevelopment of the resistance after the appearance of an earthquake. This will be elaborated from an investigating regarding the consolidation period after dynamic loading. The influence of each dynamic component from the model is also investigated in this section.

Consolidation period after dynamic loading

To visualise the behaviour of the soil after dynamic loading, a consolidation phase is added to the model from Chapter 4. In this consolidation phase the excess pore pressures are able to diminish in time. The consolidation phase ends if the pore pressures are below 1 kN/m^2. The consolidation process of excess pore pressures is presented in Figure E.3, and takes about 7 minutes.

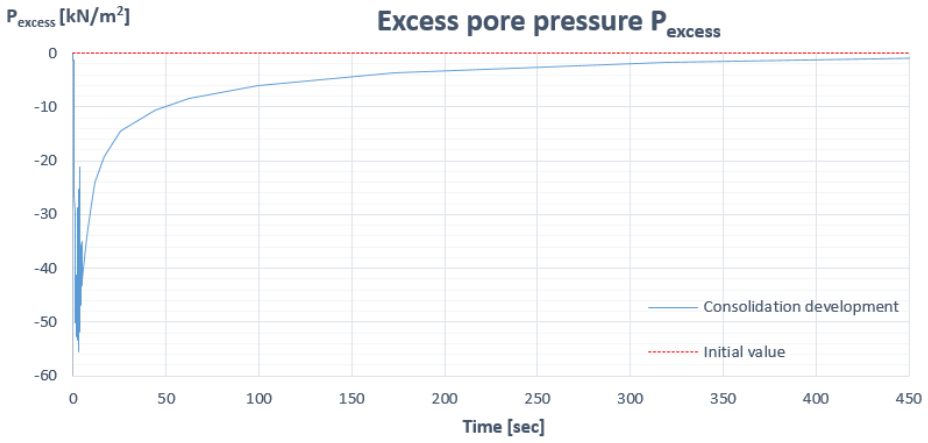

Figure E.3: Development of excess pore pressures during consolidation

It is of interest to visualise the development of the effective stresses during and after an earthquake. The new stress value equilibrium after consolidation provides insight in the deliverable resistance after an earthquake has appeared. The development of Cartesian soil stresses during the consolidation period are therefore given in the Figure E.4. The horizontal red line presents the initial stress state of the soil before dynamic loading.

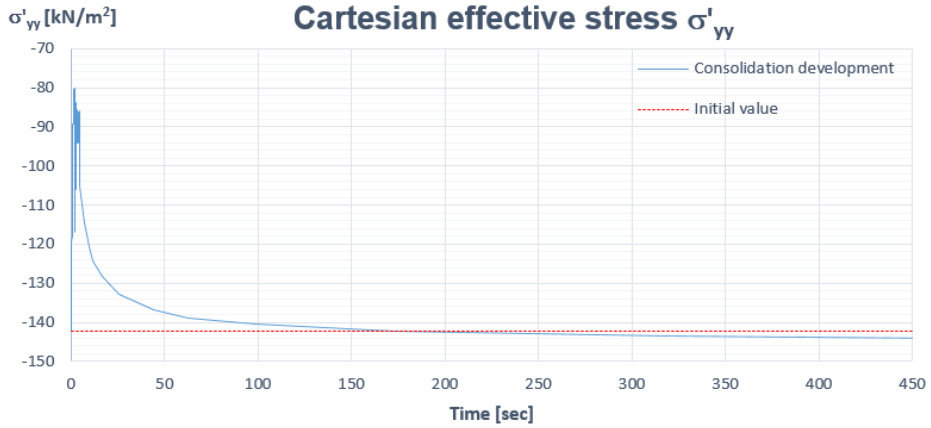

Figure E.4: Development of Cartesian effective stress during consolidation

It can be concluded that the initial Cartesian effective stress state will be reached after the excess pore pressures are disappeared. This indicates that the reduced soil stresses during an earthquake, tend to reach their initial values after the consolidation period.

Contribution of individual dynamic aspects

The output presented in Chapter 4 are based on the summation of three loading aspects, visualised in Figure E.5. Besides the static axial anchor force, the dynamic anchor movement and the acceleration input signal at the base are causing dynamic soil behaviour. It is interesting to determine the contribution of each of the two dynamic loading aspect. The results of the individual contribution of the following two loading scenarios, i.e. **Scenario 1 and 2** will be presented and compared to **scenario 3**, which includes all three load aspects simultaneously as presented in Chapter 4.

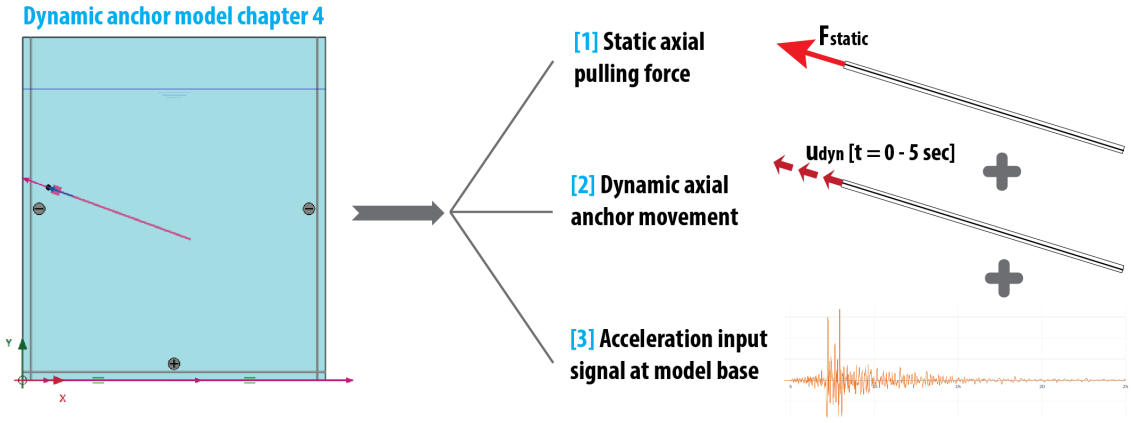

Figure E.5: Applied loading stages

The output figures from the model from Figure E.5 visualise the contribution of both load scenarios 1 and 2. In this way, the influence of both dynamic aspect becomes visible.

- **Scenario 1**: Static axial pulling force [**1**] + dynamic axial anchor movement [**2**]
- **Scenario 2**: Static axial pulling force [**1**] + acceleration input signal at model base [**3**]
- **Scenario 3**: Static axial pulling force [**1**] + dynamic axial anchor movement [**2**] + acceleration input signal at model base [**3**]

The figures correspond to the subjects handled in Chapter 4.

Volumetric strain ε_v

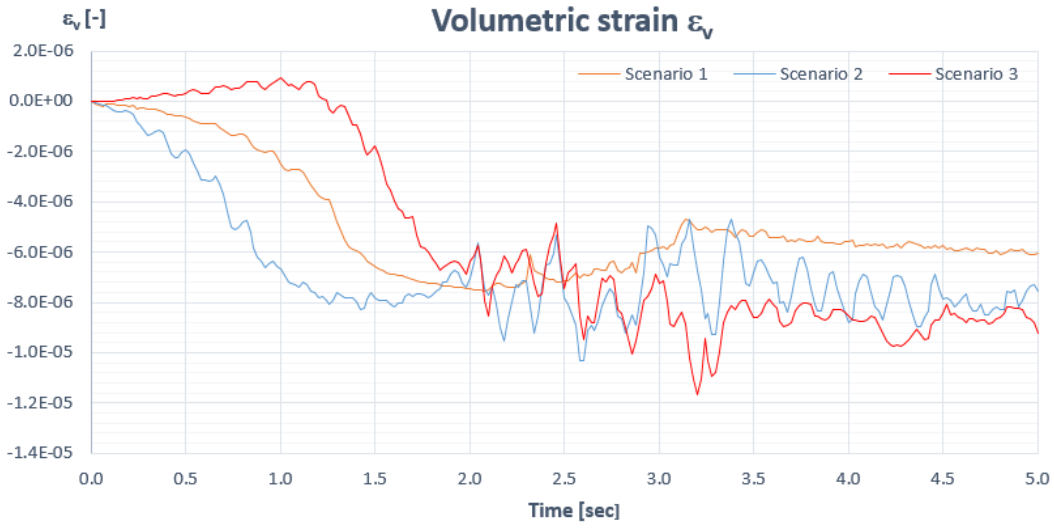

Figure E.6: Development of volumetric strains for all loading scenarios

Excess pore pressure P_{excess}

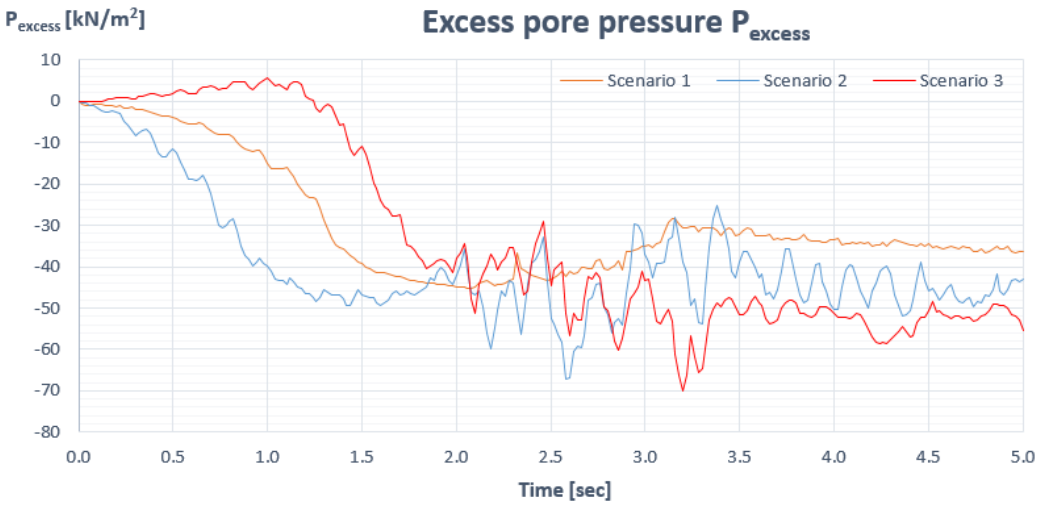

Figure E.7: Development of excess pore pressure for all loading scenarios

Principal effective stress σ'_1

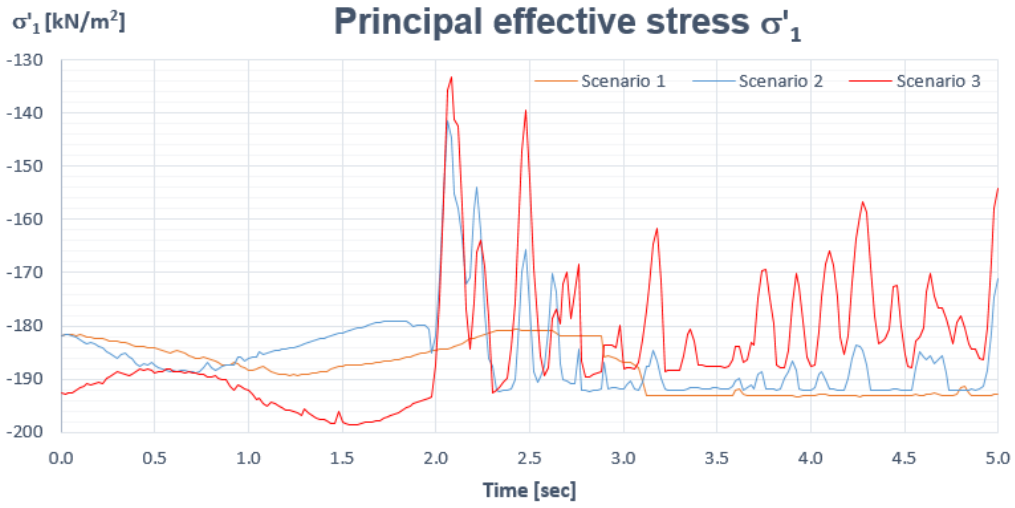

Figure E.8: Development of principal effective stress for all loading scenarios

Cartesian effective stress σ'_{yy}

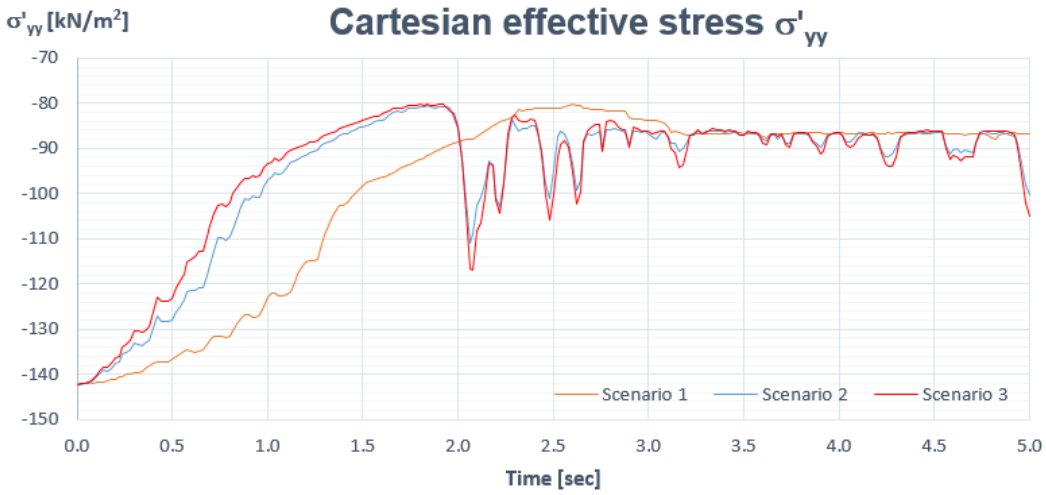

Figure E.9: Development of Cartesian effective stress for all loading scenarios

The graphs are based on a measure point close to the grout body. This stress point in PLAXIS is presented in Figure E.10 and indicated as point 'K'. To investigate if the determined stress point 'K' is representative for the general development of the soil, several other points at different locations around the grout body have been investigated. The qualitative behaviour was observed equal for the different measure points and therefore stress point 'K' is assumed to be representative.

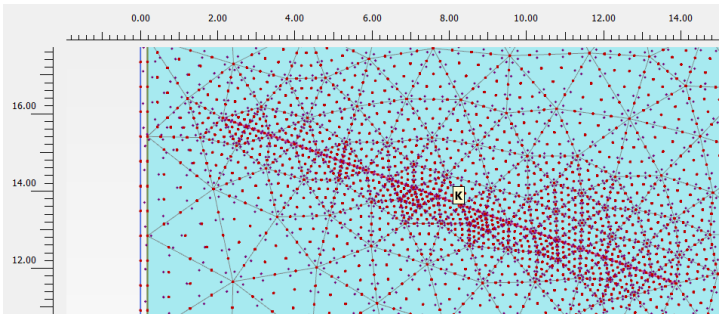

Figure E.10: Measure point close to grout body

Conclusion

The contribution of both dynamic aspects can be observed from the presented graphs above. It can be concluded that the dynamic movement of the anchor, scenario 1, develops in a relatively smooth line in comparison to scenario 3. This might be clarified from the relative low frequency movement of the anchor compared to the soil movement. It is also observed that the anchor movement tends to cause a new equilibrium value.

The contribution of the soil movement around the grout body is presented with scenario 2. This dynamic component follows the general peak developments from scenario 3. It seems that the high frequency input signal is responsible for peaked shapes in the development line. From these results is concluded that the soil movement from scenario 2, under the modelled conditions from Chapter 4, results in the largest contribution regarding the complete response of scenario 3. From a sensitivity check with an seismic signal of half the acceleration values, again the complete response is obtained. A slight reduction in the occurring effects from the original seismic signal are visible. The excess pore pressure is slightly lower, about 15% and less peak drops in the effective soil stress are visible. For a better understanding of the influence of both dynamic components, it is advised to conduct more sensitivity checks.

E.2.3. Determination of quantitative reduction of anchor resistance

The determined reduction value of 24% regarding the grout anchor resistance during an earthquake is based on the average value of the developed Cartesian effective stress. The development of this parameter is measured at eight locations close to the modelled grout body, as presented in Figure E.11. Besides the design signal (GARST) from Chapter 3, the calculation is repeated for two other seismic signals (Mid1 and KANT). These signals have been introduced in Section 3.4.5.

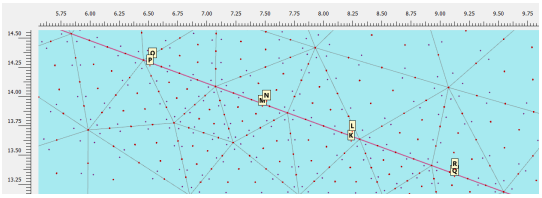

Figure E.11: Installed measure points along grout body

Table E.2 presents the measured values of σ'_{yy} in static and dynamic state from the measure points. The radial effective stress σ'_{rad} is approached as $\sigma'_{yy}/cos(18.5)$ to include the angle of the anchor with the horizontal. Multiplying σ'_{rad} with $tan(30)$ represents the shear stress σ'_{shear} for a specific location. This parameter defines the decrease of the anchor resistance. All values are expressed in kN/m^3.

GARST	K	L	M	N	O	P	Q	R	
$\sigma'_{yy,static}$	142	198	138	195	190	132	147	201	
$\sigma'_{yy,dynamic}$	87	185	85	180	175	79	87	185	
$\sigma'_{rad,static}$	149	208	145	205	200	139	155	212	
$\sigma'_{rad,dynamic}$	92	195	89	189	184	83	92	195	
$\sigma'_{shear,static}$	87	121	84	119	116	81	90	123	
$\sigma'_{shear,dynamic}$	53	113	52	110	107	48	53	113	
Change	-39%	-7%	-38%	-8%	-8%	-40%	-41%	-8%	**-24%**
Mid1	K	L	M	N	O	P	Q	R	
$\sigma'_{yy,static}$	142	197	138	195	190	130	147	201	
$\sigma'_{yy,dynamic}$	84	184	84	179	170	82	85	185	
$\sigma'_{rad,static}$	149	207	145	205	200	137	155	212	
$\sigma'_{rad,dynamic}$	88	194	88	188	179	86	89	195	
$\sigma'_{shear,static}$	87	120	84	119	116	79	90	123	
$\sigma'_{shear,dynamic}$	51	112	51	109	104	50	52	113	
Change	-41%	-7%	-39%	-8%	-11%	-37%	-42%	-8%	**-24%**
KANT	K	L	M	N	O	P	Q	R	
$\sigma'_{yy,static}$	143	198	138	195	190	131	147	201	
$\sigma'_{yy,dynamic}$	85	175	84	174	172	83	87	180	
$\sigma'_{rad,static}$	151	208	145	205	200	138	155	212	
$\sigma'_{rad,dynamic}$	89	184	88	183	181	87	92	189	
$\sigma'_{shear,static}$	87	121	84	119	116	80	90	123	
$\sigma'_{shear,dynamic}$	52	107	51	106	105	51	53	110	
Change	-41%	-12%	-39%	-11%	-9%	-37%	-41%	-10%	**-25%**

Table E.2: Output values of effective stresses around grout body

The average reduction value from the applied seismic signals is therefore assumed to be 25%. This values should be used carefully, because many simplifications are applied. These points are mentioned in Section 4.3.4.

F

Improvement measures

This appendix present additional information regarding the contents elaborated in Chapter 6 from the main report. The design load combination on the quay wall, which determines the anchor force, is further investigated to obtain the influence of each load component. This is elaborated in Section F.1. The parameters for the estimated anchor movement from Section 5.1 are presented in Section F.2. Additional information regarding both improvement measures from Section 5.4 and 5.5 are given at the end of this appendix in F.3 and F.4.

F.1. Determination of reduced safety for GSP

From Figure 5.2 of the main report, a factor of safety lower than 1 is determined during an earthquake. Goal of this section is to provide insight in the contributions of load components, which determine the increase of anchor force. The modelled load aspects are based on a design stage (N.Kraaijeveld, 2010) which might differ from the practical use of loads on the quay. Knowing the influence of each load component, a comment regarding the determined factor of safety can be made. This might bring the results from Figure 5.2 into another perspective.

Load components

The determined anchor force from Chapter 3 is calculated from a design load combination, presented in (N.Kraaijeveld, 2010). For engineering of the quay structure, several load contribution have been add up, to ensure sufficient safety during lifetime. The load combination for the design stage is however not a common load situation for daily use, but refers to an extreme situation. It is therefore of interest to indicate the contribution of each load component. The modelled load aspect with a large influence on the factor of safety should be checked on their reliability compared to the daily use of the quay. In this way, more insight in the practical safety reduction during an earthquake is obtained, instead of the determined reduction from a conservative design combination.

The design load combination can be subdivided into three main load aspects. The present soil and water behind the quay, the surface load and the force from a moored vessel. These components are earlier mentioned and presented in Appendix C. A visualisation of the load combination is given below. To estimate the contribution of the different load components, a static and dynamic calculation in PLAXIS is performed for each component. The original model van Chapter 3 is applied. The results are summarised in Figure F.1. Please note that the presented values for each component are determined to provide an initial impression of the load contributions. No conclusions can be made based on the specific values.

- *Anchor force from soil and water [S]*

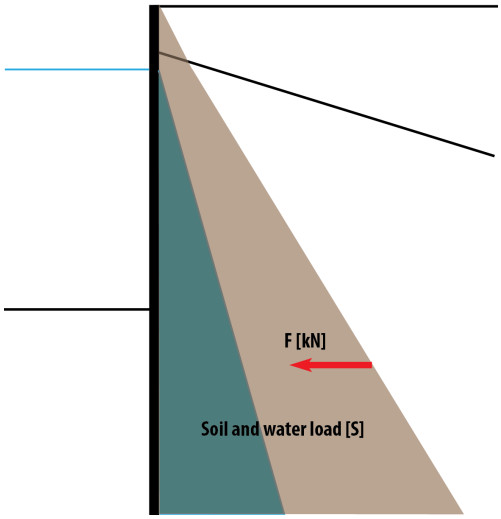

- Static anchor force: 1518 kN
- Percentage of total static anchor force: 70%
- Dynamic anchor force: 1661 kN
- Percentage of total dynamic anchor force: 67%

- *Anchor force from soil and water + surface load [S + q]*

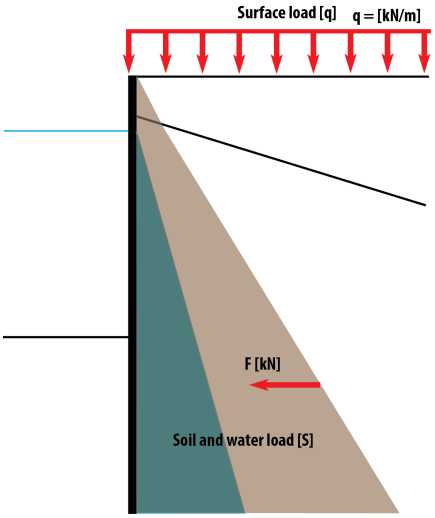

- Static anchor force: 2038 kN
- Percentage of total static anchor force: 93%
- Dynamic anchor force: 2318 kN
- Percentage of total dynamic anchor force: 94%

- *Anchor force from soil and water + surface load + vessel [S + q + V] (= DESIGN STAGE)*

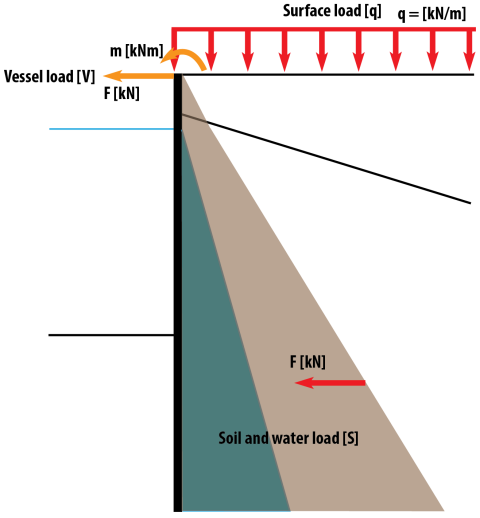

- Static anchor force: 2184 kN
- Percentage of total static anchor force: 100%
- Dynamic anchor force: 2469 kN
- Percentage of total dynamic anchor force: 100%

Overview of results

From Figure F.1 the contribution of each load component regarding the total anchor force is visualised. Difference is made between the static and dynamic state. Several conclusions can be made based on these results. The influence from a vessel at the quay is relatively small. This load component [V] does not increase significantly during an earthquake. The surface load [q] forms the governing component between both variable loads. With respect to the total anchor force, the influence of this parameters does increase due to an earthquake. The modelled values for this load are therefore important regarding the determined factor of safety.

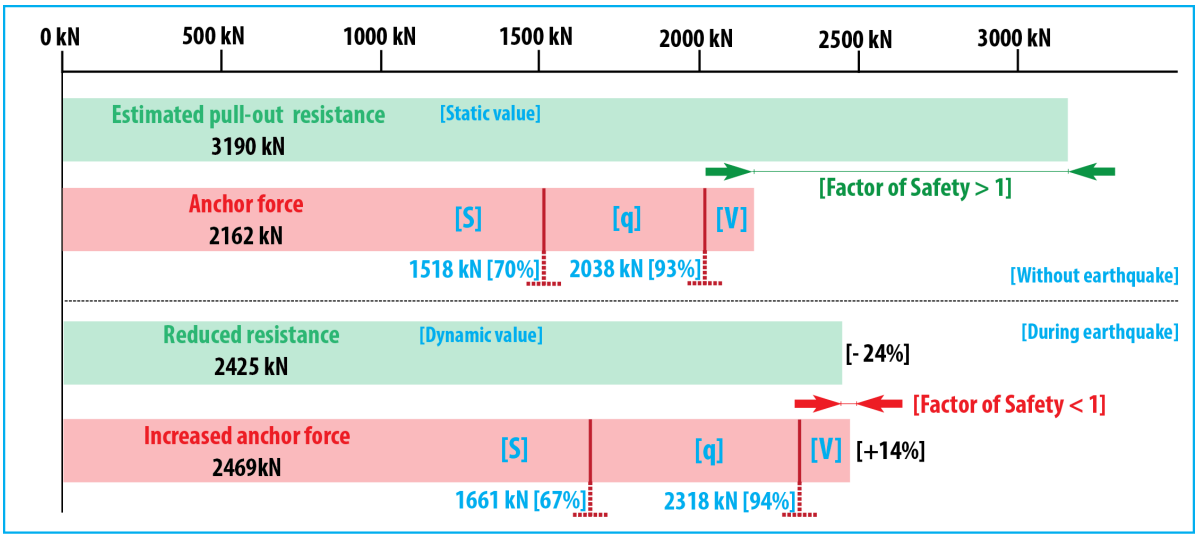

Figure F.1: Force overview with subdivision of force components(SLS values)

To comment on the reliability of the decreased factor of safety, which becomes even lower than 1 during an earthquake, the influence of the modelled load components should be taken into account. As mentioned above, the design stage includes all three load components during an earthquake, without including reduction factors. The surface load of 60 kN/m^2 is applied over the full quay area. It is however questionable if this load is acting on this complete area in practice, as modelled in the design stage. If the load area is significantly smaller than assumed in the design stage, the large influence of [q] as obtained from Figure F.1 might result in a significant lower anchor force. A factor of safety larger than 1 might be the result from including more realistic practical load values. Whether this assumption of surface load reduction is realistic should be considered in association with the authorities from Groning Seaport.

F.2. Estimation of anchor movement

The findings from Chapter 3 and 4 are translated to the existing quay structure in Section 5.1 of the main report. This section includes also an initial estimation of the anchor movement using an energy balance, schematically visualised in Figure F.2. The applied values and parameters to determine the movement are further elaborated in this section.

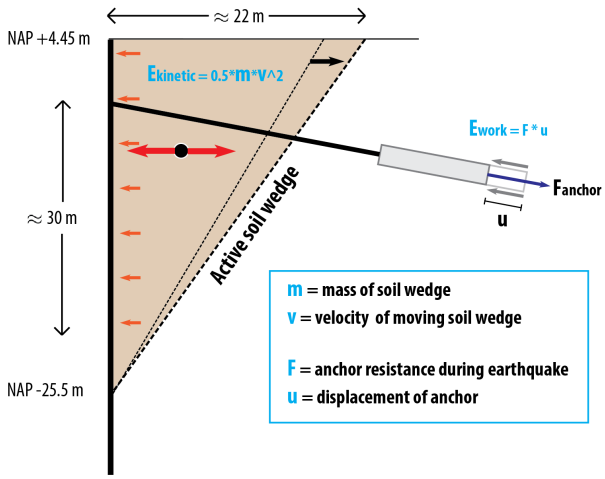

Figure F.2: Schematic overview of energy balance approach

To determine the anchor displacement, the following relation is introduced in Section 5.1:

$$E_{kin} = E_{work} \tag{F.1}$$

Which can be written as:

$$0.5 * m * v^2 = F * u \tag{F.2}$$

All parameters from Equation F.2 will be briefly elaborated below.

- Mass of soil **[m]**
  During an earthquake soil starts to move. A moving soil mass contains so called kinetic energy, know as movement energy. For this approach, all soil within the active soil wedge is assumed to influence the anchor force. The soil mass within the active soil wedge is therefore the mass which should be determined for Equation F.2.

  The active wedge is assumed to be triangle starting at the point from zero shear forces in the wall. From PLAXIS, this point is assumed to be at approximately NAP -25.5 m. From an average angle of internal friction of 29.5 degrees, the width of the active wedge will be about 17 m. During an earthquake, the soil wedge line becomes more inclined (Kramer, 1996). This additional width is assumed to be 5 m, resulting in a total active wedge width of 22 meters. The average soil density is assumed to be 2 ton/m^3. The soil mass within the active wedge is therefore approximately:

  $$0.5 * 22 * 30 * 2 = 660 ton/m$$

  The dimensions are visualised in Figure F.2.

- Velocity of moving soil **[v]**
  The velocity of the moving soil determines the corresponding energy of the moving soil mass. The higher the velocity, the higher the energy that develops in the soil mass. To determine the impact of the soil against the wall, the velocity signal during the design earthquake is used. The velocity

movement of the soil mass centre of gravity, positioned at approximately NAP -5.5 m, is given in Figure F.3. To determine the total kinetic energy, the contribution of each velocity peak is add up.

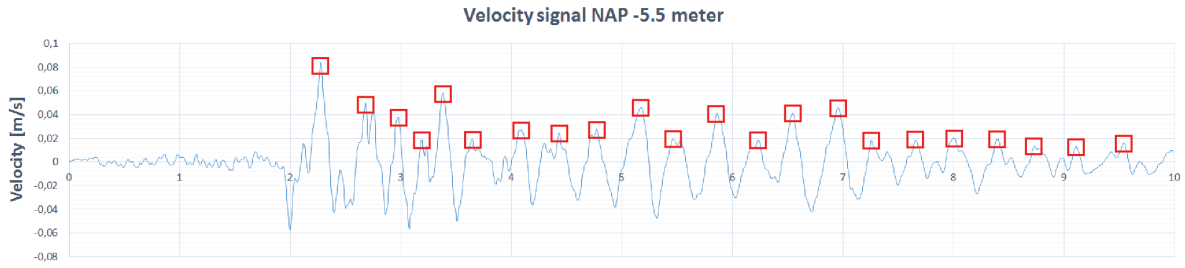

Figure F.3: Selected peak velocities from velocity signal

- Anchor resistance force [**F**]
  The anchor force resistance determines the magnitude of anchor movement as a result of the acting energy on the wall. The anchor resistance reduction from Chapter 4 should be included. The anchor resistance becomes therefore 1300 kN/m [3190 $kN/anchor$ = 1734 kN/m, including 25% reduction = 1300 kN/m]

- Anchor movement [**u**]
  The corresponding horizontal anchor movement from equation F.2 will be determined in meters.

$$u = \frac{0.5 * m * v^2}{F} = \frac{[ton/m] * [m^2/s^2]}{[kN/m]} = \frac{[kg/m] * [m/s^2] * [m]}{[N/m]} = \frac{[1/m] * [m]}{[1/m]} = [m]$$

To determine the displacement in axial anchor direction, the angle of the anchors with the horizontal should be included. The total anchor displacement in axial direction is therefore approached as:

$$u_{tot} = \frac{\left[\frac{0.5 * m * \Sigma[v^2]}{F}\right]}{cos(18.5)}$$

The resulting anchor movement of 1.25 cm is relatively small. Corresponding simplifications and assumptions regarding the applied method are elaborated in Section 5.1.

F.3. Installation of lightweight material

In Chapter 5, two improvement measures have been worked out to determine their effectiveness, applicability and corresponding construction costs. This section elaborates additional information regarding the application of lightweight material, also described as EPS material, behind the existing structure.

The applied model parameters from the PLAXIS model are described below. This model is used to determine the effectiveness of the improvement. The influence of different seismic signals regarding the anchor force including EPS is presented in Figure F.4. To ensure sufficient pressure strength, a unity check regarding this strength is presented in Section F.3.3. The final subsection elaborates the construction costs of the EPS improvement.

F.3.1. Model parameters

Except for the EPS material, the model parameters are equal to model parameters from Chapter 3, elaborated in Appendix D.2.4 and D.4. The applied EPS material is modelled as a soil polygon, with drained linear elastic material. The saturated and dry volumetric weight of EPS material are determined to be respectively 0.9 and 0.5 kN/m^3 (Aaboe). The stiffness is modelled as 12.000 kN/m^2 (Stybenex) and the poison ratio is applied as 0.2. The interface between soil and EPS is modelled with $R_{inter} = 0.7$. All other parameters are applied with default values.

F.3.2. Effectiveness for different signals

The observed results for 15 meters of EPS during the design earthquake are compared with the results from two additional design signals. In this way, a check regarding the consistency of the model is performed. The signals have been already used in Section 3.4.5. The corresponding anchor force during an earthquake from these two additional measure stations is presented in Figure F.4.

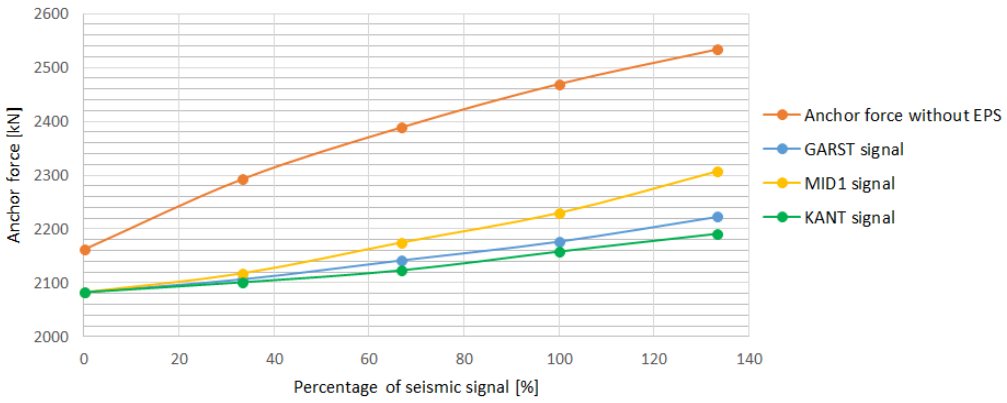

Figure F.4: Anchor development from different signals

It is concluded that the model behaves consistent for different input signals. The different characteristics between the seismic signals is revealed with the small deviation in anchor force.

F.3.3. Check on EPS pressure strength

A check on the pressure strength of EPS is required if existing soil is replaced for this lightweight material. As a starting point EPS250, at this moment the strongest type of EPS available, is applied. A check on short term and long term loading should be performed. Before the unity check on pressure strength is done, the load and resistance values should be determined.

- Loading parameters
  The loading parameters are subdivided in permanent loads, assumed as long term loading, and variable loads, assumed as short term loading. The permanent load is caused by the pavement

layer, estimated on 9.15 kPa (0.3 m of sand + 0.15 m concrete). The variable load of 60 kPa is applied as design condition for the quay structure (N.Kraaijeveld, 2010).

- Strength parameters
  Each type of EPS contains certain strength values. EPS250 refers to a short term pressure strength of 250 kPA. This value corresponds to 10% deformation of the EPS material (NEN-EN:14933-2007, 2007). The corresponding long term pressure strength is defined as $0.3 * F_{short}$ (GEOblock).

To perform a unity check, the design values for the load and resistance values are required and presented in Table F.1. These values are determined including safety factors from (GEOblock).

Load	Value	Safety factor	Design value
Variable load	60 kPa	1.5	90 kPa
Permanent load	9.15 kPa	1.35	12 kPa
Strength [EPS250 (GEOblock)]	Value	Safety factor	Design value
Short term resistance	250 kPa	1.25	200 kPa
Long term resistance	75 kPa	1.25	60 kPa

Table F.1: Design values for unity check of pressure strength EPS

The corresponding unity checks for short and long term pressure strength are:

	Load	Resistance	Unity Check
Variable/short term loading	102 kPa	200 kPa	**0.51**
Permanent loading	12 kPa	60 kPa	**0.20**

Table F.2: Design values for unity check of pressure strength EPS

Unity check values smaller than 1 indicate sufficient safety. The results from the unity check indicate therefore sufficient safety of pressure strength and possibilities for further optimisation of the EPS material. Before this optimisation is possible, the assumption with respect to: variable loads = short term loading should be investigated. No clear definition to reject this assumption is found but neither it is confirmed from literature. It might be possible that certain restrictions regarding the duration of the variable load of 60 kPA are required to meet the definition of a short loading stage.

F.3.4. Cost estimation for EPS improvement

The total construction cost of EPS are subdivided into direct costs, Table F.3 and additional costs, Table F.4. The direct costs corresponding to the different EPS widths have been determined separately. The applied prices per unit are based on average values from public tenders used within Arcadis. The direct construction costs are presented in Table F.3.

To estimate the total construction costs from Table F.4, three additional cost aspects are included in addition to the direct costs. Indirect costs, estimated to be 20% of the direct costs, and 'to be determined' costs, which are added as 5% of the direct costs form together with the direct costs from Table F.5 the so called 'Foreseen costs'. Indirect costs include aspects from execution, one time cost aspects, general costs and profit. 'To be determined' costs include several small aspects which have to be worked out later in more detail, but do no influence the general costs significantly. For those aspects it is not time efficient to work out all details in this level of cost estimation.

Including additional costs from possible risks during construction, a percentage of 5% from the foreseen costs is added. Adding these cost aspects results in an estimation of the total construction costs, as presented in Table F.4.

Assumptions from the cost estimation are summed up below Table F.4

Direct costs	Price per unit	Area	Costs
EPS 5 meters			
Removing pavement	10 $euro/m^2$	2100 m^2	21,000 *euro*
Soil works	7.5 $euro/m^3$	6300 m^3	47,250 *euro*
EPS application	162 $euro/m^3$	4375 m^3	712,031 *euro*
construct pavement	30 $euro/m^2$	2100 m^2	63,000 *euro*
			843,281 *euro*
EPS 10 meters			
Removing pavement	10 $euro/m^2$	3850 m^2	38,500 *euro*
Soil works	7.5 $euro/m^3$	11550 m^3	86,625 *euro*
EPS application	162 $euro/m^3$	8750 m^3	1,424,062 *euro*
construct pavement	30 $euro/m^2$	3850 m^2	115,500 *euro*
			1,664,688 *euro*
EPS 15 meters			
Removing pavement	10 $euro/m^2$	5600 m^2	56,000 *euro*
Soil works	7.5 $euro/m^3$	16800 m^3	126,000 *euro*
EPS application	162 $euro/m^3$	13125 m^3	2,136,094 *euro*
construct pavement	30 $euro/m^2$	5600 m^2	168,000 *euro*
			2,486,094 *euro*

Table F.3: Direct construction costs of EPS improvement

Total costs	**EPS 5 m**	**EPS 10 m**	**EPS 15 m**
Direct costs	843,281 *euro*	1,664,688 *euro*	2,486,094 *euro*
Indirect costs	168,656 *euro*	332,938 *euro*	497,219 *euro*
To be determined	42,164 *euro*	83,234 *euro*	124,304 *euro*
Foreseen costs	1,054,102 *euro*	2,080,859 *euro*	3,107,617 *euro*
Risks	52,705 *euro*	104,042 *euro*	155,381 *euro*
Total construction costs	**1,106,807** *euro*	**2,184,902** *euro*	**3,262,998** *euro*

Table F.4: Total construction costs of EPS improvement

Included assumption for cost estimation

- Soil works defines the excavation and replacement of the soil below the pavement area. Work and costs with respect to existing pipes and cables is not included. The excavated soil is assumed to be clean and without any form of contamination.
- In correspondence with a possible supplier of EPS lightweight material, an initial cost estimation for the required quantity is made. A 30% reduction on the market price per cubic meter is applied for the required EPS250 material.
- A stabilisation layer in combination with a foundation and concrete top layer is assumed for the so called pavement layer.
- The construction cost estimation does not include any engineering costs or real estate costs.
- All defined costs are excluding taxes.
- The assumed margin on the total costs is 25%. Average prices per unit are used. The cheapest values from contractors are observed to be 25% lower than the applied average values from Table F.3. The margin on determined costs is also depending on the level of design.

F.4. Installation of relieving floor

Equal to Section F.3, additional information regarding the proposed improvement measures is presented in this section. Additional information of the relieving structure behind the existing quay, as described in Section 5.5 of the main report is given. Again, the model parameters from the PLAXIS model are elaborated below. After that, a unity check regarding the bearing capacity of the proposed pile dimensions is given. Subsection F.4.3 reveals the applied values for the construction cost determination.

F.4.1. Model parameters

Except for the relieving floor, the model parameters are equal to model parameters from Chapter 3, elaborated in Appendix D.2.4 and D.4. The relieving floor is modelled as a soil polygon. Drained linear elastic material model is applied for the concrete structure. The saturated and dry volumetric weight of concrete are assumed to be 25 kN/m^3 (NEN-EN:1991-1-1, 2011). The stiffness is $31 * 10^6 kN/m^2$ and the poison ratio is applied as 0.2. The interface between soil and concrete is modelled with $R_{inter} = 0.7$. The foundation piles are implemented as an embedded beam row from elastic material. For this initial design, the pile stiffness is assumed to be $30 * 10^6 kN/m^2$. The pile type is predefined as a massive circular pile. A pile to pile distance of 3.68 m is applied. The axial skin friction is assumed to be linear containing a value of 100 kN/m. To ensure the pile base resistance to be sufficient, a maximum value of 2000 kN is modelled. All other parameters are applied with default values.

F.4.2. Determination of pile dimensions

To determine the dimensions and installation depth of the bearing piles, the software D-foundation is applied. A unity check regarding the bearing capacity of the piles is provided from the following input aspect.

- Soil layer
  The representative soil cross section from Appendix B is implemented in D-foundations. The ground level settlement after placement of the relieving structure is expected to be lower as 0.1 meters, because the structure is already installed for a number of years. Therefore, no negative skin friction is included. Positive skin friction is included for the deep sand layer from NAP -22 meter.
- Design load
  The design load for the bearing piles below the relieving floor is based on the number of applied piles and the corresponding pile-to-pile distance. For a relieving platform of 7.5 meters, initially two piles are applied for every 3.68 meters of quay length. The corresponding loading area for each pile becomes approximately 14 m^2, visualised in Figure F.5. Assuming an average volumetric weight of 20 kN/m^3 for soil and the concrete floor combined, the vertical load on one pile becomes 828 kN in case the floor is positioned at NAP +1.5 m. Including the surface load of 60 kN/m^3 results in a pile load of approximately 1660 kN for the serviceability limit state. The unity check of D-foundations will be performed using the ULS, ultimate limit state.

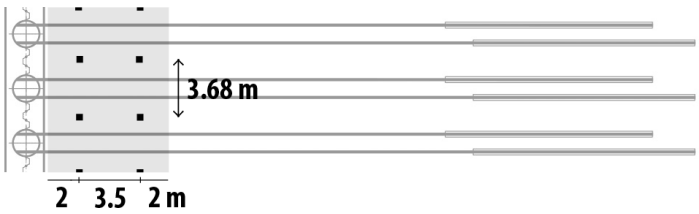

Figure F.5: Top view of bearing piles below relieving floor

- Type of pile
  As mentioned before, two types of piles are observed. The allowable installation method should be investigated in a later design state. Therefore, two different pile types with different installation methods are proposed. The prefab concrete pile will be piled into the soil to the required depth.

A tubex pile can be installed without vibrations, but is a bit more expansive. A decision between which pile to apply should be made in a later stage and is not included in this research.

Optimisation of pile dimension versus installation depth
The bearing sand layer is positions from NAP -22 meter. For the concrete prefab pile with rectangular dimensions of $0.45 * 0.45m$ the required installation depth contains -28 m NAP. The corresponding Unity Check in ultimate limit state is described as:

$$UC_{concrete-prefab-pile} = \frac{load}{resistance} = \frac{2230}{2252} = \mathbf{0.99} \tag{F.3}$$

This value is lower than 1 and is assumed sufficient.

The tubex pile requires an installation depth of -28.5 m NAP with a corresponding base diameter of 0.56 m. Grout injection along the pile shaft is assumed to reach the required depth trough the sand layers. The corresponding Unity Check in ultimate limit state is described as:

$$UC_{Tubex-pile} = \frac{load}{resistance} = \frac{2230}{2272} = \mathbf{0.98} \tag{F.4}$$

F.4.3. Cost estimation for relieving floor improvement

The total construction cost are subdivided into direct costs, determined in Table F.5 and additional costs which form together the total construction costs for the relieving structure, given in Table F.6. The subdivision between a high and low relieving floor combined with prefab concrete piles or fundex piles is taken into account. The applied prices per unit are based on average values from public tenders used within Arcadis.

The total costs are including three cost aspects, as explained in Section F.3.4. Except for the costs from possible risks, the included percentages are equal to the EPS improvement. The construction of a relieving floor is obtained to be more complex than installing EPS material. A percentage of 7.5% instead of 5% is therefore added to additional costs for risks. The estimated total costs for the relieving floor improvement are given in Table F.6.

Included assumption for cost estimation
The presented values for the determination of total construction costs include the following assumptions:

- Soil works defines the excavation and replacement of the soil below the pavement area. Work and costs with respect to pipes and cables is not included. The excavated soil is assumed to be clean and without any form of contamination.
- The prefab concrete piles are 0.45*0.45m. The determined length of piles for the low position relieving floor is 29.5 m and 32.5 m for the relieving floor at surface level.
- The diameter of the fundex piles is 0.56 m and should be 30 and 33 meters long for the low and high position relieving floor.
- The thickness of the concrete relieving floor is assumed to be 0.4 m. The applied price per unit includes an estimation regarding required form work and reinforcement. More reinforcement is required for the concrete wall.
- A stabilisation layer in combination with a foundation and concrete top layer is assumed for the so called pavement layer.
- The construction cost estimation does not include any engineering costs and real estate costs.
- All defined costs are excluding taxes.
- The assumed margin on the total costs is 25%. Average prices per unit are used. The cheapest values from contractors are observed to be 25% lower than the applied average values from Table F.5. The margin on determined costs is also depending on the level of design.

Direct costs	Price per unit	Unit	Costs
High relieving floor, prefab piles			
Removing pavement	10 $euro/m^2$	3325 m^2	33,250 *euro*
Soil works	7.5 $euro/m^3$	1469 m^3	11,222 *euro*
prefab piles	250 $euro/m^3$	6.6 $m^3/pile$	312,609 *euro*
Installation of piles	30 $euro/m/pile$	190 *piles*	185,250 *euro*
Concrete relieving floor/pavement	260 $euro/m^3$	1050 m^3	273,000 *euro*
			815,331 *euro*
High relieving floor, fundex piles			
Removing pavement	10 $euro/m^2$	3325 m^2	33,250 *euro*
Soil works	7.5 $euro/m^3$	1469 m^3	11,222 *euro*
Fundex piles	225 $euro/m^3$	8.1 $m^3/pile$	293,270 *euro*
Installation of piles	70 $euro/m/pile$	190 *piles*	250,800 *euro*
Concrete relieving floor/pavement	260 $euro/m^3$	1050 m^3	273,000 *euro*
			1,104,167 *euro*
Low relieving floor, prefab piles			
Removing pavement	10 $euro/m^2$	3325 m^2	33,250 *euro*
Soil works	7.5 $euro/m^3$	9975 m^3	74,813 *euro*
Prefab concrete piles	250 $euro/m^3$	6.0 $m^3/pile$	283,753 *euro*
Installation of piles	30 $euro/m/pile$	190 *piles*	168,150 *euro*
Concrete relieving floor	300 $euro/m^3$	1050 m^3	315,000 *euro*
Concrete wall	450 $euro/m^3$	420 m^3	189,000 *euro*
Construct pavement	30 $euro/m^2$	3325 m^2	99,750 *euro*
			1,163,715 *euro*
Low relieving floor, fundex piles			
Removing pavement	10 $euro/m^2$	3325 m^2	33,250 *euro*
Soil works	7.5 $euro/m^3$	9975 m^3	74,813 *euro*
Fundex piles	225 $euro/m^3$	7.4 $m^3/pile$	266,608 *euro*
Installation of piles	70 $euro/m/pile$	190 *piles*	228,261 *euro*
Concrete relieving floor	300 $euro/m^3$	1050 m^3	315,000 *euro*
Concrete wall	450 $euro/m^3$	420 m^3	189,000 *euro*
Construct pavement	30 $euro/m^2$	3325 m^2	99,750 *euro*
			1,426,990 *euro*

Table F.5: Direct construction costs of relieving floor improvement

Total costs	**HF,PP***	**HF,FP****	**LF,PP*****	**LF,FP******
Direct costs	815,331 *euro*	1,104,167 *euro*	1,163,715 *euro*	1,426,990 *euro*
Indirect costs	163,066 *euro*	220,833 *euro*	232,743 *euro*	285,398 *euro*
To be determined	61,150 *euro*	82,812 *euro*	87,278 *euro*	107,024 *euro*
Foreseen costs	1,039,547 *euro*	1,407,812 *euro*	1,483,737 *euro*	1,819,412 *euro*
Risks	51,977 *euro*	90,390 *euro*	74,187 *euro*	90,971 *euro*
Total construction costs	**1,095,601** *euro*	**1,478,203** *euro*	**1,563,742** *euro*	**1,910,383** *euro*

Table F.6: Total construction costs of relieving floor improvement